University College London

Modification of Peptides by Disulfide Bridging:
a Biochemical and Analytical Investigation

Sally Amanda Fletcher

A thesis submitted to University College London in accordance with the requirements of the degree of Doctor of Philosophy

Supervisor: Dr. James R. Baker

September 2014

Declaration

I, Sally Amanda Fletcher, confirm that the work presented in this thesis is my own. Where information has been derived from other sources, I confirm that this has been indicated in the thesis.

……

Abstract

The use of chemical reagents for the modification of peptides has broad applications and, as a result, is a rapidly expanding area of research. Such methods serve to improve the pharmacokinetic properties of the peptide or add functionality for a desired application. Chemical modification of peptides has facilitated the development of a variety of bioconjugates for use as analytical probes, diagnostic agents and therapeutics.

This project focuses on the modification of peptides by targeting disulfide bonds. Many peptides contain disulfide bonds which serve a crucial role in retaining their structure, function and stability. Reduction of these disulfides affords two reactive cysteine thiolates whose nucleophilicity can be exploited in peptide modification. To this end, a family of 3,4-disubstituted maleimide reagents were synthesised, designed to efficiently re-bridge a reduced, accessible disulfide bond. The bridging reagents vary in reactivity, properties and functionality but all serve to maintain the structural integrity conferred by a disulfide bond.

With these reagents in hand, the scope of their utility was tested on peptides of biological and medicinal interest. One such peptide was tertiapin Q, a neurotoxin derived from the venom of the honey bee and consisting of two disulfide bonds in close proximity. Both singly and doubly bridged variants of the peptide were synthesised and isolated. Biological activity of the modified peptide was analysed by whole-cell patch clamp experiments on cells expressing the target of the peptide toxin, the G-coupled inwardly rectifying K^+ (GIRK) channel, which tertiapin Q is known to inhibit. Loss of biological activity was observed upon modification, which led into a full structural characterisation study to determine the explanation for this intriguing result.

A second peptide target, octreotide, a stabilised analogue of the hormone somatostatin with a single disulfide bond, was modified with relative ease. Biological activity was examined by whole-cell patch clamp on cells expressing the target of octreotide, the somatostatin receptor (SSTR) subtype 2. Pleasingly, nanomolar activity of the modified peptide was observed. A novel candidate for the next generation of diagnostics for SSTR positive tumours was subsequently developed, characterised and tested by confocal microscopy.

Acknowledgements

First and foremost I wish to thank Dr Jamie Baker, my primary supervisor, for giving me the opportunity to work on such an exciting project, and for the constant support, enthusiasm and encouragement along the way. I will be forever grateful for this. I also extend my sincere gratitude to my secondary supervisor, Professor Andy Tinker, for including me into his group and for all of his shared knowledge, advice and optimism over the last four years.

I give special thanks to Dr Kersti Karu, whose wonderful help with mass spectrometry was invaluable. Dr Muriel Nobles for her continuous help with numerous aspects of the project and also for all the support and encouragement along the way. Also thanks to Dr Abil Aliev, without whom I would still be trying to assign my final NMR spectra! Thank you to Dr Carolyn Moores, for coordinating the course and for her ongoing words of encouragement.

I also would like to acknowledge our collaborators, Dr Erik Arstad and the members of the Arstad group for their help with the click chemistry, most significantly Dr Kerstin Sander and Brian Sin. Also, Dr Konstantinos Thalassinos, Ganesh Sivalingam and Adam Cryar for their initial practical help with the tandem mass spectrometry experiments.

I wish to thank all the members of the KLB and the Baker group, past and present, for making my time at UCL a truly memorable one. I thank Dr Favaad Iqbal and Dr Andrew Roupany for attempting to teach me organic chemistry, Dr Felix Schumacher for his biochemical brain, Dr Cristina Marculescu, Dr Judith Youziel, Dr João Nunes, Rosemary Huckvale and Daniel Richards for their friendship and tireless support during the ‘dramatic moments’. A special thanks goes to Liz Love and Joanna Hemming, who have become truly wonderful friends, and ones for life, I am sure. I also would like to thank all members of the Tinker group for making it such an enjoyable place to work. I thank Dr Steve Harmer and Dr Qadeer Aziz for answering all my silly questions and Alice Royal, Naomi Anderson and Dr Yiwen Li for the office chats and memorable Friday nights.

I must also extend my gratitude to all of my thesis proof-readers who have been a great help over the last few weeks, namely Dr Muriel Nobles, Dr Kersti Karu, Dr Andrew Roupany, Dr Qadeer Aziz, Daniel Richards, Andrew Swainson, Katherine McCluskey and Janna Lawrence.

I thank all of my family, friends and housemates for being so supportive and for at least pretending that they understood what I have been researching into.

Last, but my no means least, I thank my parents wholeheartedly for all of their support, both emotional and financial, over the last four years, and for giving me the courage to undertake a PhD in the first place. Thank you, this is for you both.

Sally Amanda Fletcher

Table of Contents

Abbreviations

ADC – antibody-drug conjugate

ATP – adenosine-5'-triphosphate

BME – β-mercaptoethanol

capLC-MS – capillary liquid-chromatography mass spectrometry

CCS – collision cross section

CEA – carcinoembryonic antigen

CI – chemical ionisation

CNS – central nervous system

DCM - dichloromethane

Dha – dehydroalanine

DIPEA – *N*,*N*-Diisopropylethylamine

DMF – *N*,*N*-dimethylformamide

DMSO – dimethyl sulfoxide

DNA – deoxyribonucleic acid

DTIMS – drift time ion mobility mass spectrometry

DTT – dithiothreitol

EC_{50} – half maximal effective concentration

EDTA – ethylenediaminetetraacetic acid

EGTA – ethylene glycol tetraacetic acid

EHSS – exact hard-sphere scattering

EI – electron ionisation

ELISA – enzyme-linked immunosorbent assay

Equiv. – equivalents

ESI – electrospray ionisation

Fab – antigen binding fragment

FBS – foetal bovine serum

FDA – Food and Drug Administration

FRET – fluorescence resonance energy transfer

GFP – green fluorescent protein

GIRK – G-protein coupled inwardly rectifying K^+ channel

GPCR – G-protein coupled receptor

GTP – guanosine-5'-triphosphate

h – hour

HBTU – *O*-Benzotriazole-*N*,*N*,*N'*,*N'*-tetramethyl-uronium-hexafluoro-phosphate

HEK – human embryonic kidney

HEPES - 4-(2-hydroxyethyl)-1-piperazineethanesulfonic acid

HOBt – hydroxybenzotriazole

HPLC – high-performance liquid chromatography

Hz - Hertz

IC_{50} – half maximal inhibitory concentration

IM – intra-muscular

IM-MS/MS – ion mobility-mass spectrometry/mass spectrometry

IR – infra red

IV – intravenous

LAR – long-acting release

LB – liquid broth

LC-MS – liquid chromatography-mass spectrometry

mal - maleimide

MALDI – matrix-assisted laser desorption/ionisation

MAPK – mitogen-activated protein kinase

Me – methyl

MeCN – acetonitrile

MEM – minimum essential medium

Min – minute

MOMIA – monomolecular multimodal imaging agent

m.p. – melting point

MSH – *O*-mesitylenesulfonylhydroxylamine

MS/MS – mass spectrometry/mass spectrometry (or tandem mass spectrometry)

NET – neuroendocrine tumour

NMR – nuclear magnetic resonance

OCT – octreotide

PA – projection approximation

PBS – phosphate buffered saline

PDB – Protein Data Bank

PEG – polyethylene glycol

PET – positron emission tomography

PRRT – peptide receptor radionucleotide therapy

PTP – phosphotyrosine phosphatase

RP-HPLC – reversed-phase high-pressure liquid chromatography

RT – room temperature

SC – sub-cutaneous

scFV – single chain variable fragment

SPECT – single-photon emission computed tomography

SST - somatostatin

TCEP – *tris*-(2-carboxyethyl)phosphine

TFA – trifluoroacetic acid

THF – tetrahydrofuran

THPTA – *tris*-(hydroxypropyltriazolylmethyl)-amine

TLC – thin layer chromatography

TOF – time-of-flight

TPN – tertiapin

TPNQ – tertiapin Q

UV – ultraviolet

wt – wild type

Amino Acid	*Three-letter Code*	*One-letter Code*
Alanine	Ala	A
Arginine	Arg	R
Asparagine	Asn	N
Aspartic acid	Asp	D
Cysteine	Cys	C
Glutamic acid	Glu	E
Glutamine	Gln	Q
Glycine	Gly	G
Histidine	His	H
Isoleucine	Ile	I
Leucine	Leu	L
Lysine	Lys	K
Methionine	Met	M
Phenylalanine	Phe	F
Proline	Pro	P
Serine	Ser	S
Threonine	Thr	T
Tryptophan	Trp	W
Tyrosine	Tyr	Y
Valine	Val	V

Chapter 1: Introduction

The introduction to this thesis will serve to place the project within its field; the continually expanding area of the chemical modification of proteins. The first section will cover the currently available strategies within this field and introduce the methodology employed within this project. The following sections will introduce the two peptides studied, tertiapin Q and the somatostatin analogue octreotide. Their biochemistry will be discussed before a review of the currently developed bioconjugates derived from these peptides. Finally, the electrophysiological technique of patch clamp will be described. This technique proved invaluable in the physiological analysis of the bioconjugates synthesised in this project and therefore its methodology and applications are discussed.

1.1 Chemical Modification of Proteins

1.1.1 Background

Proteins play a vast number of fundamental roles in living organisms. They function in structure and stability, cellular signalling and the catalysis of a whole host of chemical reactions. They are synthesised on the ribosome through the polymerisation of individual amino acids; the sequence and properties of which determine the subsequent structure, function and reactivity of the final folded protein.[1]

A large number of proteins undergo some form of modification following ribosomal synthesis. Some common examples of such post-translational modifications include amino acid phosphorylation, acetylation, methylation and ubiquitinylation,[2,3] shown in Figure 1.1 on a lysine residue as an example. These modifications serve to extend the diversity of a protein's amino acid functional groups beyond the 20 that naturally occur. As a result of such structural modifications, the function, location and lifetime of the protein can be altered.[2] With greater understanding of these *in vivo* modification processes and the effects that result, the possibility of imitating and extending such processes *in vitro* has become an area of ongoing research.

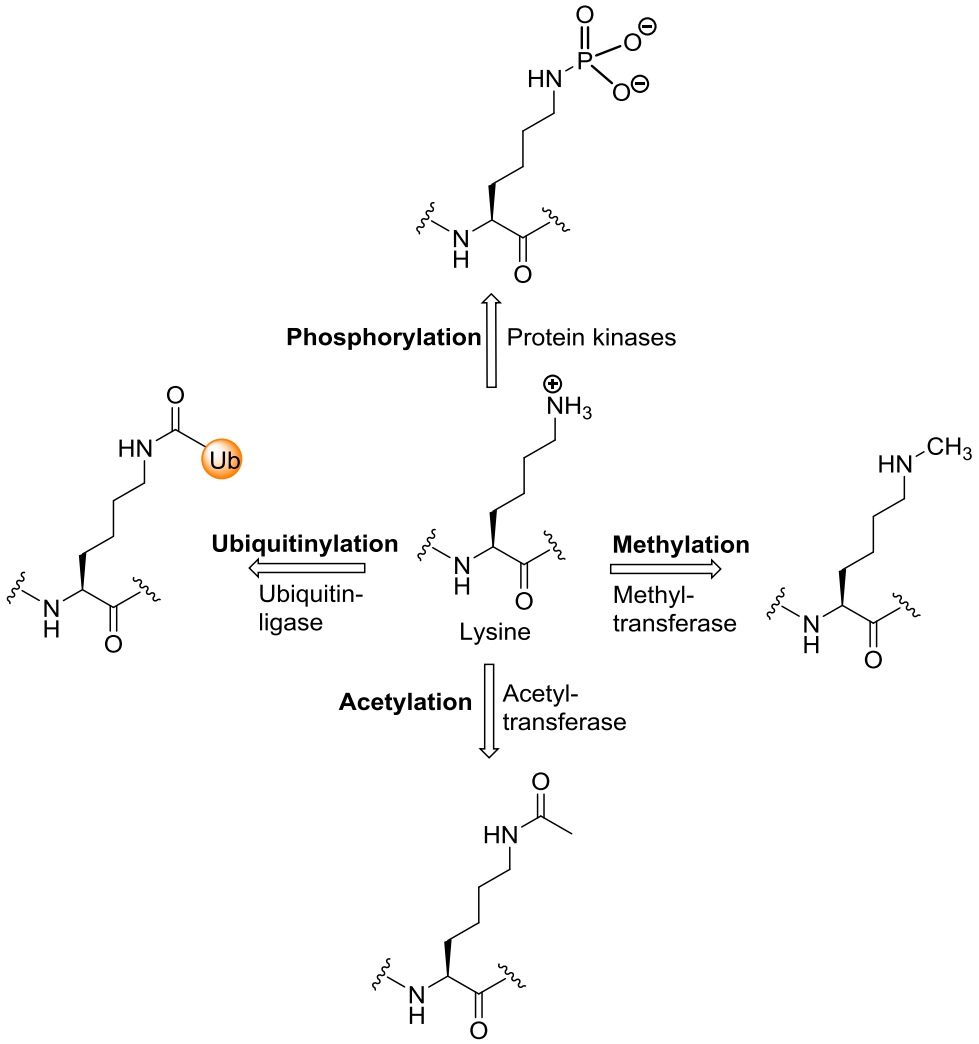

Figure 1.1 Examples of post-translational modifications of lysine.

Of key interest and importance is the idea of exploiting these processes to afford novel or improved therapeutics. Due to the poor solubility, short serum half-life, immunogenicity and protease degradation associated with protein and peptide-based therapeutics, small molecule drugs have prevailed thus far.[4,5] Tailored modifications could help to overcome such problems by improving their pharmacokinetic and pharmacodynamic properties.[6-8] In addition to therapeutics, advances in polypeptide synthesis and purification techniques have meant that these are increasingly being employed as diagnostic tools[9,10] and imaging agents[11,12]. Controlled modifications could help improve characteristics such as solubility and stability and facilitate visualisation and tracking, further extending the potential uses of peptides and proteins in these areas.[8,13,14] Much research has gone into the development of efficient strategies to

achieve this, and promising developments within this field have lead to a wide variety of novel products.

1.1.2 Site-Selective Modification

For controlled, selective modification of a peptide or protein, a specific and accessible reactive centre is needed. In other words, one particular amino acid side chain needs to be targeted in preference to those around it, of which there are often hundreds. Selectively targeting a single amino acid functional group is a significant challenge. Usually the reactivity of a nucleophilic site on a protein is exploited by functionalisation using an electrophilic modification reagent. Lysine residues are commonly targeted as their side chains bear a nucleophilic amine group.[15,16] Although lysine modifications have proved successful, they carry a distinct disadvantage; there are often multiple accessible lysine residues on the protein surface and targeting one selectively is difficult.[17] Modification reactions often result, therefore, in a mixture of products, which can make purification to obtain the desired product challenging.

Cysteine residues, with their unique sulfhydryl group, are the most nucleophilic residues in a protein, making them considerably reactive.[2,17-19] This significant nucleophilicity is a result of the relatively low electronegativity of sulfur and the fact that its electrons reside in large, diffuse orbitals that are easily polarisable, increasing electron availability. In addition to their reactivity, cysteines also have the advantage of low natural abundance, helping to reduce the amount of unwanted side reactions in cases where a single modification is desired. Miseta *et al.* quantified the relative abundance of cysteine residues in human proteins to be just 2.26%.[20] Procedures such as site-directed mutagenesis and recombinant engineering have made artificial insertion of cysteine residues at a desired location possible.[21,22] Such methods are not always ideal however, as they can be expensive and technically demanding. Additionally, incorporating a single cysteine increases the chances of protein misfolding, aggregation or disulfide scrambling.[23,24] Alternatively, native disulfide bonds can be reduced to form two free cysteines available for subsequent modification.[25,26] Exploitation of disulfides in this way will be discussed later.

As cysteines are the target of the methodology employed in this thesis, offering the most convenient attachment points for site-selective modification, reagents that target these residues will be considered next.

1.1.3 Modification Reagents Targeting Cysteine

A variety of reagents have been developed to functionalise cysteine residues. These continue to advance in efficiency and commercial availability. Some of the more widely used methods are briefly outlined.

1.1.3.1 Oxidation of Cysteine

Cysteine is renowned for rapid oxidation to form disulfide bonds. Exploitation of this reactivity has lead to a number of disulfide-containing modification reagents. Here, a reactive cysteine thiol **1** can attack one sulfur of the disulfide bond in the reagent, resulting in disulfide bond cleavage and the formation of a new mixed disulfide product **2**, as shown in Scheme 1.1.[27]

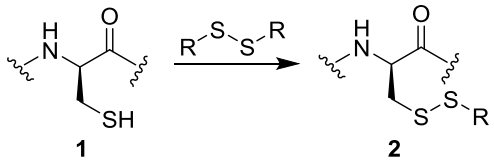

Scheme 1.1 Oxidation of cysteine (**1**) to form a new S-S bond.

These reactions carry the advantage that they proceed over a broad pH range, working well in physiological conditions, and that they are reversible through the addition of reducing agents such as *β*-mercaptoethanol (BME) and dithiothrietol (DTT). Reversibility of a protein modification is often highly desirable as it allows for functionalisation to be controlled and removable.

A classic example of a commonly used reagent of this family is Ellman's reagent (5,5'-dithiobis(2-nitrobenzoicacid)) shown in Figure 1.2. Since its introduction in 1959, Ellman's reagent has been used most recognisably for cysteine quantification[28], but more recently for modification of cysteine-containing proteins such as glutathione and haemoglobin.[29]

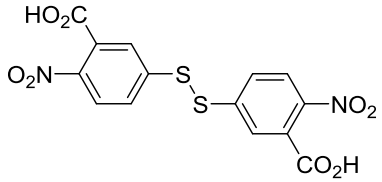

Figure 1.2: Ellman's reagent (5,5'-dithiobis(2-nitrobenzoicacid)).

1.1.3.2 Oxidative Elimination of Cysteine

Another method of cysteine modification is *via* its prior conversion to dehydroalanine (Dha). Desulfurisation of cysteine through oxidative elimination has proven an efficient strategy for the formation of Dha **3**. The resultant double bond within the residue provides a reactive site suitable for further functionalisation.[30]

Research into the best oxidative elimination strategy has been pursued most recently by Davis and co-workers. Their aim was to establish a direct route from cysteine to Dha while overcoming drawbacks of previous methods, such as lengthy reaction times and lack of substrate selectivity[31]. They explored the use of *O*-mesitylenesulfonylhydroxylamine **4** (MSH) as a potential reagent facilitating oxidative elimination (Scheme 1.2).[30] Preliminary tests on a single amino acid model gave promising results and success continued when extended to a protein model; complete conversion of a single surface-exposed cysteine to Dha **3** took place in 20 minutes.[30]

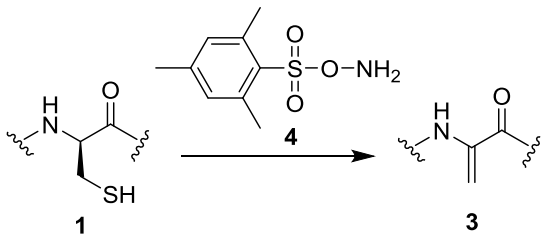

Scheme 1.2: Oxidative elimination of cysteine (**1**) using MSH (**4**).

MSH presented itself as a rapid and selective reagent for oxidative elimination. The group went on to demonstrate the versatility of Dha by further functionalising the newly incorporated double bond through the conjugate addition of nucleophiles. Phosphorylated and glycosylated protein derivatives were just a few of a number of selectively modified products successfully obtained.[30,31]

1.1.3.3 Alkylation of Cysteine

Alkylation is a common and straightforward route to the functionalisation of cysteine. A variety of different suitable electrophiles have been explored with the α-halocarbonyls (**5**, Scheme 1.3) being the first and one of the most commonly employed.[32] Iodoacetamide was originally the most popular reagent due to its high reactivity, however competing side reactions with lysine and histidine meant that chloroacetamide often prevails as the reagent of choice.[33]

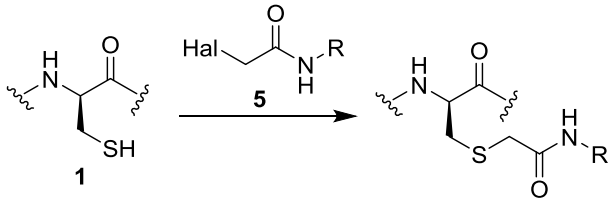

Scheme 1.3: Alkylation of cysteine (**1**) using a haloacetamide (**5**).

Such reagents have been effectively used for conjugation of proteins to other molecules such as fluorescein[34] and oligosaccharides.[35]

Another chemical functionality commonly employed in cysteine alkylation is maleimide **6**. The chemistry of this group facilitates the conjugate addition of a nucleophile,[27] such as the thiolate of a cysteine residue.[17] The resultant product is the reduced succinimide **7**.

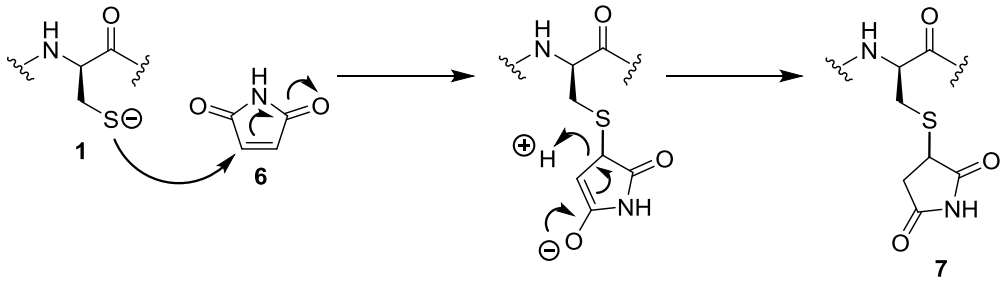

Scheme 1.4: Reaction between cysteine (**1**) and a maleimide (**6**).

These maleimides react rapidly due to the highly electrophilic nature of the alkene; this electrophilicity is caused by the electron withdrawing effects of the neighbouring carbonyl groups. When used at physiological pH, maleimides have also demonstrated high selectivity towards cysteine thiols over other nucleophilic sites in proteins; the ε-

amino of lysine or the imidazole of a histidine residue for example.[19,36] Another important characteristic of these motifs is the presence of the second point of attachment at the maleimide nitrogen, enabling facile conjugation of the maleimide complex to another biomolecule or functional moiety. Recent examples in the literature demonstrate the versatility of this concept whereby fluorophores, polymer chains and enzymes have all successfully been linked to proteins or carbohydrates *via* a maleimide (Figure 1.3).[37-40]

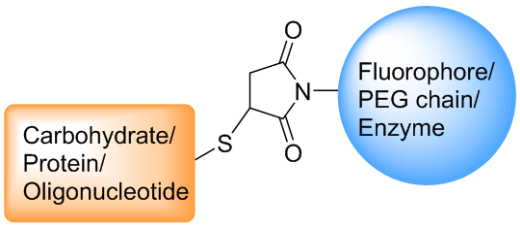

Figure 1.3: Possible uses for maleimide conjugation.

Despite its strengths for highly reactive and selective cysteine modification, maleimides still suffer limitations. Loss of the double bond through succinimide formation means that there is a limit to the extent of conjugation; only one biological or chemical entity can be attached to the protein of interest.[11] In addition, it would often be beneficial if the maleimide motif could be removed at a desired point, for instance, once the protein had reached a certain destination within the cell. The succinimide linkage was originally thought to be completely irreversible, however more recently it has been found to disassemble, by a retro-conjugate addition, over several days *in vivo*.[41] A more ideal situation would be complete and controlled disassembly at a desirable location.

There has also been evidence of some reactivity towards lysine residues where the maleimide is present in significant excess, or where the pH of the reaction is significantly increased above neutral.[42] These, however, are easily avoidable using reaction conditions that favour cysteine selectivity.

1.1.4 A New Class of Maleimides

Recent work by the Baker and Caddick groups (both UCL) has described a new class of reagents, the bromomaleimides **8**, as a next generation of maleimides, which have the ability to act as double conjugate acceptors.[19,24,43] It was proposed that incorporating a leaving group onto the double bond of the maleimide would facilitate an addition-elimination sequence. Addition of a cysteine thiolate occurs at the maleimide double

bond which results in the subsequent elimination of bromide and formation of the thiomaleimide **9** (Scheme 1.5). Maintaining the double bond means that a second nucleophile can attack and, by the same mechanism, facilitate the elimination of the cysteine substituent.[43] This makes reversibility of the cysteine modification possible.

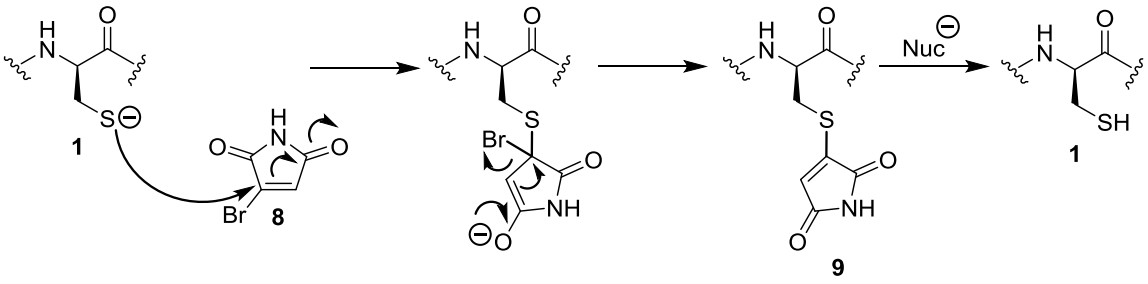

Scheme 1.5: Reaction between cysteine thiolate and bromomaleimide.

The Baker group have undertaken much research into bromomaleimide to examine its efficacy. It was first reacted with a model cysteine system, *N*-Boc-Cys-OMe (**10**), which led to the expected thiomaleimide **11** in a very fast and clean reaction; quantitative yield in less than 1 minute (Scheme 1.6).[43]

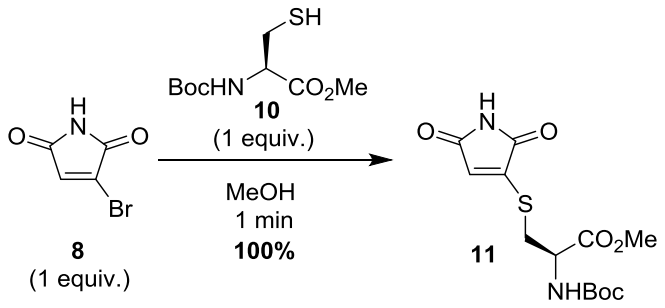

Scheme 1.6: Reaction between bromomaleimide (**8**) and *N*-Boc-Cys-OMe (**10**).

Competition experiments between maleimide **6** and bromomaleimide **8** in the presence of the model cysteine showed bromomaleimide to react faster.[43] Selectivity experiments were also conducted whereby bromomaleimide **8** was reacted with a 1:1 mixture of cysteine and propylamine. The result was the formation of the thiomaleimide product **11** exclusively,[43] showing strong selectivity for the thiol over the amine. Perhaps the most exciting finding was that when the thiomaleimide **11** was treated with the common reducing agent *tris*(2-carboxyethyl)phosphine (TCEP), its nucleophilic nature served to enable the elimination of the *N*-Boc-Cys-OMe in 98% yield.[43] This clearly

demonstrated the reversibility of the reaction suggesting that, when applied to a peptide or protein, the modification could be temporary.

Following these initial findings, through a collaboration between the Baker and Caddick groups, bromomaleimide **8** was then assessed on a protein – namely the SH2 domain of the Grb2 adaptor protein with a single point mutation (L111C) resulting in a domain with a single cysteine residue (**12**, Scheme 1.7).[19] Treatment with 1 equivalent of bromomaleimide led to total, selective modification of the single cysteine residue present to produce thiomaleimide **13**.[19] Due to retention of the maleimide double bond, it was predicted that a second conjugate addition could take place. To test this, 1 equivalent of glutathione was added to the thiomaleimide complex. The expected dithiosuccinimide **14** product was formed.[19]

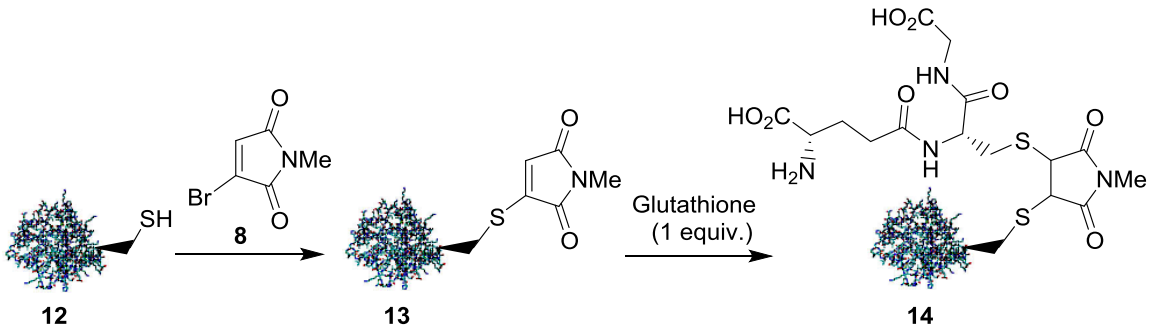

Scheme 1.7: Modification of the Grb2 SH2 domain (L111C) (**12**) with *N*-methyl-3-bromomaleimide (**8**).

From these findings it was proposed that using a 3,4-disubstituted reagent, such as dibromomaleimide **15**, would lead to the formation of the dithiomaleimide product **16** with retention of the double bond. The above reaction was repeated and this theory proven (Scheme 1.8). Retention of the double bond meant that the conjugation reaction is reversible as other nucleophiles (such as TCEP, β-mercaptoethanol or glutathione) can be employed to cleave the substituents; it is believed this is again *via* a conjugate addition-elimination sequence.[19]

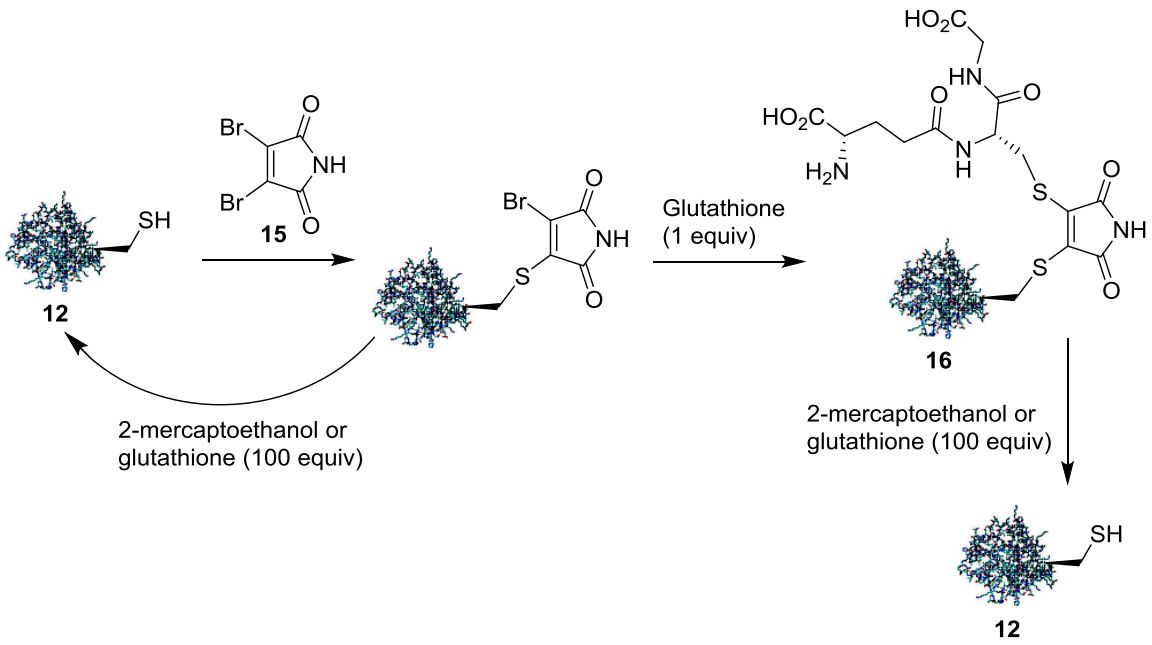

Scheme 1.8: Reversible cysteine modification using dibromomaleimide (**15**).

The ability of excess glutathione to facilitate the cleavage of the maleimide conjugates led to the intriguing possibility that the reducing conditions of the cytoplasm of cells may be ideal to facilitate this process. In passing from the extracellular to the intracellular region, the glutathione concentration increases from ~0.01 mM to 1–11 mM respectively.[44] Experimental results proved even 1 mM glutathione enough to give complete cleavage of thiomaleimide **17** and reformation of the unmodified protein **12** (Scheme 1.9).

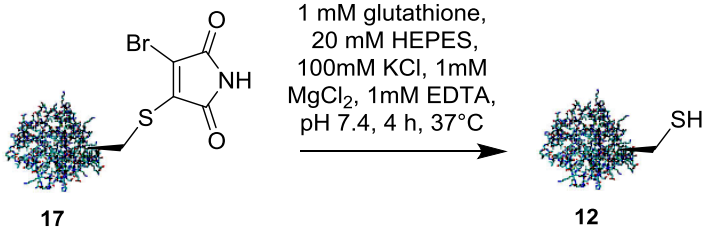

Scheme 1.9: Protein cleavage in conditions mimicking the intracellular environment.

The considerable thiol concentration difference across the cell membrane, and the cleavage that results upon crossing it, was promising as it suggested the possibility of controlling the location at which the original peptide is released. Drugs that are inactive upon administration but that become pharmacologically active when they reach their required destination, as a result of an enzymatic or chemical modification, are termed pro-drugs.[45] The search for such drugs is of great importance as they show promise in

reducing the unwanted side-effects common to many drugs currently available. Recently, using maleimides bearing a rhodamine-green fluorescent protein (GFP) fluorescence resonance energy transfer (FRET) pair, the ability of maleimide conjugates to undergo intracellular cleavage in mammalian cytoplasm was demonstrated. This highlighted the potential use of such conjugates in the targeted delivery of therapeutic cargo which is released upon internalisation into the cell.[46]

1.1.5 Targeting Disulfide Bonds as Sites of Modification

As previously mentioned, many peptides and proteins contain one or more disulfide bonds, serving to both confer stability and maintain the precise tertiary structure vital to biological activity (Table 1.1). Both therapeutic proteins and those synthesised for excretion into the extracellular environment commonly have disulfides; in these cases significant protein stability is essential.[1]

These naturally occurring disulfides are also a very attractive target for protein modification reactions as they remove the need for introducing free cysteines artificially which often suffers limitations such as low expression yields and unwanted dimerisation of proteins.[47]

Table 1.1 Examples of therapeutic proteins displaying one or more solvent-accessible disulfide bonds[48].

Protein	*Disulfide Linkage(s)*	*Medical Application*
IFN-β	Single intra-chain	Treatment of multiple sclerosis
IL-2	Single intra-chain	Treatment of certain cancers
TNF-α	Single intra-chain	Treatment of soft tissue carcinoma
Hirudin	Two intra-chain	Anti-coagulant
Insulin	Two inter-chain and one intra-chain	Treatment of diabetes
Antibodies	Two inter-chain and two intra-chain	Various

Non-covalent interactions between amino acid side chains and the formation of disulfide bonds is coupled with resultant protein folding. In biological systems this is facilitated by the presence of two enzymes: protein disulfide oxidoreductase and protein disulfide isomerase.[49,50] Due to the rigidity of the peptide bond, neighbouring cysteine residues cannot couple to form a disulfide. This is also true for the case in which the

two cysteines are separated by just one other residue (C-X-C). Due to the nature of both the α-helix and β sheet arrangement of an amino acid chain, cysteines are only able to form disulfides when spaced by at least two other residues (C-X-X-C) resulting in a viable cysteine-cysteine alignment.[20]

The reactivity of the disulfide bond, and that of the two cysteine residues produced upon reduction, has been found dependant upon both the immediate local environment[51,52] and its accessibility within the protein structure.[53] Both Wang *et al.* and Britto *et al.* describe findings whereby cysteine residues in proximity to basic amino acid residues such as arginine, histidine and lysine had enhanced reactivity. They conclude that the positive charges on these basic residues may help promote deprotonation of the cysteine thiol (-SH) to the significantly more reactive thiolate ($-S^-$). Conversely, a negatively charged local environment, caused by proximity to acidic residues such as aspartic acid and glutamic acid, led to suppression of thiol dissociation and a resultant decrease in cysteine reactivity.[51,52]

With regards to disulfide accessibility, it has been found that disulfide bonds residing in the hydrophobic core of a protein are significantly less reactive.[54] This, however, is a necessary characteristic as these disulfide bonds are often integral to the function and tight packing of the protein and modifying these buried disulfides may lead to undesired effects such as unfolding and loss of biological activity.[23] Accessible disulfides on the other hand, such as those on the surface of the protein, tend to contribute mainly to the stability of a protein and hence are not so fundamental to protein structure and function.[23,55] Consequently, these accessible disulfides present themselves as a more attractive target for modification. Reduction of such disulfides leads to the formation of a pair of very reactive thiolate nucleophiles whose reactivity holds great potential for subsequent modification reactions.

The chemical modification strategies described in Section 1.1.3 and 1.1.4 were designed for the modification of single cysteine residues, either naturally occurring, artificially inserted or from the reduction of a disulfide to form two modifiable cysteines. In the case of the latter, loss of the disulfide bond removes any structural integrity that it previously conferred which could be detrimental to protein function in many cases. This

will be most significant in cases where the disulfide bond is in proximity to the pharmacophore of the peptide or protein.

A recent alternative to modification of the individual cysteines of a reduced disulfide bond is the idea of 're-bridging' the two cysteines whilst simultaneously incorporating the desired functionality. Research into the re-bridging of an accessible disulfide bond as a protein modification strategy was originally pioneered by Brocchini *et al.*, who aimed to exploit the reactivity of both the sulfur atoms of the reduced disulfide. They developed the polyethylene glycol (PEG) linked mono-sulfone **18** which, by means of sequential addition-elimination reactions, served to install a three-carbon bridge spanning the original disulfide bond to produce the PEGylated product **19**. The proposed mechanism of the reaction is shown in Scheme 1.10.[23]

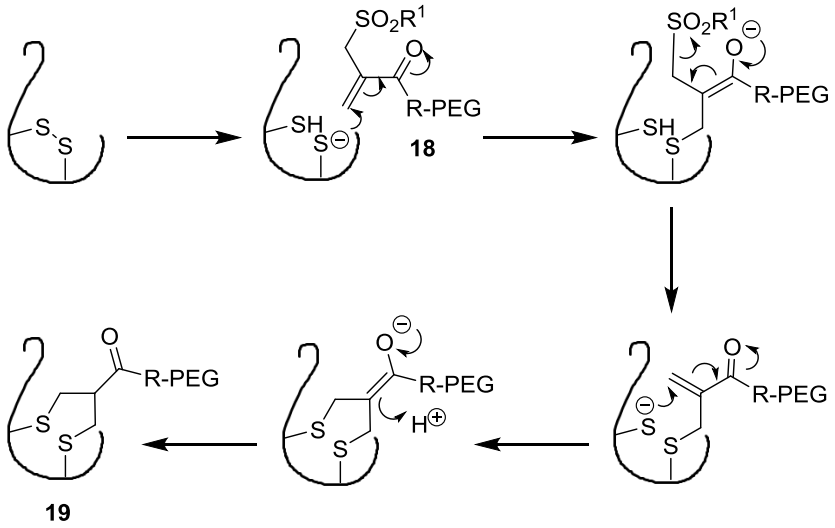

Scheme 1.10: Disulfide modification using a PEG-linked monosulfone (**18**) to connect cysteines via a three-carbon bridge.

Brocchini *et al.* found that, through using these reagents, the fundamental tertiary structure of a peptide could be maintained, despite incorporation of an unnatural cysteine-cysteine linkage. They demonstrated this on a number of peptides, such as somatostatin, L-asparaginase, glutathione, interferon α-2b and an anti-CD4 antibody fragment. Only in the case of L-asparaginase was any reduction in biological activity observed, presumed to be as a result of the steric hindrance caused by the extended PEG component.[23,56]

Brocchini also commented on the use of mild reduction conditions to selectively target only the accessible disulfides in situations where multiple bridges are present. This helps to reduce the number of possible products obtained, making purification easier, as well as further reducing the chances of abolishing biological activity by modifying integral disulfides crucial to protein structure and function.[23,56]

Following this work, in 2010 Baker *et al.* realised the potential of dibromomaleimide, which was previously employed for single cysteine modification, in the selective targeting of disulfides. It was envisaged that dibromomaleimide could circumvent the undesireable formation of an additional chiral centre and would result in a sulfur-sulfur linkage formed with just two carbon atoms,[19] rather than the three reported above.

1.1.6 3,4-disubstituted Maleimides as Disulfide Modification Reagents

Research by Baker *et al.* progressed to examine the ability of dibromomaleimide **15** to modify a disulfide bond by addition of both cysteine thiolates upon its reduction. Somatostatin **20**, which is discussed in greater detail in Section 1.3, was employed as a suitable peptide model on which to test this. Native somatostatin is produced in the body to serve as a regulatory hormone in the pancreas and gastrointestinal tract, a neurotransmitter in the central nervous system and an inhibitor of hormone release at the pituitary.[57] Somatostatin is a cyclic peptide of 14 amino acids formed by proteolytic cleavage from a larger peptide precursor.[57] Most importantly, it contains a single, accessible disulfide bond. Somatostatin **20** was treated first with 1 equivalent of TCEP to reduce the disulfide, followed by 1.1 equivalents of dibromomaleimide **15** at pH 6.2. This resulted in complete conversion to the maleimide-bridged construct **21** (Scheme 1.11). Subsequent treatment with β-mercaptoethanol led to reversal back to the reduced peptide, confirming the reversibility of the modification.[19] These results were promising and presented dibromomaleimide as the first known reagent for selective and reversible disulfide bridging.

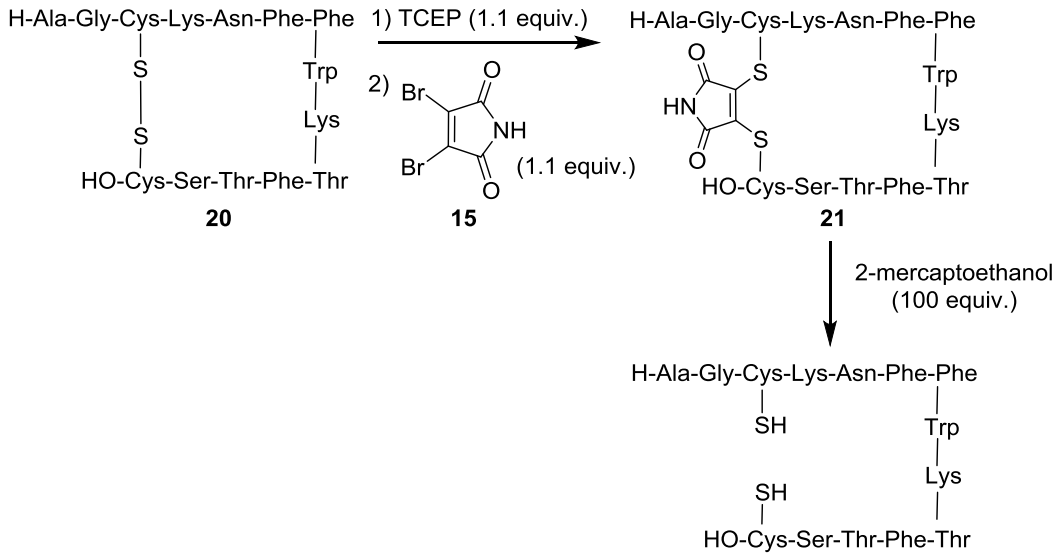

Scheme 1.11: Reversible disulfide bridging of somatostatin (**20**) by dibromomaleimide (**15**).

Following this, the prospect of using the maleimide nitrogen as a third point of attachment was investigated. *N*-fluorescein-dibromomaleimide was synthesised and reacted with somatostatin; the fluorescently labelled, bridged peptide was formed efficiently.[19] In addition, *N*-PEG dibromomaleimide has also been synthesised and used in the bridging of somatostatin. PEGylation is a common strategy employed to help improve water-solubility and *in vivo* half-life and to reduce potential antigenicity of a protein[12] - such a reagent could be invaluable in the site-specific PEGylation of therapeutic peptides and proteins.

Both reagents have shown comparable biological activity to native somatostatin.[24] These results give great promise for use of these maleimides in the field of bioconjugation.

Research in the Baker group later turned to overcoming one of the more restricting problems with dibromomaleimide and its derivatives - the significant time the reduced disulfide bond is left un-bridged before addition of the maleimide moiety. This is problematic as it can lead to protein unfolding and loss of tertiary structure or, if more than one accessible disulfide is present, scrambling of the disulfides, both potentially resulting in loss of protein function.[24,58] If, upon reduction of a protein's disulfide bonds, its tertiary structure is largely maintained, the proximity of the free thiolates increases the chances of correct cysteine connectivity upon re-bridging. However, if the

reduction process leads to a large disruption of the tertiary structure and the free thiols move too far apart, then the propensity to form the correct cysteine pairs is greatly reduced.

To overcome this, the ideal protocol would be an *in-situ* approach, where a reducing agent and a bridging reagent could be present at the same time to facilitate rapid bridging upon reduction. Attempts to achieve this with dibromomaleimide failed as it was found to have substantial reactivity towards TCEP, the commonly used reducing agent, and therefore was not suitable for *in-situ* use.[24] Instead, dithiomalemides were presented as an alternative reagent that might be more resistant to attack by the reducing agent. Comparison *in-situ* reactions of somatostatin **20** with dibromomaleimide and dithiophenolmaleimide **22** were conducted. While dibromomaleimide appeared to be attacked by TCEP leading to incomplete somatostatin bridging, the use of dithiophenolmaleimide **22** led to quantitative conversion to the bridged peptide **21** within 20 minutes (Scheme 1.12).[24] These findings presented dithiophenolmaleimide as the first known disulfide bridging reagent for effective use in an *in-situ* protocol.[24]

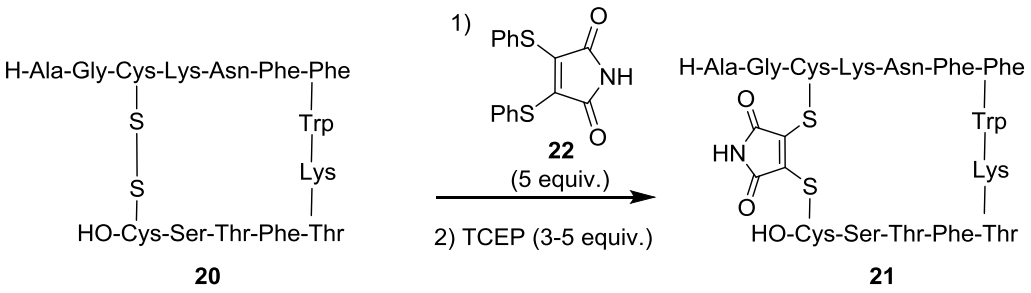

Scheme 1.12: The *in-situ* protocol with TCEP for disulfide bridging of somatostatin.

TCEP cross reactivity promoted a screen of other potential reducing agents suitable for use in an *in-situ* protocol. While DTT and mercaptoethanol were incompatible due to their thiol-based nature causing them to react with the maleimides themselves, benzeneselenol proved efficient when used in conjunction with dithiophenolmaleimide. Control reactions revealed that the released thiophenol serves as a reducing agent itself, achieving efficient disulfide cleavage in the presence of benzeneselenol.[15]

1.1.7 Towards Novel Bioconjugates by Disulfide Bridging

The scope of the *in-situ* protocol using 3,4-disubstituted maleimides for disulfide modification continues to be investigated. Most recently, its application to the modification of the disulfide bonds of antibodies and antibody fragments has been optimised and published. In this work, a disulfide-stabilised single chain variable fragment (sscFv) was employed, namely shMFE **23**, which displays carcinoembryonic antigen (CEA) specificity. Pre-incubation of shMFE with as little as 2 equivalents of dithiophenolmaleimide-based bridging reagents before addition of 25 equivalents of the reducing agent benzeneselenol led to quantitative conversion to the functionalised antibody fragment **24** (Scheme 1.13).[59]

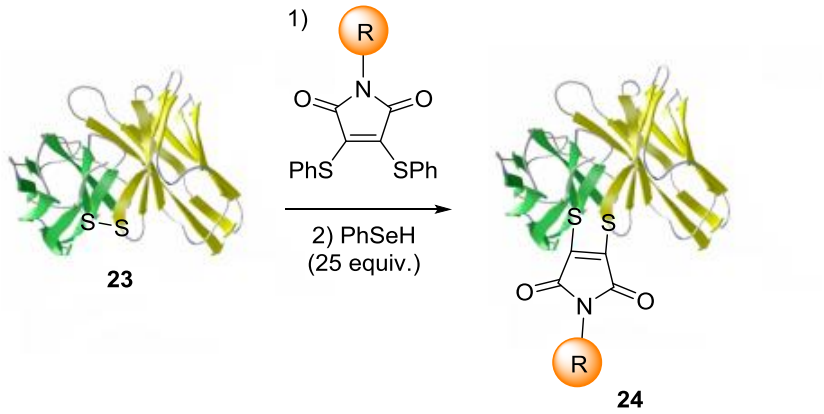

Scheme 1.13: In situ disulfide bridging of the disulfide bond of shMFE (**23**). R = PEG, fluorescein, biotin or spin label.

Remarkably, the binding affinity of the bridged sscFv fragments was not just retained but actually increased, as determined by ELISA. The observed increase in binding affinity is postulated to be as a result of the release of some of the strain associated with the incorporated disulfide bond, altering the geometry of the protein in such a way as to facilitate improved antigen binding.[59] Subsequent to these promising results, functionalization of the sscFv fragment was achieved by employing maleimides incorporating fluorescein, biotin, PEG and a nitroxide spin label. Pleasingly, rapid conversion to the desired products was observed in all cases, with yields of homogenous product of between 80-90%. All analogues produced exhibited the same improved binding as observed previously. Subjecting the functionalised derivatives to reducing agents or intracellular concentrations of glutathione led to the regeneration of the unmodified sscFv **23** through cleavage of the maleimide bridge.[59] This highlights the possibility of selective and controlled intracellular delivery using such functionalised antibody fragments.

Following this success, work has focused on the production of antibody-drug conjugates (ADCs) using this chemistry. This is a rapidly expanding area owing to the great demand for targeted delivery of cytotoxic drugs to cancerous cells in order to minimise undesirable side effects common to current cancer therapeutics. Minimising side effects will undoubtedly lead to improved patient tolerability and compliance.[60] Preliminary work utilising this chemistry in this area, published by Castañeda *et al.*, involved the synthesis of a dithiophenolmaleimide derivative linked to a cytotoxic drug; doxorubicin was chosen as the first anticancer warhead of choice. Synthesis of the functionalised maleimide **25** (Figure 1.4) was straightforward and produced excellent overall yields.[61]

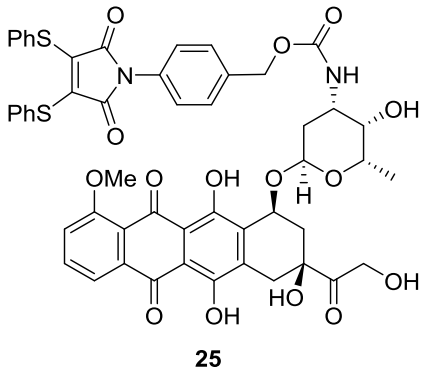

Figure 1.4: N-doxorubicin dithiophenolmaleimide (**25**).

Conjugation of this reagent was tested on the antigen binding fragment (Fab) of the monoclonal IgG1 antibody trastuzumab (marketed as Herceptin™) as this fragment has one inter-chain disulfide bond and is known to internalise upon binding to its target, the HER2/neu receptor. In this case, the disulfide bond of the Fab fragment **26** was first reduced with 3 equivalents of TCEP for 1 hour before addition of 5 equivalents of the doxorubicin-linked maleimide **25** to produce the desired conjugate **27** in near-quantitative yields within 1 hour (Scheme 1.14).[61]

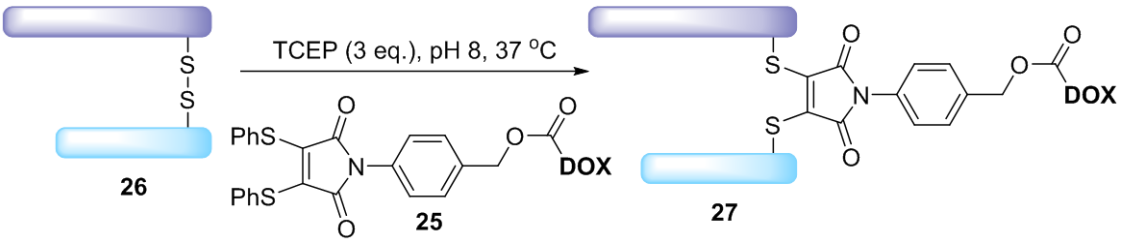

Scheme 1.14: Disulfide bridging of the trastuzumab Fab fragment using *N*-doxorubicin dithiophenolmaleimide.

ELISA analysis suggested no loss of binding affinity when comparing native trastuzumab-Fab **26** to that functionalised by maleimide **25**. In addition, incubation of the Fab conjugate **27** in lysosome-mimicking conditions (37 °C, pH 4.5) led to continued release of the cytotoxic cargo over time.[61] This demonstrates the potential of such conjugates in the targeted delivery and controlled release of anti-cancer drugs which could make a valuable contribution to the expanding field of ADCs.

Another area in which disulfide bridging using functionalised maleimides has been used effectively is in the improvement of the pharmacodynamic properties of therapeutic proteins. Palanki *et al.* recently published their work on their progress towards formulating a long acting growth hormone receptor agonist.[62] In order to treat the effects of growth hormone deficiency, recombinant growth hormone is administered daily to patients *via* subcutaneous injection; this is as a result of its short serum half-life (20-30 minutes). A stabilised derivative which could be administered weekly is highly sought after. Palanki *et al.* developed a conjugate of human growth hormone connected, *via* the disulfide bridging linker **28**, to an aldolase carrier antibody. In this way, the antibody serves to improve the pharmacokinetics and biodistribution of the growth hormone in order to increase its circulatory lifetime. Linker **28** consists of the dithiophenolmaleimide moiety at one end, for insertion into the disulfide bonds of growth hormone, and an electrophile at the other end, designed to react selectively with a free lysine on the aldolase antibody (Figure 1.5).[62]

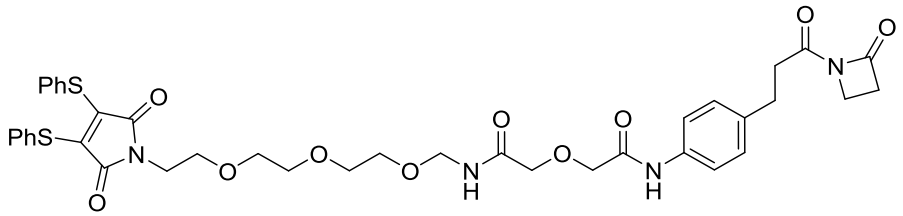

28

Figure 1.5: The linker used in the work by Palanki *et al.*[62]

The group successfully managed to isolate their desired conjugate in around 30% yield. Interestingly, despite the presence of two disulfide bonds in human growth hormone, they found they achieved 95% selectivity for one disulfide over the other.[62] With subsequent analysis of their conjugate, they found that conjugation of the protein by disulfide bridging had lowered its affinity for the growth hormone receptor. Its cellular

response is still elicited to a certain extent, but a lesser amount is internalised and, thus, satisfactory circulatory levels of growth hormone are maintained for longer. In addition, conjugation of growth hormone to the aldolase antibody gives protection from proteolysis, further improving the half-life of the protein. Animal studies have given promising evidence to suggest that, after administration of the conjugate, weight stabilisation is achieved for at least five days.[62] Pre-clinical studies continue on this promising therapeutic candidate.

1.1.8 Fine Tuning the Maleimide Reagents

Tuning the groups attached to the maleimide is also proving to be a powerful method for controlling the reactivity and utility of the reagent. It was recently reported by Marculescu *et al.* that substituting the thiophenol moieties for phenol leads to a bridging reagent with attenuated reactivity, postulated to aid selectivity in some bioconjugations.[63] In addition, the phenoxymaleimides were found to efficiently install a succinimide bridge within the disulfide bond of somatostatin; a result not possible with the more reactive mono-substituted maleimides such as bromomaleimide **8**. Addition of 1.5 equivalents of phenoxymaleimide **29** to reduced somatostatin led to complete conversion to the succinimide bridged peptide **30** (Scheme 1.15) in 1 hour.[63]

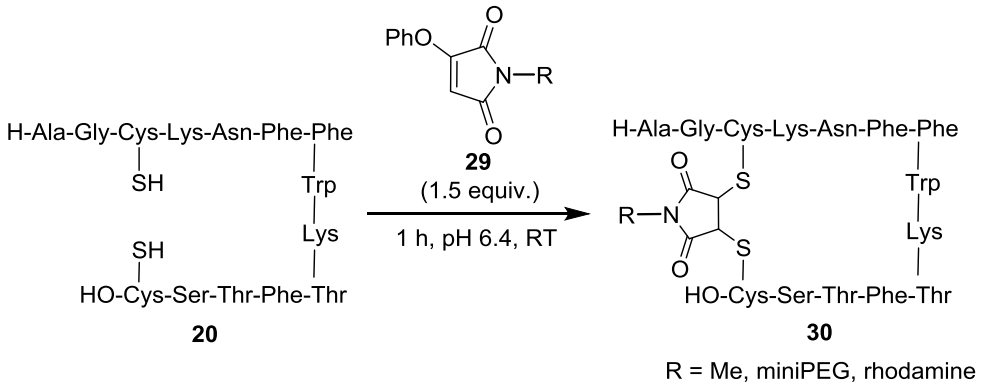

Scheme 1.15: The succinmide bridging of somatostatin (**20**) using phenoxymaleimide (**29**).

Such succinimide bridges were expected to have differing reactivity towards thiols in comparison to their maleimide equivalent. In fact, thiol reactivity of the succinimide bridge was found to be dependent upon the system in which it was employed; a succinimide bridged ds-scFv showed complete resistance towards thiol cleavage, whereas succinimide bridged somatostatin **30** was fully cleavable.[63] This differential stability is reasoned to be as a result of the local environment of the disulfide. The succinimide bridge presents itself as a novel disulfide bridging reagent with properties

distinct from that of the maleimide bridge. It has already demonstrated its applicability in the dual labelling of a peptide in an efficient one-pot procedure.[63]

Another method of tailoring the maleimides is by the means of attachment of moieties to the maleimide nitrogen. Although the reversible modification of peptides and proteins is both novel and invaluable, there are undoubtedly circumstances in which a permanent modification is desired. Recently, bromomaleimides have been synthesised whose stability can be controlled by a simple hydrolysis procedure.[64] In this way, protein bioconjugates can be designed to be either stable or cleavable in the presence of excess thiol. It was found that an *N*-linked aromatic moiety on the maleimide (Scheme 1.16) led to reagents that hydrolyse rapidly at pH 8; the resulting maleamic acid **32** being no longer cleavable by excess thiol.[64] Incorporating such reagents into proteins produces conjugates in which the stability can be tempered to achieve reversible or irreversible modification as desired. This could prove useful in the synthesis of labelled proteins, where reversibility may be a hindrance.

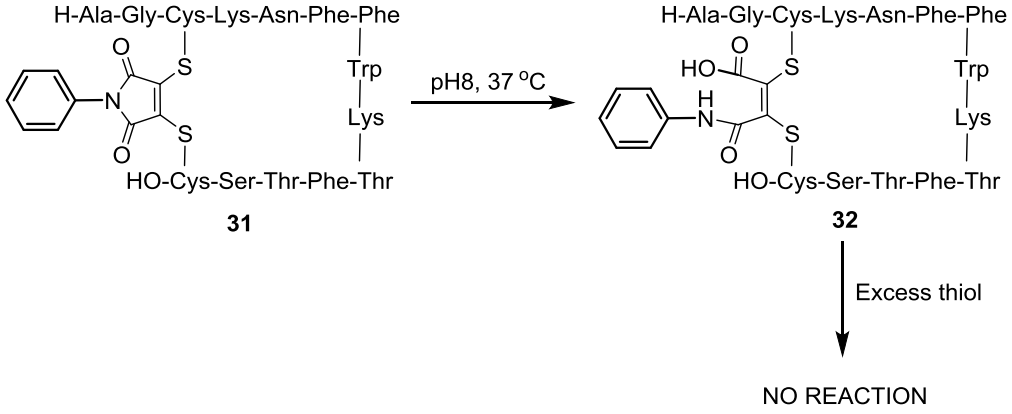

Scheme 1.16: From reversible to irreversible modification using *N*-phenylbromomaleimide in the modification of somatostatin.

1.1.9 Summary

In summary, the potential of protein and peptide modification for various applications has been described and the current methods for modification introduced. Modification of native, accessible disulfide bonds by re-bridging presents itself as a new and efficient method for selective and controlled functionalisation. With the advent of *in-situ* modification protocols, retention of tertiary structure and biological activity is possible. Careful design of the modification reagent and protocol employed has proven to

facilitate broad application of this chemistry. The project herein continues to evaluate the scope of this chemical modification strategy. The peptides to be investigated in this project will now be introduced.

1.2 Tertiapin Q & its Applications

1.2.1 Introduction to Toxins

A toxin is a poisonous substance produced by the natural metabolic activity of a number of living organisms.[65] They have evolved in plants, animals and microbes as a means of catching prey and as a self defence mechanism.[66] Toxins are usually small peptides, of between 8 and 70 amino acids, with a very compact structure and are usually associated with the ill-effects that occur as a result of absorption and accumulation into body tissues, owing to their significant toxicity. Peptide toxins are usually found in animal venom, and by association with specialised envenomation apparatus, they are delivered into the soft tissue via intravenous or subcutaneous routes[66]. Evolution had helped fine-tune these peptides to elicit great stability, potency and target selectivity.

It has long been realised that a substance is only poisonous at a specific dose, a threshold dose, and above this almost any substance could be classified as "poisonous"[67] It is with this knowledge that poisons and toxins began to establish themselves as valuable therapeutic and analytical tools. Studies in toxicology have facilitated the determination of the level at which the toxin becomes poisonous and elicits its undesirable effects and, as a result, much research has been focused on exploitation of these substances at low doses for beneficial applications.

Ion channels are a common target for many plant and animal toxins and play a fundamental role in cellular signalling within the body; modification or disruption of this can have dramatic effects. Furthermore, studies have shown toxins to be highly selective for their particular channel target, to have low immunogenicity, little accumulation in organs and high chemical and thermal stability.[68] Combined, these factors make toxins very promising candidates for channel-targeting therapeutics for a range of human diseases and disorders. The pharmaceutical industry has increasingly begun to employ toxin mimetics as therapeutics for cancer,[69] pain,[70] epilepsy[71] and both neurological and cardiovascular disorders[66,72]; a variety of these are currently in clinical trials.

In addition to drug discovery, a second invaluable application of such toxins is the characterisation of the channels and receptors to which they are targeted.[68] They have

proven highly effective as pharmacological probes to help elucidate the structure and consequent function of various ion channels. An example is the characterisation of the nicotinic acetylcholine receptor where initially the peptide neurotoxin α-bungarotoxin, from a Taiwanese banded krait, to which it selectively binds, was used to isolate the receptor in an affinity chromatography assay.[73] Following this a second toxin, α-conotoxin, derived from the *Conus* family, was employed to characterise the receptor.[74]

1.2.2 Tertiapin and Its Structure and Function

Tertiapin is a twenty one amino acid neurotoxin derived from the venom of the honey bee. It was isolated over thirty years ago when it was believed that bee venom contained substituents with anti-arthritic properties[75]. In the search for these substituents many small peptides, including tertiapin, were isolated and examined for their biological activity.[75] Since its isolation, a significant amount of work on the structure and biological activity has been undertaken. In 1993, Xu and Nelson published their work presenting the solution structure of the peptide determined by two-dimensional NMR and circular dichroism.[76] Superimposition of the data showed tertiapin to be a very rigid and compact molecule, owing to the strong interactions between amino acid side chains. Four cysteine residues form two disulfide bonds adding further to the stability of the molecule. Within the structure are an α-helix and a Type 1 reverse turn connected by a β strand (Figure 1.6).[76-78]

Figure 1.6: Three-dimensional solution structure of tertiapin determined by NMR. Disulfide bonds (cys3-cys14 and cys5-cys18) shown (PDB code: 1TER).[78]

In the elucidation of the biological role of the small peptides isolated from the bee venom, tertiapin was found to selectively inhibit a particular class of potassium (K^+) channel, namely the G protein-gated inwardly rectifying K^+ (GIRK) channel.[76,77,79] These channels are activated by muscarinic M_2, α_2 adrenergic, D_2 dopaminergic,

histamine, adenosine A_1, $GABA_B$ and somatostatin receptors.[80] Upon neurotransmitter release, these receptors are activated, leading to the dissociation of the $G_{\beta\delta}$ subunit of a G-protein from the G_α subunit. It is the binding of this $G_{\beta\delta}$ to the *C*- and *N*- termini of the GIRK channel which directly activates it.[80,81] To date, four different GIRK subunits have been identified, GIRK1-4, and these are found as dimers differentially distributed within the body. GIRK1 is found almost invariably in all GIRK-expressing tissues whilst GIRK2 is widely expressed in neurons and GIRK4 found mainly in the cardiac tissue.[82] The name 'inward rectifier' comes from the propensity of the GIRK channels to allow movement of a large flux of K^+ ions in the inwards direction, and only a comparatively small amount in the outwards direction. The mechanism for selective current flow direction in GIRK channels was for a long time unknown. There is now significant evidence to suggest that it is the blocking of the channel from the intracellular side by Mg^{2+} ions and polyamines which prevent outward K^+ flow.[83,84]

GIRK1/2 channels (a channel made up of both GIRK1 and GIRK2 subunits) play an important role in regulating action potential firing in the central nervous system. They allow movement of a small amount of K^+ in the outwards direction in order to maintain a hyperpolarized state and consequently decreased neuronal excitability.[85] The crucial role of the GIRK channels has been demonstrated by experiments on weaver mice which carry a mutation in the pore region of the GIRK2 subunit. The mutation has been proven to cause decreased K^+ selectivity and loss of channel function, leading to seizures and neuronal cell death.[86,87] In the heart, GIRK1/4 channels are activated by acetylcholine in response to vagus nerve stimulation. Here, the small outward K^+ current through the GIRK channels serves to slow the heart rate by elongating the refractory period of cardiomyocytes.[88,89]

GIRK channel subunits have just two transmembrane domains (M1 and M2 in Figure 1.7) with a pore-forming loop between the two, as depicted in Figure 1.7. Four of these subunits assemble to form the complete channel.[90] In recent years, research has been carried out to further elucidate the structure and resultant function of the inward-rectifying channels. The role of particular residues of the pore-forming loop as an ion selectivity filter,[91] the mechanism by which the channel pore is opened for K^+ flux[92] and the secondary structure of the *N*- and *C*-terminal regions forming the cytoplasmic pore[93] have all been studied.

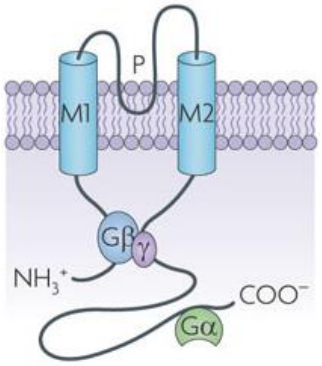

Figure 1.7: A GIRK subunit showing the two transmembrane segments (M1 and M2), the pore forming loop (P) and the interaction with G-protein.[94]

However, due to a lack of high-affinity ligands that selectively bound to GIRK channels, some areas of the pharmacology and the functioning of the channel remained relatively unknown. In 1998, Jin and Lu ran a screen of venoms from various sources for their inhibitory action against the channel and, once a successful candidate was found, isolated the component which was active.[75] Searching protein databases revealed this active component to have the same structure as tertiapin. Comparison studies between the isolated peptide and synthetic tertiapin led to complete confirmation that the isolated peptide was tertiapin. Tertiapin was found to inhibit the GIRK channel with an IC_{50}[i] of 8.5 nM.[79,95]

It was later found that one of the methionine residues in tertiapin, number 13 (Figure 1.8), is readily oxidised by air and that this greatly hinders the peptide's ability to bind to the channel.

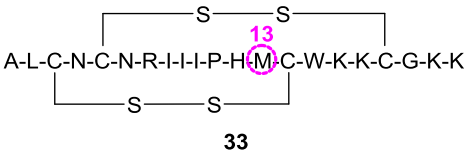

33

Figure 1.8: Tertiapin (**33**), amino acid chain representation (methionine 13 highlighted).

In 1999, Jin *et al.* aimed to overcome this problem by making mutants of the peptide; replacing the methionine residue, one at a time, with fourteen other amino acids before testing their activity and affinity for the channel (Table 1.2).[79]

[i] The IC_{50} of a substance is defined as the half-maximum inhibitory concentration.

Table 1.2: The K_i[ii] values for wild type tertiapin **33** and fourteen mutants.[79]

Species	*Mean K_i (nM)*	*Standard Error of the Mean*	*Number of Experiments*
wt	2.04	0.02	50
M13A	19.31	2.51	4
M13D	21.54	1.82	4
M13E	299.63	17.65	4
M13F	33.74	1.98	3
M13G	96.81	6.32	4
M13I	7.21	0.45	8
M13L	16.23	1.91	4
M13N	40.41	3.04	4
M13Q	**1.25**	**0.01**	**50**
M13S	38.93	4.25	4
M13T	21.41	2.06	4
M13V	12.54	1.08	4
M13W	40.14	2.34	3
M13Y	27.12	1.65	3

From this screen, it was found that replacing methionine with glutamine produced a variant that had specificity and affinity comparable to that of wild type tertiapin but was not susceptible to spontaneous oxidation in air. This variant, named tertiapin Q, presented itself as an effective new pharmacological probe.

Work on tertiapin and tertiapin Q progressed to determine how they elicit their inhibitory action. Experiments, again by Jin *et al.*, included an alanine scan whereby each residue (except for the four cysteines involved in disulfide bonding) of the peptide was mutated, in turn, to alanine and the activity of the mutant tested. It was found that mutating histidine 12, lysine 17 or lysine 20 resulted in a much greater IC_{50} value.[77] It was hypothesised that these residues were integral to channel binding. Based on the fact that residues 12-19 make up the α-helix of the peptide's secondary structure, this

[ii] The K_i of a substance is the inhibition constant and is the concentration required to occupy 50% of the target channel or receptor.

evidence strongly suggests that this region was primarily responsible for the interaction with the channel surface. Mutagenesis studies on the channel itself showed residues in the channel pore to be involved in the channel-toxin interaction. From a combination of these, a hypothesis arose whereby the toxin blocks the channel by insertion of its α-helix into the pore, leaving the remainder protruding into the extracellular environment.[77]

It was recently found that tertiapin Q is not completely selective for GIRK channels and that it also has an inhibitory effect on voltage-dependent Ca^{2+} activated large conductance K^+ (BK) channels.[96] Studies by Khanjan *et al.* show that the inhibition characteristics vary between GIRK and BK channels; inhibition of BK channels by tertiapin has proven to be much slower, voltage dependent and has a lower IC_{50} of 5.8 ± 1.0 nM.[96]

1.2.3 Application of Tertiapin Q

There is increasing demand for high affinity probes to elucidate the pharmacology of different ion channels. Tertiapin Q has already been presented as a good candidate and has been put to use as an analytical tool for studying GIRK channels. For example, a tertiapin Q derivative radiolabelled with ^{125}I was synthesised by Felix *et al.*[97] They decided to attach the label at the N-terminus as this is known not to be involved in the interaction with the GIRK channel. They found their derivative to be of very similar potency to tertiapin Q and suggest its use in quantifying cell surface channel expression.[97] Whilst a novel product resulted, its synthetic route had its drawbacks. Site-directed mutagenesis was required to incorporate a tyrosine residue as native tertiapin Q lacks these. Tyrosine was chosen as its reactivity enables further functionality, covalent attachment of ^{125}I in this case. Additionally, the conversion to the iodinated product was not quantitative, with both the native peptide and the di-iodinated peptide also formed meaning subsequent purification by HPLC was required.[97] No further attempts at functionalising tertiapin Q appear to have been reported.

In addition to pharmacological probes, tertiapin Q, like many other toxin peptides, has been proposed as a potential therapeutic due to its notably high channel selectivity. Recent studies have proposed that targeting GIRK channels could be an effective way of treating atrial fibrillation, a common cardiac arrhythmia.[98] Constitutively active GIRK1/4 channels in the heart have been observed and have shown to sustain the

arrhythmia and, therefore, controlled inhibition of the GIRK channels has been proposed at a therapeutic possibility. Tertiapin Q has good inhibitory potential, and selectively inhibits GIRK1/4 channels of cardiac tissue at low nanomolar concentrations.[99] Experiments have demonstrated that tertiapin Q can efficiently terminate vagus nerve-induced atrial fibrillation in canines[99,100] and reduce GIRK1/4 current in the atrial myocytes from patients with chronic atrial fibrillation.[98]

Despite promising results, tertiapin Q has unwanted pharmacological characteristics, such as immunogenicity and short serum half-life, which could prevent its use as a therapeutic.[4,5] It is these factors which have previously led to a shortage of peptide-based therapeutics, regardless of their advantages over small molecule drugs. Increasing realisation of the advantages of utilising peptides, such as their ease of synthesis and high target specificity and affinity, has gone hand-in-hand with advances in chemical synthesis techniques and methods to overcome poor physiochemical properties.[5] As a result, prospects for peptide-based therapeutics have begun to, and look set to continue to, improve.

1.2.4 Summary

In summary, tertiapin Q presents itself as an ideal candidate for bioconjugation. Its nanomolar affinity for its target makes it ideal for use as a probe to study the pharmacology of the GIRK channel family; incorporation of a visualisation agent could greatly advance research in this area. In addition, the inhibitory activity of tertiapin Q could be exploited for the treatment of atrial fibrillation provided the discussed limitations can be overcome. Despite this potential, progress in this area is minimal and not widely reported on in the literature.

1.3 Somatostatin, its Analogues & their Applications

1.3.1 Somatostatin and Its Structure and Function

Somatostatin is a natural cyclic peptide hormone originally discovered and isolated from the bovine hypothalamus. There are two natural forms, somatostatin-14 (Figure 1.9, **20**) (sst-14) and somatostatin-28 (sst-28); sst-28 consists of the same 14 amino acids as sst-14, but with an extra 14 amino acids extending from its *N*-terminus. Although there is some evidence to suggest that sst-28 is a precursor to sst-14, it is also known to act as a hormone in its own right, with very similar pharmacological actions to sst-14.[101] The two forms of somatostatin are commonly expressed in both the central nervous system (CNS), where it acts as a neurotransmitter, and in the gastrointestinal tract, acting as an inhibitor of growth hormone, glucagon, insulin and gastrin release.[102]

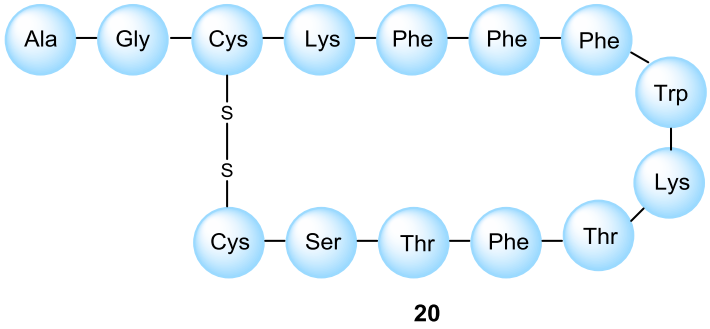

20

Figure 1.9: Amino acid sequence of somatostatin-14 (**20**).

Somatostatin targets the somatostatin receptor which has been located in the CNS, the gastrointestinal tract and in many cells of neuroendocrine function. Recently, five human receptor subtypes have been cloned and identified (sst1-5) with largely variable, tissue-dependant expression suggesting significant diversity in the function of the receptor in each tissue type.[103] The somatostatin receptors form a distinct subset of the G-protein coupled receptor (GPCR) superfamily; they comprise the characteristic seven-helix membrane-spanning structure, where the extracellular domain binds the associated ligand and the intracellular domains are responsible for signal transduction inside the cell.[103] All 5 receptor subtypes bind the two natural forms of somatostatin and do so with low nanomolar affinity. In addition, the subtypes share common intracellular signalling pathways upon activation by somatostatin, namely the activation of phosphotyrosine phosphatase (PTP), inhibition of adenylyl cyclase, activation of K^+/Ca^{2+} channels and the modulation of mitogen-activated protein kinase (MAPK). It is

these pathways that mediate the subsequent inhibitory effects on hormone release and cell growth, which are the effects characteristically associated with somatostatin.[103,104]

It is well accepted that the binding of somatostatin to its receptors is predominantly through amino acid residues 7-10; these residues together comprise the hormone pharmacophore. Only very minor modifications can be made to these residues without incurring a huge loss in biological activity – threonine can be exchanged for valine and tryptophan exchanged for its enantiomer with little effect, but lysine must always be conserved.[105,106] There is a disulfide bond between the two cysteine residues of somatostatin (3 & 14) which, like with most cyclic peptides, is fundamental to the structural integrity, rigidity and function of the hormone. The two phenylalanines (6 and 11) neighbouring the pharmacophore have been shown exhibit a stabilising effect on the peptide structure, potentially by means of a non-covalent aromatic interaction of the amino acid side chains, but do not directly interact with the receptor.[105]

Somatostatin receptors are known to be over-expressed in various pathologies, perhaps most importantly in cancers; ovarian, kidney, breast, thyroid and neuroendocrine tumours are a few examples. As a consequence of this, there is great interest in exploiting this differential receptor expression and the pharmacological action of somatostatin for clinical applications.[104] The ability of somatostatin to control the release of active peptide hormones that are being over-produced by these receptor-bearing tumours makes somatostatin an ideal candidate as an anti-proliferative therapeutic. However, the short *in vivo* half-life (2-3 minutes in plasma) due to rapid enzymatic degradation, along with the relatively low selectivity of the peptide for one of the five receptor subtypes, are considerable drawbacks making somatostatin itself not ideal for use in the clinic.[101,102]

1.3.2 Somatostatin Analogues

Efforts to circumvent these drawbacks through the synthesis of analogues with improved pharmacokinetic properties have been ongoing since the 1980's. Importantly it was discovered that, by exchanging L-tryptophan for the D- enantiomer, the half-life of the peptide could be significantly improved. This is believed to be because of the more favourable interaction between the indole ring of D-tryptophan with the side chain of the neighbouring lysine residue; when in the D- configuration, tryptophan is more

able to shield the aliphatic chain of lysine. It was found that exchanging these enantiomers led to minimal alteration to the overall conformation and architecture of the peptide, but rather served to increase structural stability by stabilising the hair-pin turn motif.[105] In addition, D-amino acids are known to confer greater resistance towards proteases, further adding to prolonged *in vivo* half-life.[101,105] In addition to this, shortening of the chain length of the peptide also had beneficial effects. Removal of amino acids from either side of the pharmacophore, with exception of the two cysteines required for maintenance of the disulfide bond, lead to derivatives with a smaller ring size and decreased flexibility.[105] This served to increase the potency and specificity of the peptide; native somatostatin has almost no specificity for any of the 5 receptor sub-types.[104,105] These significant improvements to the pharmacokinetic properties of the peptide made it a more attractive candidate for use in the clinic, and recently a few of these synthetic analogues have successfully made it onto the market for treatment of somatostatin receptor positive tumours. These are displayed in Table 1.3.

Table 1.3: The pharmacokinetic properties of somatostatin and its analogues (adapted from publication by Veber *et al*.).[106]

Name	*Size*	*Half-life*	*Target receptor*	*Administrative route*	*Development stage*
Somatostatin (20)	14/28 amino acids	~3 min	sst1-5	IV	-
Octreotide (34)	8 amino acids	2 h	Primarily sst2 (partially sst5)	IV, SC, IM	Approved & marketed
Lanreotide	8 amino acids	2 h	Primarily sst2 (partially sst5)	SC, IM	Approved & marketed
Pasireotide	6 amino acids	12 h	Primarily sst5 (partially sst1-3)	SC, IM	Approved & marketed

(IV: intravenous, SC: sub-cutaneous, IM: intramuscular)

Perhaps the most well-documented of all analogues to date is octreotide **34**; originally synthesised and reported by Wilfried Bauer in 1979 and today marketed by Novartis Pharmaceuticals under the brand name Sandostatin® (Figure 1.10).[107]

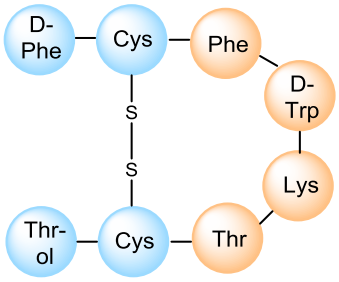

34

Figure 1.10: The amino acid sequence of octreotide (**34**) (Sandostatin®) with the pharmacophore depicted in orange.

Octreotide binds almost exclusively to sst2 and has shown to be 20 times more potent than native somatostatin.[104,107] It has been approved by the U.S. Food and Drug Administration (FDA) for the treatment of patients with various types of neuroendocrine tumours (NETs). NETs have been found to overexpress the sst2 receptor at high levels, making octreotide an ideally targeted therapeutic.[104] The bioavailability of octreotide is good, approximately 100% for a sub-cutaneous administration, and distribution of the peptide is rapid.[101] More recently, long-acting formulations of the peptide have been designed by incorporation of octreotide into micropsheres made from a biodegradable polymer. This variant, known as Sandostatin-LAR® (long-acting release), was shown to release low levels of octreotide for about 7 days after administration before slowly increasing its release rate over the subsequent week and maintaining its maximal concentration for 28-35 days.[104,108]

1.3.3 Somatostatin Analogues as Imaging Agents

1.3.3.1 Radiolabelled Derivatives

As well as being used as a therapeutic in its own right, octreotide has also been investigated as a targeting agent by conjugation of the peptide to another active biomolecule. One such example is the coupling of octreotide to a radioactive isotope to allow imaging and localisation of somatostatin receptor positive tumours. One of the first labelled variants synthesised was ^{123}I-labelled tyr$_3$-octreotide **35** by Krenning *et al.* in 1989 - here the phenylalanine residue at position 3 was substituted for a tyrosine; a structurally similar amino acid which would facilitate attachment of ^{123}I (Figure 1.11).[109]

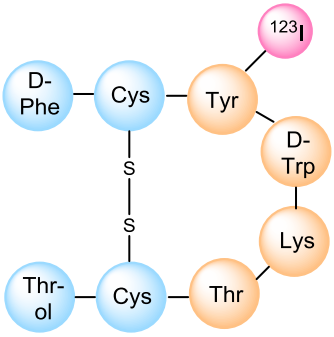

35

Figure 1.11: The structure of Oct-tyr-^{123}I (**35**).

Successful radioiodination allowed visualisation of receptor positive tumours *in vivo* with use of a gamma camera.[109] However, this imaging agent was found to suffer drawbacks such as poor bioavailability due to rapid clearance by the liver and relatively short radioactive half-life (~13 hours).[10,110]

The next generation of octreotide-based imaging agents designed to overcome these drawbacks comprised a chelating group attached at the peptide termini. The first and most well established example of this is ^{111}In-pentetreotide **36**, developed by Bakker *et al*., which has diethylene triamine penta-acetic acid (DTPA) conjugated to the *N*-terminus of octreotide. DTPA is a chelating group which allows radiolabelling by chelation with indium-111 (Figure 1.12).[111] ^{111}In-pentetreotide was found to be very effective in visualisation of a variety of somatostatin receptor positive tumours and was marketed as a radiopharmaceutical by Mallinckrodt Medical Inc. under the commercial name of OctreoScan®.

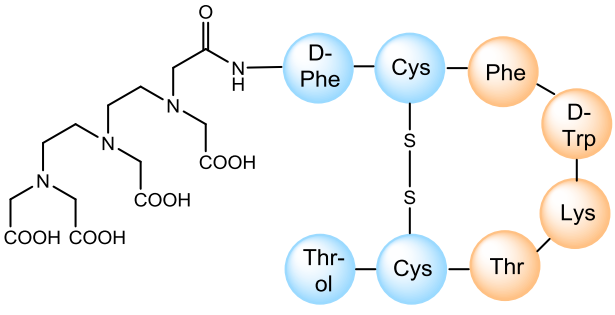

36

Figure 1.12: The structure of OctreoScan® (**36**).

In comparison to ^{123}I-octreotide, OctreoScan was found to have a significantly longer half-life of ~68 hours and to be cleared predominantly by the kidneys. These superior

kinetics and biodistribution profiles help reduce background interference and false positives from accumulation in normal healthy gut structures.[10,110] An average dose of 6.0 mCi of OctreoScan is given to a patient before whole-body imaging by scintigraphy is carried out to produce 2D images like those in Figure 1.13 below.

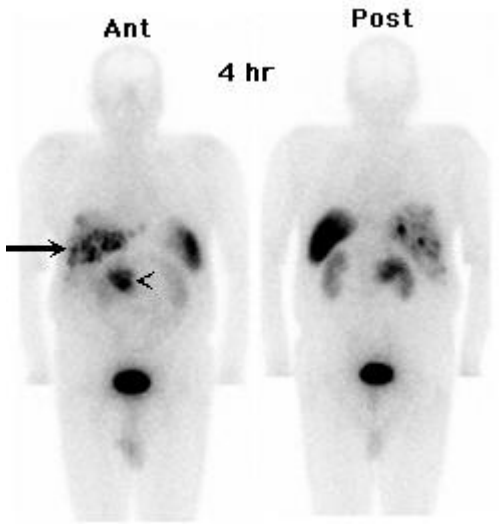

Figure 1.13: Scintigram obtained 4 h after injection with OctreoScan (**36**). Arrow shows tracer accumulation at the liver, while the arrow head shows accumulation in an area of the pancreas. (Normal tissue accumulation is also seen in the kidneys and bladder as a result of normal tracer clearance).[112]

This imaging is easily interpretable and allows the localisation and assessment of tumours – clinicians are then able to decide on subsequent treatment and whether somatostatin or octreotide therapy could prove effective.[110] The main limitation with this construct is that the DPTA chelating agent is restricted to the binding of gamma-emitting particles only, it has poor affinity for beta-emitting particles such as ^{60}Y and ^{186}Re; these are known as 'bone seekers' and, if not tightly bound by a chelator, will accumulate in the bone marrow and cause irreparable damage.[10]

To overcome this limitation, Heppelar *et al.* designed a new chelator comprising of 1,4,7,10-tetraazacyclododecane-1,4,7,10-tetraacetic acid (DOTA) which can bind a number of different radiometals. This was subsequently conjugated to octreotide to create DOTATOC **37** shown below in Figure 1.14.[113]

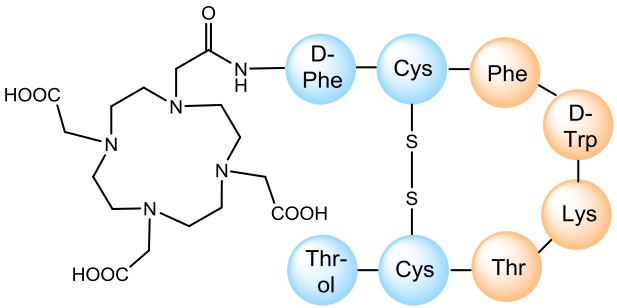

37

Figure 1.14: The structure of DOTATOC (**37**).

Careful choice of the radiometal added to DOTATOC produces constructs suitable for varying applications; ^{67}Ga and ^{111}In can be used for single photon emission tomography (SPET), ^{68}Ga and ^{86}Y for positron emission tomography (PET) and ^{90}Y, ^{68}Ga and ^{177}Lu for peptide receptor radionucleotide therapy (PRRT). Different radiometals have different physical properties, for example the emission products of their decay and the energy at which these are emitted. This in turn affects the degree of tissue penetration possible and, therefore, the therapeutic potential. ^{111}In emits gamma-radiation and Auger electrons; these are low energy and lead to minimal tissue penetration (0.02-10 μm) making ^{111}In-based constructs suitable for imaging but not for radiotherapy. Radiometals such as ^{90}Y, however, emit beta-radiation which is of much higher energy and hence facilitates much deeper tissue penetration (up to 12 mm).[114] Investigations into the use of ^{90}Y-DOTATOC as treatment for somatostatin receptor positive tumours gave promising results (tumour size stabilisation or regression in many cases).[113,115] This is owed, in part, to the 'cross-fire effect' which is pronounced when using radiometals with such high tissue penetration levels and is the term used to describe the elimination of cells that had not come into direct contact with the radiotherapeutic agent itself. This can, however, be a drawback if this cross-fire effect causes unwanted toxicity to neighbouring organs. ^{177}Lu emits intermediate-range beta-radiation resulting in a tissue penetration of around 2 mm, presenting this radiometal as an ideal choice for medium-sized or surrounded tumours.[114] The versatility of the DOTA chelating agent gives it great value as both an imaging agent and a radiotherapeutic and thorough consideration of the radiometal employed facilitates tailoring of the construct for each individual patient case.

A drawback to the discussed routes to radiolabelled octreotide derivatives is the synthetic strategy required to create them. Octreotide is routinely produced by means of

solid phase peptide synthesis, however the presence of a nucleophilic lysine residue within the pharmacophore of the peptide makes functionalization more challenging. In order to avoid attaching the chelating moiety to this lysine residue, which would undoubtedly be detrimental to the biological activity of the peptide, a protected lysine must instead be incorporated. Addition of the chelating group is then restricted to the *N*-terminal NH_2 group, but a subsequent deprotection step is then required to regain the natural lysine residue.[116] An example is shown in Scheme 1.17, showing the incorporation of DTPA onto the *N*-terminus of octreotide. The peptide is first treated with di-*tert*-butyl-dicarbonate ($(Boc)_2O$) to protect the inter-chain lysine residue before coupling of DTPA-dianhydride at the *N*-terminus selectively. This is then purified on silica gel to remove the unwanted doubly substituted DPTA derivative and un-reacted starting material before deprotection of the lysine residue using TFA. Finally, another purification step was added to obtain the desired homogenous product in a low yield of 10%, even before the final radiolabelling step.[111,116]

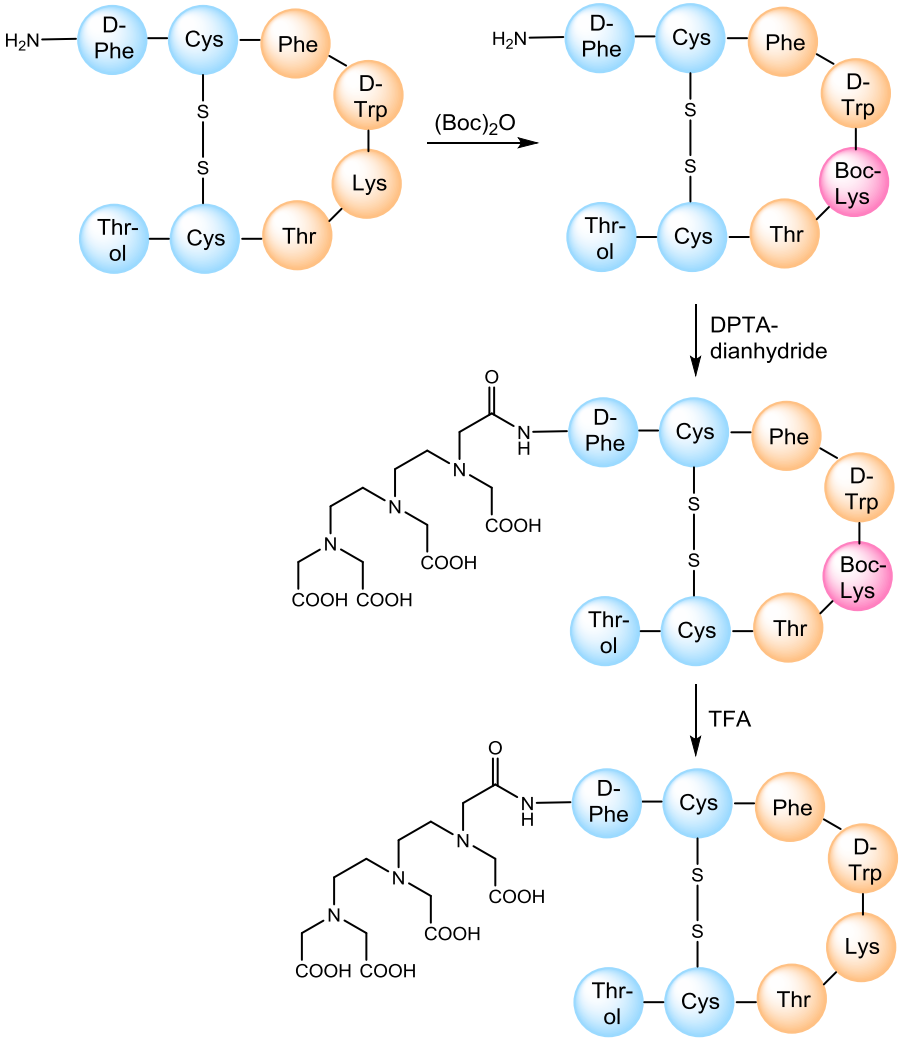

Scheme 1.17: The synthetic route to OctreoScan® (**36**).

1.3.3.2 Fluorescent Derivatives

Fluorescence detection presents itself as another attractive method by which to image tumours for early stage tumour diagnosis. The high sensitivity of this method means that femtimolar quantities of a near-infra red fluorescent dye can be detected with ease. In addition, it removes the need for the patient to be exposed to the ionising radiation present in radiometal imaging techniques.[117] Cyanine dyes have been widely investigated for use as a contrast agent in optical imaging; the first receptor targeting molecules employed with these dyes were monoclonal antibodies that bound to receptors known to be expressed on the surface of tumour cells.[118] Despite the high specificity of the antibody-receptor binding, the drawback with utilising antibodies as a targeting moiety is their significantly long *in vivo* half-life and high immunogenicity.

In 2001, Becker *et al.* reported the use of indocarbocyanine dyes linked to octreotide at the *N*-terminus forming the fluorescent conjugate **38** (Figure 1.15). Their synthetic strategy involved synthesising the octreotide chain with a Boc-protected inter-chain lysine and trityl-protected cysteine residues. With this in hand, the carboxylic acid-functionalised cyanine dye was coupled to the *N*- terminal amine of octreotide by means of a classic HBTU facilitated coupling. Following this, the protected residues were deprotected using TFA and the peptide cyclised by disulfide bond formation before finally being purified by HPLC.[119] Final yields were not reported.

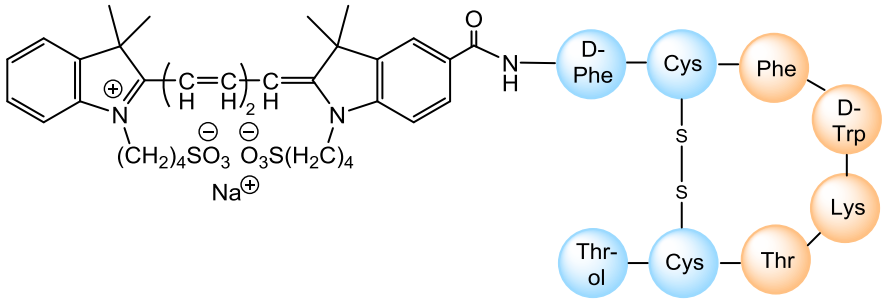

38

Figure 1.15: The structure of indodicarbocyanine dye-linked octreotide (**38**).

In this key publication, they effectively demonstrated that this conjugate displayed specific and long-lasting targeting of tumours whilst maintaining desirable pharmacokinetic properties.[117] The figure below shows the contrast between tumour and normal tissue in a mouse bearing a RIN38/SSTR2 tumour before and 6 hours after administration of the conjugate. Localisation of the tumour is very effective due to high

accumulation in the tissue over-expressing the somatostatin receptor. In addition, contrast enhancement was found to be rapid, with ~75% maximum contrast reached within 1 hour post injection. Interestingly, the group also investigated the effect of exchanging the two cysteines of octreotide with methionine – in this mutant, which resultantly lacks its disulfide bond, the binding and accumulation of the dye-linked conjugate was significantly reduced shown by the lack of contrast in panels B and D of Figure 1.16.[117]

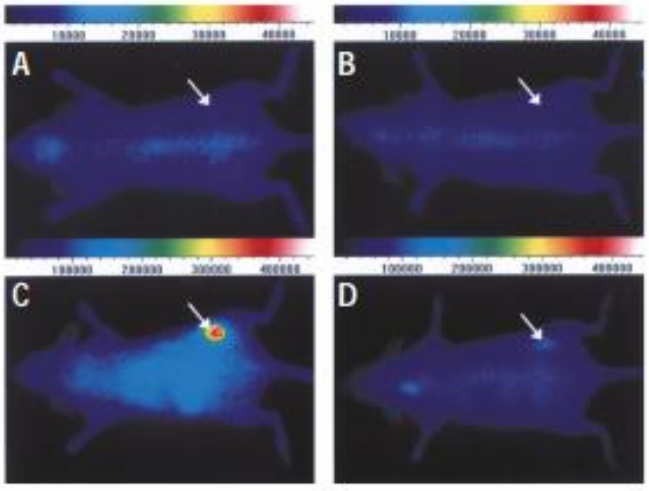

Figure 1.16: In vivo fluorescent images of RIN38/SSTR2 tumour bearing mice both before (panels A and B) and after 6 hours (panels C and D) administration of the conjugate **38**. Panels A and C show the effect of the conjugate using native octreotide, panels B and D show the effect of a double mutant of octreotide (C2M, C7M).[117]

This finding further demonstrates the crucial structural contribution of the disulfide bond, as discussed at the start of this chapter. Fluorescent octreotide **38** proved to be a highly selective and sensitive method for visualisation of tumours by optical imaging. One of the few drawbacks with this method, however, is the low penetration levels of near infra-red light in living tissue, limiting the use of such conjugates to superficial lesions, breast carcinomas or gastric cancers rather than tumours in deeper set organs.[117,120]

Octreotide has been linked to other fluorophores with similar success. Recently Fottner *et al.* synthesised a 5-carboxy-fluorescein linked octreotate derivative which they used with a miniaturised confocal laser scanning microscope, facilitating, for the first time, the morphological and functional imaging of somatostatin receptor positive tumours in real time. This allowed for instantaneous, high-resolution, hisopathological evaluation

of organs *in vivo*. This novel technique is envisaged to be of use in confocal endoscopy, facilitating intraoperative visualisation of tumours during surgery.[121]

1.3.3.3 Multimodal Derivatives

Employing two complimentary imaging techniques synergistically can allow for more accurate staging and localisation of tumours and is a concept that has started to be explored. Administering two separate imaging agents carries problems as both will have differing pharmacokinetic properties to consider and the toxic effects of each component may well be additive. To circumvent this, incorporation of multiple imaging agents into nanoparticles, micelles and liposomes has been investigated,[122,123] however, these carry their own drawbacks as such large molecules have inherently slow diffusion rates into the target tissue and rapid uptake by the liver. Most recently, efforts have been focused on incorporating the desired imaging agents into one, relatively small entity. Monomolecular multimodal imaging agents (MOMIAs) are single molecules consisting of two or more imaging agents in a 1:1 signalling ratio, both providing different but complimentary information.[124] Coupling optical imaging with a radionuclear method allows for the drawbacks of each individual method to be negated. Deep tissue tumours can be detected using a short-lived radioisotope without the depth limitations of optical imaging and subsequently, once the diseased region had been located, precise imaging of the tumour can be carried out by optical imaging outside of radioactivity exposed areas.[124,125] The challenge lies in incorporation of the two active molecules onto a targeting moiety, without disrupting the activity, efficiency or selectivity of any of the components.

In 2008, Edwards *et al*. reported on their octreotate derivative LS172 (**39**) which incorporates the DOTA chelating group at the *N*-terminus for binding of either ^{177}Lu or ^{64}Cu and the near-infrared fluorescent dye cypate conjugated at the *C*-terminus of the peptide.[125] Carefully controlled protection and deprotection steps throughout the solid phase synthesis procedure were required to form the desired product shown in Figure 1.17.

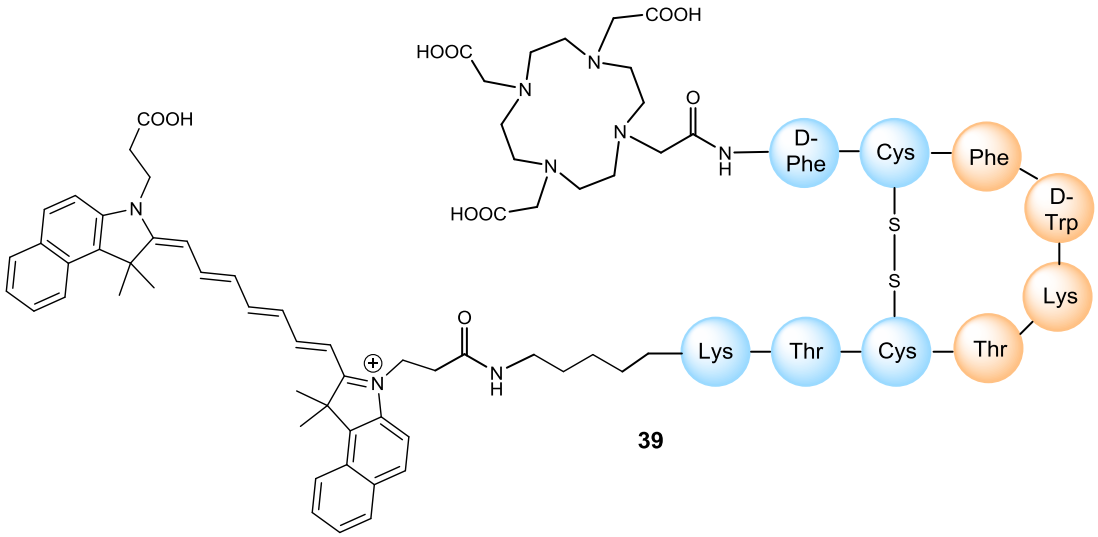

Figure 1.17: The LS172 MOMIA (**39**).

They found that binding of the radiometal to the chelator affected binding affinity of the conjugate, for example, binding of ^{64}Cu to DOTA reduced the affinity of LS172 by approximately 5-fold. Despite this, their experiments demonstrated excellent correlation in the biodistribution of the MOMIA with both optical and radionuclear imaging techniques and high binding affinity for the somatostatin receptor. A detrimental problem they encountered with LS172 was low tissue accumulation owing to poor receptor internalisation upon receptor binding.[125] Accumulation of the contrast agent is essential for precise tumour assessment and, as a result, this will hinder the potential use of LS172 as a MOMIA in the clinic.

1.3.4 Summary

In summary, radio- and fluorophore-labelled somatostatin derivatives are a valuable tool in the diagnosis and, in some cases, treatment of somatostatin receptor positive tumours. Despite their usefulness, synthetic routes to these conjugates are indirect and hence often low yielding.

Research into utilising octreotide as a targeting moiety for a MOMIA continues. Efficient and straightforward routes to enable the incorporation of the imaging moieties onto the peptide are required for the concept to progress.

1.4 An Introduction to the Patch Clamp Technique

1.4.1 General Introduction

The plasma membrane of a cell is a semi-permeable barrier, less than 10 nm in thickness, which separates the cytoplasm and intracellular organelles from the extracellular environment. This membrane is predominantly formed of a phospholipid bilayer within which proteins are embedded; these proteins are fundamental for cell recognition and the transport of chemicals and ions, both into and out of the cell.[126] Knowledge on this system is vast and well-documented but not within the scope of this introduction.

The aforementioned proteins responsible for ion transport are channels that span the entire plasma membrane to allow effective transport of ions from one side to another. These channels show ion-type selectivity and are gated by either changes in pH, ligands, mechanical stress or by changes in electrical potential.[126] Through precise regulation of ion transport, these channels are responsible for an extensive array of physiological processes, from control of hormone secretion to maintaining the heart beat. As a result of this, extensive research continues to be conducted into understanding the properties and functions of the various channel families and the pharmacological treatment of diseases associated with them.

1.4.2 Studying Ion Channels Using the Patch Clamp Technique

Patch clamp is a very powerful, high-resolution technique used to measure ionic currents across a cell membrane. It was originally developed by Erwin Neher and Bert Sakmann who demonstrated how the technique could be used to measure incredibly small electrical currents passing through a single ion channel in a patch of frog skeletal muscle[127,128]; for this work, and for pioneering the patch clamp method, they were awarded the Nobel Prize in Physiology and Medicine in 1991.[129]

The original method by Neher and Sakmann describes gently pressing the blunt tip of a heat polished micropipette onto the surface of a single cell, as depicted in Figure 1.18. The small (0.5-2 μm) tip diameter, when in contact with the plasma membrane, creates a megaohm (MΩ) seal allowing isolation of a tiny patch of membrane; this can contain as little as one single ion channel. It is through this that the electronic recordings were

then made.[129] Since its original development, the patch clamp technique has been greatly refined and is responsible for a wealth of information on the biophysics of ion channels and the cell membrane. A seminal discovery leading to significant improvement of the accuracy of recordings was that gentle suction, or negative pressure, applied to the pipette could create a seal in the gigaohm (GΩ) range – this led to reduced ion leak.[130]

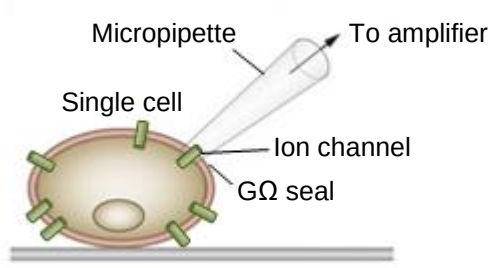

Figure 1.18: The basic patch clamp technique.[131]

Formation of this high-resistance seal leads to complete electric isolation of the patch of membrane beneath the pipette tip; this ensures that any ions that flow through this patch of membrane will enter the pipette and be recorded.[132] The pipette is filled with a solution of desired ionic composition allowing the extracellular environment to be completely controlled by the operator. Recording in this fashion is known as the 'cell-attached' configuration and is the most non-invasive of all patch clamp methods, with the cell remaining attached throughout the experiment.[131,132] With this method, single channels can be isolated, as depicted in Figure 1.19, but the intracellular environment cannot be controlled.

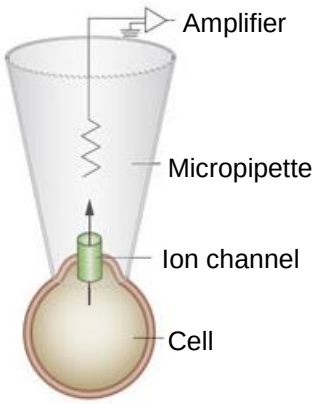

Figure 1.19: The 'cell-attached' patch clamp mode.[131]

If, subsequent to seal formation, the negative pressure is significantly increased, the patch of membrane under the pipette can rupture and access to the intracellular region is gained. Upon membrane rupture, the solution and the electrode within the pipette come into contact with the cell cytoplasm. The volume of the cell is negligible relative to the volume of the micropipette and so the intracellular composition is said to be that of the pipette solution and, thus, is completely controlled by the operator.[132] In this way, both the intra- and extracellular environments can be controlled by tailoring of the pipette solution and bath solution respectively. This method is known as the 'whole-cell' configuration and allows for recordings from all ion channels within the cell membrane as depicted in Figure 1.20.[78,131,132]

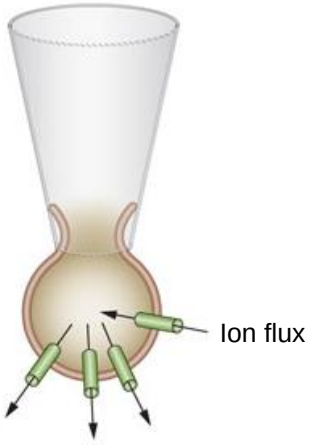

Figure 1.20: The 'whole-cell' patch clamp mode.[131]

Recording is done using a silver electrode within the micropipette which is connected to a very sensitive amplifier. The rate of ion flow through an ion channel is typically around ten million ions per second; this equates to a current of just a few picoamperes and hence highly sensitive detection and amplification is fundamental for precise recordings.[132] A second electrode is connected to form a circuit and is maintained in the extracellular bath solution, this is the bath (or ground) electrode. This can be modelled by the equivalent circuit illustrated in Figure 1.21 for the whole-cell configuration.

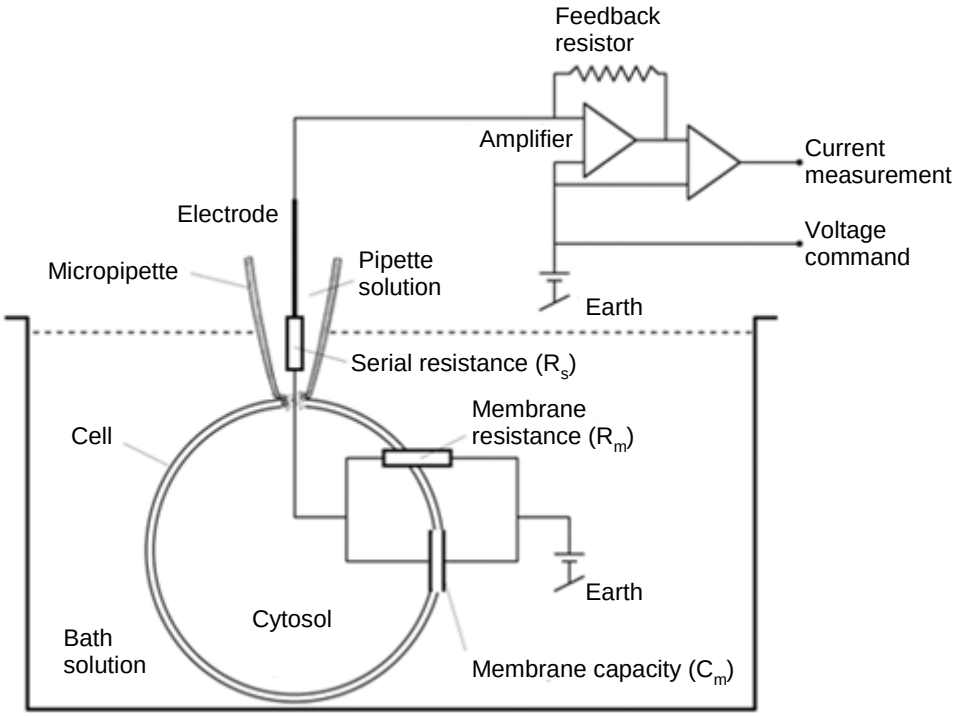

Figure 1.21: The whole-cell mode setup.[133]

Within the circuit formed there is an observable resistance from the pipette, shown in Figure 1.21 as serial resistance (R_s), and also the resistance from the cell membrane itself, shown as membrane resistance (R_m). The latter is the largest of the two and, with formation of a complete circuit, the current through R_m can be determined.[134] The whole-cell configuration is the most commonly employed and two modes are available: the voltage-clamp mode facilitates the holding of the membrane potential at a set voltage, allowing for the quantification of membrane current as the sum of the total ion flux though the cell membrane (i.e. through R_m) whilst in the current-clamp mode, the membrane current is held constant while changes in membrane potential are observed.[132]

Besides the original cell-attached and most common whole-cell configurations, there are a few less common variants that can be employed as alternatives. Adding pore-forming agents (commonly antibiotics such as amphotericin B) to the pipette solution while in the cell-attached configuration creates a partially permeable membrane under the pipette tip; this facilitates the ionic continuity between the pipette solution and cytoplasm whilst ensuring intracellular proteins stay within the cell. This is known as the 'perforated-patch' method and is depicted in Figure 1.22.[131,132]

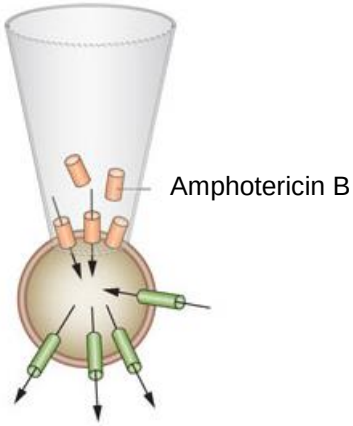

Figure 1.22: The perforated patch clamp mode.[131]

It is also possible to make recordings using a small patch of membrane rather than the whole cell. This again allows for both the intra- and extracellular environment to be controlled and increases the chances of obtaining recordings through single channels. In the 'inside-out' configuration (Figure 1.23a), the cytosolic face of an excised patch of membrane is exposed, allowing for the study of the effect of intracellular ligands on the ion channel of interest. Conversely, in the 'outside-out' configuration (Figure 1.23b), the extracellular face is exposed and the effect of extracellular ligands then studied.[131,132]

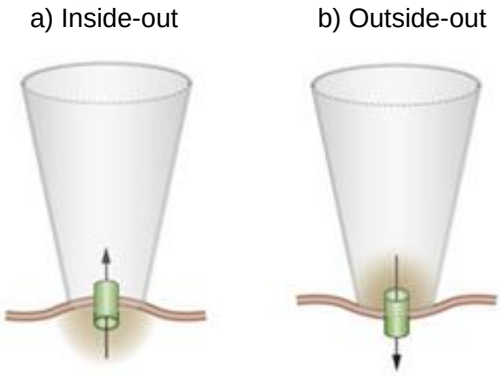

Figure 1.23: The a) 'inside-out' and b) 'outside-out' patch clamp modes.[131]

1.4.3 Membrane Potential and Capacitance

The intra- and extracellular media possess a number of different inorganic ions in varying concentrations. The gross distribution of these ions is relatively consistent among a vast number of cell types and is displayed in Table 1.4 below.

Table 1.4: The ionic distribution across the animal cell membrane.[132]

Ion Species	*Intracellular concentration range (mM)*	*Extracellular concentration range (mM)*
Na^+	5.00-20.0	130-160
K^+	130-160	4.00-8.00
Ca^{2+}	$0.05\text{-}1.00 \times 10^{-3}$	1.20-4.00
Mg^{2+}	10.0-20.0	1.00-5.00
Cl^-	1.00-60.0	100-140

The differences in ion distribution create a concentration gradient across the plasma membrane for each ion species. These concentration gradients lead to the diffusion of ions down this gradient, from higher to lower concentration environments.[132] This diffusion of ions changes the existing electric potential across the membrane (the membrane potential). This new potential creates an electric force on the ions which opposes the diffusion force on the ions. As the diffusion of the ionic species continues, the electric potential gradient opposing the diffusion gets steeper. Once these two opposing forces are equal, equilibrium is reached and there is no net movement of ions across the membrane.[134]

The relationship which describes the electrical potential at which an ionic gradient is at equilibrium is given by the Nernst equation:[132,134]

$$E = \left(\frac{RT}{zF}\right) ln \frac{[ion]_i}{[ion]_o}$$

Where E is the equilibrium potential for a given ion, R is the universal gas constant (8.31 J mol^{-1} K^{-1}), T is temperature in Kelvin, z is the oxidation state of the given ion, F is the Faraday constant (9.65 x 10^4 C mol^{-1}) and $[ion]_o$ and $[ion]_i$ are the extra- and intracellular concentrations of the given ion respectively.

The potential difference across the cell membrane, i.e. the membrane potential, is due to both the overall distribution of ions and the relative permeability of the plasma membrane to each ionic species at any one moment. At rest, the typical membrane potential is around -50 to -80 mV.[132]

If the membrane potential is not equal to the equilibrium potential for a given ion at any one moment, then that ion will move across the membrane accordingly. This movement of ions is a movement of charge and, in electronic terms, is expressed in current:[132]

$$I = {}^{dQ}/_{dt}$$

Where I is current in amperes (A) and dQ/dt is the change in charge over time in coulomb (C).

The current caused by ion flux is dependent upon two variables: the net electrical potential acting on the ion, which is the difference between the membrane potential and the equilibrium potential, and the resistance from the membrane. The fewer channels open for transport of the ion, the greater the resistance imposed by the membrane (R_m).[132]

The membrane also exerts a capacitance effect, meaning it has the ability to store charge. It does so by accumulating ions of opposite charge on the inner and outer faces of the membrane by forces of attraction. It follows that the larger the surface area of the membrane, the greater the capacitance of the cell as there is greater area over which to accumulate ions. As a result of this capacitance associated with the plasma membrane, a change in membrane potential will always come into effect with some delay; the change must first overcome the stored charge present at that given moment.[132]

The resistance, capacitance and potential of a cell membrane are all factors that are taken into consideration when conducting electrophysiological experiments to study ionic currents and there are methods to quantify and compensate for them accordingly.

1.4.4 Application of the Patch Clamp Technique

Patch clamp is a valuable technique employed when approaching physiological questions about ion channels. Patch clamp can be carried out on cultured cells, excised dissociated cell samples or on tissue slices; the latter creating the most physiologically relevant environment[133]. In addition, the ion channel of interest can be heterogeneously introduced and expressed by transfection of a stable cell line. The patch clamp technique is used in many areas of research, most notably in the area of neuroscience and the research into the physiology of excitable cells. Methods for efficient cell isolation have broadened the scope of possibilities through patch clamp. Recently, high resolution recordings from brain slices were obtained[135] and even recordings from the brain *in vivo* have been conducted successfully.[136] The great significance of this advance in the patch clamp technique is demonstrated in its recent use to study

fundamental electrophysiological processes such as electrical transmission at synapses[136,137] and the study of vital ion channels in neurones of the brain.[138,139]

1.5 Project Aims

As discussed in the introduction, maleimides present themselves as one of the most commonly employed motifs for the chemical modification of cysteine. Most recently, their utility in the re-bridging of a reduced disulfide bond as a strategy for protein modification has been realised and, as a result, is becoming a rapidly expanding and exciting field.

A preliminary aim of this project is to broaden the library of 3,4-disubstituted maleimide reagents available; careful design of the chemistry of these reagents should allow their reactivity, properties and functionality to be fine-tuned. We plan to explore the effect of varying the substituents of the 3,4-disubstituted maleimides in order to either increase or decrease reactivity, or to tailor the chemical properties of the reagents (Scheme 1.18). Perhaps most significantly, a solution to the issue of the poor water-solubility associated with the currently available maleimides is sought. The modification protocols devised thus far all employ significant amounts of organic solvents which are known to disrupt non-covalent interactions and which may have a detrimental effect on protein structure.[140,141] Improving the water-solubility of our reagents could be greatly beneficial and widen the scope of their utility.

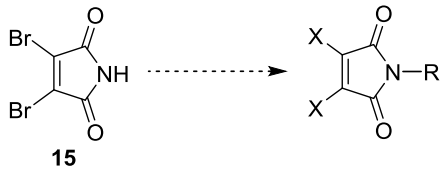

Scheme 1.18: From dibromomaleimide **15** to novel next generation maleimides.

We are also interested in probing the selectivity of the maleimides; site-selectivity in the field of bioconjugation is a fundamental criteria but one that can prove challenging to achieve. Many peptides and proteins of therapeutic interest have disulfide bonds, often multiple. Thus far, research within the group had been restricted to systems with a single disulfide bond. Those with multiple disulfides present themselves as more challenging targets. We aim to probe the ability of our maleimide reagents to selectively target a disulfide by exploiting the differential accessibility and reactivity of the bonds. Recently published work by Brocchini *et al*. describes similar studies on their disulfide-bridging monosulfone reagents with promising results[56]; we are interested in how well

3,4-disubstituted maleimide reagents compared in the pursuit for truly site-selective disulfide modification reagents.

An *in situ* protocol for maleimide modification has recently been reported, which serves to immediately re-bridge two cysteine residues upon reduction, effectively minimising the opportunity for protein or peptide unfolding and aggregation.[24] In the case of multiply disulfide bonded systems, this protocol is hypothesised to reduce the likelihood of disulfide scrambling – an important consideration for these more complex systems. We plan to examine the scope of this *in situ* protocol in overcoming such limitations associated with the presence of more than one disulfide bond within a target.

In order to examine the aforementioned concepts, we have chosen the small peptide neurotoxin tertiapin Q **40** as a target (Scheme 1.19). This peptide has two disulfide bonds in relatively close proximity. As described, this peptide has potential for use as an ion channel probe or as a therapeutic for atrial fibrillation; success in the selective modification of the disulfide bond/s of tertiapin Q could open the doors to the formation of novel, functional bioconjugates for such applications.

Scheme 1.19: Towards a maleimide modified derivative of tertiapin Q (**40**).

We aim to accurately assess the effects of the incorporation of an unnatural two-carbon bridge within the disulfide bond/s of tertiapin Q. To accomplish this, we plan to use the electrophysiological technique of patch clamp to assess any alterations to the binding and resultant effects of maleimide modified tertiapin Q on its target, namely the GIRK channel family. If biological activity is successfully maintained, work will focus on the synthesis of the desired, functional bioconjugates.

Concurrent with this, we plan to examine the scope of the small peptide octreotide as a target for maleimide modification. Octreotide has considerable coverage in the literature as both a therapeutic in its own right, and as a precursor for bioconjugation. Its high

affinity for the somatostatin receptor makes it the ideal candidate for the diagnosis and treatment of somatostatin-receptor positive tumours, of which there are numerous. We hope to use maleimide modification to contribute to this field, by the design and synthesis of some novel, next-generation bioconjugates (Scheme 1.20). Of particular interest is whether we could create a functional diagnostic MOMIA via an efficient synthetic route.

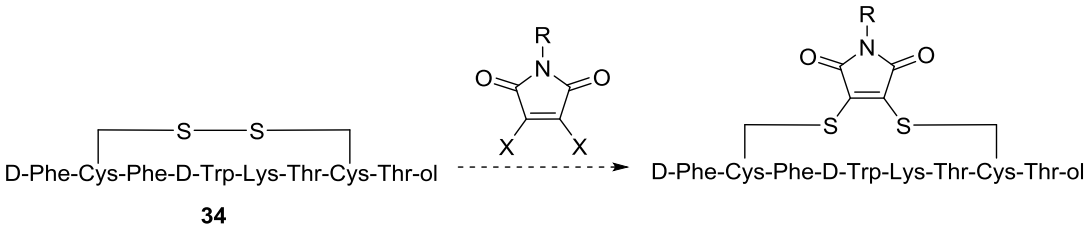

Scheme 1.20: Towards novel bioconjugates of octreotide (**34**).

Subsequent to the preliminary yet promising research carried out by the Baker and Caddick groups, and alongside the complimentary work conducted by the Brocchini group, this project will investigate the 3,4-disubtituted maleimides as reagents for disulfide modification. Of key interest is their efficacy when used on therapeutically relevant targets and those with multiple disulfide bonds – a challenging idea but one that would vastly broaden the scope of the maleimide modification technique. A primary goal is to devise sound methods for both accurate structural analysis and biological activity testing of our modified products. Finally, we aim to create useful and innovative bioconjugates from our chosen target peptides, with the vision of creating products that fulfil gaps within the clinical market.

Chapter 2: Results & Discussion

2.1 Maleimide Synthesis & Reactivity

2.1.1 Maleimide Synthesis

After promising results from research in the Baker group on dibromomaleimide and, perhaps more significantly, dithiophenolmaleimide, it was proposed that a family of modified thiophenolmaleimide reagents be synthesised and examined.[24] Altering the substituents on the aromatic ring of dithiophenolmaleimide should serve to tune the reactivity of the compounds. The target molecules first envisaged were designed to vary in their substituents in the *ortho*- position on the thiophenol ring. Introducing steric bulk at these positions was postulated to help decrease susceptibility towards unwanted attack by bulky nucleophilic reducing agents employed in the disulfide bridging protocols. Dithiophenolmaleimide **22** and the *ortho*-substituted derivatives **41**-**43** were chosen and synthesised using dibromomaleimide and the corresponding substituted thiophenols, both of which commercially available (Scheme 2.1). In each case, the synthesis was straightforward and yielded a solid product with varying yellow colouration.

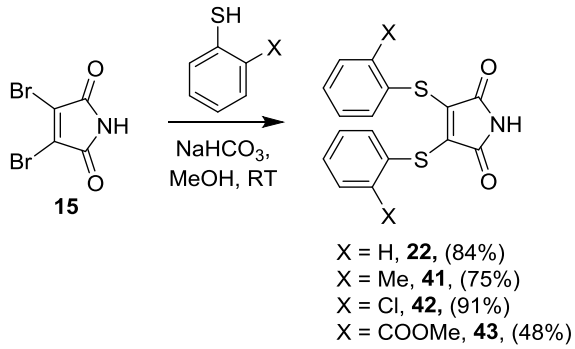

Scheme 2.1: Synthetic route to maleimides **22** and **41**-**43**.

All syntheses were very fast; all starting material had reacted within 15 minutes in each case, as confirmed by thin-layer chromatography (TLC). The yield of maleimide **43** is significantly lower; this was reasoned to be as a result of the competing side reaction in this synthesis, the formation of the disulfide, which was not isolated due to its tendancy to elute alongside maleimide **43** during attempts at purification.

2.1.2 Addition of Cysteine to Maleimides

To examine how efficient these new maleimides would be at reacting with thiols via the addition-elimination reaction, a preliminary test was carried out using a protected cysteine analogue, *N*-Boc-Cys-OMe (**10**) (Scheme 2.2). The reaction was carried out in pH 6.2 phosphate buffer in order to mimic conditions suitable for use with proteins. After protocol optimisation, DMF (15%) was employed in order to facilitate the solubilisation of the maleimides.

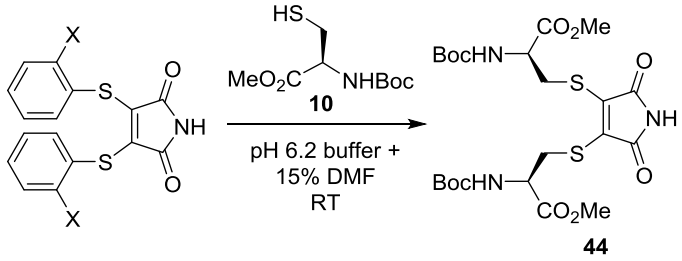

Scheme 2.2: The reaction of maleimides **22** and **41**-**43** with N-Boc-Cys-OMe (**10**).

Table 2.1: Yield of dicysteine-maleimide obtained for maleimides **22** and **41**-**43**.

Maleimide	*Reaction time (min)*	*Yield of Product* **44** *(%)*
22 (X=H)	30	85
41 (X=Me)	120	37
42 (X=Cl)	60	49
43 (X=COOMe)	30	86

In the case of maleimides **22** and **43**, the reaction was fast; all starting material had reacted within 15 minutes, affording good yield of the product **44** after purification. In contrast, with maleimides **41** and **42**, starting material remained, even after elongated reaction times of over an hour, and it appeared that no further reaction was taking place. This is consistent with the fact that maleimides **41** and **42** contain electron donating and sterically encumbering groups respectively, which will serve to reduce the rate of nucleophilic substitution. This may also lead to competing reactions, such as disulfide formation, which would prevent full conversion to the desired product.

2.1.3 TCEP Cross Reactivity with Maleimides

As described in Chapter 1, a potential limitation of targeting disulfide bonds in protein modification is the likelihood of scrambling, aggregation or unfolding during the reduction process. The ideal bridging protocol adopts an *in situ* approach whereby the bridging reagent and the reducing agent must be present together in order to decrease the time the reduced disulfide is left unbridged. For this to be possible however, the maleimides must be resistant to cross reactivity with the reducing agent employed. Due to the fact that dithiothreitol (DTT) and β-mercaptoethanol (BME) are thiol-based, they have been found to be, as expected, inefficient at disulfide reduction when used in combination with thiophenolmaleimide **22** due to their propensity to react with the maleimide itself.[24] As a result, the phosphine-based reducing agent TCEP has routinely been employed thus far. Reactivity towards TCEP has been observed for dibromomaleimide and, to a lesser extent, for thiophenolmaleimide. This decreased susceptibility of cross-reactivity with dithiophenolmaleimide is perhaps due to the increased steric hindrance imparted by the aromatic rings, blocking the access of TCEP. To examine the reactivity of maleimides **22** and **41**-**43** towards TCEP they were reacted together in pH 6.2 phosphate buffer for 15 minutes (Scheme 2.3) and the yield of recovered maleimide calculated. The results obtained are shown in Table 2.2.

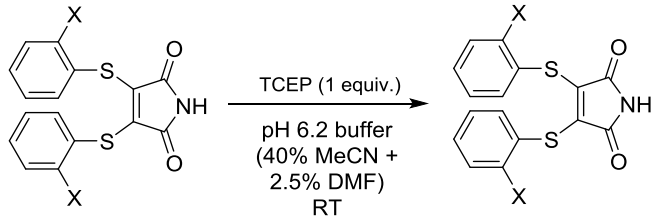

Scheme 2.3: Reaction conditions to determine cross reactivity of maleimides **22** and **41**-**43** with TCEP.

Table 2.2: Yield of maleimide recovered after cross-reactivity experiment.

Maleimide	*Yield Recovered (%)*
22 (X=H)	94%
41 (X=Me)	100%
42 (X=Cl)	96%
43 (X=COOMe)	95%

All maleimides tested seemed to exhibit resistance towards cross reactivity with TCEP. Variation between the recovered yields is negligible, suggesting the extent of cross reactivity is not dependent upon the protection by the substituent on the aromatic ring.

2.1.4 Bridging Somatostatin in a Step-wise Protocol

Work progressed onto testing the disulfide bridging capability of the maleimide reagents on a model peptide system. Somatostatin **20**, a 14 amino acid peptide hormone discussed in detail in Section 1.3, was employed. Somatostatin has a single, accessible disulfide bond and proved simple to prepare and characterise by the desired analytical methods. Initially, utility of the maleimides **22** and **41**-**43** in the step-wise bridging protocol was investigated.[24] This is a two stage process, the first being reduction of the disulfide bond using TCEP to reveal the two nucleophilic cysteine thiols. The second stage is addition of the maleimide reagent to install a two-carbon bridge between the cysteines, as depicted in Scheme 2.4, creating maleimide bridged somatostatin **21**.

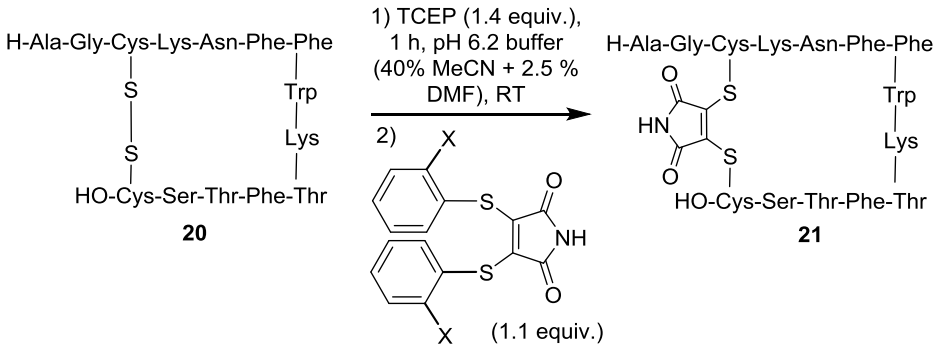

Scheme 2.4: Step-wise bridging of somatostatin (where X = H (**22**), Me (**41**), Cl (**42**) or COOMe (**43**)).

After addition of 1.4 equivalents of TCEP and incubation at room temperature for 1 h, somatostatin was fully reduced. This was determined by apparent conversion by LC-MS. Successful reduction was identified by the increase in mass from *m/z* 1638 to *m/z* 1640 accounting for the protonation of both cysteine sulphurs. A subsequent mass increase to *m/z* 1733 was observed upon addition of the maleimide reagents accounting for the incorporation of the bridge between the two cysteine residues and formation of bridged somatostatin **21**. The species were commonly observed as the doubly charged ions; typical mass spectra are shown in Figure 2.1 **A**-**C**.

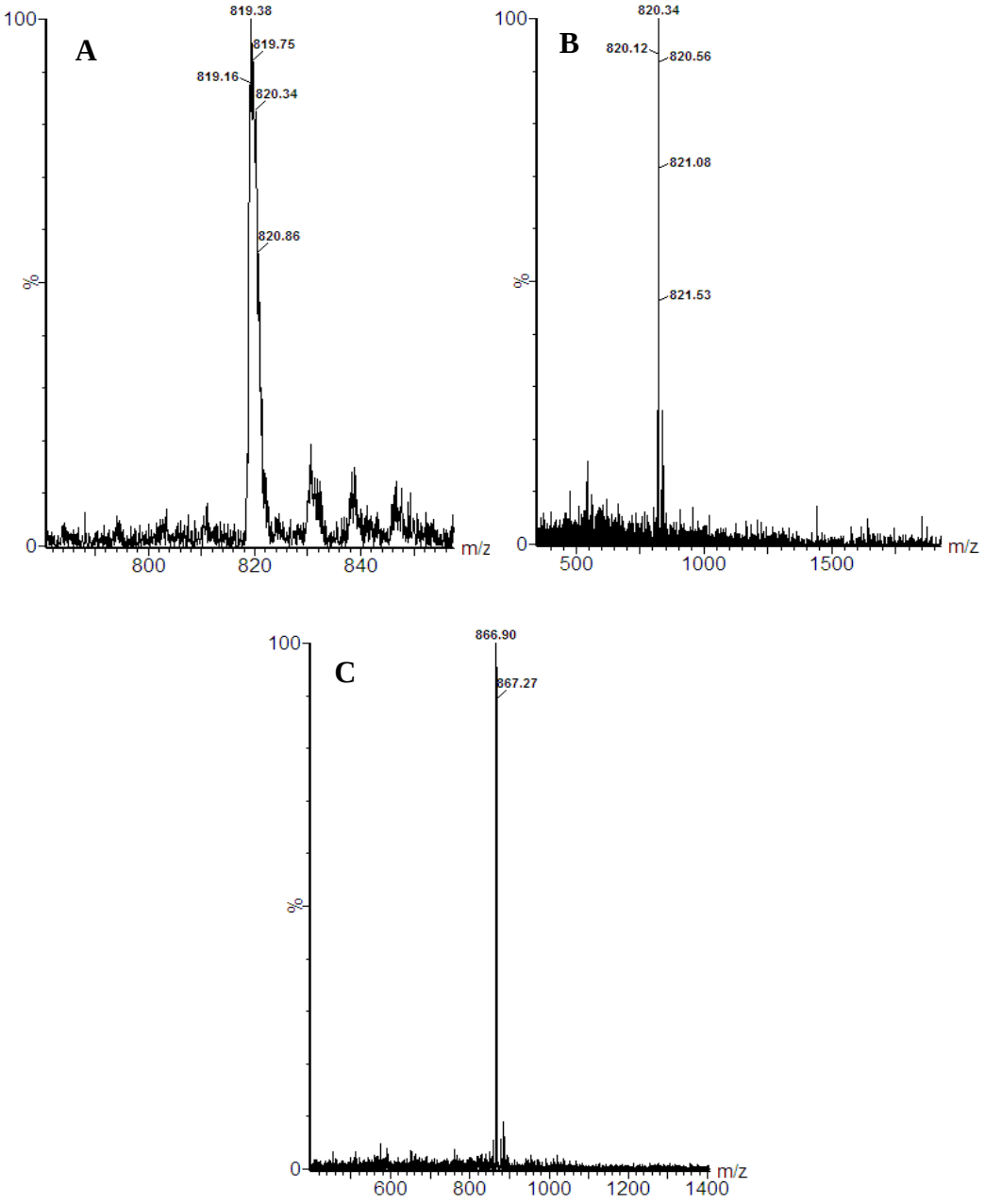

Figure 2.1: ***A-C:*** ESI mass spectrum of **A**) peak at *m/z* 819.38 corresponding to the doubly charged ion of native somatostatin **20** (expected mass = *m/z* 818.95). **B**) peak at *m/z* 820.34 corresponding to the doubly charged ion of reduced somatostatin (expected mass = *m/z* 819.95) and (**C**) peak at *m/z* 866.90 corresponding to the doubly charged ion of maleimide-bridged somatostatin **21** (expected mass = *m/z* 866.50).

LC-MS readings were taken at 1, 10 and 60 minutes, and despite all of the maleimides showing rapid bridging, there were some noticeable differences between their rates of reaction. Apparent conversion to the bridged product **21** over time for each of the four maleimide reagents is shown in Figure 2.2. Conversion percentages are determined by peak height in the LC-MS spectra and are normalised accordingly if more than one

species is detected. Such analysis is not perfectly quantitative, but gives a good representation of conversion rates and product ratios.

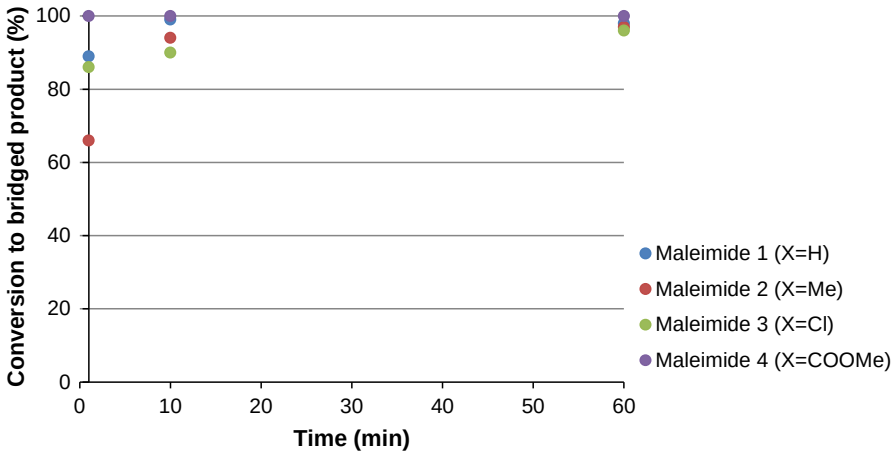

Figure 2.2: Percentage conversion to bridged somatostatin **21** over time for maleimides **22** and **41**-**43**.

From Figure 2.2, it is apparent that the rate of conversion to modified somatostatin **21** follows the trend **43** > **22** > **42** > **41**. This is as expected and supports the observations from the previous experiment using protected cysteine. Maleimide **43** reaches quantitative conversion to the bridged product **21** within 1 minute, owing, as previously discussed, to the effects of the electron withdrawing methyl-ester group on the aromatic ring, increasing its reactivity towards the cysteine thiolate. Conversely, maleimide **41** had only reached 70% conversion to bridged product **21** in this time; the electron donating methyl substituent decreasing the reactivity of the maleimide and therefore slowing the rate of reaction. Maleimides **22** and **42**, with their thiophenol and chlorothiophenol substituents respectively, have intermediate bridging speeds, the un-substituted and halogenated aromatic rings having a lesser effect on the maleimide reactivity.

Maleimide **43** presents itself as a very effective bridging reagent capable of complete conversion to bridged somatostatin within 1 minute. When compared to maleimide **22** which was found, both in this study and in previous literature, to afford complete conversion within 10 minutes[7], this further heightens the potential for **43**. Increased speed of the bridging reaction consequently means that the free cysteines of the reduced disulfide have less opportunity to participate in disulfide scrambling, or for the

structural integrity of the peptide or protein to be lost by unfolding, both of which could be detrimental.

2.1.5 Bridging Somatostatin in an *In Situ* Protocol

Following these promising results, the utility of these maleimides in the *in situ* protocol described was assessed. In this procedure, the peptide is pre-incubated with the maleimide reagent prior to addition of the reducing agent. It should follow that, as soon as the disulfide bond is cleaved, there is a maleimide present to immediately re-bridge the free cysteine thiols. In reference to a previously published protocol,[24] 5 equivalents of maleimides **22** or **41**-**43** were added to somatostatin **20** before 3 equivalents of TCEP (Scheme 2.5). LC-MS recordings were taken after 1, 5, 10, 20 and 30 minutes.

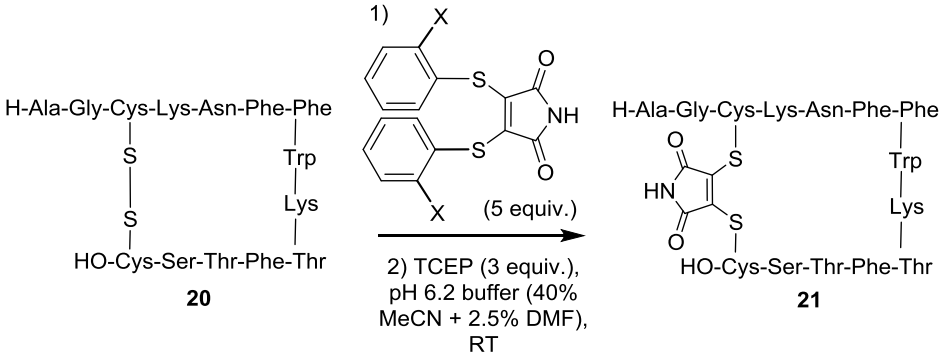

Scheme 2.5: *In situ* bridging of somatostatin (where X = H (**22**), Me (**41**), Cl (**42**) or COOMe (**43**)).

Apparent conversion to the bridged product **21** over time is plotted in Figure 2.3.

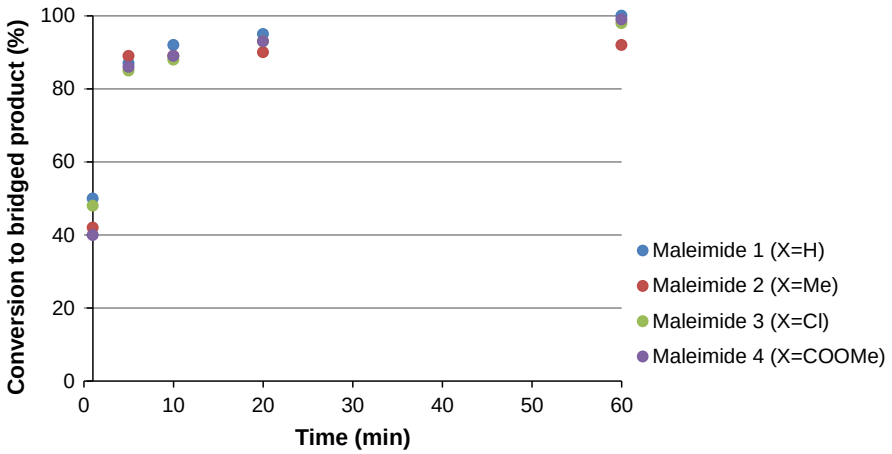

Figure 2.3: Percentage conversion to bridged somatostatin **21** over time for maleimides **22** and **41**-**43** (3 equiv TCEP).

From these results, it is apparent that the difference between maleimides **22** and **41**-**43** in the rate of conversion to the bridged product **21**, which was seen in the step-wise protocol, is no longer apparent and the rate of conversion is almost identical in each case. For all maleimides tested, only 40-50% conversion was observed after 1 minute, which is significantly less than the conversion observed using the step-wise protocol. This suggests that it is in fact the reduction of the disulfide by TCEP that is the rate limiting step in this reaction sequence, rather than the speed at which each maleimide can re-bridge the free thiols. Interestingly, it took longer than the 20 minutes previously reported using thiophenolmaleimide **22** to reach complete conversion to the bridged product **21** in such a protocol[1]. With exception to maleimide **41**, all other reagents led to the desired product within 60 minutes.

2.1.6 Towards Reagent Stoichiometry in the *In situ* Protocol

Ideally, a stoichiometric system would exist, whereby there are no unused reagents remaining after complete conversion to the bridged product; this facilitates the ease of product purification and minimises the likelihood of any undesirable side reactions occurring. Using dibromomaleimide this is difficult to achieve due to the previously observed cross reactivity with TCEP. As previously demonstrated, the thiophenol-based maleimide reagents show much greater resistance and therefore could potentially be applicable to a stoichiometric system. Experiments were carried out in an attempt to reduce the amounts of each reagent employed.

By initially employing TCEP as the limiting reagent, somatostatin was incubated with 5 equivalents of maleimide **22** for 10 minutes, before addition of 1 equivalent of TCEP. The reaction was monitored over 90 minutes by LC-MS. Product formation is shown in Figure 2.4.

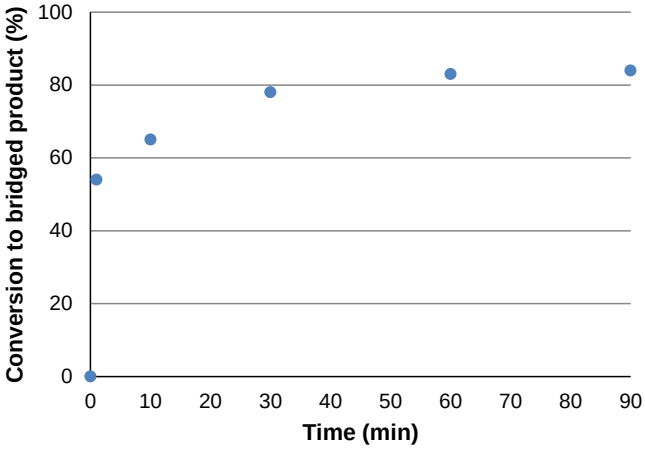

Figure 2.4: Percentage conversion to bridged somatostatin **21** over time using the *in situ* protocol with 5 equivalents of maleimide **22** and 1 equivalent of TCEP.

Using a stoichiometric (with respect to the number of disulfide bonds) amount of reducing agent revealed a very fast initial reaction, with 55% conversion to the bridged product **21** within 1 minute. Subsequent to this, the rate of reaction drops significantly. Maximal product formation is seen soon after 30 minutes, and from this point onwards there is negligible increase. To determine the exact stoichiometry at which full conversion to bridged somatostatin is obtained, a second experiment was conducted whereby 1 equivalent of TCEP was added primarily as before, and then, as the percentage of conversion stopped increasing over time, 0.1 equivalents of TCEP were then added incrementally. Product formation is shown in Figure 2.5.

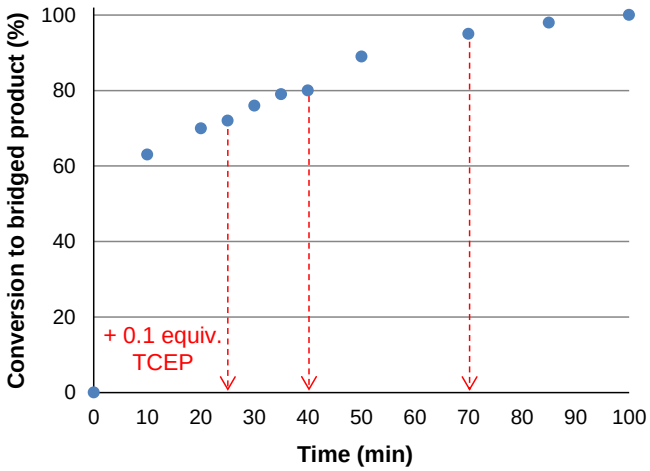

Figure 2.5: Conversion to bridged somatostatin **21** over time using the *in situ* protocol with 5 equivalents of maleimide **22** and 1 equivalent of TCEP, followed by 0.1 equivalents at 25, 40 and 70 minutes.

A further 0.3 equivalents of TCEP is required to push the conversion to completion by full disulfide bond reduction. This may be as a result of a very small degree of cross reactivity with the maleimide reagents. Nevertheless, 1.3 equivalents of TCEP is pleasingly close to the stoichiometric ideal.

Turning next to the minimisation of bridging reagent employed in the *in situ* protocol, somatostatin was pre-incubated with a minimum amount of maleimide **22** before addition of TCEP. Product formation is shown in Figure 2.6. It was found that with as little as 1.1 equivalents of maleimide **22** used in conjunction with 1.3 equivalents of TCEP, full conversion to bridged somatostatin **21** could be obtained.

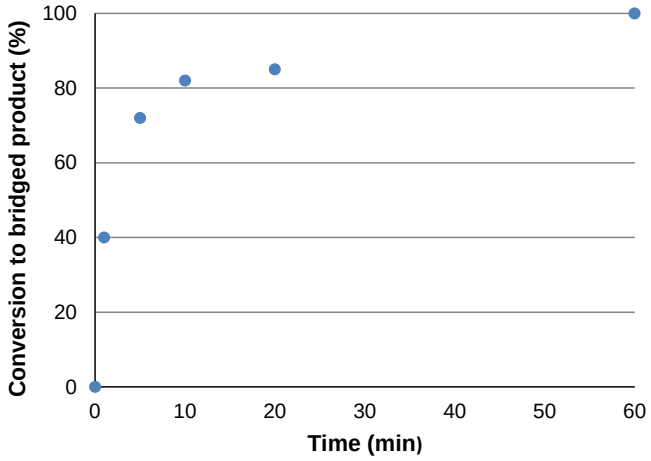

Figure 2.6: Conversion to bridged somatostatin over time using the *in situ* protocol with 1.1 equivalents of maleimide **22** and 1.3 equivalent of TCEP.

In comparing this to the results in Figure X where 5 equivalents of maleimide are employed, it is apparent that this only serves to increase the rate of the reaction; 80% conversion to the bridged product **21** is achieved within 5 minutes in this case.

Again this gives promise that cross-reactivity between the reagents used is very low, and that near-stoichiometric amounts of reducing agent and maleimide can be employed with minimal compromise on the rate of the disulfide bridging reaction.

2.1.7 An *In situ* Protocol using Benzeneselenol-Catalysed Reduction

As previously mentioned, at pH 6.2, the common reducing agents DTT and BME are not compatible in an *in situ* protocol, due to their thiol-based nature. In the search for alternatives, it was found that selenol-based reagents were used to catalyse the reduction

of disulfide bonds with great efficiency.[24] When a catalytic amount was used in conjunction with DTT in the reduction of the disulfide bond of α-chymotrypsinogen, disulfide reduction rates were increased by a factor of ~100.[142] In light of this, previous studies in the group investigated the use of benzeneselenol alongside dithiophenolmaleimide **22** and such a protocol proved effective in the rapid *in situ* modification of the disulfide bond of somatostatin.[24] The devised protocol was repeated using maleimides **22** and **41**-**43**; pre-incubation with 10 equivalents of the maleimide before addition of 5 equivalents of benzeneselenol (Scheme 2.6). Conversion to the bridged peptide **21** was monitored over time.

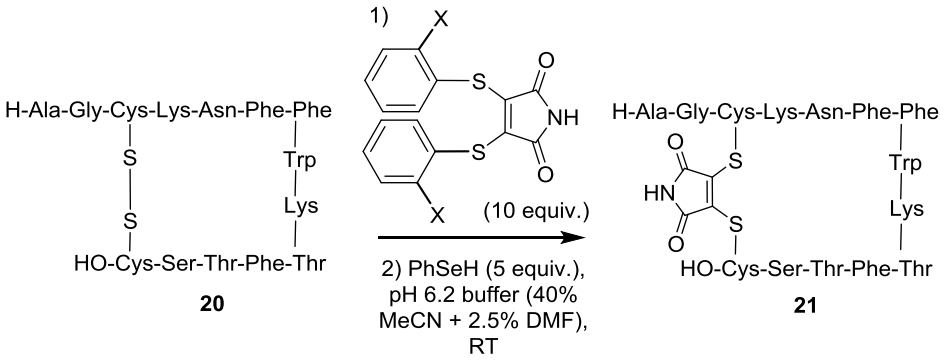

Scheme 2.6: *In situ* bridging of somatostatin using catalytic benzeneselenol (PhSeH) (where X = H (**22**), Me (**41**), Cl (**42**) or COOMe (**43**)).

The apparent conversions to bridged peptide **21** by LCMS are shown in Figure 2.7.

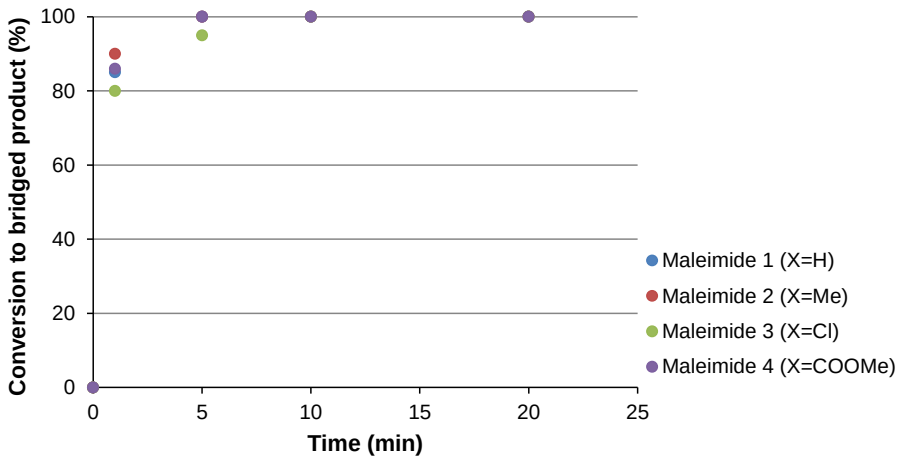

Figure 2.7: Percentage conversion to bridged somatostatin **21** over time for **22** and **41**-**43** (5 equiv. benzeneselenol).

All maleimides reach quantitative conversion to bridged somatostatin **21** and, with the exception of **42**, do so within 5 minutes with negligible variation in rate of reaction.

This suggests that benzeneselenol has dramatically increased the rate of disulfide reduction in comparison to TCEP. The speed of the bridging itself is also increased, but can be accounted for by the excess (10 equivalents) of maleimide present. In conclusion, benzeneselenol presents itself as an efficient alternative to TCEP to facilitate very rapid disulfide reduction.

2.1.8 Towards an Organic Solvent-Free *In Situ* Protocol

The four maleimide compounds tested thus far, although efficient in the bridging protocol, were found to be somewhat insoluble. Because of this, acetonitrile (40% v/v) and DMF (2.5% v/v) were routinely added to the buffer in which somatostatin is dissolved in order to aid solubility of the maleimide compounds once added. This is highly undesirable when trying to mimic physiological reaction conditions.[140,143] Organic solvents such as these have been found to have a detrimental effect on protein structure and function.[144] For this reason, maleimide **45** where X = COOH was synthesised (Scheme 2.7), on the premise that the carboxylic acid should greatly increase the solubility of the whole compound. Deprotonation to form a charged carboxylate moiety should improve its dissolution in water.

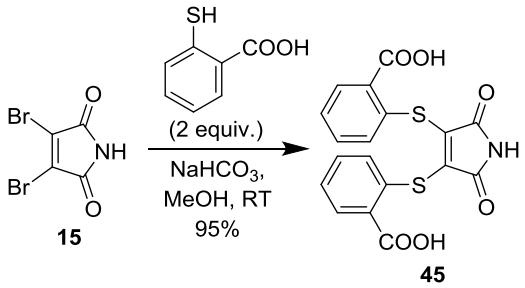

Scheme 2.7: The synthetic route to maleimide **45**.

Pleasingly, maleimide **45** was found to be soluble in pH 6.2 phosphate buffer, with no added organic solvents, up to a concentration of 7 mM. This concentration is suitable for the disulfide modification experiments. The reactivity of this reagent was comparable to that of the other thiophenolmaleimide derivatives. 1.1 equivalents of this compound were used in the *in situ* bridging of somatostatin, alongside 1.3 equivalents of TCEP and full conversion to the bridged product **21** was seen within 60 minutes (Scheme 2.8).

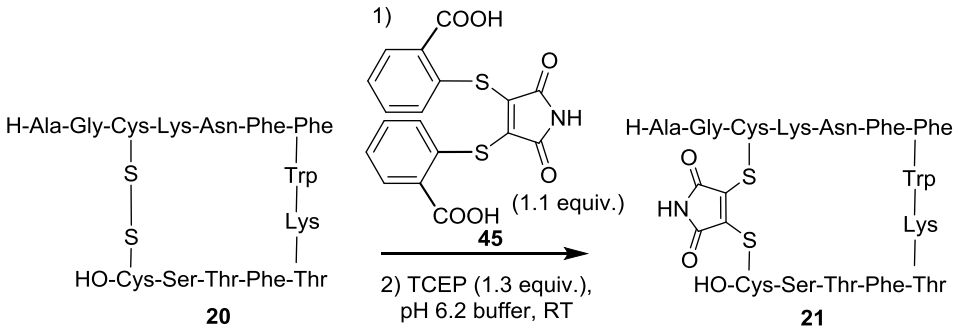

Scheme 2.8: *In situ* bridging of somatostatin **20** using maleimide **45** in organic solvent-free conditions.

Maleimide **45** proved to be the first example of a disulfide bridging reagent compatible with a completely organic solvent-free system. This reagent, and other water soluble maleimide derivatives, could prove invaluable in cases where the peptide or protein shows sensitivity towards organic solvents.[63]

2.1.9 Summary of Results

In summary, new functionalised thiophenolmaleimides with differing chemistry have been synthesised successfully. They varied in their reactivity depending on the nature of the group in the *ortho* position of the aromatic ring, electron withdrawing groups aiding faster rates of reaction; maleimide **43** presented itself as the fastest acting bridging reagent to date. Results confirmed that maleimides **22** and **41**-**43** are all unreactive towards the reducing agent TCEP, as desired. The maleimides were all capable of bridging the disulfide bond of somatostatin in both the step-wise and *in situ* protocol with TCEP as the reducing agent. Near-stoichiometric conditions can be achieved, minimising the amount of unused reagent remaining and aiding product purification. Employing benzeneselenol as a reducing agent in the *in situ* protocol lead to improved reduction rates compared to those observed with TCEP. Incorporation of a carboxylic acid moiety on the aromatic rings of the maleimide serves to improve water-solubility to such an extent that completely organic solvent-free conditions can be achieved with maleimide **45**.

Tuning of the reactivity of the maleimides goes further than that studied in this project, and is the focus of other members of the group. In continuation of this study, the effect of altering the location of the ring substituent to the *meta*- and *para*- positions would be of interest but was not within the scope of this project.

2.2 Modification of Tertiapin Q

From initial experiments with somatostatin giving promise that our 3,4-disubstituted maleimide reagents could effectively re-bridge an accessible disulfide bond, we wished to examine the scope of this modification strategy. Somatostatin presented itself as a relatively simple model owing largely to the fact it consists of a single disulfide bond. We were intrigued by how this chemistry would translate to more complex systems; those with multiple disulfide bonds were a key interest. As discussed in Chapter 1.1, disulfide bonds are prevalent in many extracellular or surface-exposed peptides and proteins where they play fundamental roles in conferring structure and stability and in the tuning of biological function.[1] Examples of those containing multiple disulfides are also numerous. For the purpose of our study, we chose a small 21 amino acid neurotoxin peptide called tertiapin Q. This peptide is discussed in detail in Chapter 1.2, but most notably it consists of two disulfide bonds which serve to maintain its rigid and compact structure and consequently help confer great affinity for its GIRK channel target.[76] We hypothesised exploring the scope of the maleimide reagents on this system; to determine whether sufficient control of the bridging could be obtained to allow selective disulfide modification whilst retaining the correct cysteine connectivity, to examine to what extent the biological activity of the peptide is altered as a result of modification and to synthesise novel, functional bioconjugates of tertiapin Q for various applications.

2.2.1 Dose-Response Analysis of Native Tertiapin Q

It is a well-known concept that the response elicited by a given substance is dependent upon the concentration. Substances such as toxins often show the characteristic dose-response relationship whereby, at very low doses, the substance is non-toxic, at intermediate doses a response is seen and the level of which steeply increases and, at very high doses, the effect tends to plateau as the effect reaches its maximum.[145]

Analysis of the effect of increasing doses of native tertiapin Q on the inhibition of both inwards and outwards flux of K^+ through the GIRK1/4 channel would serve as control with which to compare the biological activity of any modified derivatives. Whole-cell patch clamp experiments were conducted on HEK293 cells stably expressing the GIRK 1/4 channel subtype.[146] This subtype was chosen as, in cardiac cells, these predominate

and therefore is the most physiologically relevant system to employ in out experiments. The typical current traces for a recording of GIRK1/4 currents at both rest and after application of tertiapin Q are shown in Figure 2.8.

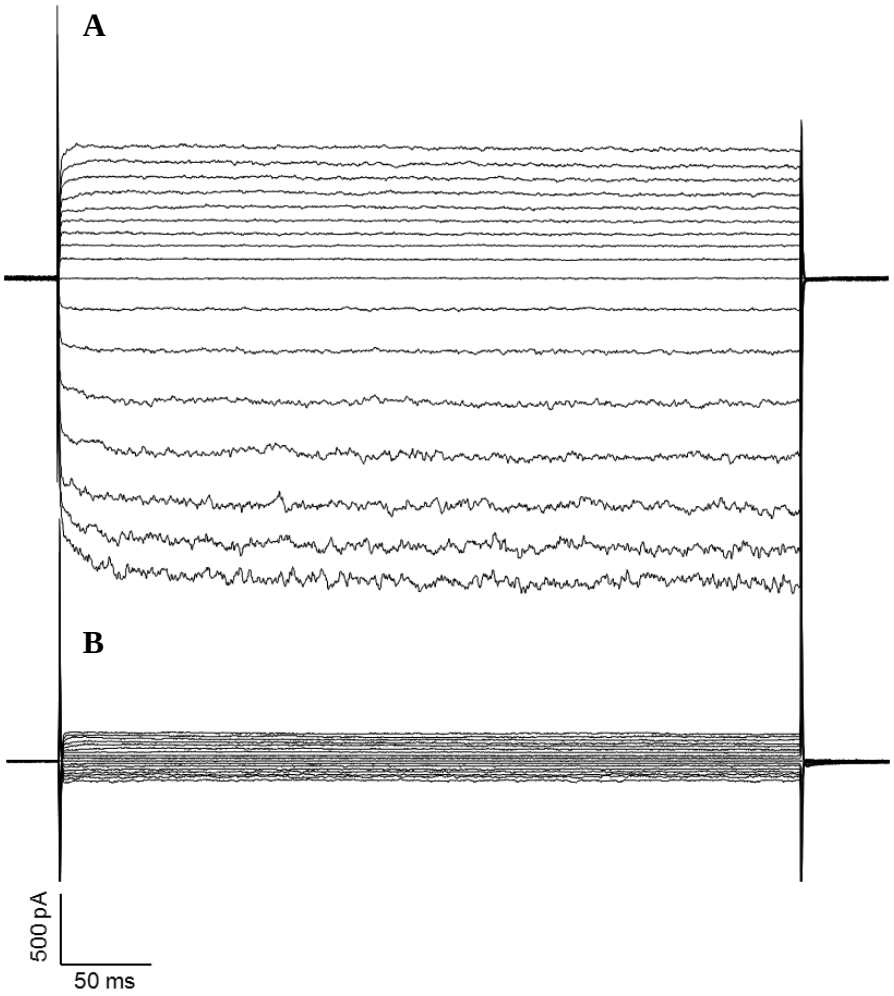

Figure 2.8: Current recordings of **A**) the resting GIRK1/4 channel and **B**) GIRK1/4 channel inhibition by tertiapin Q (100 nM). Current was recorded over 20 mV voltage steps, over a range of -120 to +40 mV from a holding potential of -50 mV.

These representative recordings show the large inwards currents and smaller outwards currents of the GIRK1/4 channel at rest (Figure 2.8**A**). Immediate current activation is observed following capacitive transient spikes. Upon administration of tertiapin Q, inhibition of the GIRK1/4 channel is seen by reduction in both the inwards and outwards currents (Figure 2.8**B**).

Recordings were taken at regular intervals whilst increasing doses of tertiapin Q (ranging from 1 nM to 100 nM) were subjected to the cells via continuous perfusion.

This allows for the recording of the total amount of current from K^+ flux through all GIRK1/4 channels in the cell membrane. The results obtained are shown in Figure 2.9.

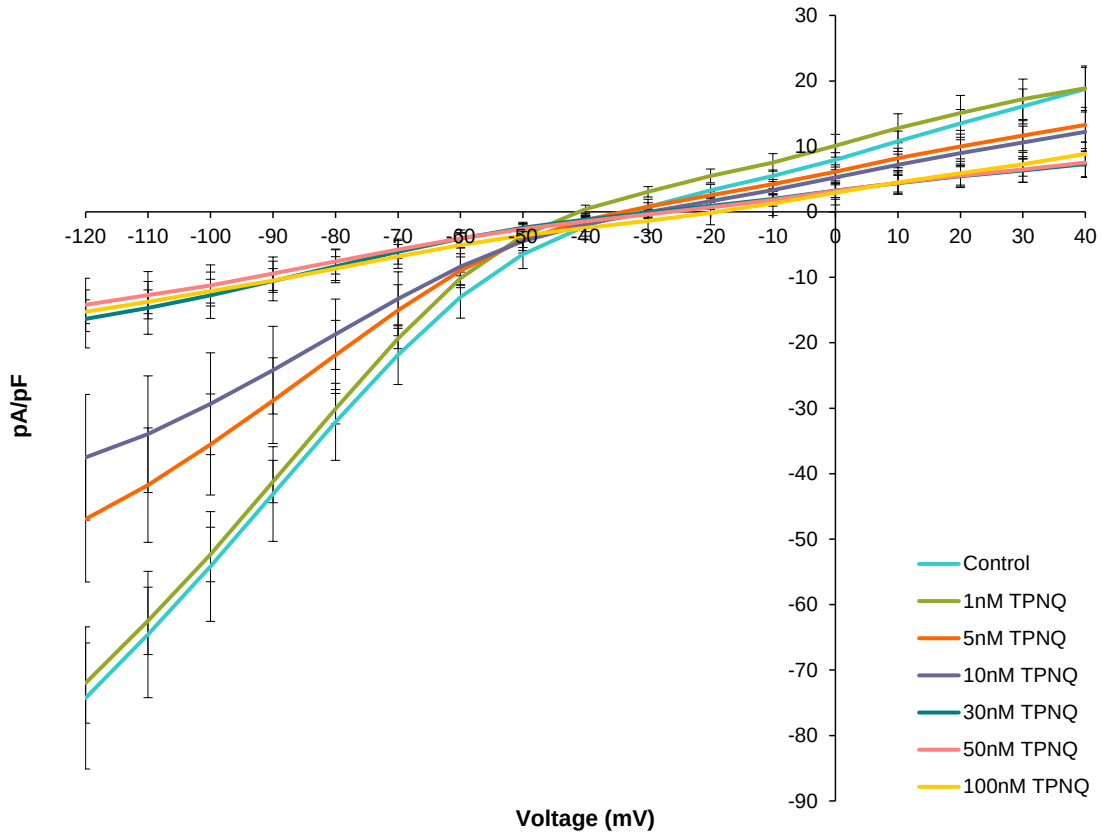

Figure 2.9: Current-voltage relationship: average K^+ current (pA/pF) over a range of membrane potentials (-120 to +40 mV) in response to changing concentrations of tertiapin Q. The error bars shown are calculated as the standard error of the mean.

Figure 2.9 shows the change in K^+ current over the full range of membrane potentials tested. The graph shows the characteristic trace of an inwardly rectifying channel – a significantly large inwards K^+ current, seen between -120 and around -40 mV, and a smaller outwards K^+ current seen between around -40 and +40 mV.[147] The point at which the lines cross the x-axis is where the ion flux switches from being in the inwards direction to being outwards. The expected value of this for a particular ion, known as the reversal potential, has the same numerical value as the equilibrium potential of that ion. This is defined by the Nernst equation:

$$E = \left(\frac{RT}{zF}\right) ln \frac{[ion]_i}{[ion]_o}$$

The Nernst equation where R is the universal gas constant (8.31 $Jmol^{-1}$ K^{-1}), T is the temperature in Kelvin, z is the oxidation state of the ion, F is the Faraday constant ($9.65x10^4$ $Cmol^{-1}$) and $[ion]_o$ and $[ion]_i$ are the extracellular and intracellular concentrations of the ion of interest respectively.

For K^+, at a temperature of 298 K, the physiological equilibrium potential is calculated as -83.7 mV. In this investigation, the compositions of the intracellular and extracellular solutions produce an equilibrium potential of -48.0 mV. In the patch clamp protocol used, the holding potential is -50 mV, close to the equilibrium potential calculated where there is no net movement of ions across the cell membrane. Experimentally, Figure 2.9 shows the reversal potential to be between around -40 mV prior to the addition of tertiapin Q. The small discrepancy is due to endogenous currents present in HEK293 cells,[148] and also some small current leak as a result of the whole-cell patch clamp procedure. Figure 2.9 also shows that tertiapin Q inhibits the GIRK channels at all membrane potentials tested, confirming that its effect is voltage independent, concurrent with previous literature.[96]

At the lowest tertiapin Q concentration, 1 nM, there is very little change in the level of K^+ current passing through the GIRK channels, although a very small inhibitory response is still seen. Increasing the concentration from 1 nM to 5 nM sees a dramatic increase in the inhibitory response, shown by the large drop in the level of K^+ current recorded. This effect continues up to 30 nM, but increasing the concentration above 30 nM leads to no further increase in channel inhibition. Even with tertiapin Q concentrations as high as 100 nM, the current level does not seem to reach 0, where there is no flux of K^+; this residual current has also been noticed in similar experiments by Kanjhan *et al.*.[96]

In order to obtain a numerical value to quantify the potency of tertiapin Q as an inhibitor, the IC_{50} value should be determined. In this case, this is the concentration at which half maximum inhibition of the GIRK channel is obtained. To do this, the average degree of channel inhibition, as a percentage, by each concentration of tertiapin Q tested is plotted (Figure 2.10). From this, the concentration for half maximum inhibition can be determined.

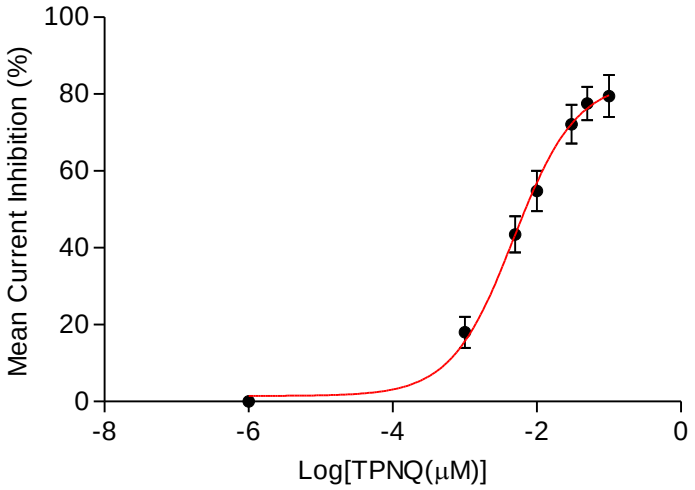

Figure 2.10: Mean current inhibition (%) with increasing concentration of tertiapin Q (plotted as log [tertiapin Q (μM)]. The sigmoidal fit line (red) was produced using a fit with function y = Bottom+(Top-Bottom)/(1+10^(X-LogIC$_{50}$)). R^2 = 0.9976. X at Y_{50} = -2.32. The error bars shown are calculated as the standard error of the mean. Raw data in Appendix Table 1.

The sigmoid shape of the graph in Figure 2.10 is highly characteristic of a dose-response study. The equation used to fit the data assumes a Hill slope of -1.0; this corresponds to a 1:1 ratio of ligand to receptor binding and can be utilised in this analysis due to extensive literature precedent confirming this stoichiometry to be true.[145] The IC_{50} value was calculated to be 4.78 nM. This is similar to the value quoted in the literature which is 8.5 nM.[79] With an R^2 of 0.9976, the data values fit well within the sigmoid trend line suggesting the IC_{50} value obtained can be taken with confidence.

From this analysis, it is clear that tertiapin Q is a potent inhibitor of GIRK1/4 channels, eliciting its effects at concentrations as low as 1 nM. This potency, along with its great selectivity, makes tertiapin Q an ideal candidate for studying the characteristics and physiology of these channels.

2.2.2 Tertiapin Q Wash-Out Analysis

It is often the case that ion channel inhibitors that physically block the channel by binding in the pore region act reversibly and that washing out the inhibitor can lead to recovery of original function.[145] Chemical modification of tertiapin Q also has the potential to alter not only the inhibitory potential of the toxin, but also the ability for the inhibition to be reversed by washing out the toxin from the channel pore. If toxins such as tertiapin Q are to be used for analytical or medical applications then these

characteristics are important. To test this, after the maximum concentration of tertiapin Q had been administered to the cells and maximal GIRK channel inhibition observed, perfusion was switched to extracellular solution and currents monitored for return to resting levels. Figure 2.11 shows the current recovery after administration of 100 nM tertiapin Q. After GIRK channel inhibition by the maximum concentration of tertiapin Q, some recovery of K^+ flux is possible with continuous wash-out with extracellular solution. At the most negative membrane potential, -120mV, there is about 35% current recovered. Resting current levels were not fully regained.

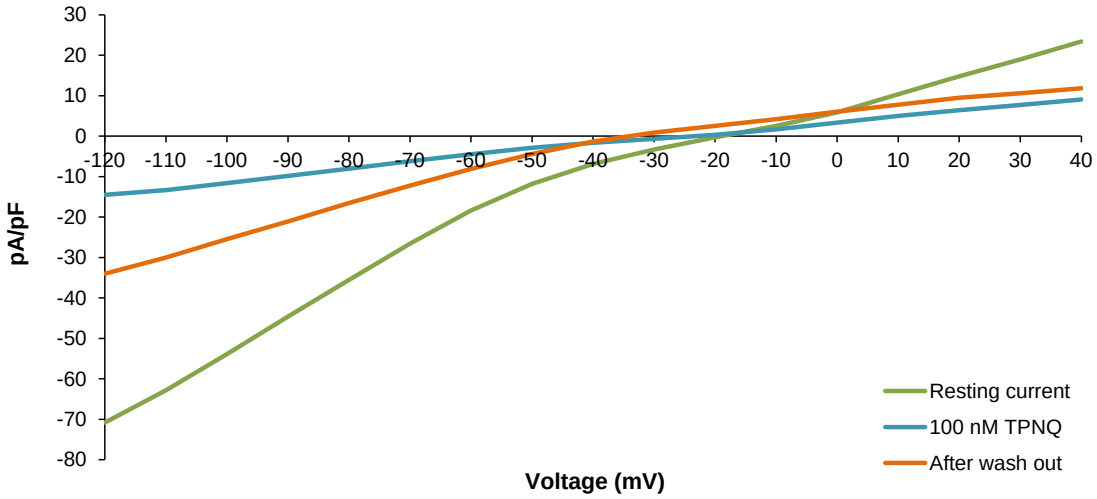

Figure 2.11: K^+ current (pA/pF) inhibition over a range of membrane potentials (mV) with 100nM tertiapin Q and K^+ current recovery after washing with extracellular solution.

These particular results were recorded after 25 minutes of perfusion with extracellular solution which suggests that current recovery is significantly slow. This experiment was repeated with similar results; only between 25-45% of the baseline current levels were ever observed. These findings are concurrent with others in the literature[95]; however there are also cases where more complete recovery is seen[88]. This variation is most probably due to the differing cell types employed and the limiting amount of time that patch-clamp recordings can be taken for as the seal on the cell membrane is easily lost.

This analysis of native tertiapin Q serves as a control for comparison with any modified derivatives synthesised.

2.2.3 Maleimide Modification of Tertiapin Q

With our study on native tertiapin Q complete, we turned to examining the scope of maleimide modification on this doubly disulfide bonded system. Initial studies employed non-functionalised maleimides for simplicity and ease of purification and analysis; if biological activity is retained using these then the desired functionalised maleimides could subsequently be employed. The products in Figure 2.12 were envisaged.

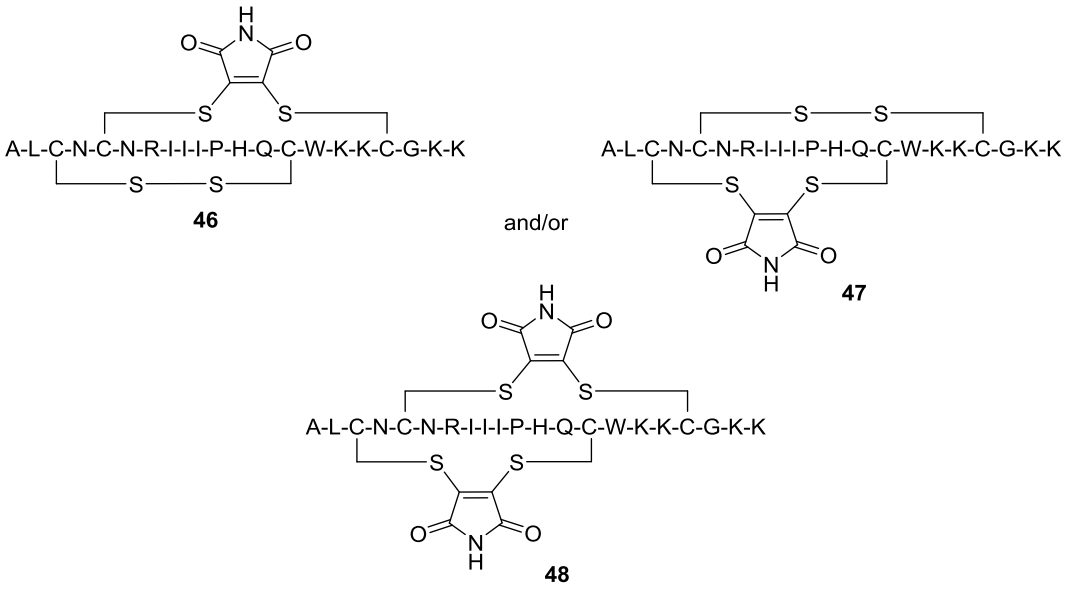

Figure 2.12: The envisaged products from bridging tertiapin Q disulfide/s with maleimide reagents: Singly modified products **46** and **47** and doubly modified product **48**.

2.2.4 Probing Disulfide Reactivity

Solvent accessibility of a disulfide bond within a peptide or protein is variable and sequence dependent and is an important factor to consider when attempting to modify a peptide or protein at this site. Increased accessibility often equates to increased reactivity as reagents can often reach the disulfide more easily.[53] In the case of tertiapin Q, being formed of only 21 amino acids means it has only limited tertiary structure; it lacks the hydrophobic core created in larger polypeptides and proteins during protein folding which helps bury the disulfide bonds and shield them from surrounding solvent. When studying the published NMR solution structure shown below in Figure 2.13, both disulfide look relatively solvent accessible but the C3-C14 disulfide perhaps a little more so. Only so much information can be taken from such an image however, and to what extent this expected accessibility is observed experimentally was of interest.

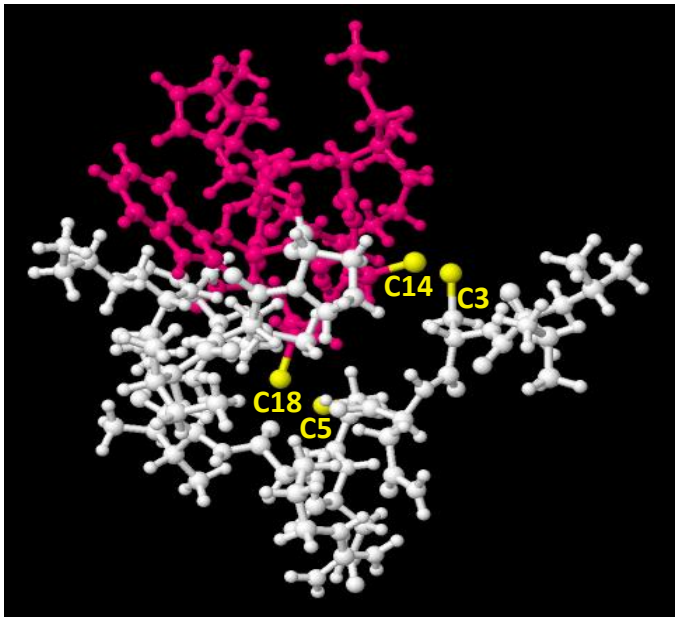

Figure 2.13: Three-dimensional solution structure (ball and stick representation) of tertiapin determined by NMR. Cysteines (cys3-cys14 and cys5-cys18) shown in yellow.[78]

In order to assess the accessibility of the two disulfides within the tertiary structure of tertiapin Q, an initial experiment was conducted to find out whether they were both solvent accessible and reactive. As in the step-wise protocol, the reducing agent is first added to the peptide and left to reduce for a given amount of time before 10 equivalents of dibromomaleimide **15** were subsequently added in each case to re-bridge any reduced disulfides (Scheme 2.9). The reducing agents TCEP and DTT were both tested for their efficacy in reduction, and were tested in varying equivalents. The effect of pH on the reactivity of the disulfides was also investigated.

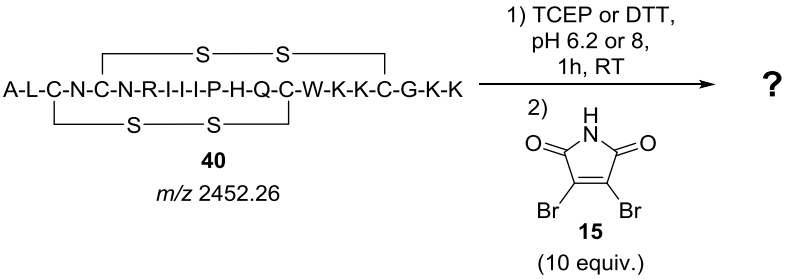

Scheme 2.9: Reduction and modification of the disulfide bond/s of tertiapin Q using TCEP or DTT (varying equivalents) in conjunction with maleimide **15** (10 equivalents) at pH6.2 or 8.

Formation of the singly modified products **46** and/or **47** and doubly modified product **48** were recorded by monitoring apparent conversion by LC-MS. The reaction mixture was injected into the LC-MS instrument and all product peaks from the LC trace selected for mass analysis. From the obtained mass spectrum, containing peptide ions in multiple

charge states, a deconvolution algorithm was run to facilitate ease of interpretation. A typical LC trace, mass spectrum and deconvoluted mass spectrum are shown in Figure 2.14 and 2.15 **A** and **B** – these are for reduced tertiapin Q, but are typical of all peptide species analysed.

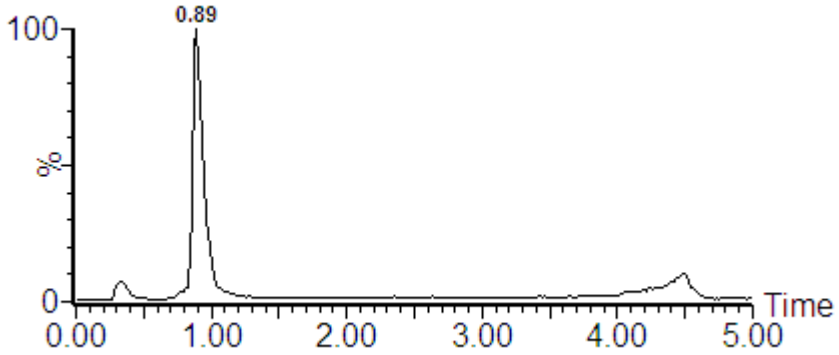

Figure 2.14: The LC chromatogram of reduced tertiapin Q. Peak eluting at 0.89 min was selected for mass analysis.

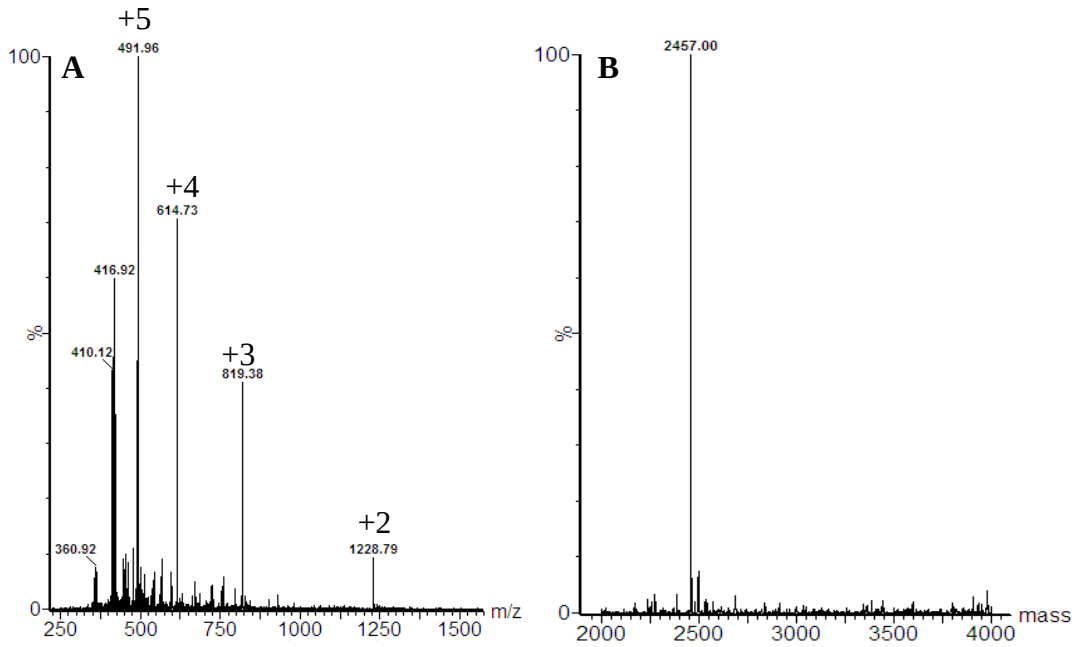

Figure 2.15: **A**) ESI mass spectrum of the chromatographic peak eluting at 0.89 min (Figure 2.14) corresponding to the +2, +3, +4 and +5 reduced tertiapin Q ions of *m/z* 1228.79, 819.38, 614.73 and 491.96 respectively. **B**) Deconvolution of spectrum **A**. Peak at *m/z* 2457 corresponding to reduced tertiapin Q (Expected mass = *m/z* 2456.29).

Upon reduction, the expected mass increase from *m/z* 2452 to *m/z* 2456 is observed upon protonation of the free cysteine thiolates. Incorporation of one maleimide bridge to produce product **46** and/or **47** sees a subsequent mass increase to *m/z* 2547, while incorporation of two maleimide bridges to produce the doubly modified product **48** sees

a mass increase to *m/z* 2642. Product formation was normalised to a total of 100%; the observed ratios are shown below in Table 2.3.

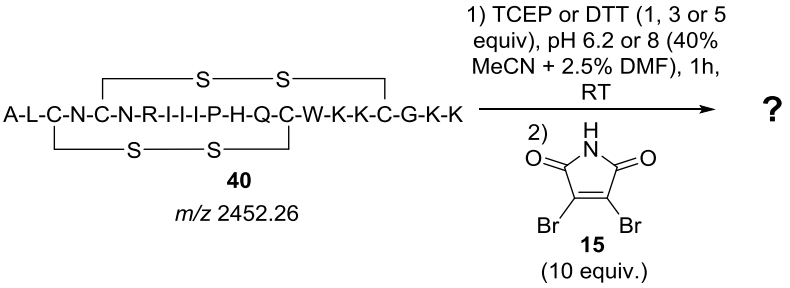

Scheme 2.10: Experimental conditions of the reduction study of tertiapin Q **40** using the reducing agents TCEP or DTT (1, 3 or 5 equiv.) for 1 h before addition of excess dibromomaleimide **15**.

Table 2.3: Reduction study of tertiapin Q: apparent conversion to singly modified peptide **46** and/or **47** and doubly modified peptide **48** under varying reaction conditions.

Experiment	*Reducing Agent*	*Time left reducing*	*pH*	*Amount of native TPNQ* **40***(%)*	*Amount of* **46**/**47** *(%)*	*Amount of* ***48*** *(%)*
1	TCEP (1 equiv.)	1h	6.2	37%	18%	45%
2	TCEP (3 equiv.)	1h	6.2	0%	0%	100%
3	TCEP (5 equiv.)	1h	6.2	0%	0%	100%
4	TCEP (1 equiv.)	1h	8	50%	0%	50%
5	TCEP (3 equiv.)	1h	8	0%	0%	100%
6	TCEP (5 equiv.)	1h	8	0%	0%	100%
7	DTT (2 equiv.)	3h	6.2	69%	0%	31%
8	DTT (5 equiv.)	3h	6.2	41%	0%	59%

With a significant excess (10 equivalents) of dibromomaleimide present, it should follow that any disulfide that is reduced will be subsequently bridged. When an excess of the reducing agent TCEP is used, both disulfides are modified; even 3 equivalents of TCEP is enough to fully reduce both bonds (experiments 2 and 5). This suggests that both disulfides are solvent accessible and can be reduced and re-bridged. This is as initially expected from studying the NMR structure of tertiapin Q (Figure 2.13).

In an attempt to reduce and modify just a single disulfide, the effect of adding sub-stoichiometric (with respect to disulfide bonds) amounts of TCEP was tested. The major products in these cases are the double-modified peptide **48** and the native peptide **40**

(experiments 1 and 4). Interestingly, very little of the single modified peptide is observed. This suggests that selective reduction of a single disulfide is not possible. The fact that formation of the double bridged peptide **48** is favourable suggests that when one disulfide is reduced the second then becomes more reactive to reduction. This could be reasoned by the slight alteration of the conformation of the peptide upon reduction of one disulfide bond, causing a slight change in the local environment of the second and resulting in a more favourable situation for its reduction. Alternatively, due to the proximity of the disulfide bonds in tertiapin Q, thiol-disulfide exchange reactions could potentially occur, whereby upon reduction of one disulfide to form two reactive cysteine thiolates, these could subsequently attack a cysteine residue of the neighbouring second disulfide, leading to its reduction.[149] Scheme 2.11 shows one permutation of this, but of course there would be multiple.

Scheme 2.11: One example of a thiol-disulfide exchange reaction occurring between two disulfides (R_1S-SR_2 and R_3S-SR_4).

Within such a system, the equilibrium constants of the disulfide exchange reactions depend on the differences in stability between the possible disulfide connectivities. Such intramolecular reactions are fast and naturally occur during the process of protein folding whereby the most stable disulfide arrangement is sought.[149] In this case, such exchange reactions would limit the selectivity that TCEP may have had for one disulfide over the other.

The effect of altering pH on the disulfide reactivity of tertiapin Q was tested. Environmental pH plays an important role in determining the reactivity of a disulfide; at a pH above the pKa of the cysteine thiol (-SH), which is approximately ~8.2 (depending on the structural context), the cysteine prefers to reside in its more reactive thiolate ($-S^-$) form. The thiolate is known to be ($5x10^{10}$)-fold more reactive than the protonated thiol and hence participates in reactions involving nucleophilic attack more readily.[150] When considering the conditions for site-selective modification, a compromise has to be made however. At pH 8, although cysteine reactivity is increased, the likelihood of other nucleophilic sites within the peptide or protein also increasing in reactivity is heightened. Lysine residues, for example, with a pKa of approximately 10.5, could

potentially react with a Michael acceptor such as a maleimide and cause unwanted side products. In the case or tertiapin Q, where there are four lysine residues within the amino acid sequence, this could potentially be a significant problem.[151] The experimental results show that increasing the pH to 8 has no significant effect on disulfide reactivity in the case of tertiapin Q, and so employing a pH 6 system will be more ideal. This will help prevent any unwanted lysine modification occurring.

Also notable from the results table is that DTT does not show greater efficacy in reduction of the disulfides in comparison to TCEP. This is a beneficial result as, due to the fact that DTT is itself a thiol and will therefore react with a maleimide reagent, it would have to be removed from the reaction prior to maleimide addition to ensure an efficient reaction and complete conversion to the desired product. To remove unwanted reagents, a purification method is needed, during which re-oxidation to the disulfide is an unwanted but likely result.[151] Instead employing TCEP removes the issues of maleimide cross-reactivity.

To conclude from this analysis, the most significant observation is that, despite sub-stoichiometric amounts of reducing agent, both disulfides on tertiapin Q appear accessible and, as a result, are reactive towards the reducing agents and bridging reagents used in this project.

2.2.5 Step-Wise Modification of Tertiapin Q

From the reactivity study, it was apparent that obtaining solely the singly bridged products **46** and/or **47** was going to be challenging. For this reason, we concentrated on obtaining complete conversion to the doubly bridged product **48**. Providing that the cysteines are joined in the native connectivity and that the incorporation of a two carbon bridge between the two residues does not have a detrimental effect on the structure of the peptide, incorporating two maleimides as opposed to one was not envisaged to pose a problem. The step-wise protocol employed in Section 2.2.4 proved efficient in formation of the desired product. In order to facilitate ease of purification and reduce chances of reagent cross reactivity, a dithiophenolmaleimide reagent was chosen. Maleimide **45** presented itself as ideal due to its high reactivity previously observed with somatostatin modification, and also its water-solubility. Employing this reagent meant that tertiapin Q was successfully converted to the doubly modified derivative **48**,

using minimal equivalents of reagent in completely organic solvent-free conditions (Scheme 2.12)

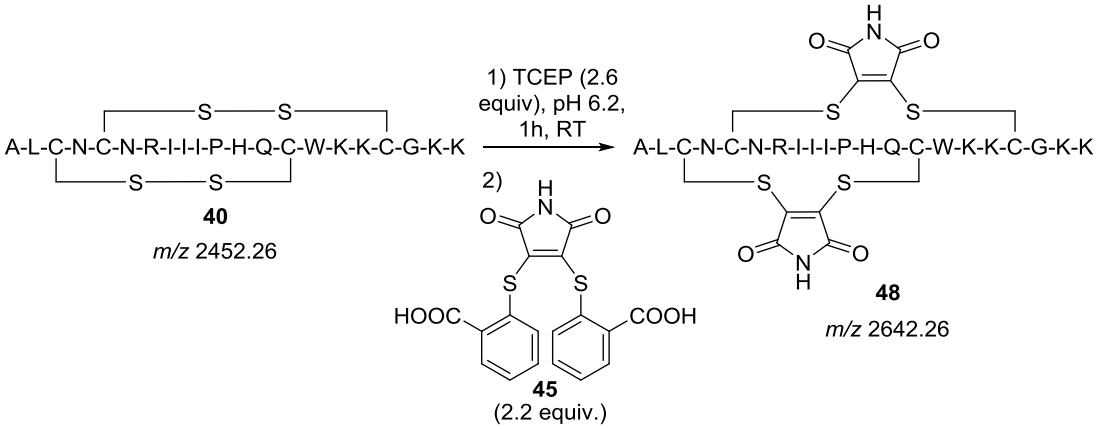

Scheme 2.12: The step-wise modification protocol: reduction using TCEP (2.6 equiv.) for 1 h followed by addition of maleimide **45** (2.2 equiv.).

Using this protocol, clean conversion to the doubly bridged product **48** (Figure 2.16) was observed within 10 minutes of addition of maleimide **45** to the reduced peptide.

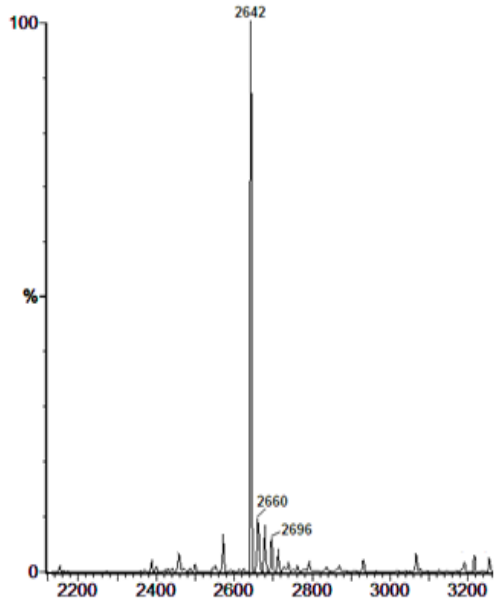

Figure 2.16: Deconvoluted mass spectrum of the reaction mixture. Peak at *m/z* 2642 corresponding to doubly modified tertiapin Q **48** (Expected mass = *m/z* 2642.27).

Despite almost stoichiometric reagent ratios, for accurate characterisation and future biological testing, purification of the desired product was required. Attempts to use dialysis to filter off any remaining TCEP and maleimide and to remove the salts from the buffer employed were unsuccessful. The yield of recovered product dropped by 70-80% repeatedly. This was hypothesised to be due to the small and hydrophilic nature of

the peptide making it difficult to retain. RP-HPLC purification presented itself as a superior method, providing further analysis of the modification reaction as well as a means of purification. Injection of the reaction mixture onto the C18 RP-column allowed the separation of four different species. The LC chromatogram from the reaction mixture is shown below in Figure 2.17, with the species labelled **A**-**D**.

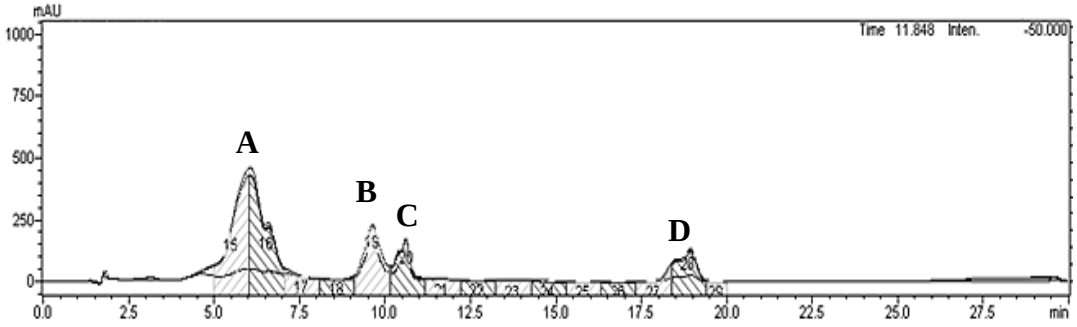

Figure 2.17: LC chromatogram of the reaction mixture (Retention time of **A**: 6.0 min, **B**: 9.5 min, **C**: 10.5, **D**: 18.5-19.0 min).

A more complex mixture of product than expected was observed in the chromatogram. In order to determine the nature of these products they were isolated, concentrated under vacuum and characterised by MALDI mass spectrometry. Peaks **C** and **D** appeared not to consist of peptide-based products. Surprisingly, both peaks **A** and **B** proved to be the doubly modified product **48**, as shown in the mass spectra in Figure 2.18.

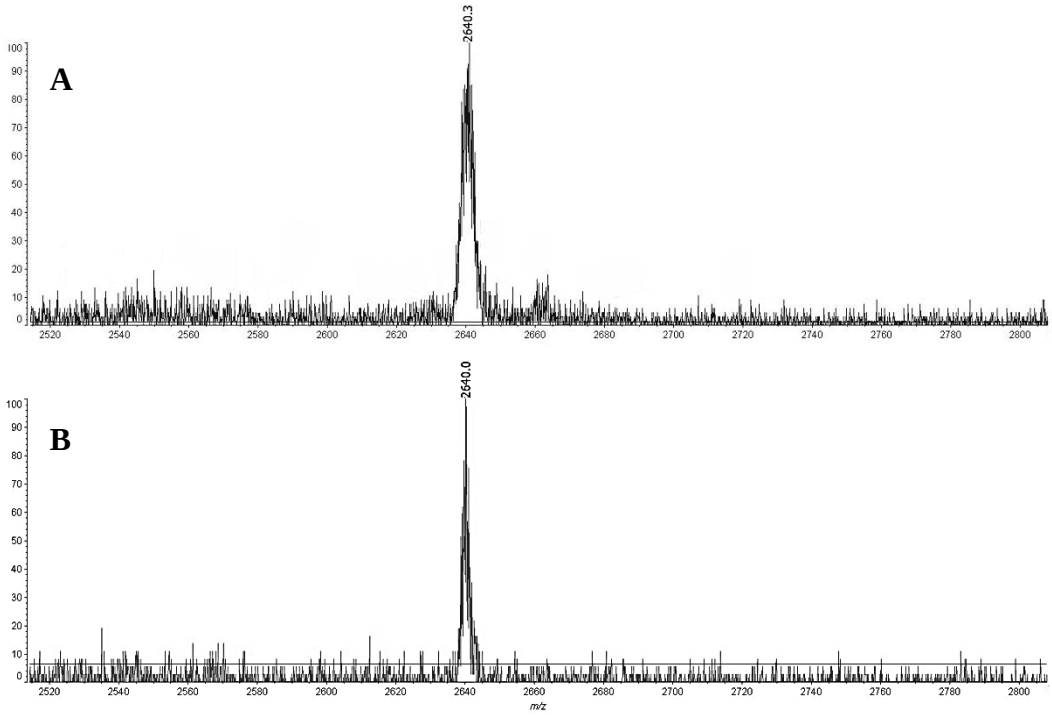

Figure 2.18: MALDI mass spectra of peaks **A** and **B** from the LC chromatogram in Figure 2.17. Peaks at *m/z* 2640.3 and *m/z* 2640.0 respectively correspond to the doubly modified peptide **48** (Expected mass = *m/z* 2642.26).

The fact that both peaks represented species of the same mass, yet were differentially eluted from the column, suggests they vary in configuration or conformation. It was hypothesised that **A** and **B** could be regioisomers from differing cysteine-cysteine connectivity. In the protocol used, the disulfide bonds are left to reduce for one hour in which time tertiapin is able to unfold, facilitated further by its limited secondary structure which would normally help keep the peptide together. It seems, therefore, not unlikely that upon addition of the maleimide reagent, incorrect cysteine pairing could result as a consequence of partial or complete unfolding. In addition, if the previously proposed thiol-disulfide exchange reactions are occurring during reduction, then this again would also facilitate the bridging of a non-native pair of cysteines. Subsequent to isolation and concentration, the modified peptide in both **A** and **B** was reconstituted in distilled water and the peptide concentration determined using the absorbance at 280 nm. **A** was found to have a concentration of 136 μM and **B** of 306 μM and, from this, a yield of 23% and 52% was calculated respectively. This suggests the latter was the more predominantly formed product from this reaction, with the cumulative yield of doubly modified peptide **48** calculated to be 75% after RP-HPLC purification.

Following these findings, efforts focussed on determining whether biological activity of the modified peptide had been retained. Whole-cell patch clamp experiments were undertaken, analogous to those carried out on native tertiapin Q. HEK293 cells stably expressing the GIRK1/4 channel were again employed. The modified tertiapin Q samples **A** and **B** were kept separate at all times and prepared over a range of concentrations (from 1 nM to 100 nM). These solutions were perfused over the cells in a sequential manner with increasing concentration. Negligible inhibition of the GIRK1/4 channels by either sample **A** or **B** was seen in this case, as shown in Table 2.4.

Table 2.4: Changes to K^+ current levels through GIRK1/4 channels after administration of 100 nM **A** or 100 nM **B**.

Experiment	*Current remaining after addition of 100 nM of* **A** *(%)*	*Current remaining after addition of 100 nM of* **B** *(%)*
1	98	95
2	96	98
3	98	92
Average	97	95

From the results in Table 2.4, almost maximal current is observed in each case; the doubly modified derivatives appeared unable to block the GIRK1/4 channel and K^+ flux. To ensure that this was not due to very low channel expression, native tertiapin Q was also tested on the cells (data not shown) and the expected current inhibition was observed confirming the GIRK1/4 channel was present and functional.

To ensure that the loss of inhibitory activity of the peptide was not a result of the purification method, a simple control was conducted. Low pH environments caused by addition of acid to the solvents in HPLC protocols can lead to protein unfolding and denaturation in some cases.[152] In our protocol, 0.1% TFA is added to both eluents, lowering the pH to around pH 2. Perhaps this caused unfolding of the peptide. To examine whether the RP-HPLC procedure caused loss of activity, native tertiapin Q was subjected to the same RP-HPLC protocol as employed above and was concentrated and prepared for testing identically. Results showed that the 'purified' native peptide retained biological activity (data not shown) concluding that, as expected, the purification method was not an issue.

It therefore seemed conclusive that the inactivity of the modified peptide was a result of maleimide modification of the disulfide bonds. Even small distortions to a peptide or protein's tertiary structure can be detrimental and perhaps tertiapin Q cannot tolerate such modification. In addition, if the maleimides have bridged the cysteine residues in incorrect pairs then this is likely to abolish biological function; this can be easily reasoned in this case where a step wise protocol was employed. An *in situ* method was sought in order to overcome the problem.

2.2.6 *In Situ* Modification of Tertiapin Q

Preliminary *in situ* method development began - maleimide **45** was again employed so that aqueous conditions could be used in every attempt to not perturb the tertiary structure of tertiapin Q. Tertiapin Q was firstly incubated with 5 equivalents of maleimide **45**, before addition of varying amounts of TCEP as shown in Scheme 2.13. Product formation was again monitored by apparent conversion by LC-MS. An unexpected side product was observed during the reaction. Results are displayed in Table 2.5.

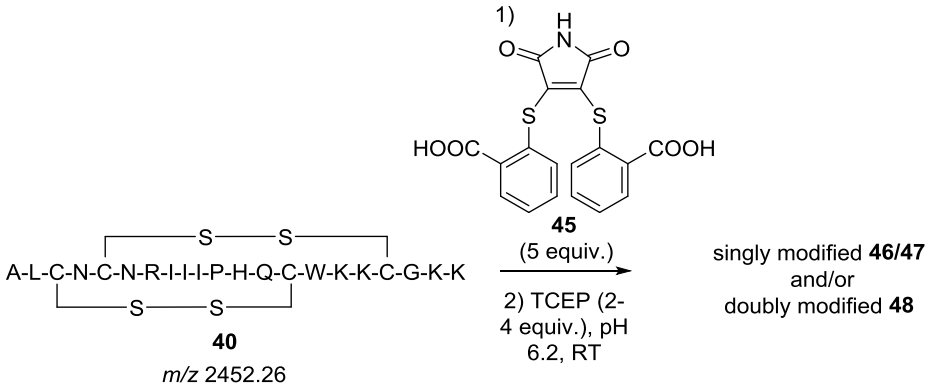

Scheme 2.13: The *in situ* modification protocol using maleimide **45** (5 equiv.) and TCEP (2-4 equiv.).

Table 2.5: Product formation (by apparent conversion by LC-MS) after 5 minutes using maleimide **45** (5 equiv.) with varying equivalents of TCEP (2-4 equiv.).

No. of equivalents of TCEP	Native TPNQ (%)	Singly Bridged TPNQ **46/47** (%)	*m/z 2798 product (%)*	*Doubly Bridged TPNQ* **48** *(%)*
2	37	43	-	20
3	9	9	77	5
4	8	9	77	6

In this case, formation of the doubly bridged product **48** appears to be hindered by the formation of a side product. Deconvolution of the recorded mass spectra revealed this product to be of *m/z* 2798. It was predicted that this could be as a result of one of two products, the first arising from addition of TCEP to the singly bridged product and has *m/z* 2797 (**49**), and the second from retention of thiosalicylic acid on the doubly bridged product with *m/z* 2796 (**50**) (Figure 2.19).

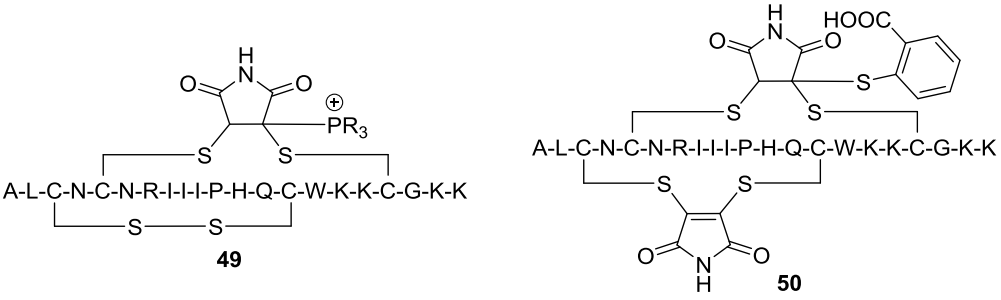

Figure 2.19: The possible adducts **49** and **50** formed in the *in-situ* reaction.

In order to determine for certain the nature of this adduct, the *in situ* experiment was carried out using thiophenolmaleimide **22**. If the adduct is formed by retention of the

eliminated leaving group, which is now thiophenol, then in this case the mass of the adduct formed will be *m/z* 2751. As before, 5 equivalents of maleimide **22** were incubated with tertiapin Q before addition of TCEP, 2 equivalents in this case, and the reaction monitored over time. The results are shown in Table 2.6.

Table 2.6: Product formation (by apparent conversion by LC-MS) over time using maleimide **22** (5 equiv.) with 2 equivalents of TCEP.

No. of equivalents of TCEP	*Reaction Time (mins)*	*Native TPNQ (%)*	*Singly Bridged TPNQ* **46/47** *(%)*	*m/z 2751 product (%)*	*Doubly Bridged TPNQ* **48** *(%)*
2	1	81	19	-	-
2	15	32	23	-	45
2	30	5	0	-	100

From these results we can confirm that the adduct cannot be from attack by TCEP, as none of the *m/z* 2798 adduct is observed. However, there was also no evidence of the *m/z* 2751 adduct corresponding to retention of a thiophenol moiety. This suggests that the adduct formed using maleimide **45** is characteristic of that maleimide reagent solely. This is postulated to be as a result of the ability of the carboxylic acid group, when existing as the carboxylate, to form a stabilising salt bridge with the maleimide nitrogen. This may well limit its utility in an *in situ* protocol.

Undeterred by this, we revised our *in situ* protocol. We decided to compromise on an organic solvent-free system in order to use a maleimide with no side reactivity. We also decided to investigate benzeneselenol as reducing agent; this requires organic solvent to keep it in solution, unlike TCEP which is water soluble, however it showed significantly rapid bridging speeds on previous experiments with somatostatin in Section 2.1.7. Maximising the speed at which the disulfides are re-bridged upon reduction should help to reduce the likelihood of peptide unfolding and disulfide scrambling.[24]

Analogous to the benzeneselenol protocol employed with somatostatin, we employed maleimide **22** as the bridging reagent. 20 equivalents of maleimide **22** were added to tertiapin Q before addition of 1.1 equivalents of benzeneselenol. Product formation was monitored over time by LC-MS. Results are shown in Figure 2.20.

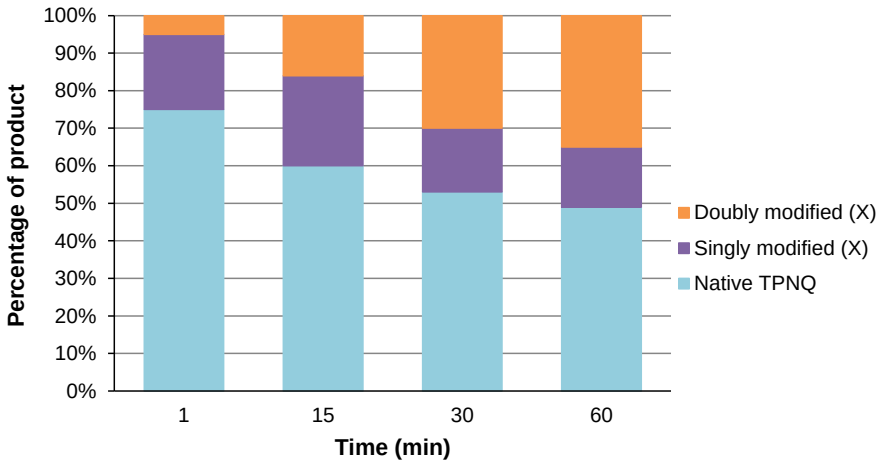

Figure 2.20: Product formation of singly modified product **46**/**47** and doubly modified product **48** over time using 1.1 equivalents of benzeneselenol.

Similarly to TCEP, using 1.1 equivalents of benzeneselenol does not give selective modification of a single disulfide; formation of the doubly modified product **48** is observed as soon as after 1 minute. This sub-stoichiometric amount of benzeneselenol appears not to be sufficient to push the reaction to completion. Despite being catalytic in disulfide reduction, selenols have the propensity to oxidise to form the diselenide when exposed to air which hinders their reductive potential. As a result, an excess is often required to compensate for this. As disulfide selectivity appeared again not possible, the reaction was repeated using 5 equivalents of benzeneselenol in order to achieve complete conversion to the doubly modified peptide **48**. Results are shown in Figure 2.21.

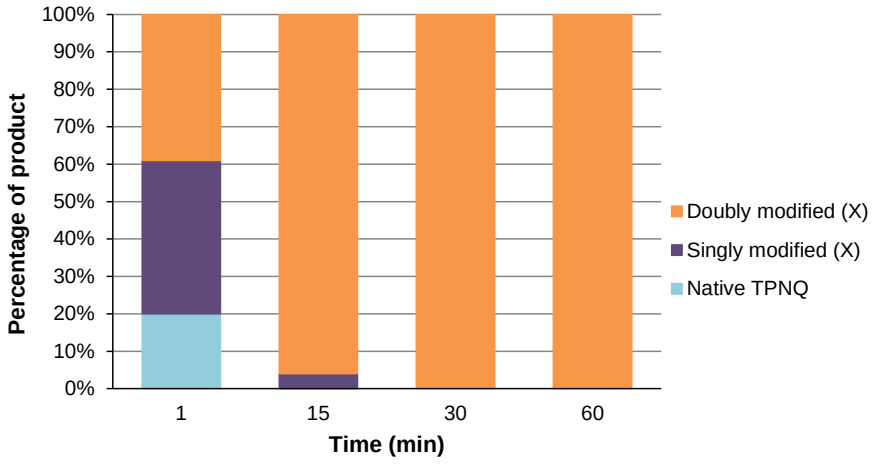

Figure 2.21: Product formation of singly modified product **46**/**47** and doubly modified product **48** over time using 5 equivalents of benzeneselenol.

Using 5 equivalents of benzeneselenol gave efficient conversion to the doubly modified product **48**, with no unwanted side products observed. In these reactions, 20 equivalents

of maleimide **22** were used; further experiments revealed that as little as 5 equivalents gave the same efficient conversion (data not shown).

With the desired product in hand, it was purified by RP-HPLC to remove any excess reagents, buffer salts and organic solvents. Chromatographic separation revealed three products, **A**-**C**. The LC chromatogram is shown in Figure 2.22.

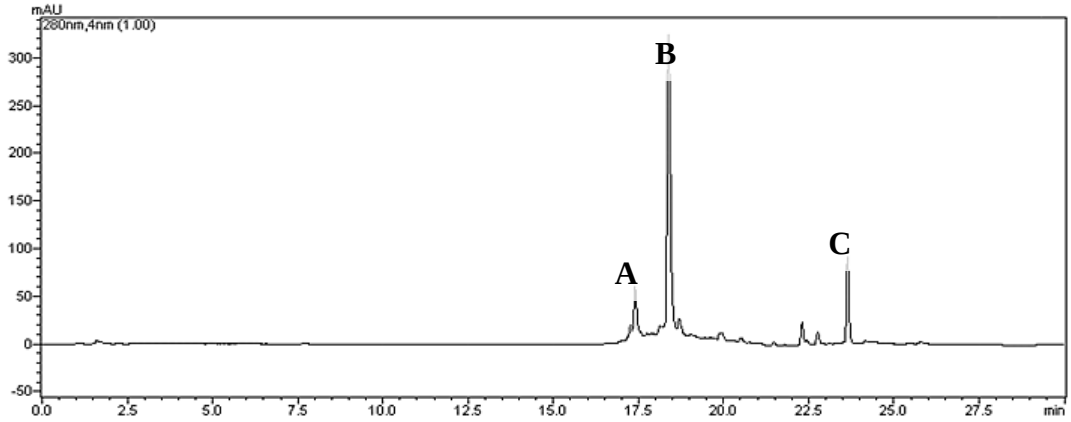

Figure 2.22: LC chromatogram of the reaction mixture (Retention time of **A**: 17.25 min, **B**: 18.5 min, **C**: 23.75 min).

The LC chromatogram showed one main product (peak **B**) believed to be the desired doubly modified product **48**. To determine whether peak **A** or **C** was unreacted peptide, the reaction mixture was co-injected with native tertiapin Q **40**. The LC chromatogram is shown in Figure 2.23.

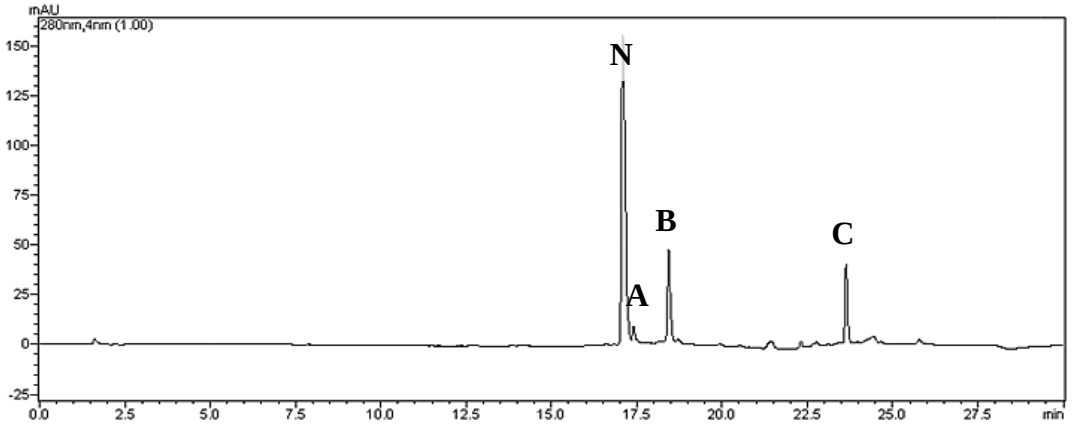

Figure 2.23: LC chromatogram of the co-injection of the reaction mixture and native tertiapin Q (Retention time of **N**: 17.0 min, **A**: 17.25 min, **B**: 18.5 min, **C**: 23.75 min).

Native tertiapin Q (peak **N**) does not appear to directly co-elute with either **A** or **C**. Peaks **A**-**C** were carefully isolated before characterisation by MALDI mass

spectrometry. Peaks **A** and **C** appeared not contain peptide-based products and the spectra obtained were messy and uninterpretable. The spectrum of peak **B** is shown in Figure 2.24, and confirms the formation of the desired doubly modified peptide **48**.

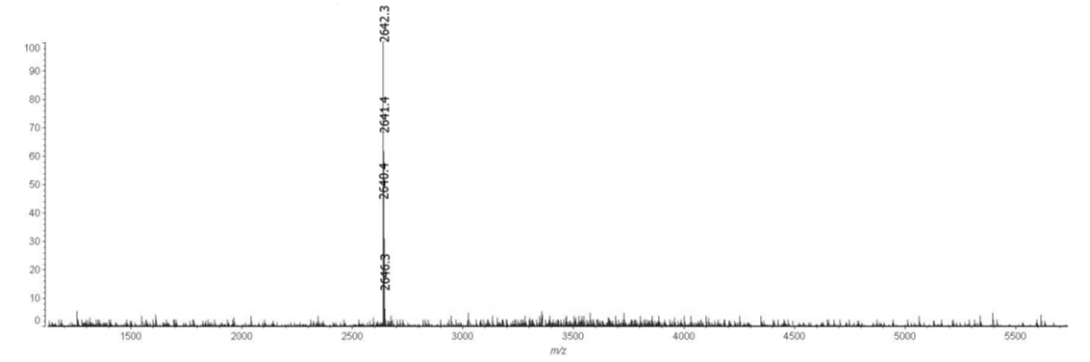

Figure 2.24: MALDI mass spectra of peak **B** from the LC chromatogram in Figure 2.22. Peak at *m/z* 2642.3 corresponds to the doubly modified peptide **48** (Expected mass = *m/z* 2642.26).

Pleasingly, a very clean mass spectrum was obtained from the RP-HPLC purification and this product was taken on for biological testing to determine whether inhibitory activity had been retained by disulfide modification through the *in situ* protocol. Whole-cell patch clamp experiments were conducted. HEK293 cells stably expressing the GIRK1/4 channel were again employed. The modified tertiapin Q was prepared at a concentration of 100 nM and perfused over the cells whilst monitoring for inhibition of the K^+ currents. Again, disappointingly, negligible inhibition of the GIRK1/4 channels was observed, as shown in Table 2.7.

Table 2.7: Changes to K^+ current levels through GIRK1/4 channels after administration of 100 nM native tertiapin Q or 100 nM of purified **B** (doubly modified product **48**).

Experiment	*Current remaining after administration of 100 nM native TPNQ (%)*	*Current remaining after administration of 100 nM **B** (%)*
1	17	87
2	12	92
3	14	104
Average	14	94

Similarly to tertiapin Q modified by the step wise protocol, biological activity of the peptide appears to have been abolished by incorporation of the maleimide bridges. An

average of 94% of the resting current was recorded even after continuous perfusion with the modified peptide. This suggests that this *in situ* protocol, which has been designed to reduce potential disulfide scrambling by facilitating rapid bridging upon reduction, does not maintain the correct tertiary structure of tertiapin Q.

We were interested in deciphering whether the loss of activity was due to the structural influence of the maleimide bridge on the peptide structure or rather as a result of disulfide scrambling from incorrect cysteine-cysteine connectivity. The former seemed less likely as maleimide modification of somatostatin, which again is a small peptide with limited tertiary structure, demonstrated retention of biological activity.[24] It should be noted, however, that the concentration of modified somatostatin tested in this case was 20 μM – more than an order of magnitude greater than the EC_{50}[iii] of the native peptide, making it not truly comparable to the native situation. The relatively small size of the maleimide in comparison to the peptide itself also adds to the premise that it should not significantly interfere with tertiary structure. All systems should be seen as unique, however, and this should not be overlooked as a possibility.

For these reasons, disulfide scrambling was the more probable scenario, thus, we decided to focus our efforts on trying to establish whether this had occurred. For this, we turned to tandem mass spectrometry. Initially, we collaborated with Dr. Kostas Thalassinos, UCL. Using their equipment and expertise, we were able to conduct ion-mobility-tandem mass spectrometry (IM-MS/MS) analysis on a hybrid quadrupole-ion mobility-orthogonal acceleration time-of-flight (oa-TOF) mass spectrometer (Synapt HDMS, Waters).[153]

Tandem mass spectrometry (MS/MS), as its name implies, utilises two mass spectrometers in tandem. The first detects all species within the introduced sample, the species of interest (parent ion) is then selected and subsequently fragmented within a collision cell to produce a series of fragments (daughter ions) which are detected in the second mass analyser (Figure 2.25). The end result is a mass spectrum containing ions characteristic of the selected peptide species from which information regarding the structure and amino acid sequence can be obtained.[154]

[iii]The EC_{50} of a substance is defined as the half-maximum effective concentration.

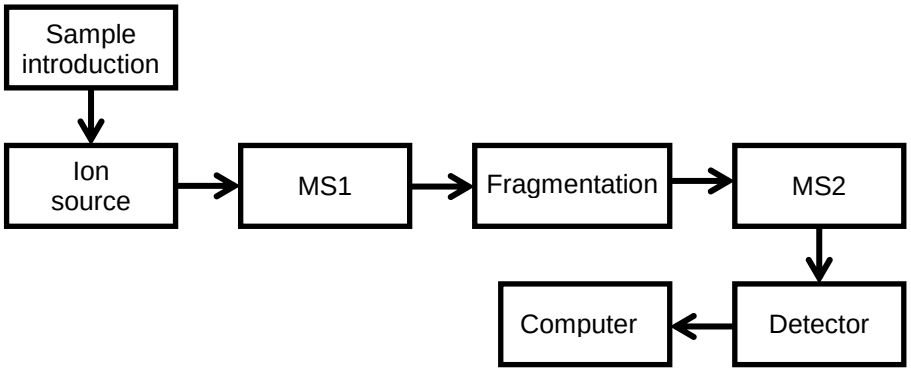

Figure 2.25: The stages of MS/MS analysis; after sample introduction, the species are ionised prior to *m/z* separation at MS1. After manual selection for the species of interest, the species is fragmented in a collision cell filled with an inert gas. A second round of *m/z* separation occurs before fragment ions arrive at the detector and are recorded.

MS/MS has become an increasingly useful and popular technique for the structural characterisation and analysis of complex molecules as a result of its great accuracy, efficiency and sensitivity. In addition, the information obtained from such a technique allows for the localisation of post-translational or chemical modifications at the amino acid residue level.[155,156] In theory, it should be possible to unequivocally locate the site of maleimide modification within the sequence of tertiapin Q, providing good fragmentation can be achieved.

Fragmentation of peptides requires the involvement of a proton at the cleavage site, in other words it is 'charge-directed'. It therefore follows that, if an amino acid side-chain tightly binds or 'sequesters' that proton, increased energy will be required to move that proton from the basic side-chain to the peptide backbone, in order to induce the dissociation event. The nomenclature of the daughter ions generated during such fragmentation was originally established by Roepstorff and Fohlmann,[157] and later revised by Biemann,[158] and describes the fragments extending from the *N*-terminal as *b*-ions and those extending from the *C*-terminal as *y*-ions (Figure 2.26).

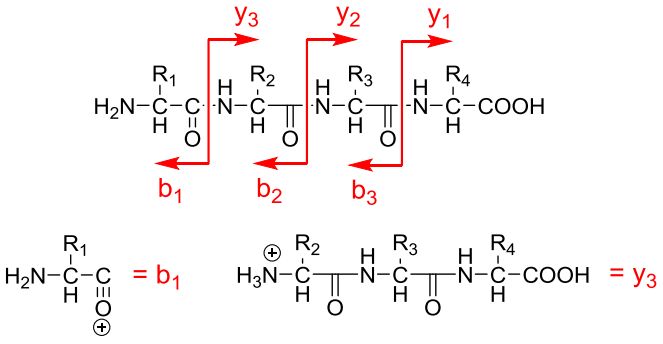

Figure 2.26: Fragmentation paths yielding *b*- and *y*-ions characteristic of an amino acid chain.

A peptide species will have a characteristic fragmentation pattern which is governed largely by its amino acid sequence and depends on how readily the peptide can be cleaved at each site within this sequence.[156] In order to assess the intrinsic fragmentation pattern of tertiapin Q, MS/MS analysis of the native peptide was undertaken, both in the oxidised and reduced state. As can be expected, the oxidised tertiapin Q did not fragment well owing to the compact and rigid nature of the peptide; the disulfide bonds serving to limit the number of possible dissociation sites. Conversely, reduced tertiapin Q exists in a much more open and extended conformation, making fragmentation easier and, thus, more complex yet conclusive MS/MS spectra are obtained. The peptide was introduced to the instrument by direct infusion ESI and the full mass spectrum was recorded. The spectrum yielded the doubly, triply, quadruply and quintuply charged ions, as shown in Figure 2.27.

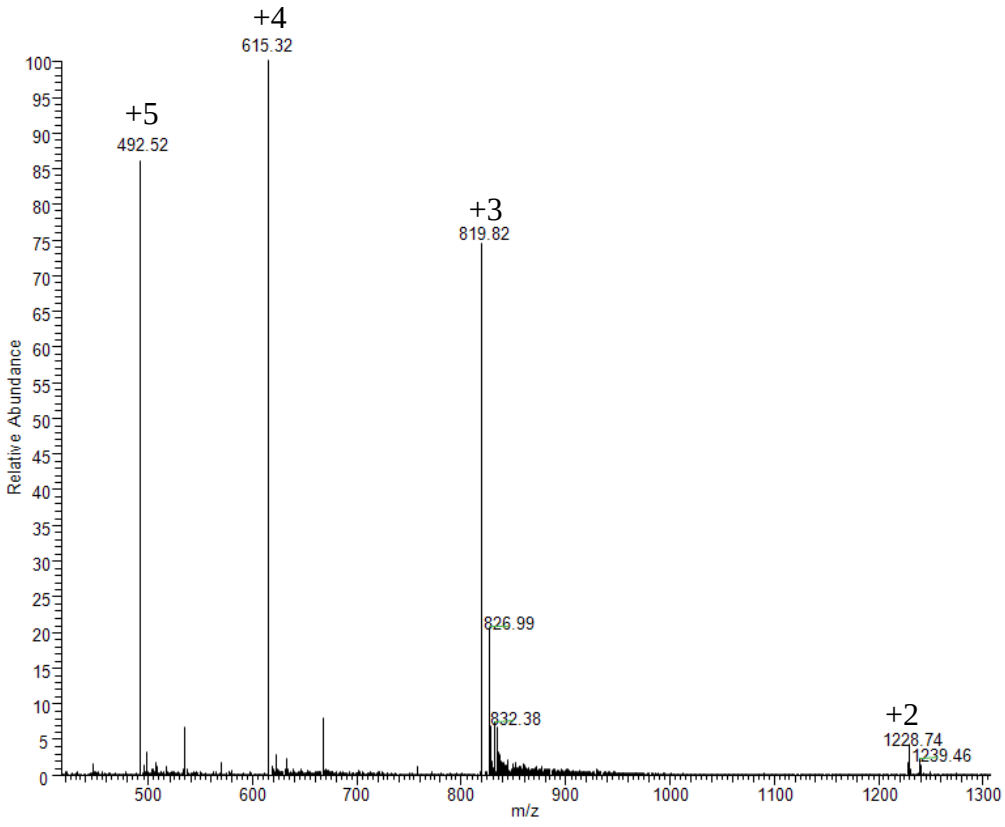

Figure 2.27: Full MS of reduced tertiapin Q recorded at a peptide concentration of ~500 pg/µL in water + 0.1% formic acid. Peaks correspond to the +2, +3, +4 and +5 reduced tertiapin Q ions of *m/z* 1228.74, 819.82, 614.32 and 492 respectively.

After isolation of the species of interest, this was subjected to manually controlled collision energies in order to fragment the peptide. The resulting fragments were then conveyed to a TOF-mass analyser and the MS/MS spectra was recorded. If few fragments were detected by the mass analyser, the collision energy was increased

accordingly to produce spectra with maximum information. The MS/MS spectrum of the doubly charged reduced peptide ion at *m/z* 1228.74 is presented in Figure 2.28, showing the fragments b_9, b_{10}, b_{11}, b_{13}, b_{14}, b_{15}, b_{16}, y_{11}, y_{12}, y_{13} and y_{14}.

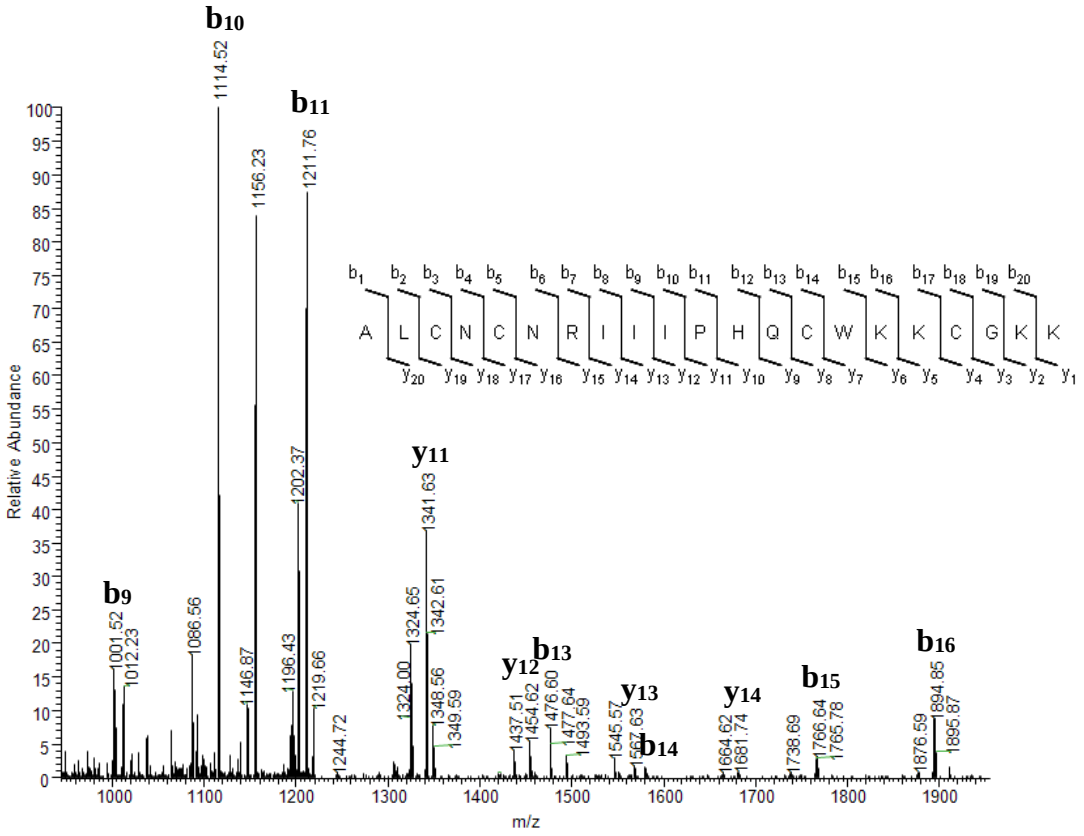

Figure 2.28: MS/MS spectrum of the +2 reduced tertiapin Q ion at *m/z* 1228.74. Shown in the inset is the peptide's amino acid sequence, *b*- and *y*-ions are formed by peptide bond cleavage with charge retention on the *N*- and *C*-termini.

The reduced peptide fragments well, with the most intense fragment peaks being those of the b_{10} and b_{11} ions, which are the sites either side of the proline-11 residue. This suggests the amide bonds connecting proline are significantly more labile. With the characteristic fragmentation of native tertiapin Q examined, work progressed on to locating the maleimide modification in our product. A mass increase corresponding to the monoisotopic mass of a maleimide bridge should be observed within the spectra.

Work began by determining the possible number of regioisomers that could arise from inserting two maleimide bridges in between the four cysteine residues of tertiapin Q. Similarly to natural disulfide formation through oxidation, the number of possible connectivities increases with increasing number of cysteine residues. Sela and Lifson[159] described the formula for the number of regioisomers (*i*) formed when *n* cysteine residues oxidise to form *p* disulfide bonds as:

$$i = \frac{n!}{p!(n\text{-}2p)!2^p}$$

This is assuming all cysteines are in an appropriate environment and are suitably close enough to form a bond. In the case where all cysteine residues within the peptide or protein participate in disulfide bonding, the formula can be simplified to:

$$i = \frac{n!}{(n/2)!2^{(n/2)}}$$

In the case of tertiapin Q with its four cysteine residues, there are three possible disulfide regioisomers and, thus, three possible ways in which a maleimide could bridge the fully reduced peptide. These are shown schematically in Figure 2.29.

C3-C14/C5-C18 (native) connectivity:

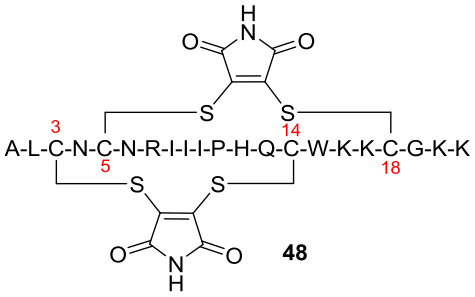

C3-C5/C14-C18 connectivity:

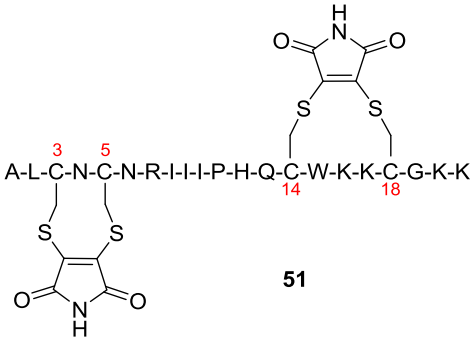

C3-C18/C5-C14 connectivity:

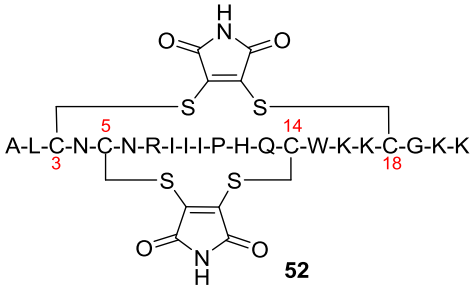

Figure 2.29: The three possible cysteine-cysteine connections in a doubly maleimide modified tertiapin Q **48** (native connectivity) and **51** and **52** (scrambled connectivities).

Using these predictions, a library of possible peptide fragments which could occur from each cysteine-cysteine connection was created. This was done by taking each case, and removing amino acids consecutively from both the *N*-terminus (creating *y*-ions) and *C*-terminus (creating *b*-ions) and accurately calculating the mass of each of these theoretical fragment species.

With this library in hand (see Appendix Tables 3, 4 and 5), experimental analysis began. As before with native tertiapin Q, the purified product **48** was introduced to the instrument by direct infusion ESI and the species of interest is then selected for. The triply, quadruply and quintuply charged ions were observed, as shown in Figure 2.30.

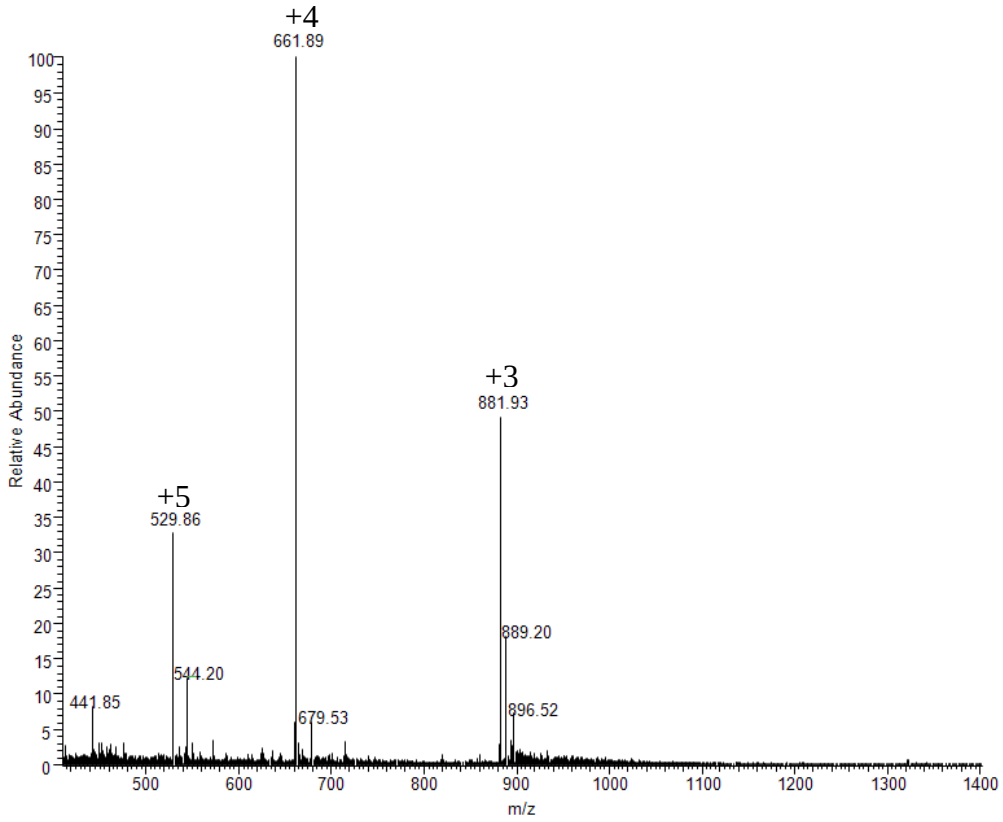

Figure 2.30: Full MS of doubly modified tertiapin Q **48** recorded at a peptide concentration of ~500 pg/µL in water + 0.1% formic acid. Peaks correspond to the +3, +4 and +5 modified tertiapin Q ions of *m/z* 881.93, 661.89 and 529.86 respectively.

Subsequent fragmentation of the *m/z* 881.93, 661.89 and 529.86 ions generated MS/MS spectra. Analysing the MS/MS spectra of the triply charged peptide ion gave quite conclusive results. From searching our fragment library for species that correspond exclusively to one of the three possible regioisomers, a number of matching masses were identified.[160] The data suggested in was in fact one of the scrambled variants

produced, specifically the C3-C5/C14-C18 regioisomer. From the MS/MS spectrum in Figure 2.31, the b_8, b_9, b_{10}, y_{10} and y_{11} ions can be seen.

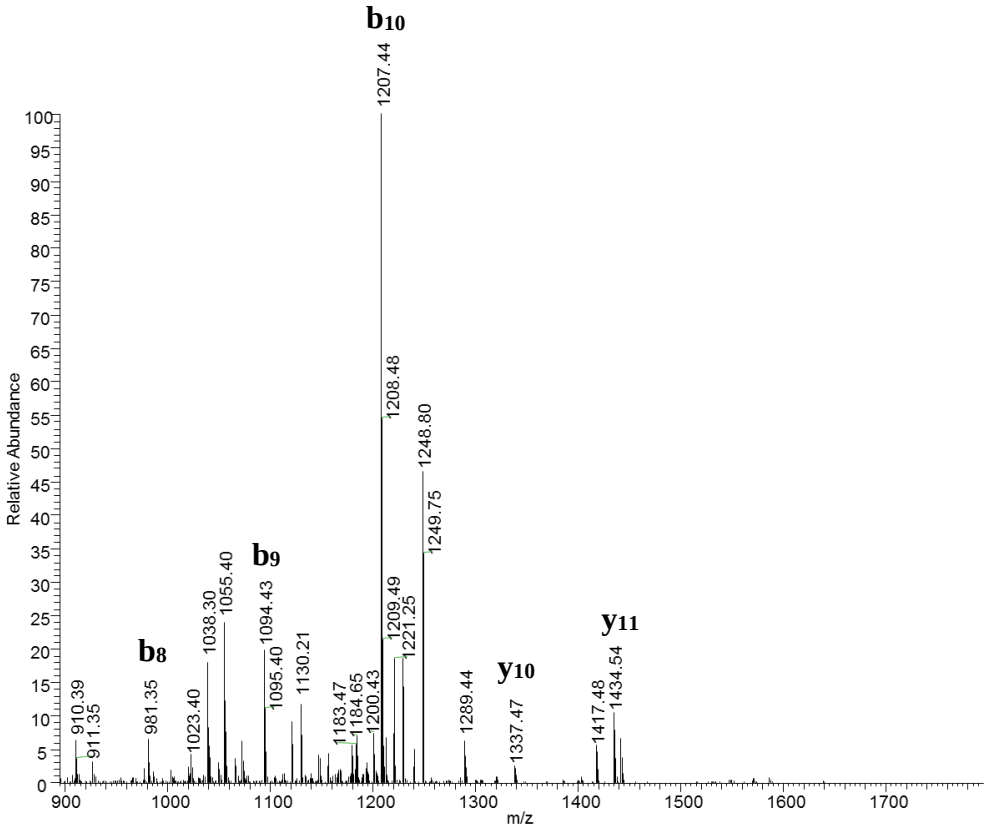

Figure 2.31: MS/MS spectrum of the +3 modified tertiapin Q ion at *m/z* 881.93.

In addition to the species labelled in the spectrum, other fragment species were also identified and are listed in Table 2.8. In this case, the monoisotopic masses calculated and the mass ions experimentally observed incorporate the mass of a maleimide bridge. The way in which the modified peptide fragments well between cysteine 5 and cysteine 14, and that the fragments within this region all incorporate the exact mass associated with addition of a maleimide bridge give sound evidence to prove the incorrect bridging connectivity. The C3-C5/C14-C18 regioisomer (**51**) appears to be the product formed from the modification reaction.

Table 2.8: The expected and observed fragment peaks from the MS/MS spectra of doubly modified tertiapin Q. (+ mal = + mass of maleimide bridge).

Fragment	*Sequence*	*Regioisotope connectivity*	*Expected monoisotopic mass (m/z)*	*Observed mass (m/z)*
b_5	ALCNC + mal	C3-C5/C14-C18	598.18	598.17
b_6	ALCNCN + mal	C3-C5/C14-C18	712.22	712.23
b_7	ALCNCNR + mal	C3-C5/C14-C18	868.32	868.34
b_8	ALCNCNRI + mal	C3-C5/C14-C18	981.40	981.35
b_9	ALCNCNRII + mal	C3-C5/C14-C18	1094.49	1094.43
b_{10}	ALCNCNRIII + mal	C3-C5/C14-C18	1207.57	1207.44
b_{11}	ALCNCNRIIIP + mal	C3-C5/C14-C18	1304.62	1304.67
b_{12}	ALCNCNRIIIPH + mal	C3-C5/C14-C18	1441.68	1441.71
b_{13}	ALCNCNRIIIPHQ + mal	C3-C5/C14-C18	1569.74	1569.77
y_{10}	KKGCKKWCQH + mal	C3-C5/C14-C18	1337.64	1337.47
y_{11}	KKGCKKWCQHP + mal	C3-C5/C14-C18	1434.69	1434.54
y_{12}	KKGCKKWCQHPI + mal	C3-C5/C14-C18	1547.75	1547.78

This is depicted in Figure 2.32. The product fragmented in a similar fashion to the reduced, native peptide analysed previously, suggesting the structure is relatively open and extended. Sites in-between the maleimide bridged cysteines, which would have given the fragments corresponding to b_3 and b_4 (or y_{17} and y_{18}) and b_{14}- b_{17} (or y_4-y_7), are not observed, which would be expected if this cysteine connectivity be true.

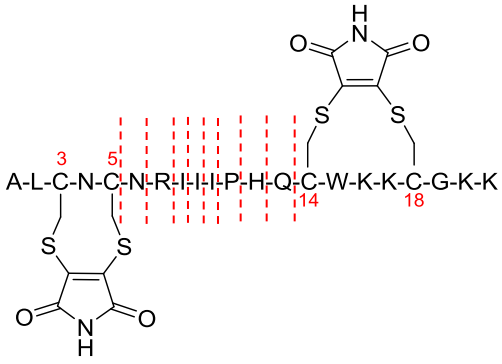

Figure 2.32: The C3-C5/C14-C18 connectivity of regioisomer **51** and the sites of fragmentation observed.

This suggests the maleimides bridge two cysteine residues before the peptide re-folds into its native conformation, preventing the formation of the desired product **48**. Had the maleimides bridged tertiapin Q in the correct, native fashion, we would have expected

minimal fragmentation, owing to the compact nature of the peptide as previously discussed. Only the few terminal residues from the *N*- and *C*- terminus are expected to be cleaved in this case. Good fragmentation was observed in our experiments, again suggesting that the correct regioisomer was not the product formed.

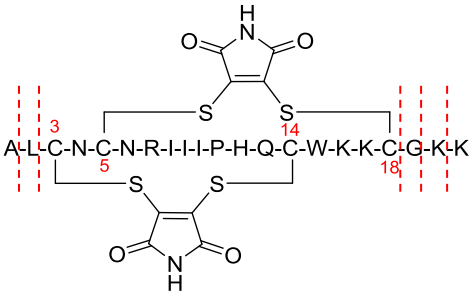

Figure 2.33: The native C3-C14/C5-C18 connectivity of desired doubly modified product **48** and the expected possible sites of fragmentation.

These results would provide a good explanation for the loss of biological activity of modified tertiapin Q as disulfide scrambling is often detrimental to the biological activity of peptides and proteins. As discussed in the introduction, disulfide bonds play a fundamental role in maintaining a precise and unique tertiary structure which is crucial to defining activity. We decided to investigate further this idea of disulfide scrambling in the tertiapin Q model.

Molecular modelling is a technique commonly used to visualise molecules and proteins and analyse their structure and behaviour. In order to gain a better understanding of what happens to the structure of teriapin Q during the modification protocol, the modelling program Chimera was used with the PDB file for tertiapin (1TER).[78] As described in the literature, tertiapin has a very compact and rigid structure, with the two disulfide bonds connecting the *C*-terminal α-helix and the more extended *N*-terminal β-strand (Figure 2.34).

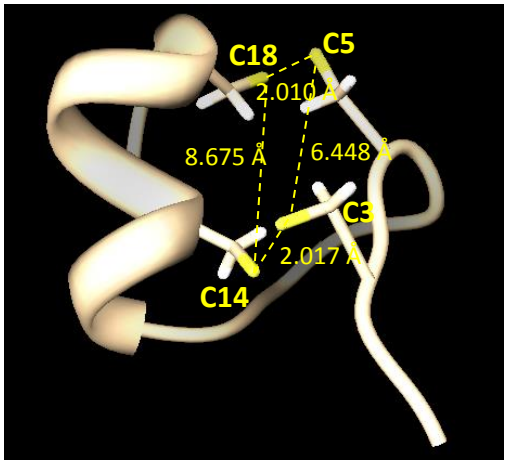

Figure 2.34: NMR solution structure (cartoon representation) of tertiapin. Cysteines are highlighted and the distance between the thiol atoms indicated. (PDB code: 1TER)

From the NMR structure, we see that in the native state both the C3-C14 and C5-C18 disulfide bonds span a distance of about 2 Å whilst the disulfide pairs themselves are between about 6.4 to 8.7 Å away from each other. Removing the disulfide bonds and, using the energy minimisation tool in Chimera, letting tertiapin adopt its lowest energy state effectively mimics the effect of disulfide reduction during the maleimide modification protocols. The energy minimised conformation is shown in Figure 2.35.

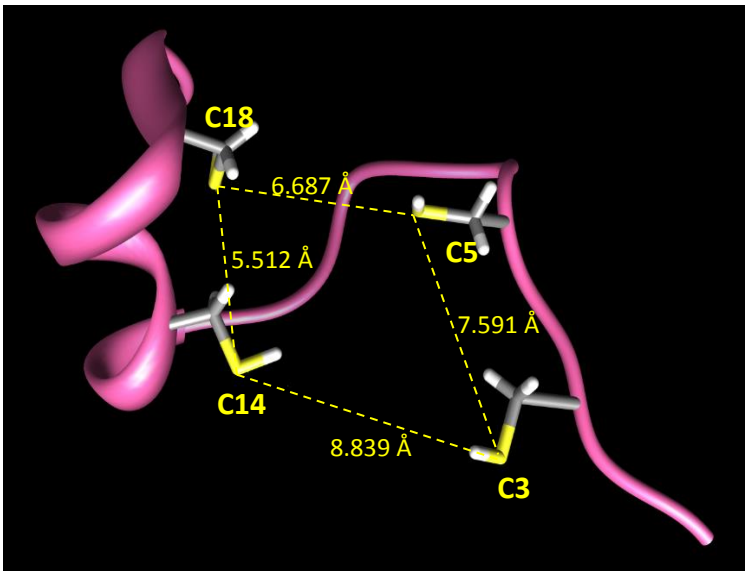

Figure 2.35: NMR solution structure (cartoon representation) of tertiapin Q after energy minimisation and the resultant distances between cysteine residues.

It is apparent that, when the disulfide bonds are reduced, the peptide will unfold into a more extended conformation and the cysteine residues move into very different proximities. The native pairs C3-C14 and C5-C18 are now around 8.8 and 6.7 Å apart

respectively; markedly greater than the 2 Å at which they are held at before reduction. In contrast, the C14 and C18 residues, which are 8.7 Å apart in the native state, move significantly closer together with about 5.5 Å distance now between them. This is in fact the closest pair of cysteine residues as a result of the change in peptide conformation. This further supports the hypothesis that the disulfide bonds could have scrambled as a result of maleimide modification as the cysteines appear to no longer reside in distances which would favour the native C3-C14/C5-C18 connectivity. In addition, the fact that residues C14 and C18 are now significantly closer would add weight to the evidence from the fragmentation study above, that in fact C3-C5 and C14-C18 are now bridged pairs.

This theoretical analysis correlates well with some further results obtained from the IM-MS/MS work. Prior to fragmentation in the instrument, the peptide moves through an ion mobility separation chamber. Ion mobility can separate species dependant on shape; it has the ability to separate species of the same mass-to-charge (*m/z*) ratio existing in different conformations. Complementary to NMR and x-ray crystallography, it is used to study three-dimensional protein structure and for analysis of complex mixtures.[161] Ion mobility is based on the time taken for individual species to transverse the mobility chamber which contains an inert gas and is under the influence of a weak electric field. This time, known as drift time (t_d), is related to the mass, charge and collision cross section of the ion species. The collision cross section is the area of an ion that is accessible for the carrier gas molecules to strike. The smaller this collision cross-section, meaning the smaller and more compact the species ion, the less area available for carrier gas to collide with and impede the ion's drift. As a result, the ion requires less time to migrate through the drift chamber.[153,161]

Experimentally, the t_d of both native and doubly modified tertiapin Q was recorded (Figure 2.36 **A** and **B**). This data was then converted into a corrected collision cross section using a calibration curve. This calibration curve was constructed using two calibrants, cytochrome c and myoglobin, which both have known cross sections existing in a variety of charge states (Appendix Figure 1). Using this calibration curve and the known t_d values, a corrected, rotationally averaged collision cross section was determined for tertiapin Q. Absolute collision cross sections were derived from these figures by correcting for the charge of the species.

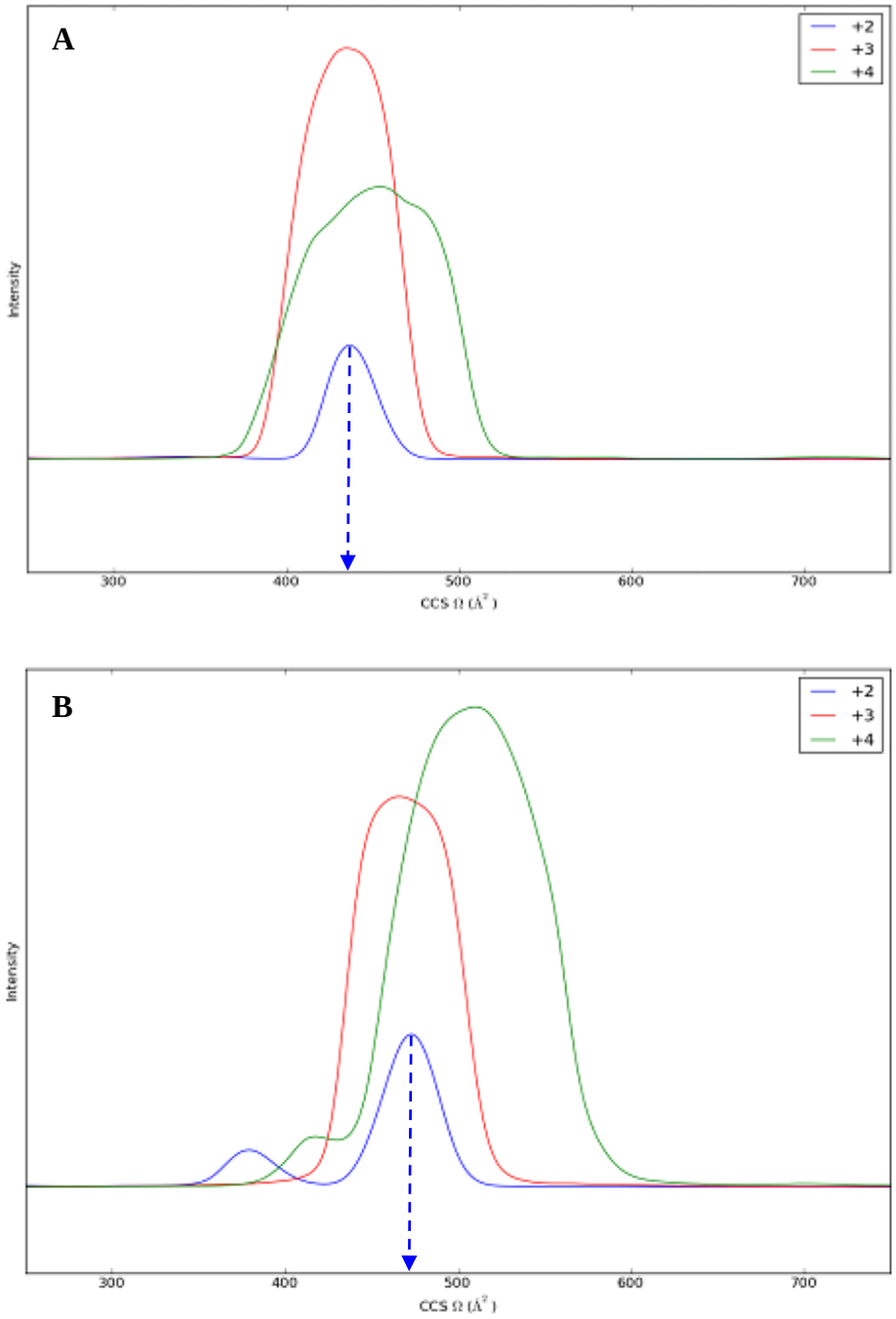

Figure 2.36: Ion mobility spectra showing collision cross section obtained for **A**) native tertiapin Q and **B**) doubly bridged tertiapin Q.

From the experimental data obtained, native and doubly modified tertiapin Q have collision cross sections of 435 and 473 $Å^2$ respectively. The fact that there is such a difference between these values suggests that they have quite different tertiary structures. Furthermore, the increased cross section size of the modified peptide in comparison to the native peptide implies that the modified peptide has now adopted a more extended, open conformation, which served to increase its t_d. These

experimentally obtained cross sections can be compared to theoretical values calculated using MOBCAL from the PDB file. Here the theoretical cross section of the native peptide was calculated to be 427 $Å^2$; not dissimilar to the experimentally obtained value for native tertiapin Q, but again significantly different to that of the modified peptide. This adds evidence to suggest that the tertiary structure has certainly been perturbed by the modification in such a way that its structure is no longer so compact.

All of our structural information obtained suggests that the maleimides have bridged the cysteine residues in non-native pairs. Fragmentation patterns, ion mobility analysis and modelling experiments suggest that C3-C5/C14-C18 is the preferential regioisomer formed, i.e. regioisomer **51**. Tertiapin Q is believed to elicit its inhibitory activity towards the GIRK channel family by means of insertion of its α-helix into the pore of the channel.[77] The fact that two of the cysteine residues we are targeting reside within the α-helix itself suggests that such disulfide scrambling observed would not be well tolerated. Such modification would be expected to have a detrimental effect on biological activity.

The propensity to form such a scrambled product suggests that either a) both disulfides are reduced before maleimide bridging occurs or b) reduction of the first disulfide initiates thiol-disulfide exchange reactions, effectively scrambling the peptide before it is bridged by a maleimide. In order to try and overcome these issues, we must carefully control reduction whilst maximising the speed of the bridging reaction. If we could selectively reduce and immediately re-bridge just one disulfide at a time, one would hope a correct native pair could be targeted.[23]

2.2.7 Towards Controlled Disulfide Reduction

As thiol-based reducing agents are unsuitable in our *in situ* protocol due to cross reactivity issues they were not suitable for this work, despite potentially having the desired attenuated reductive potential. Benzeneselenol is also unsuitable as it has been found to be catalytic and reduce disulfides very rapidly as a result. For these reasons, we returned to TCEP. In order to try and slow the reduction by TCEP it was postulated that incremental addition of very small amounts of the reducing agent may be the only way to slow reduction. We continued to employ the fast reacting maleimide **22**; envisaging

that, if added in significant success, we could promote immediate bridging during a slow and controlled reduction process.

Twenty equivalents of maleimide **22** were pre-incubated with tertiapin Q **40**, prior to addition of 0.3 equivalents of TCEP every 15 minutes (Scheme 2.14) and product formation monitored by LC-MS.

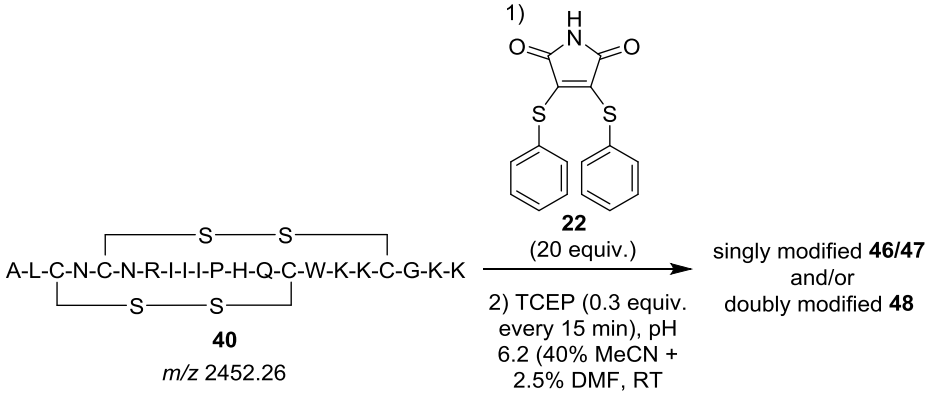

Scheme 2.14: The *in situ* modification protocol using maleimide **22** (20 equiv.) and incremental addition of TCEP (0.3 equiv. every 15 min).

In this case, we were not focused on pushing the reaction to completion, rather assessing whether or not the correct product was being formed. For this reason, when suitable conversion to singly modified products **46** and/or **47** or doubly modified product **48** was observed, the sample was immediately taken on to MS/MS analysis. For this point onwards, a different MS instrument was utilised - in this case, a capillary-LC-MS/MS; this allows for separation by chromatography prior to MS/MS analysis. As a result, RP-HPLC purification of any product was not essential before analysis and the mixture could be introduced into the instrument directly. Once again, the doubly, triply and quadruply charged ions of the doubly modified product **48** were recorded (data not shown) and subsequent fragmentation of the doubly and triply charged peptide ions provided the most conclusive information. The MS/MS spectrum of this doubly charged peptide ion at *m/z* 1322.13 after fragmentation is shown below in Figure 2.37.

The fragments observed in both spectra are listed below in Table 2.9. Once again, results suggest formation of the undesired C3-C5/C14-C18 regioisomer. High abundance of the b_{10} and b_{11} fragment ions especially suggests ease of fragmentation at these sites, indicative of the scrambled, open conformation.

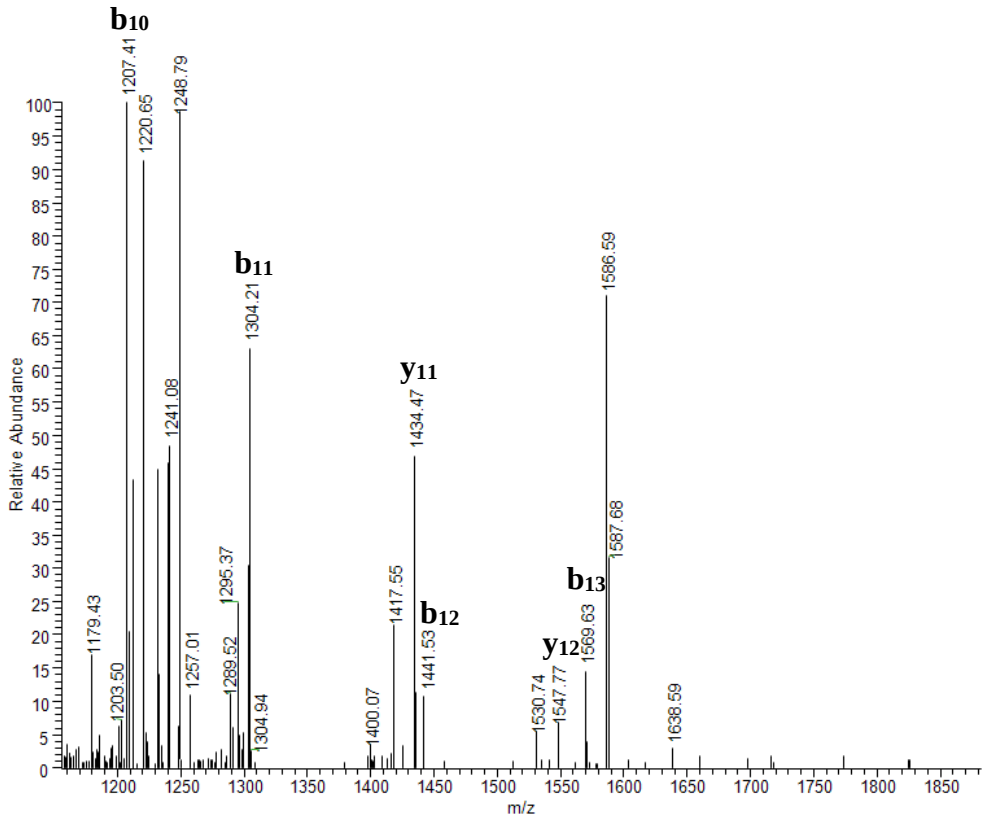

Figure 2.37: MS/MS spectrum of the +2 modified tertiapin Q ion at *m/z* 1322.13.

Table 2.9: The expected and observed fragment peaks from the MS/MS spectra of doubly modified tertiapin Q. (+ mal = + mass of maleimide bridge).

Fragment	*Sequence*	*Regioisotope connectivity*	*Expected monoisotopic mass (m/z)*	*Observed mass (m/z)*
b_8	ALCNCNRI + mal	C3-C5/C14-C18	981.40	981.35
b_9	ALCNCNRII + mal	C3-C5/C14-C18	1094.49	1094.43
b_{10}	ALCNCNRIII + mal	C3-C5/C14-C18	1207.57	1207.41
b_{11}	ALCNCNRIIIP + mal	C3-C5/C14-C18	1304.62	1304.21
b_{12}	ALCNCNRIIIPH + mal	C3-C5/C14-C18	1441.68	1441.53
b_{13}	ALCNCNRIIIPHQ + mal	C3-C5/C14-C18	1569.74	1569.63
y_{10}	KKGCKKWCQH + mal	C3-C5/C14-C18	1337.64	1337.47
y_{11}	KKGCKKWCQHP + mal	C3-C5/C14-C18	1434.69	1434.47
y_{12}	KKGCKKWCQHPI + mal	C3-C5/C14-C18	1547.78	1547.77

It appears that even attempts to attenuate the reduction speed during the reaction do not lead to formation of the desired product. Even though conversion to modified tertiapin is slower, selectivity for the correct disulfide is not achieved. Once again this suggests

that either the reduction is still not achieving selectivity for a single disulfide, and/or the re-bridging by the maleimide reagent is not fast enough to prevent the process of thiol-disulfide exchange leading to the isomerisation of the disulfide bonds and therefore allowing the formation of the undesired C3-C5/C14-C18 product **51**(Figure 2.38).

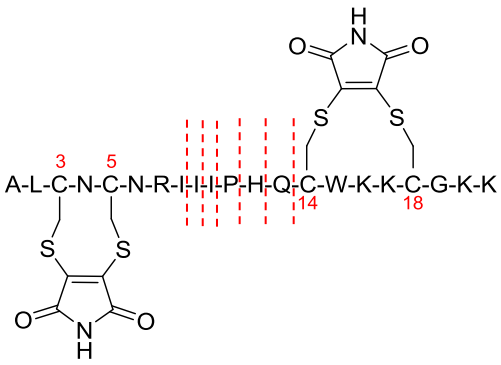

Figure 2.38: The C3-C5/C14-C18 connectivity (regioisomer **51**) and the sites of fragmentation observed.

Another consideration during this part of the project was whether tertiapin Q had an intrinsic propensity to scramble and misfold during synthesis. Of course *in vivo* there are cellular mechanisms including molecular chaperones to aid peptide and protein folding and to ensure correct tertiary structure is obtained.[49,50] Although the *in vitro* situation is very different, the tertiapin Q employed in this project was made synthetically by means of solid phase synthesis. During this procedure, there are various protection and deprotection steps to ensure correct bonding between desired residues, including the disulfide bonds. We were interested to determine whether tertiapin Q, once reduced, refolds into its native state when unaided by such chaperones and protection strategies. Often the secondary structure of a peptide or protein is sufficient to facilitate the templating of the amino acids into the correct conformation[162]; as frequently drawn upon in this study, however, every system will behave differently and should be considered individual.

Tertiapin Q in pH 6.2 buffer was fully reduced using TCEP before being left at room temperature for 72 hours to re-fold and re-oxidise. Analytical RP-HPLC was used to monitor the product formation of the reaction. The resulting chromatograms are shown in Figure 2.39.

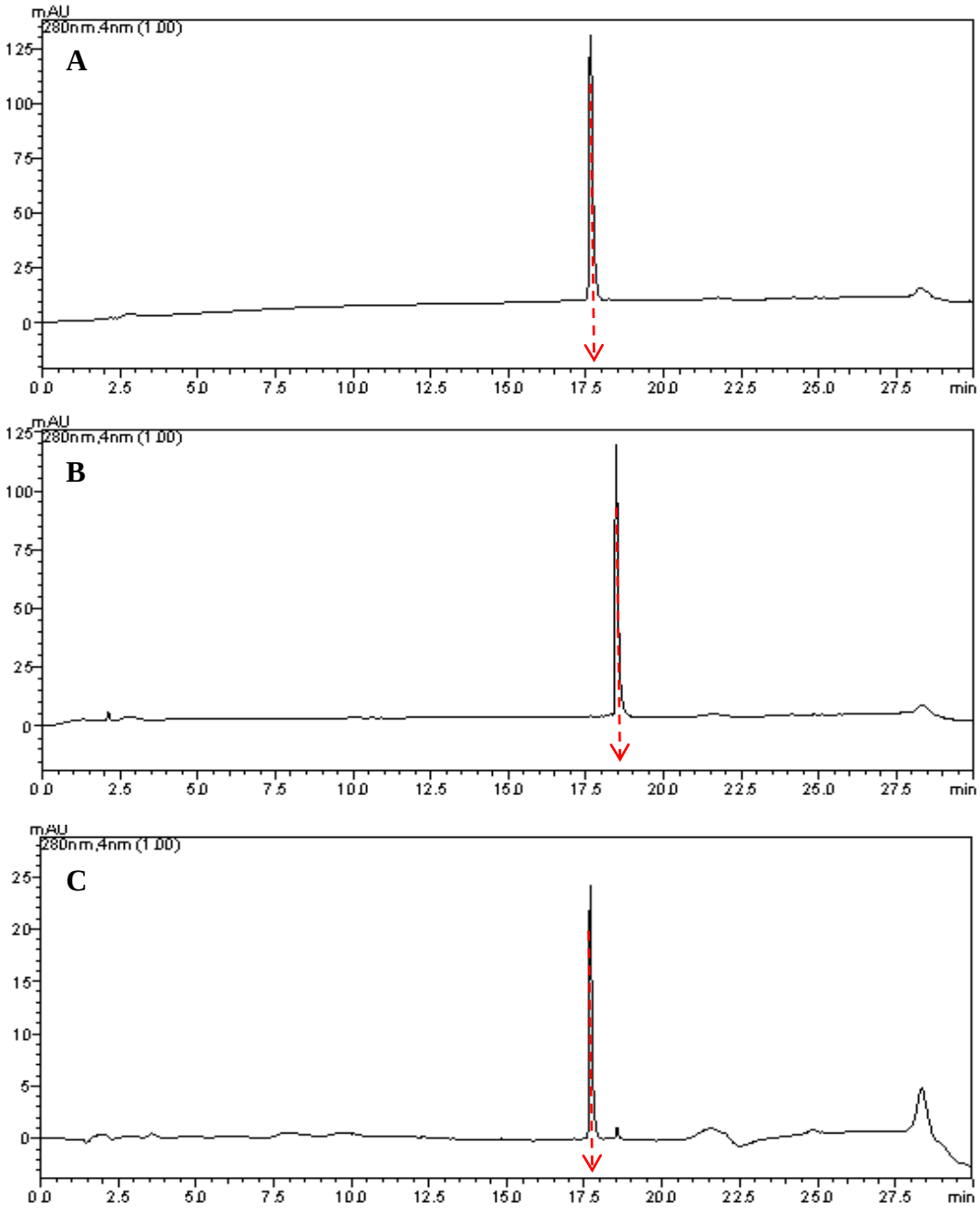

Figure 2.39: LC chromatogram of **A)** native tertiapin Q (Retention time: 17.75 min), **B**) reduced tertiapin Q (Retention time: 18.50 min) and **C**) tertiapin Q after 72 h re-oxidation (retention time: 17.75 min).

From the chromatograms, an increased retention time is observed upon reduction of the peptide. Upon re-oxidation, the retention time of the re-folded peptide appears to be exactly that of the original native peptide. This suggests the same conformation has been achieved. Additionally, there appears to be just one peak formed implying this is the sole product. The effect of organic solvent on this process was also considered. This

analysis was repeated using the solvent conditions routinely employed in our modification protocols, pH 6.2 buffer with 40% MeCN and 2.5% DMF (Figure 2.40).

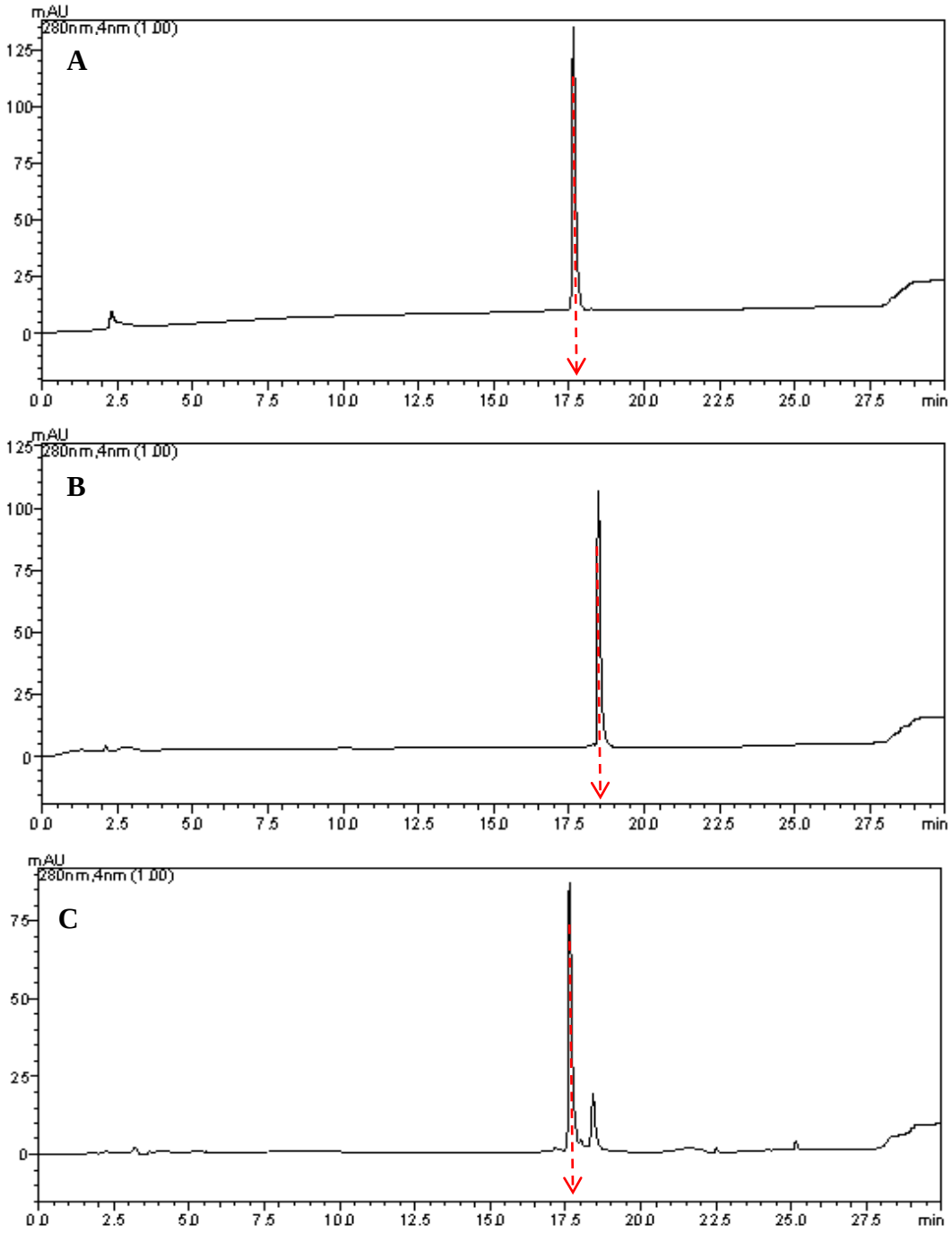

Figure 2.40: LC chromatogram of **A**) native tertiapin Q (Retention time: 17.75 min), **B**) reduced tertiapin Q (Retention time: 18.50 min) and **C**) re-oxidised tertiapin Q after 72 h (retention time: 17.75 min) in organic solvent.

In this case, the same increased retention time is seen upon reduction of the peptide. The re-oxidation is slower than in organic solvent-free conditions; some reduced peptide still remains after 72 hours. However, after re-oxidation the peptide appears to, once again,

adopt the native conformation. The organic solvents do not seem to hinder the templating of the peptide suggesting they shouldn't have had a negative effect in the modification protocols.

Results suggest that, during natural disulfide formation, tertiapin Q has the ability to adopt the correct structure, suggesting correct disulfide connectivity. Scrambling does not therefore appear to be an inherent problem during peptide folding.[163] It seems conclusive that the, thus far unavoidable, issue of incorrect cysteine-cysteine bridging during maleimide modification is as a result of the reagents and protocols employed in the strategy. Selective reduction of a single disulfide bond is not achievable and therefore facilitates formation of an unwanted product.

2.2.8 Towards Controlled Disulfide Modification

The thiomaleimides are known to react very fast; it was hypothesised that a less reactive reagent may be more effective at selectively targeting a single disulfide. To this point, using thiophenol-based maleimides has always resulted in formation of the doubly modified product, even when sub-stoichiometric amounts of reagent were employed. The aryloxymaleimides have been reported to display attenuated reactivity towards cysteines.[63] Compared to the thiophenol, aryloxy substituents contribute an increased mesomeric effect into the maleimide ring, reducing their electrophilicity. It was envisaged that such reagents could aid modification selectivity in some systems.

Investigation into whether such reagents could be of use in the selective modification of tertiapin Q began; if one of the disulfides was even slightly more accessible or reactive then perhaps it could be targeted using an aryloxymaleimide. Synthesis of maleimide **53** was straightforward but relatively low-yielding (Scheme 2.15). After the first addition of phenol to form *N*-methyl mono-bromo, mono-phenoxymaleimide, addition of the second phenol group was slow. Attempts to increase reaction time from 48 to 72 hours and increase reaction temperature from room temperature to 60 °C did not lead to increased yields.

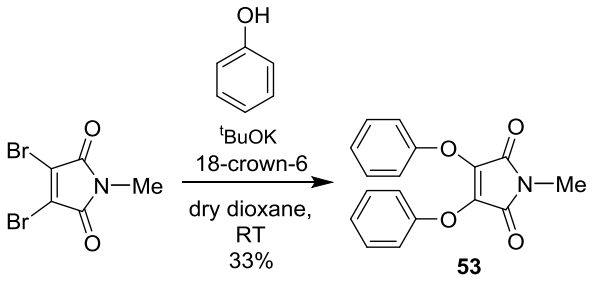

Scheme 2.15: The synthetic route to *N*-methyl di-phenoxymaleimide **53**.

Efforts to optimise the synthesis were not in our interest at this point, so work progressed onto the utility of this reagent in the *in situ* modification of tertiapin Q. When considering which reducing agent to employ it was decided that benzeneselenol was unsuitable; its catalytic nature proved to favour the reduction and modification of both disulfides significantly. For this reason, we chose to return to TCEP. Starting with less than 2 equivalents of both maleimide **53** and TCEP (Scheme 2.16), the reaction was monitored for product formation over time, by LC-MS analysis.

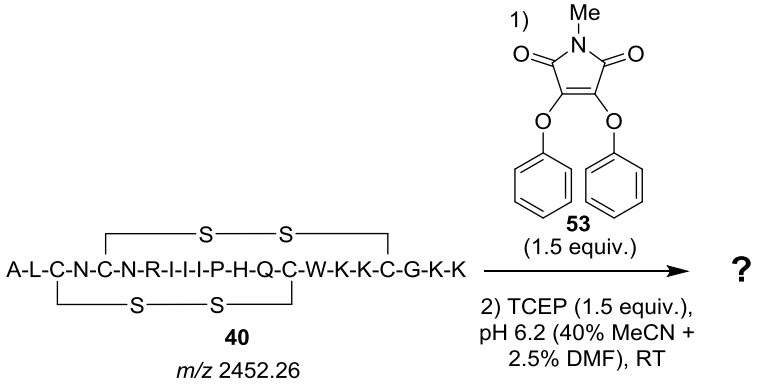

Scheme 2.16: The *in situ* modification protocol using maleimide **53** (1.5 equiv.) and TCEP (1.5 equiv.).

Significant amounts of the singly modified peptide **46** and/or **47** were observed during this reaction. When formation of the singly modified product started to plateau, 0.5 equivalents of TCEP were added to the reaction in attempt to maximise the yield. The results of the analysis are displayed in Table 2.10.

Table 2.10: Formation (by apparent conversion by LC-MS) of the singly modified product **46** and/or **47** and the doubly modified product **48** over time.

Total Reaction Time (h)	*Total equivalents of TCEP*	*Total equivalents of Maleimide*	*Native TPNQ* **40** *(%)*	*Singly Bridged* **46**/**47** *(%)*	*Doubly Bridged* **48** *(%)*
1	1.5	1.5	59	41	0
2	1.5	1.5	55	45	0
3	2.0	1.5	37	63	0
4	2.0	1.5	35	65	0
5	2.5	1.5	23	77	0

Pleasingly, using maleimide **53** in conjunction with TCEP yielded almost 80% of the singly modified product, with no evidence of the doubly modified product forming, even after 5 hours reaction time. An example of the LC-MS spectra observed is shown in Figure 2.41.

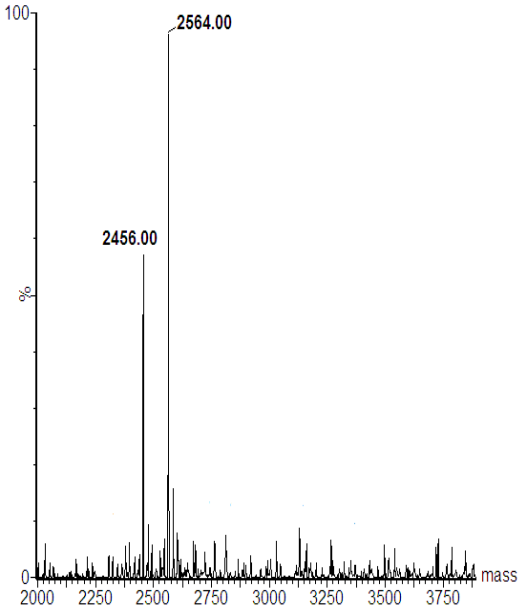

Figure 2.41: Deconvoluted mass spectrum of the reaction mixture, over the mass range *m/z* 2000-4000. Peak at *m/z* 2456 corresponding to reduced tertiapin Q (expected mass = *m/z* 2456.29) and *m/z* 2564 corresponding to singly modified peptide **46**/**47** (expected mass = *m/z* 2563.29).

This is the first time the single bridged peptide has been observed without concurrent formation of the double bridged product. The attenuated reactivity of the maleimide can be clearly observed by the amount of unreacted native peptide remaining in each case. In order to determine whether incremental addition of the reducing agent was a necessary procedure to aid single modification, the established *in situ* protocol using

TCEP was repeated, but this time the reducing agent was added as a single portion. The results are shown in Table 2.11.

Table 2.11: Product formation (by apparent conversion by LC-MS) from the *in situ* modification of tertiapin Q with addition of TCEP in a single portion.

Total Reaction Time (h)	*Total equivalents of TCEP*	*Total equivalents of Maleimide*	*Native TPNQ* **40** *(%)*	*Singly Bridged* **46**/**47***(%)*	*Doubly Bridged* **48** *(%)*
1.5	2.5	1.5	20	69	11

Although the singly bridged peptide was formed faster (70% conversion in 1.5 hours compared to 4-5 hours previously), a small amount of the doubly bridged peptide was also formed. Incremental addition of TCEP appears to be beneficial. In order to make subsequent purification of the desired product easier, the number of species should be minimised, therefore we chose the incremental TCEP addition protocol as standard.

Intrigued by the efficient formation of a singly modified product, localisation of the maleimide bridge was the next task. Despite facilitating single modification, whether or not maleimide **53** has been selective for a particular disulfide remained to be determined. In this case, there are 6 possible regioisomers that could be formed as a result of bridging just two cysteines. After its conclusive results previously, MS/MS analysis was again employed to determine which regioisomer, or combination thereof, had been formed. The possible regioisomers are depicted in Figure 2.42.

C3-C14 or C5-C18 (native) connectivity:

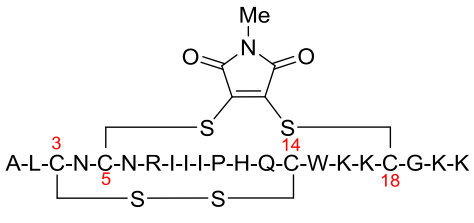

54

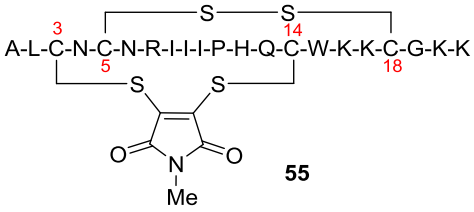

55

C3-C5/C14-C18 connectivity:

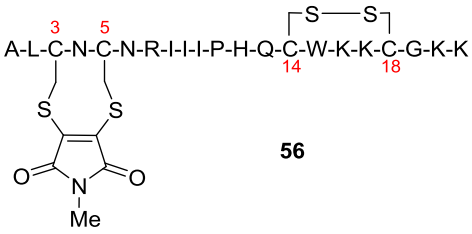

56

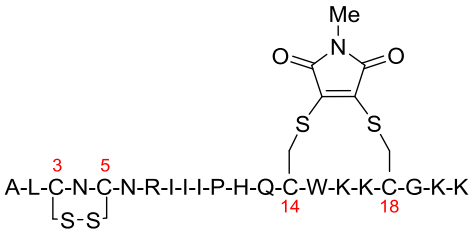

57

C3-C18/C5-C14 connectivity:

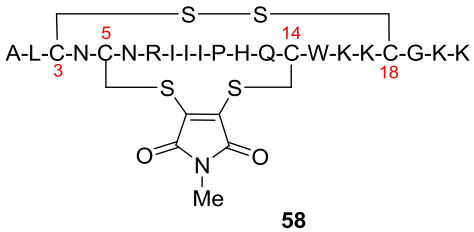

58

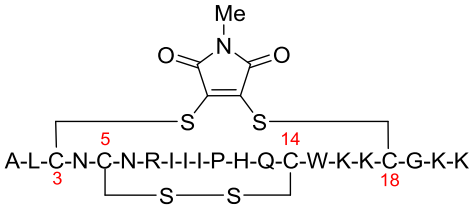

59

Figure 2.42: The six possible cysteine-cysteine connections in a singly modified species. Regioisomers **54** and **55** (native connectivity) and **56-59** (scrambled connectivities).

A new library of possible fragments that could arise from each of regioisomer was constructed (see Appendix Tables 6-11), again by sequentially removing each amino acid in turn and calculating the monoisotopic mass of the resultant fragment. Figure 2.43 shows the full mass spectrum of the singly modified product. The doubly, triply and quadruply charged peptide ions were all recorded.

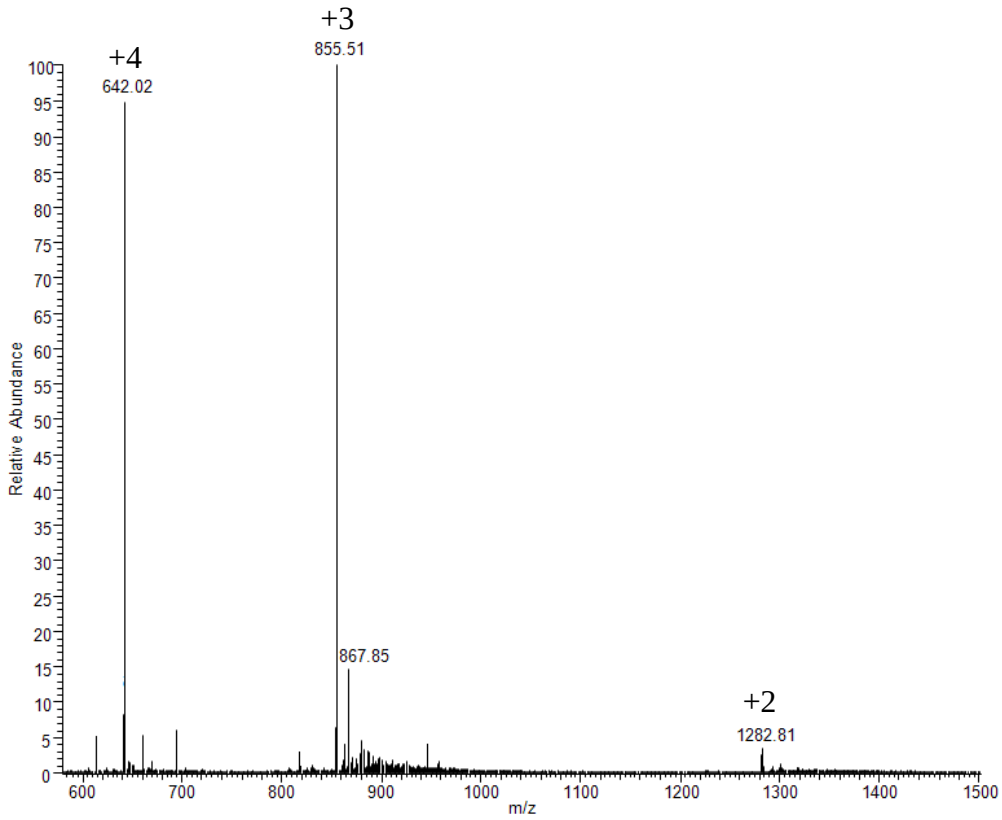

Figure 2.43: Full MS of singly modified tertiapin Q recorded at a peptide concentration of ~500 pg/µL in water + 0.1% formic acid. Peaks correspond to the +2, +3 and +4 modified tertiapin Q ions of *m/z* 1282.81, 855.51 and 642.02 respectively.

After selecting the parent ion of the desired singly modified product, it was fragmented as before and the resulting MS/MS spectra analysed. In this case, the doubly and triply charged ions yielded the most conclusive information. The spectrum from fragmentation of the doubly charged ion of *m/z* 1282.81 is shown in Figure 2.44.

Although fewer fragments were observed in these experiments, there was conclusive evidence to suggest incorrect cysteine-cysteine connectivity once again. The fragments observed that suggest this are listed below in Table 2.12.

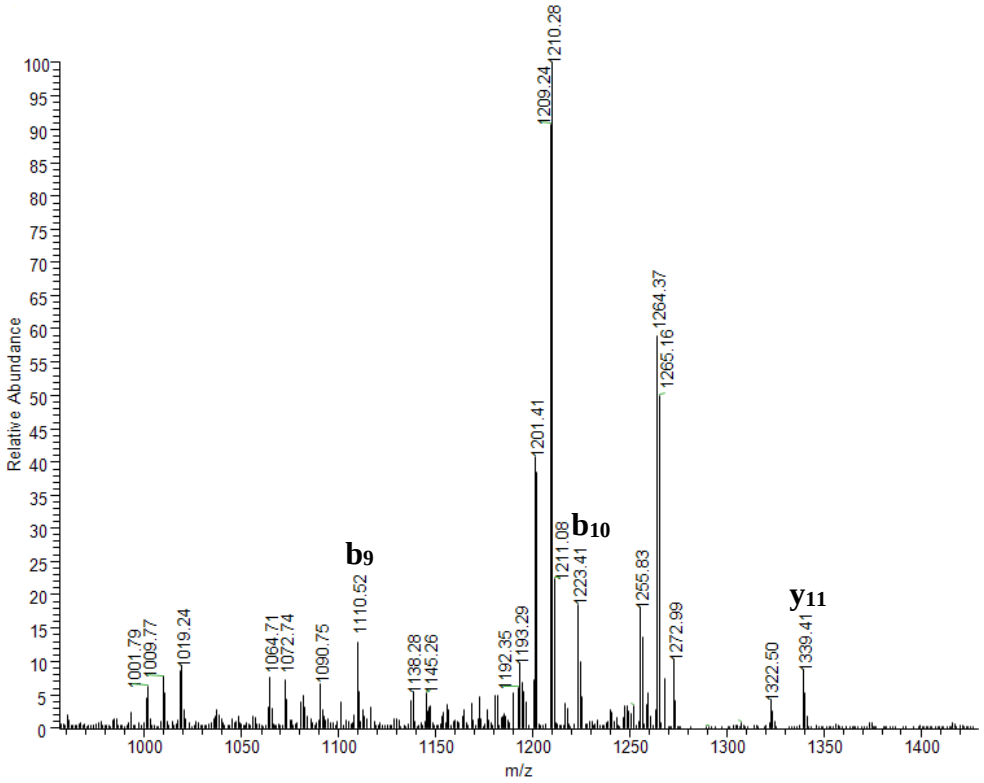

Figure 2.44: MS/MS spectrum of the +2 modified tertiapin Q ion at *m/z* 1282.81.

Table 2.12: The expected and observed fragment peaks from the MS/MS spectra of singly modified tertiapin Q. (+ mal = + mass of maleimide bridge).

Fragment	*Sequence*	*Regioisotope connectivity*	*Expected monoisotopic mass (m/z)*	*Observed mass (m/z)*
b_7	ALCNCNR + mal	C3-C5	884.35	884.30
b_8	ALCNCNRI + mal	C3-C5	997.43	997.26
b_9	ALCNCNRII + mal	C3-C5	1110.52	1110.52
b_{10}	ALCNCNRIII + mal	C3-C5	1223.60	1223.41
b_{12}	ALCNCNRIIIPH + mal	C3-C5	1457.71	1457.50
b_{13}	ALCNCNRIIIPHQ + mal	C3-C5	1585.77	1585.47
y_{11}	KKGCKKWCQHP + mal	C3-C5	1339.69	1339.46
y_{12}	KKGCKKWCQHPI + mal	C3-C5	1452.77	1452.45

The results suggest that it is neighbouring cysteines that have again been bridged; more specifically the C3 and C5 residues. The b_9 and b_{10} fragments were again observed, a location at which one would not expect tertiapin Q to fragment at had it be bridged with the correct, native connectivity. This propensity to fragment at these sites is also observed with the native, reduced peptide suggesting the compact structure has again been lost. Interestingly, no fragments corresponding to any other regioisomer were

observed, implying the C3-C5 connectivity, i.e. the regioisomer **56**, to be the major or sole product formed. It appears that maleimide **53** is selective for a pair of cysteine residues and suggests C3 and C5 are the most reactive; however, this is not a desired native pair. We would expect that inhibitory activity would have again been lost due to the associated structural perturbation.

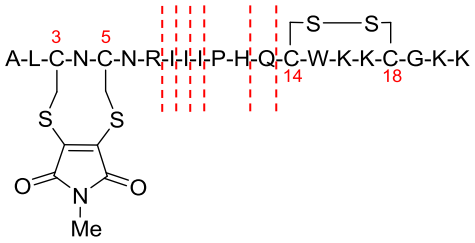

Figure 2.45: The C3-C5 connectivity (regioisomer **56**) and the sites of fragmentation observed.

Finally, we wished to confirm that both disulfides were reduced during this protocol, again facilitating such incorrect bridging. To test this, 1.5 equivalents of maleimide **53** was added to tertiapin Q followed by subsequent addition of 0.5 equivalents of TCEP every hour, as before. After two hours, 10 equivalents of maleimide **6** were added; adding such a reagent in excess should serve to cap any free thiols of tertiapin Q. In this way, it should be possible to determine by LC-MS whether the second, unmodified disulfide is in its oxidised or reduced state – a reduced disulfide should lead to a mass change of +190.02 *m/z* upon addition of maleimide, and formation of product **60** (Scheme 2.17). Results are shown in Table 2.13.

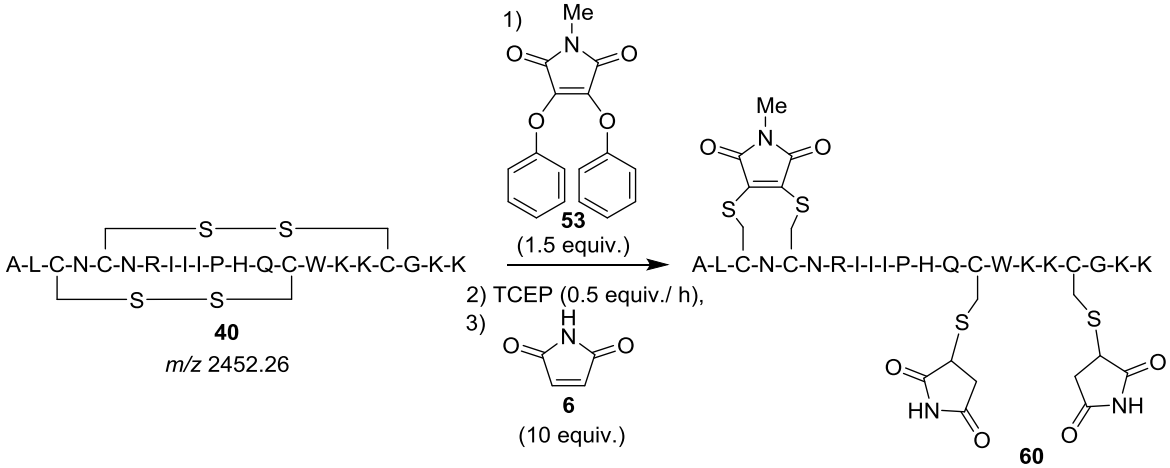

Scheme 2.17: The *in situ* modification of tertiapin Q using maleimide **53** (1.5 equiv.) and incremental addition of 0.5 equivalents of TCEP every hour - free thiols capped with maleimide **6** at these 1 h time points.

Table 2.13: The results of the *in situ* modification with maleimide **53** and TCEP with free thiol capping with maleimide **6**.

Total Reaction Time (h)	*Total equivalents of TCEP*	*Native TPNQ* (**40**) *(%)*	*Singly Bridged + 2 x maleimide* (**60**) *(%)*	*Singly Bridged* (**56**) *(%)*
2	1.0	23	58	19

A large proportion of product **60**, the singly bridged product capped by maleimide, confirms the presence of two free thiols. This proves that the second disulfide is often also reduced, facilitating the bridging of an incorrect cysteine-cysteine pair by the maleimide.

In this case, the attenuated reactivity of maleimide **53**, although facilitating a slower modification reaction and the formation of a singly modified product, cannot overcome the continual issue of complete reduction of the disulfide bonds of tertiapin Q by TCEP. As with the thiophenolmaleimide **22**, selectivity for native cysteine pairs is not possible.

2.2.9 Summary of Tertiapin Q Modification

Tertiapin Q presented itself as an ideal candidate for probing the utility of the 3,4-disubstituted maleimide reagents. Until the start of this project, analysis of such reagents had been limited to systems with a single disulfide bond, where modification was straightforward and efficient. In the case of tertiapin Q, its two disulfide bonds allowed us to probe a more challenging system, to test the scope of the methodology and whether controlled reduction and/or bridging was possible.

Analysis of the reactivity of the disulfides to the reducing agents TCEP, DTT and benzeneselenol revealed them both to be solvent accessible and reactive; this was quite expected from the small size and limited tertiary structure of the peptide resulting in the lack of a hydrophobic core in which to bury and protect essential residues and bonds.

Initial work using an organic solvent-free, step-wise protocol to modify both the disulfide bonds of tertiapin Q resulted in, what appeared to be, a fast and efficient reaction to form the doubly modified product **48**. However, subsequent analysis of biological activity by patch clamp analysis demonstrated the product formed had negligible inhibitory activity towards the GIRK 1/4 channel. It was postulated that this

was due to disulfide scrambling as a result of the extensive time the peptide is left to reduce and unfold during the protocol.

Focus quickly turned to development of an *in situ* protocol in attempt to overcome this predicted problem. Initial attempts using the water-soluble maleimide **45** were unsuccessful however, due to, what we postulate to be, retention of the thiosalicylic acid moiety. Unable to employ organic solvent-free conditions effectively led us back to dithiophenolmaleimide **22** and, to try and make the reaction as rapid as possible in order to circumvent disulfide scrambling, benzeneselenol to aid reduction catalysis. Again rapid formation of the doubly modified peptide **48** was observed. Patch clamp experiments revealed that unfortunately biological activity of the tertiapin Q had again been abolished by the modification. It was predicted that this must again be due to disulfide scrambling, but we wished to prove this to be the case. In order to do so, we embarked on tandem MS analysis. Pleasingly, efficient fragmentation and careful comparison of the acquired mass spectra with the predicted regioisomers formed allowed us to determine the exact location of the maleimide bridges. Incorrect cysteine-cysteine pairing by the maleimide had occurred, more specifically the C3-C5/C15-C18 regioisomer **51**, which would explain the loss of biological activity. Such an isomer would undoubtedly have a significantly different tertiary structure to the native peptide.

In attempts to overcome this issue, we tried to obtain selectivity by attenuating the reduction reaction. We were limited by the compatibility of the reducing agents we had available to us meaning that TCEP was the only suitable option. To try and aid slow and selective disulfide reduction we added TCEP in small aliquots to the peptide in excess maleimide **22**. We hoped that, as soon as one disulfide was reduced there would be a maleimide reagent in close proximity to immediately re-bridge the cysteines. Once again, despite being able to slow the reaction, selectivity was still not obtained. Double modification resulted and, when analysed by tandem MS, the resultant product was the commonly observed C3-C5/C15-C18 regioisomer **51**.

We also tried to achieve selective modification of just one disulfide bond. We investigated maleimide reagents with attenuated reactivity as a means to selectively modify solely the most reactive disulfide. Despite successfully obtaining high yields of the desired singly bridged product, tandem MS experiments revealed that incorrect

cysteine-cysteine pairing had again occurred. The fragments observed in the mass spectra suggested C3-C5 cysteines were modified exclusively, forming regioisomer **56**. Once again the structural changes that this would confer would undoubtedly affect the inhibitory activity of tertiapin Q.

In conclusion, despite various attempts to obtain a maleimide modified derivative of tertiapin Q, the proximity of the disulfide bonds meant that this remained a challenge throughout. It appeared that reduction of one disulfide led to the almost immediate reduction of the second meaning that selectivity was not possible; tertiapin Q had a propensity to exist in the completely reduced state. We hypothesise that this is either due to a slight conformational change upon reduction of the first disulfide leading to increased reactivity of the second, or due to rapid thiol-disulfide exchange causing disulfide scrambling prior to maleimide bridging. This was an issue that our maleimide modification reagents could not overcome and modification of the correct cysteine pairs was not possible in any case. It also became apparent that modification of the C3-C5 pair was most favourable, being found in every protocol tested. This could be reasoned by the proximity of these two cysteines within the peptide chain, residing in a favourable distance for a maleimide to react.

This demonstrates a limitation to the applicability of the 3,4-disubstituted maleimides in the modification of small, multiply disulfide bonded systems. Although each system is variable in nature, the structure of the peptide or protein, and the location of the disulfide bonds and their local environment need to be carefully considered before applying such a modification strategy.

2.3 Modification of Octreotide

2.3.1 Native Octreotide Analysis

2.3.1.1 Dose-Response Analysis

As described in the introduction, octreotide is a known agonist of the somatostatin receptor. With its longer half-life and improved potency it presents itself as a more attractive clinical candidate than the natural peptide somatostatin and, as a result, there continues to be interest in using octreotide for therapeutic and diagnostic applications.[107] Unlike the more promiscuous somatostatin, octreotide displays almost exclusive selectivity for the somatostatin receptor subtype 2, with additional low selectivity for subtype 5. In order to assess the agonistic activity of octreotide in its native state, activation of the somatostatin receptor was analysed.[107] It is reported that somatostatin and its analogues cause hyperpolarisation of neuroendocrine and neuronal cell membranes as a result of activation of GIRK channels; in fact, it is the hyperpolarisation of the cell membrane of pituitary cells in this fashion which is responsible for the characteristic inhibition of growth hormone release associated with somatostatin.[164] Studies have shown that the somatostatin receptor 2 couples most efficiently to the GIRK channel family over any of the other receptor subtypes. Co-expression of somatostatin receptor 2 with GIRK1 followed by administration of somatostatin leads to strong activation of inwards potassium currents through the GIRK channel. This activation of GIRK channels *via* the somatostatin receptor is mediated by G-protein.[164]

With this information in hand, we designed our octreotide activity analysis accordingly. A HEK293 cell line stably expressing the GIRK1/2a channel subtype was transiently transfected with the somatostatin receptor 2. The GIRK1/2a subtype was chosen as it is reported to predominate in neuroendocrine cells, providing the most physiologically relevant system for these experiments.[146] Successful transfection of the somatostatin receptor was observed by epifluorescence from eGFP which was also transfected into the cells as a visible indicator. With this engineered cell line, whole-cell patch clamp experiments were conducted. Typical current recordings for the GIRK1/2a channel, both at rest and after administration of native octreotide, are shown in Figure 2.46.

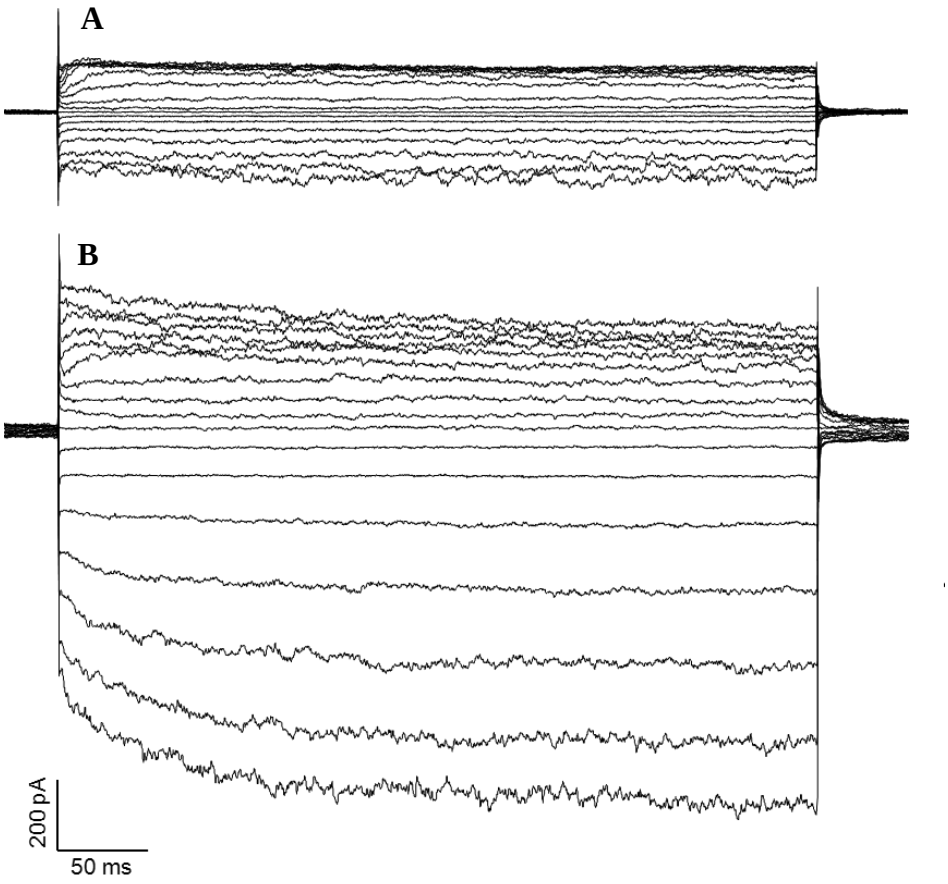

Figure 2.46: Current recordings of **A**) the resting GIRK1/2a channel and **B**) GIRK1/2a channel activation by octreotide (100 nM). Current was recorded over 20 mV voltage steps, over a range of -120 to +40 mV from a holding potential of -50 mV.

These representative recordings show the larger inwards currents and smaller outwards currents of the GIRK1/2a channel at rest (Figure 2.46 **A**). Immediate current activation is observed following capacitive transient spikes. Upon administration of octreotide, rapid activation of the GIRK1/2a channel is seen; both the inwards and outwards currents are enlarged, the inwards current significantly more so which is characteristic of inwardly rectifying channels (Figure 2.46 **B**).

Native octreotide was prepared over a range of concentrations (from 0.01 nM to 100 nM), and these were subsequently perfused over the cells in a sequential manner with increasing concentration. Octreotide was washed out between each concentration step by perfusion with extracellular solution in order to regain the resting current levels. The recordings we acquired using Axon™ pCLAMP™ 10.2 software and analysed using Axon™ Clampfit™ 10.2 software. The mean of the maxiumum inwards currents through the GIRK1/2a channels in response to increasing concentrations of octreotide was plotted (Figure 2.47).

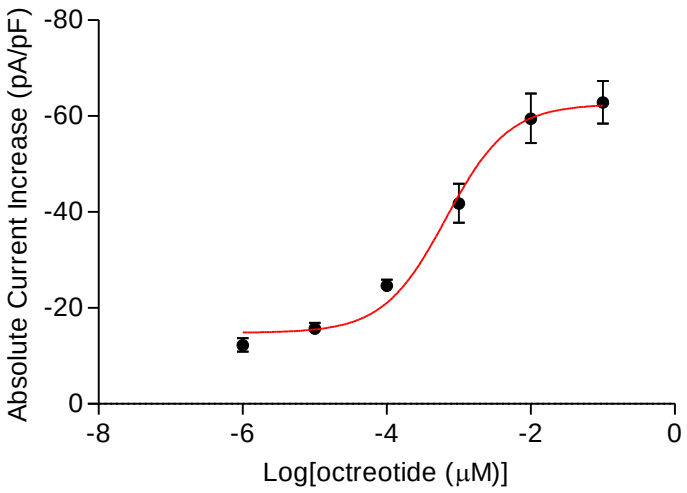

Figure 2.47: Mean absolute current increase (pA/pF) with increasing concentration of native octreotide (plotted as log [octreotide (μM)]). The sigmoidal fit line (red) was produced using a fit with function y = Bottom+(Top-Bottom)/(1+10^(X-LogIC$_{50}$)). R^2 = 0.9905. X at Y_{50} = -3.18. The error bars shown are calculated as the standard error of the mean. Raw data in Appendix Table 12.

The data points plotted were fitted using a standard dose-response curve and this created the sigmoidal fit line characteristic of a dose-response analysis. At the lowest concentrations tested (0.1 nM) we observe negligible current suggesting minimal activation of the somatostatin receptor. As octreotide concentration is increased we observe significant current activation; octreotide is binding to and activating the somatostatin receptor, which in turn activates the GIRK channel, allowing increased inwards flux of potassium. At the highest tested concentrations of octreotide (100 nM) the current increase begins to plateau as maximal activation is reached. This concentration dependence on activity is characteristic of agonists and antagonists. The high R^2 score of the fit line demonstrates a very reliable fit of the data. From the curve we can determine a numerical value for the half-maximal effective concentration (EC_{50}) in order to quantify the agonist activity. From this study, an EC_{50} of 0.66 nM was obtained which demonstrates the high potency of the peptide in activation of the somatostatin receptor subtype 2. This value correlates well with the literature which reports the EC_{50} of octreotide as greater than 0.1 nM, often around 0.5 nM, for somatostatin receptor 2.[165]

During the patch clamp analysis, it was observed that, shortly after maximal current activation had been achieved after administration of octreotide, the current levels began to diminish despite continuing perfusion with the agonist. This is a typical feature

commonly observed in GPCR-mediated signalling and is a result of desensitisation of the receptor with prolonged agonist exposure. There are a variety of mechanisms by which this desensitisation can occur such as receptor phosphorylation, palmitoylation and internalisation; the mechanism is dependent upon receptor type and the cell type expressing it.[166,167]

2.3.1.2 Wash-Out Analysis

It is also reported in the literature that, for somatostatin receptor subtypes 2-5, baseline current levels can be recovered upon wash-out of somatostatin.[164] This was observed during this study, with baseline level current regained rapidly with all concentrations of octreotide tested by continuous perfusion with extracellular solution. An example of this is shown below in Figure 2.48. Resting current levels are first recorded (green) before administration of 1 µM octreotide where the associated activation of inwards potassium currents is observed (blue). Upon maximum activation, subsequent agonist wash-out brings the current levels back to the resting state (orange).

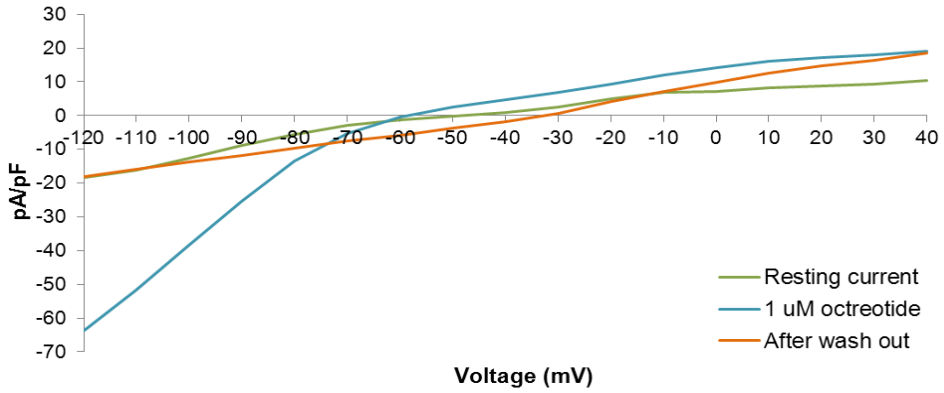

Figure 2.48: K^+ current (pA/pF) activation over a range of membrane potentials (mV) with 1 µM octreotide and baseline K^+ current recovery after washing with extracellular solution.

The conclusions obtained from studying the activity of native octreotide on this system serves as a sound control for comparison with the octreotide derivatives synthesised, analysed and discussed later.

2.3.2 Maleimide Modified Octreotide

2.3.2.1 Maleimide Modification of Octreotide

With the vision of creating novel derivatives of octreotide by maleimide modification we wanted to ensure that insertion of the maleimide bridge into the disulfide bond of the peptide did not have a detrimental effect on its action as an agonist. Previous work on tertiapin Q demonstrated just how sensitive these small peptides are to perturbations to their tertiary structure. In this case, the presence of a single disulfide bond rules out the possibility of disulfide scrambling, the main issue faced when working with multiply disulfide bonded systems. In addition, previous work in the group on somatostatin, which is structurally similar to octreotide, demonstrated that the modification of its disulfide was facile and did not lead to loss of biological activity.

Conditions were developed to rapidly bridge the disulfide bond of octreotide **34**. Due to the simplicity accompanied with just having a single disulfide bond, a step-wise protocol could be employed. By reduction of the disulfide bond with 1.2 equivalents of the reducing agent TCEP before addition of 1.2 equivalents of the dithiophenolmaleimide **22**, full conversion to the bridged peptide **61** was obtained within 10 minutes (Scheme 2.18)

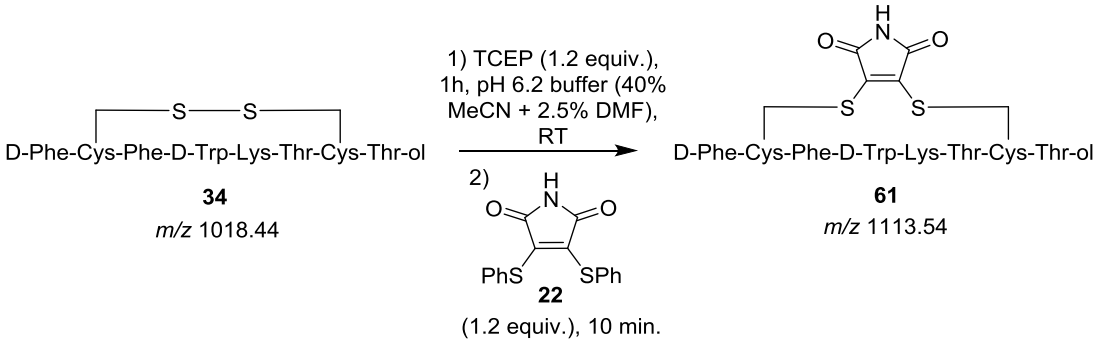

Scheme 2.18: The step-wise maleimide modification of octreotide **34** by reduction with TCEP (1.2 equiv.) for 1 h followed by addition of maleimide **22** (1.2 equiv.).

Conversion to the bridged peptide **61** was determined by observation of the appropriate mass change by LC-MS. An example of such spectra is shown below in Figure 2.49.

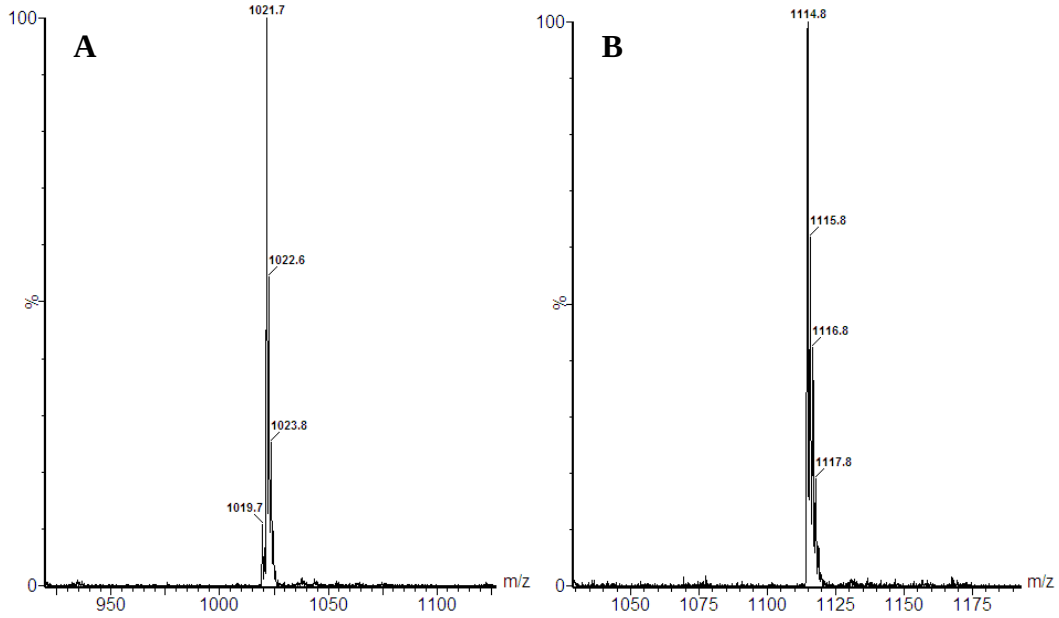

Figure 2.49: ESI mass spectrum of **A**) peak at *m/z* 1021.7 corresponding to reduced octreotide (expected mass = *m/z* 1021. 3) and **B**) peak at *m/z* 1114.8 corresponding to modified octreotide **61** (expected mass = *m/z* 1115.2).

2.3.2.2 Purification & Characterisation of Modified Octreotide

With the desired product in hand, it was purified by RP-HPLC using an analytical C-18 column, in order to remove the unwanted buffer salts and unreacted starting materials. The RP-HPLC trace obtained is shown below in Figure 2.50, with analysis at 280 nm.

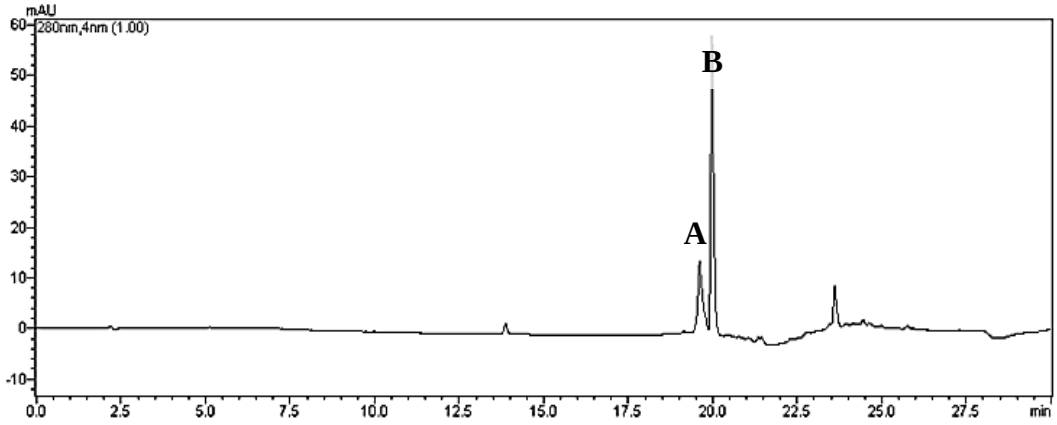

Figure 2.50: HPLC chromatogram (absorbance at 280 nm) of the octreotide modification reaction mixture (peak **A** retention time: 19.6 min, peak **B** retention time: 20 min).

Peaks **A** and **B** were isolated, concentrated and characterised by MALDI mass spectrometry. The spectra obtained are shown below in Figure 2.51.

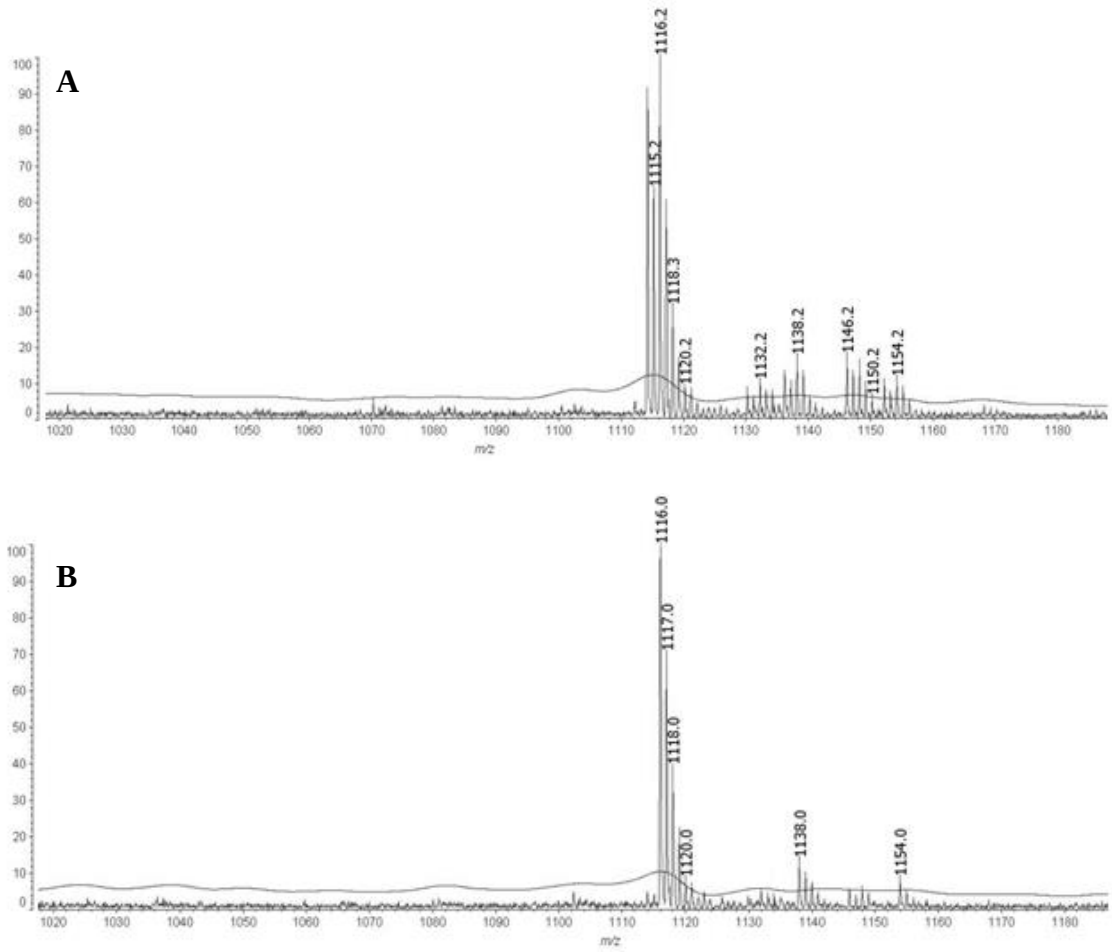

Figure 2.51: MALDI mass spectra of peaks **A** and **B** from the LC chromatogram in Figure 2.50. Peak at *m/z* 1116.0 corresponds to the modified peptide **61** (Expected mass = *m/z* 1115.2). The sodiated product (+23 *m/z*) and potassiated (+35 *m/z*) products are also visible.

From the spectra obtained it is apparent that both peaks observed by RP-HPLC, despite their slightly differing retention times, appear to have the mass corresponding to the bridged octreotide **61**. No unreacted starting material, expected at *m/z* 1019, is detected confirming the reaction had reached full conversion to the desired product. Interestingly, the main difference between these two products appears to be their isotopic distribution profile, with that of the peak **A** being uncharacteristic of what has been previously observed for octreotide. This suggests that perhaps there is an impurity within this sample causing the observed effect. The major product, peak **B**, was successfully isolated from such impurities and an overall yield of 68% after purification was obtained. This product only was used for further analysis.

It was also noted during RP-HPLC purification that upon co-injection with native octreotide, the peptides co-eluted (Figure 2.52).

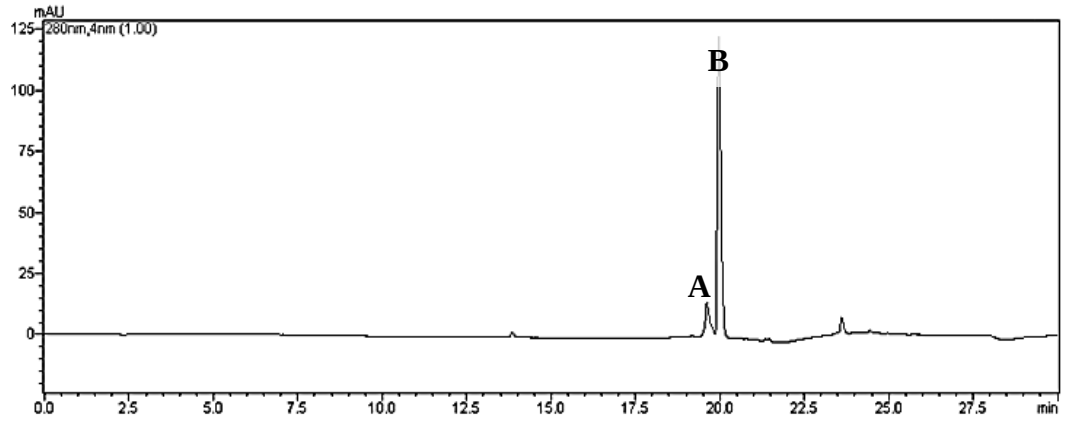

Figure 2.52: RP-HPLC chromatogram (absorbance at 280 nm) of the octreotide modification reaction mixture doped with native octreotide (peak **A** retention time: 19.6 min, peak **B** retention time: 20 min).

Modified octreotide **61** and native peptide **35** have identical retention times; in comparison to Figure 2.50 the only difference observed is an increase in peak **B** integration. Despite numerous attempts at tuning the solvent gradient to achieve the desired separation, surprisingly the two different species could not be separated. It was reasoned that perhaps incorporation of the small maleimide bridge within the peptide structure did not alter its conformation or hydrophobicity significantly enough to differentiate the two products on the column.

2.3.2.3 Biological Activity of Modified Octreotide

With the pure maleimide modified peptide in hand, analysis of biological activity was conducted. In analogous fashion to with native octreotide, whole-cell patch clamp experiments were carried out on the HEK293 cell line stably expressing the GIRK1/2a channel and transiently transfected with both somatostatin receptor subtype 2 and eGFP. Modified peptide **61** was administered over a range of concentrations (from 1 nM to 10 μM) and the agonist was washed out with extracellular solution between each concentration tested. The current recordings were analysed as previously described and results obtained are shown in Figure 2.53 below in the form of a dose-response curve.

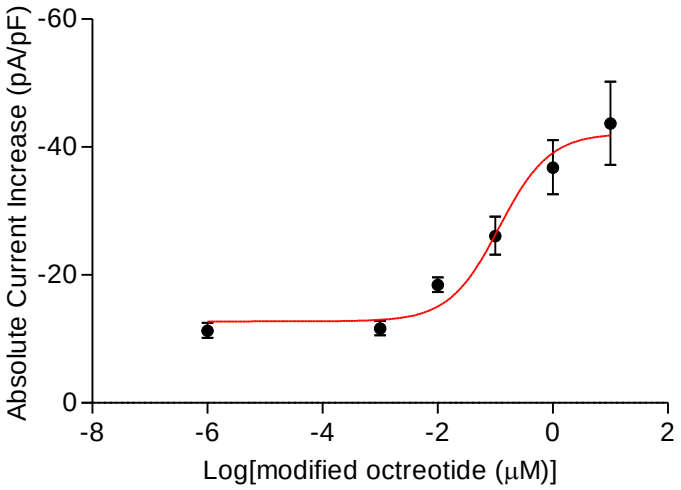

Figure 2.53: Mean absolute current increase (pA/pF) with increasing concentration of modified octreotide **61** (plotted as log [modified octreotide (μM)]). The sigmoidal fit line (red) was produced using a fit with function y = Bottom+(Top-Bottom)/(1+10^(X-LogIC$_{50}$)). R^2 = 0.9734. X at Y_{50} = -0.929. The error bars shown are calculated as the standard error of the mean. Raw data in Appendix Table 13.

Similarly to with native octreotide, the fit of the data produces a sigmoidal dose-response relationship, with an R^2 value of 0.9937 confirming a reliable fit. It became apparent while conducting the patch clamp experiments that the level of current elicited by modified octreotide **61** was significantly lower than with the native peptide and, as a result, higher concentrations were also tested. From the fit line, an EC_{50} value of 118 nM was determined. Overlaying the dose-response curve of modified octreotide with that of the native peptide allows for ease of comparison of the two agonists (Figure 2.54).

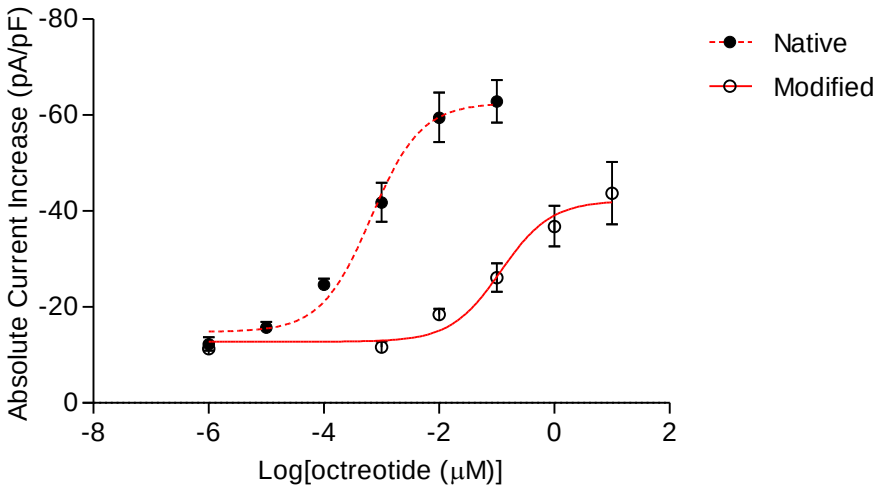

Figure 2.54: Overlay of the mean absolute current increase (pA/pF) with increasing concentration of modified octreotide **61** (solid line) and native octreotide (dashed line) (plotted as log [octreotide (μM)]).

In comparison to native octreotide with an EC_{50} value of 0.66 nM, there has clearly been an attenuation of agonist affinity as a result of disulfide bond modification. The way in which, despite being tested at higher concentrations, the modified peptide **61** does not elicit a maximum current increase comparable to the native peptide suggests a decrease is agonist efficacy also. In this way, the modified peptide **61** shows pharmacological action of a partial agonist.[145]

This decrease in agonist affinity and efficacy can be well reasoned by the proximity of the disulfide bonded cysteines to the pharmacophore of the peptide (Figure 2.55) – the cysteines directly neighbour the four residues (Phe-Trp-Lys-Thr) that make up the receptor binding site of octreotide. It is well known that sequence alterations to this fundamental region of the peptide are not tolerated, suggesting geometrical changes like those resulting from maleimide bridging could also be detrimental.[106]

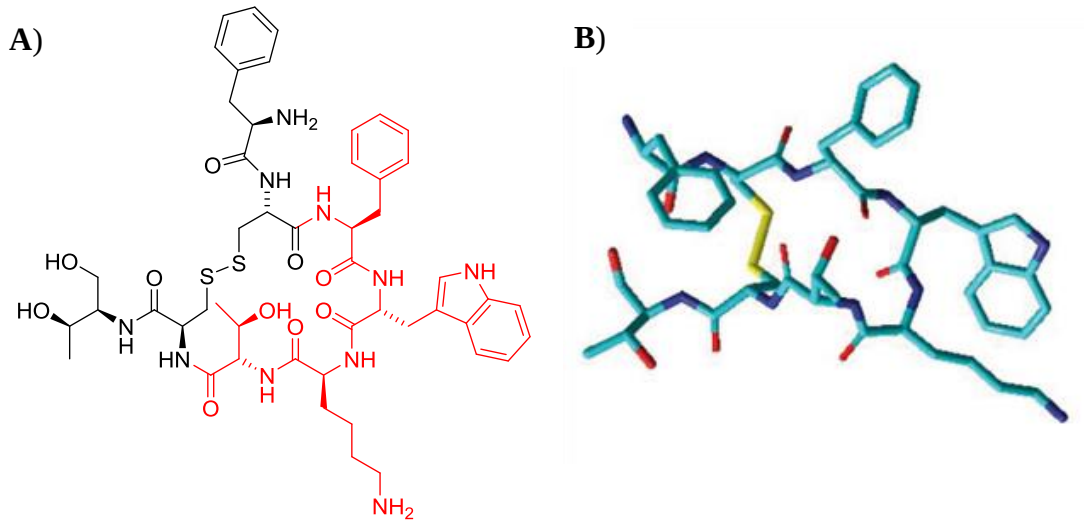

Figure 2.55: The structure of octreotide **A)** the atomic structure with the pharmacophore shown in red **B)** the solution NMR structure (PDB entry code 1SOC).[78]

It is not unreasonable to assume that insertion of a two-carbon bridge into the disulfide bond could distort the structure in such a way as to hinder the binding of the peptide to its receptor target. The average length of a disulfide bond is 2.05 Å and the ideal C-S-S-C dihedral angle is around 90°[168]; such geometric constraints mean the disulfide bond has a significant influence on the conformation of the local amino acid environment. A maleimide bridge is expected to hold the two cysteine sulphur atoms at a slightly larger distance of 2.5 Å[169]. This, albeit small, difference could in turn alter the geometry of

neighbouring bonds. It appears that this is not tolerated in octreotide and a negative effect on receptor binding results.

Despite this, maleimide bridging does not abolish biological activity, and EC_{50} is still within the nanomolar range. This suggests that the modified octreotide **61** retains the ability to bind to the somatostatin receptor and elicit its agonist effects to a certain degree. Research progressed on to designing an octreotide-based bioconjugate using this chemistry for novel therapeutic or diagnostic applications. It was hypothesised that incorporation of an alkyne on the nitrogen of the maleimide ring would activate it in such a way that a compatible, functional biomolecule of choice could subsequently be attached.

2.3.3 Alkyne Functionalised Octreotide

2.3.3.1 Maleimide Modification of Octreotide

N-alkyne functionalised maleimide **63** was readily synthesised in two steps from dibromomaleimide, as depicted in Scheme 2.19[170]. The first step involved converting the maleimide nitrogen into the corresponding carbamate **62** in order to activate it; this was done using *N*-methylmorpholine and methyl chloroformate. Subsequent addition of a stoichiometric amount propargylamine and stirring with excess silica efficiently installed the desired alkyne moiety, with an overall yield of maleimide **63** of 74%.

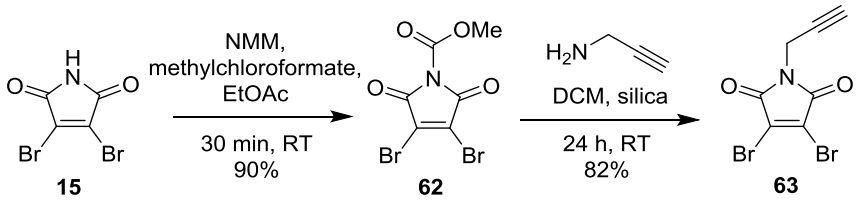

Scheme 2.19: The synthesis of *N*-alkyne dithiophenolmaleimide **63**.

With this reagent in hand, the same step-wise protocol employed previously was followed in order to insert the functionalised maleimide **63** into the disulfide bond of octreotide (Scheme 2.20).

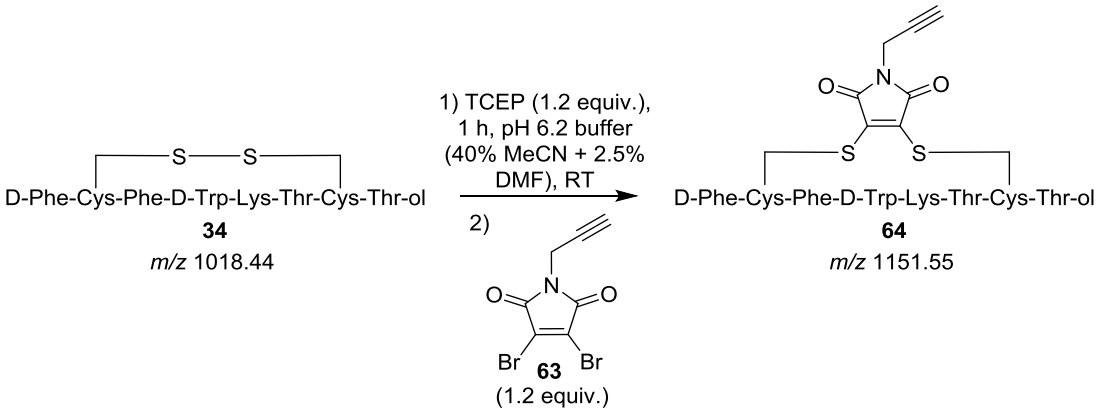

Scheme 2.20: Step wise modification of octreotide **34** by reduction with TCEP (1.2 equiv.) and addition of maleimide **64** (1.2 equiv.).

Conversion to the modified peptide **64** was determined by observation of the appropriate mass change by LC-MS, an example of such spectra is shown below in Figure 2.56.

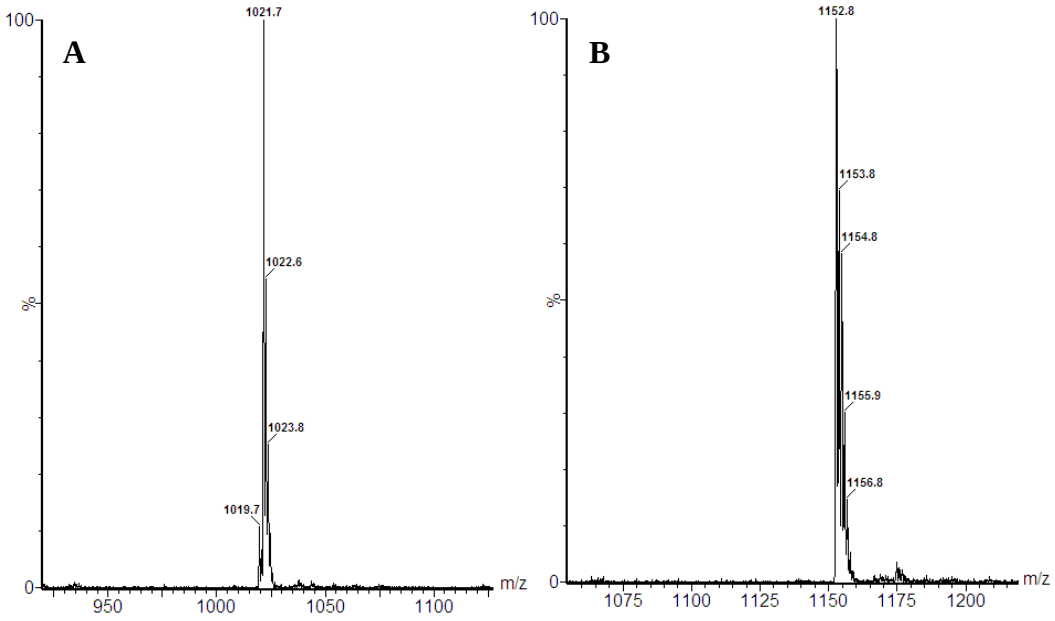

Figure 2.56: ESI mass spectrum of **A**) peak at *m/z* 1021.7 corresponding to reduced octreotide (expected mass = *m/z* 1021. 3) and **B**) peak at *m/z* 1152.8 corresponding to alkyne modified octreotide **64** (expected mass = *m/z* 1151.55).

Complete conversion to the modified peptide **64** was observed within 10 minutes and was reproducible.

2.3.3.2 Purification & Characterisation of Functionalised Octreotide

As before, isolation of the desired product was carried out by RP-HPLC purification. The RP-HPLC trace obtained is shown below in Figure 2.57, with analysis at 280 nm.

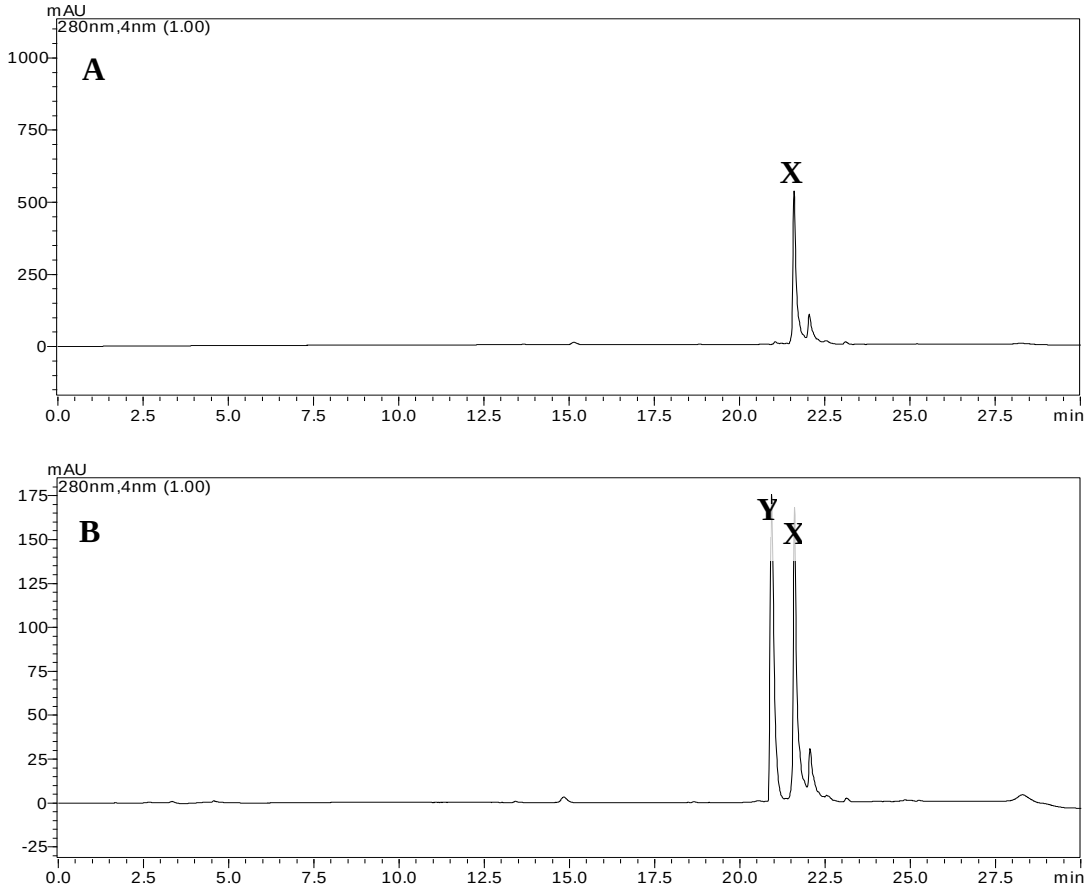

Figure 2.57: RP-HPLC chromatograms of **A**) octreotide modification reaction mixture and **B**) octreotide modification reaction mixture doped with native octreotide (peak **X** retention time: 21.7 min, peak **Y** retention time: 20.8 min).

From the RP-HPLC trace **A**, modified octreotide **64** (peak **X**) has a retention time of 21.7 minutes. This peak was collected, concentrated under vacuum and re-dissolved in deionised water before analysis by MALDI to assess the purity of the product. The MALDI spectrum obtained is shown below in Figure 2.58. The recovered yield of modified peptide after RP-HPLC purification was calculated to be 77%. By co-injection of the reaction mixture with native octreotide (RP-HPLC trace **B**, peak **Y**) we can observe the associated retention time shift as a result of maleimide modification. This confirms that there was no unmodified octreotide in our reaction mixture. The shift in retention time is relatively small, giving hope that the structure of the peptide had not been drastically altered.

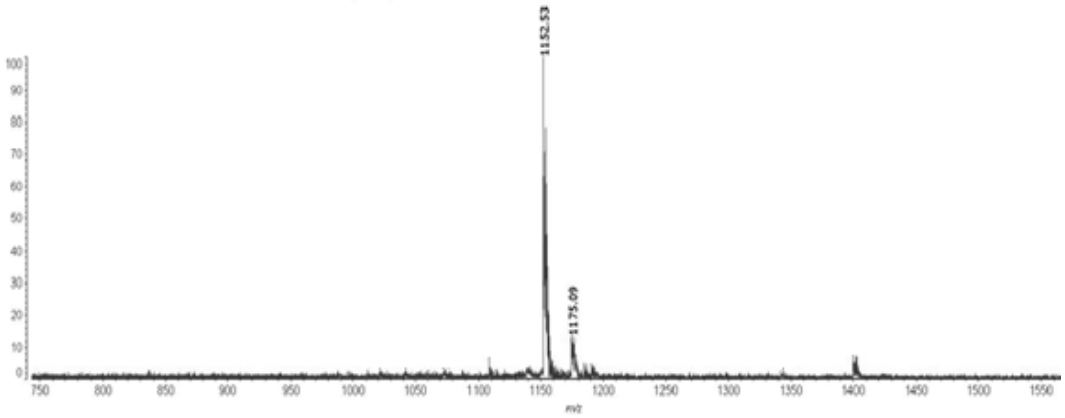

Figure 2.58: MALDI mass spectrum of peak **X** from the LC chromatogram in Figure 2.57**A**. Peak at *m/z* 1152.53 corresponds to the modified peptide **64** (Expected mass = *m/z* 1151.55). The sodiated product (*m/z* +23) is also visible (*m/z* 1175.09).

Satisfied with the purity of the desired product, the biological activity was next evaluated.

2.3.3.3 Biological Activity of Functionalised Octreotide

Whole-cell patch clamp experiments were again carried out on the HEK293 cell line stably expressing the GIRK1/2a channel and transiently transfected with both somatostatin receptor subtype 2 and eGFP. Modified peptide **64** was administered over a range of concentrations (from 1 nM to 10 µM), again with agonist wash out between each tested concentration. The resulting dose-response curve from the recorded currents is shown below in Figure 2.59.

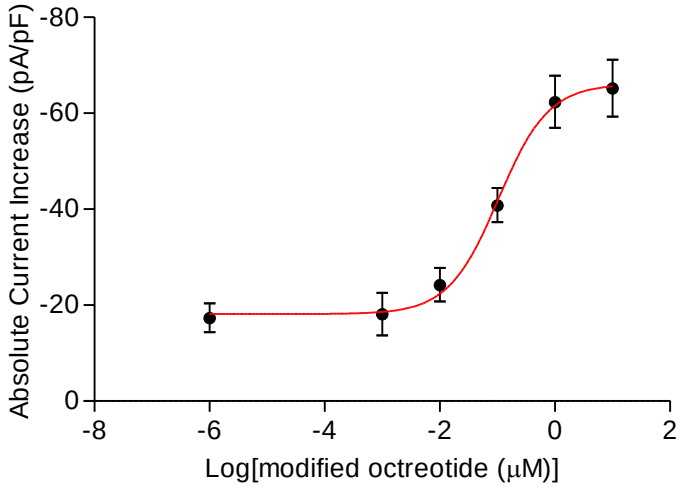

Figure 2.59: Mean absolute current increase (pA/pF) with increasing concentration of modified octreotide **64** (plotted as log [modified octreotide (µM)]). The sigmoidal fit line (red) was produced using a fit with function y = Bottom+(Top-Bottom)/(1+10^(X-LogIC$_{50}$)). R^2 = 0.9975. X at Y_{50} = -0.981. The error bars shown are calculated as the standard error of the mean. Raw data in Appendix Table 14.

Similarly to modified octreotide **61**, the fit of the data for alkyne functionalised octreotide **64** produces a sigmoidal dose-response relationship with an R^2 value of 0.9975. From the fit line, an EC_{50} value of 105 nM was determined. Once again, overlay of the dose-response curve of the modified peptide **64** with that of the native peptide facilitates ease of comparison of the two agonists (Figure 2.60).

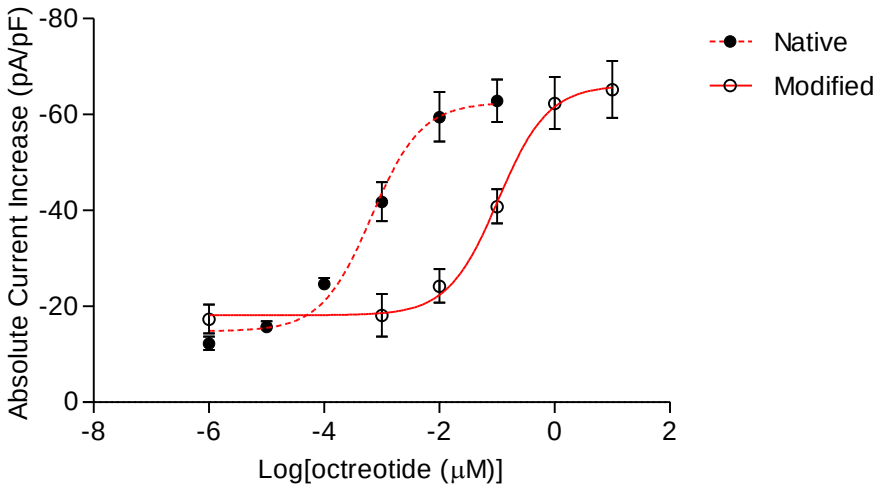

Figure 2.60: Overlay of the mean absolute current increase (pA/pF) with increasing concentration of modified octreotide **64** (solid line) and native octreotide (dashed line) (plotted as log [octreotide (μM)]).

As expected, in comparison to native octreotide with an EC_{50} value of 0.66 nM, a decrease in agonistic affinity, i.e. an increase in EC_{50}, is observed. The loss of biological activity is of similar magnitude to that of maleimide modified octreotide **61**, whose EC_{50} was calculated to be 118 nM. This adds further conclusive evidence to suggest that incorporation of a two-carbon bridge within the disulfide bond of octreotide perturbs the tertiary structure and hinders, but does not abolish, binding to the somatostatin receptor. Interestingly, the decrease in agonist efficacy observed previously with modified octreotide **61** is not seen in this case; maximal current increase is observed by administration of the modified octreotide **64**, albeit at a higher dose than in the native case. This suggests the modified peptide displays full agonist characteristics.[145]

This variance between the observed efficacy of the two modified derivatives could be as result of the nature of the chemical modification, perhaps the differing chemical conformation of each serves to alter agonist efficacy considerably in the case of a small

peptide such as octreotide. To confirm this hypothesis, higher concentrations of modified peptide **61** would be tested, to fully confirm the partial agonistic activity.

Despite the attenuated affinity of the alkyne functionalised octreotide **64**, and with the knowledge that nanomolar activity is still viable for certain applications, efforts towards a novel octreotide-based bioconjugate continued. Alkyne functionalised octreotide **64** was subsequently investigated as a precursor for attachment to a desired biomolecule by means of click chemistry.

2.3.3.4 Click Reactions of Functionalised Octreotide

Click chemistry is a powerful synthetic strategy for covalently combining two molecules. One of the most utilised reactions of this kind is the Huisgen 1,3-dipolar cycloaddition between an alkyne and an azide to yield 1,2,3-triazoles. A copper catalyst is often utilised to selectively produce the 1,4-disubstituted triazole **65**, which can proceed under aqueous conditions, as shown in Scheme 2.21 below. This reaction is renowned for being highly reliable and selective and has proven to be an incredibly versatile bond forming process, as proven by its extensive coverage in the literature.[171]

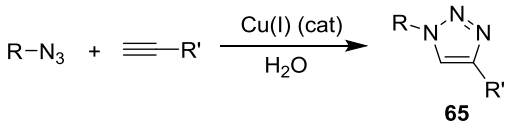

65

Scheme 2.21: The copper(I) catalysed cycloaddition between an alkyne and an azide.

A key application for this reaction has been found in bioconjugation, whereby biomolecules such as proteins, peptides or nucleic acids can be attached to a second entity of choice, for example fluorophores, therapeutic drugs or affinity tags.[172-174] This type of click cycloaddition proves efficient here due to the ease at which the alkyne and azide moieties can be incorporated into organic compounds, the selectivity of the reaction partners and the bioorthogonal nature of the reaction.[171]

We envisaged utilising our alkyne-labelled octreotide as a precursor onto which a second functional molecule could be attached. By utilising functionalised azides, an array of different bioconjugates could be created. To first determine whether the alkyne labelled octreotide was functional in a click cycloaddition reaction, a test reaction was run using the small PEG-azide **66** as shown in Scheme 2.22. The conditions employed

were based on those described by Hong *et al.*.[175] Sodium ascorbate is the chosen reducing agent to produce Cu(I) from the $CuSO_4$ salt *in situ*, employed largely because of its good water-solubility. To prevent further reduction or re-oxidation of the Cu(I), a stabilising ligand is often added. Tris-(hydroxypropyltriazolylmethyl)amine (THPTA) was chosen in this case, due to its reported efficiency and, again, water-solubility. These reagents allow the reaction to be carried out in fully aqueous, biologically compatible conditions.[173]

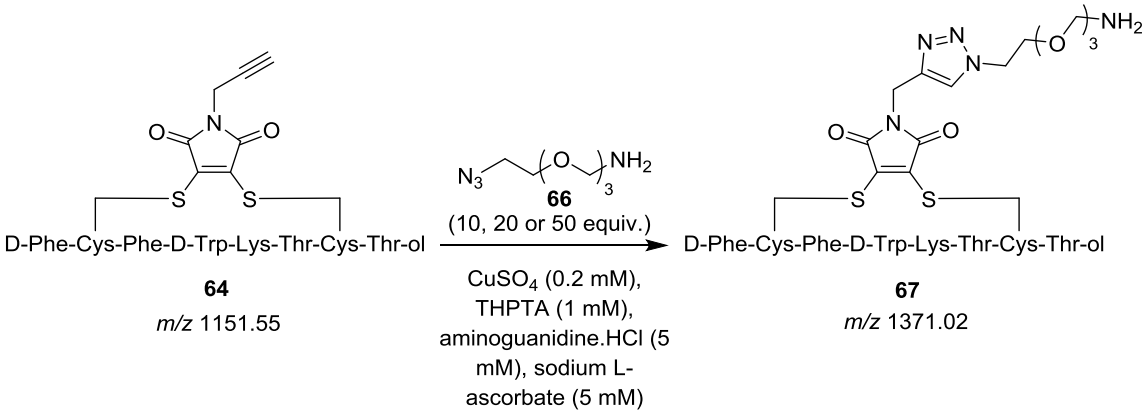

Scheme 2.22: The copper(I) catalysed click cycloaddition between alkyne functionalised octreotide **64** and PEG-azide **66** at varying equivalents (10, 20 or 50).

The reaction was carried out using varying number of equivalents of the PEG-azide, being in excess in all cases. All other possible variables remained constant throughout. The results are summarised in Table 2.14.

Table 2.14: The effect of increasing equivalents of PEG-azide **66** on formation of the desired product **67** (by apparent conversion by LC-MS).

Number of equivalents of PEG-azide **66**	*Yield of desired product* **67** *(apparent conversion by LC-MS)*
5	0%
10	48%
20	95%

The reaction proceeded well, with 20 equivalents of azide leading to the greatest formation of modified product **66**. The LC-MS spectrum of the product is shown below in Figure 2.61. Increasing the number of equivalents further lead to a more complex mixture of unidentifiable products.

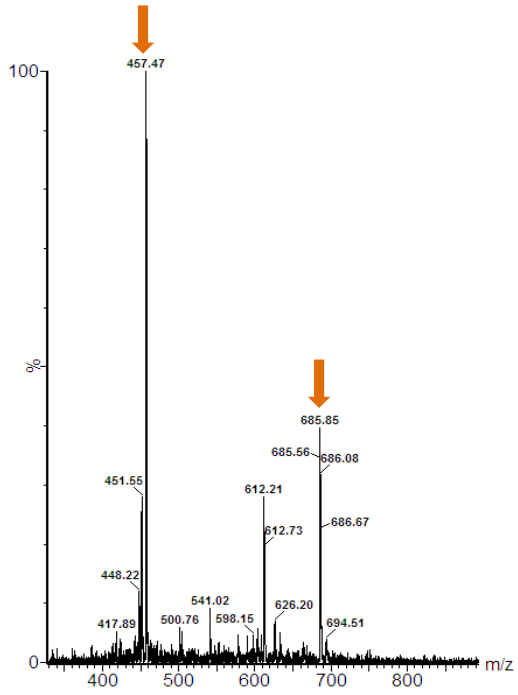

Figure 2.61: ESI mass spectrum of the reaction mixture with 20 equivalents of PEG-azide **66** with the peak at *m/z* 685.9 and *m/z* 457.47 corresponding to the doubly and triply charged ions of the expected click product **67** respectively (expected mass = *m/z* 685.7 and *m/z* 457.2).

With good evidence to suggest that, despite the alkyne moiety being attached to a peptide, the click cycloaddition is efficient, work progressed onto incorporation of a functional azide. The first example chosen was azide functionalised derivative of the therapeutic drug doxorubicin. Doxorubicin is a chemotherapeutic given for the treatment of a number of different cancers and exerts its pharmacological effect by means of DNA intercalation. Although the drug has proven effective in the treatment of many cancer patients, it is well known that it often causes numerous unwanted side effects such as alopecia, nausea, vomiting and neutropenia, to name just a few, and these limit its clinical usefulness. Attempts to improve tumour cell selectivity include encapsulation of the drug into liposomes[176], formation of doxorubicin hydrogels[177] and conjugation of the drug to a targeting moiety.[178,179]

We envisaged direct conjugation of doxorubicin to octreotide as a means to deliver the drug to tumours expressing the somatostatin receptor. As discussed in the introduction, many tumours tissues such as breast, kidney, thyroid and neuroendocrine have been found to overexpress this receptor, making it a popular means by which to differentiate and target tumour cells from healthy ones. In turn this can help minimise undesirable side effects. We attempted to attach doxorubicin as shown in Scheme 2.23 below. The azide functionalised drug **68** was synthesised and kindly donated by Dr João Nunes.[180]

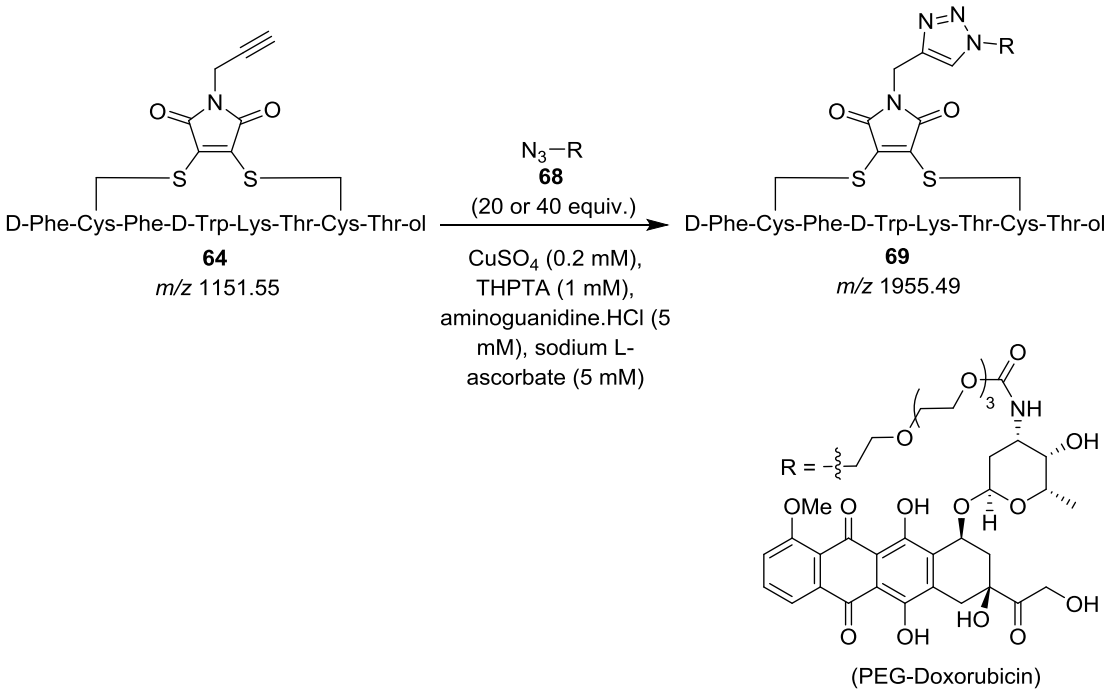

Scheme 2.23: The copper(I) catalysed click cycloaddition between alkyne functionalised octreotide **64** and doxorubicin-azide **68** in varying equivalents.

Despite using identical reagent ratios as previously described, the reaction between the alkyne-labelled octreotide **64** and doxorubicin-azide **68** did not proceed efficiently. A complex mixture of products was obtained, perhaps as a result of the degradation of doxorubicin by the copper iodide. There was evidence of product formation as shown in Figure 2.62, but the yield was low and difficult to quantify. Despite attempts at purification by RP-HPLC, the desired product **69** could not be isolated. Attempts to improve the efficacy of the reaction included increasing azide to 40 equivalents and extended reaction time of 24 hours, but with no improvement.

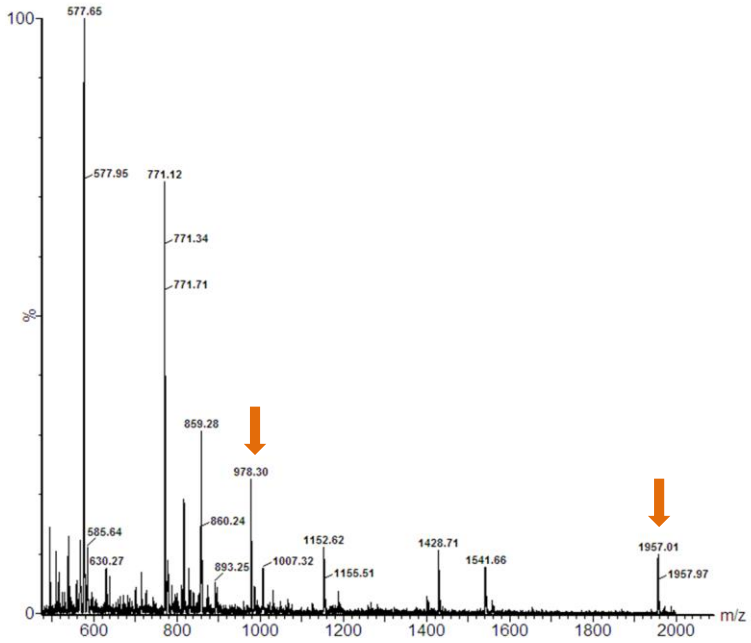

Figure 2.62: ESI mass spectrum of the reaction mixture with 20 equivalents of doxorubicin-azide **68** after 1 h. Peak at *m/z* 1957.00 and *m/z* 978.30 corresponding to the singly and doubly charged ions of the expected click product **69** respectively (expected mass = *m/z* 1955.49 and *m/z* 977.6).

After experiencing difficulties with this route to a functionalised octreotide bioconjugate, we sought an alternative strategy. It was envisaged that, conducting the click cycloaddition between the azide and the maleimide-alkyne to create a functionalised maleimide *prior* to insertion into the peptide disulfide could overcome the issue; the disulfide bridging reaction was consistently efficient and quantitative. With a concomitant shift in our focus from a drug-based conjugate to new methodology development for multimodal imaging, efforts in this alternative strategy were pursued and are discussed below.

2.3.4 Octreotide as a Monomolecular Multimodal Imaging Agent (MOMIA)

As described in the introduction, in cancer diagnosis, employing multiple imaging agents in conjunction helps to improve the accuracy of the staging and localisation of tumours. There are a variety of imaging techniques currently used in the clinic, each using different imaging moieties.[181] A relatively new concept is the combining of two or more of these moieties into a single molecule in order to minimise the number of doses administered to the patient and the pharmacokinetic variance associated with giving each diagnostic agent separately.[124] We envisaged making such a molecule, by employing octreotide as a somatostatin receptor targeting moiety, as before, and then

attachment of two different imaging modalities using a maleimide functionalised with both. A schematic of such a construct is shown below in Figure 2.63.

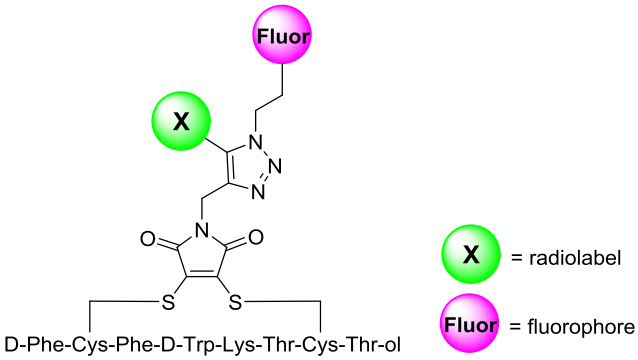

Figure 2.63: The proposed octreotide-based multimodal imaging agent.

2.3.4.1 Maleimide Synthesis

There were a number of synthetic considerations to be taken into account when designing the molecule of choice:

- The fluorophore needs to modifiable without detriment to its fluorescence lifetime or quantum yield. Rhodamine B **70** is commercially available at relatively low cost, has good photostability, quantum yield and water-solubility and has a carboxylic acid group which lends itself to functionalization.[182] It was decided that this would be a suitable fluorophore to enable visualisation.

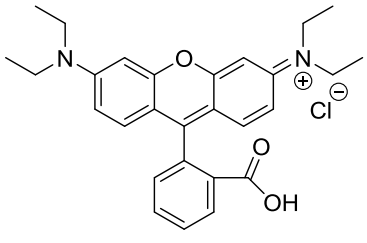

70

Figure 2.64: Rhodamine B (**70**).

- In order for the molecule to be 'clickable', alkyne or azide functionality needed to be incorporated. An azide was chosen, connected to the fluorophore by a 6-carbon linker; this is important as the bulky rhodamine molecule may hinder the click cycloaddition if it is too close to the reactive site.

- It was decided that this linker should be adjoined to rhodamine by means of an amide connectivity; amide bonds being less prone to hydrolysis than the corresponding ester linkage. To install this, a piperidine moiety was utilised, this way a tertiary amide is produced in connection with the rhodamine molecule (Figure 2.65). This should inhibit any intramolecular cyclisation which is reported to occur with secondary amide connectivity – this is found to cause loss of fluorescence.[183]

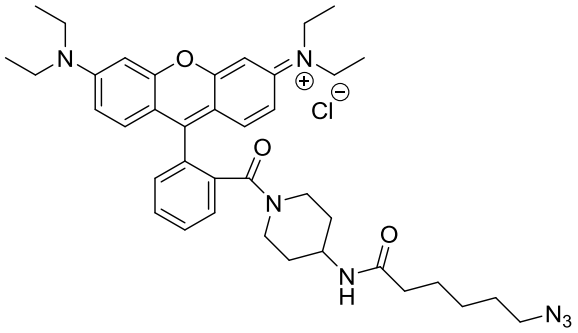

Figure 2.65: Azide functionalised rhodamine B

- It was proposed that a radiolabel would be a beneficial second imaging modality. This would enable imaging by SPECT or PET. A novel route to incorporate ^{125}I into the triazole product of a click cycloaddition in a one-pot, three component, copper(II)-mediated reaction has been pioneered by the Arstad group at UCL and described by Yan *et al.*[184] (Scheme 2.24); it was envisaged that this could be employed in conjunction with our rhodamine-azide and *N*-alkyne maleimide.

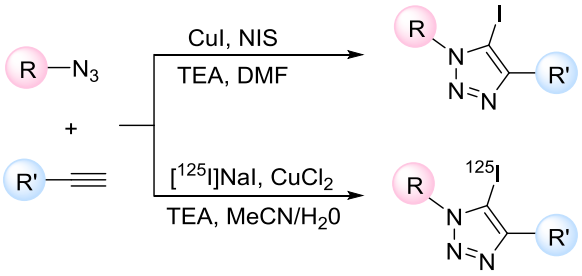

Scheme 2.24: Synthesis of 5-[^{125,127}I]Iodo-1,2,3-triazoles.[184]

- Lastly, the nature of the *N*-alkyne maleimide was considered. The dibromomaleimide derivative **63** was considered but, in order to eliminate the chance of any halogen exchange reactions occurring between the iodine in the

click reaction and the bromine eliminated during the disulfide bridging reaction, the dithiophenol derivative **71** was synthesised and utilised instead.[170]

The synthetic strategy devised is shown below (Scheme 2.26). The carboxylic acid of rhodamine B was first converted to the more reactive acid chloride **72** using excess oxalyl chloride. This reaction is fast and efficient and was quantitative, meaning further purification was not necessary. This acid chloride was taken on immediately to avoid degradation. It was reacted with the *N*-Boc amino piperidine, with $CsCO_3$ as a base, to produce the product **73** with the desired tertiary amide linkage in 67% yield.[46] Deprotection of this with TFA lead to quantitative formation of the desired rhodamine moiety as the TFA salt **74**.

Meanwhile, 6-bromohexanoic acid was converted to the azide **75** by reaction with sodium azide and heating at 50 °C (Scheme 2.25).[185] Despite attempts with longer reaction times and solvent mixtures, the yield of this reaction remained at around 40% which is lower than expected but still acceptable.

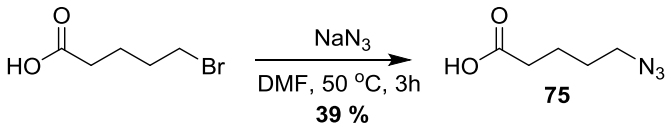

Scheme 2.25: The synthetic route to 6-azidohexanoic acid.

Acid **75** was coupled to the rhodamine-TFA salt by means of a classic *N,N,N′,N′*-Tetramethyl-*O*-(1*H*-benzotriazol-1-yl)uronium hexafluorophosphate (HBTU) coupling with catalytic 1-hydroxybenzotriazole (HOBt) and *N,N*-diisopropylethylamine (DIPEA) as a base. Yields of the desired azide **76** were good, between 65-77% over 3 attempts.

Finally, this azide-functionalised rhodamine B **76** was taken on to the final step, the click reaction with *N*-alkyne dithiophenolmaleimide **71**. As previously mentioned, this reaction has been pioneered by the Arstad group at UCL, with whom we worked in collaboration for this section of the project. The group have carried out thorough optimisation of the protocol to obtain high yields of the iodinated triazoles from a range of alkynes and azides. The mechanism of the reaction remains largely elusive; various speculations are discussed in their published paper.[184] For structural characterisation and future imaging studies and activity testing the nonradioactive ^{127}I containing compound

77 was synthesised. This uses Cu(I) iodide, TEA and *N*-chlorosuccinimide (NCS) with the alkyne and azide in a one-pot protocol, as shown in Scheme 2.24. In this case, a 37% yield of the desired product **77** was obtained as a dark purple solid and was kept for further experiments. The synthetic strategy is shown below in Scheme 2.26.

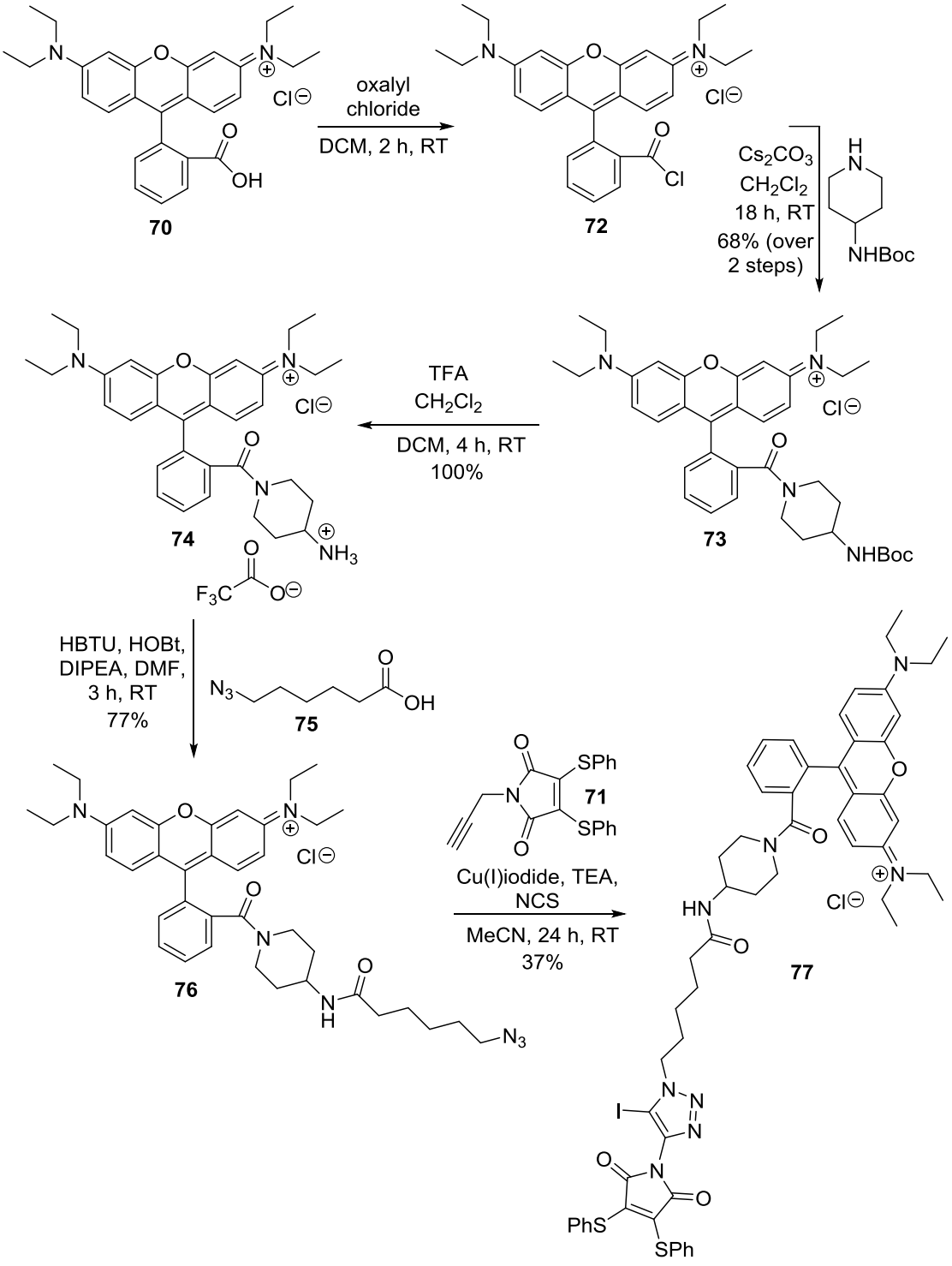

Scheme 2.26: The synthetic route to the desired MOMIA-maleimide reagent (**77**).

When synthesising the radioactive derivative **78**, which was carried out by our collaborators, the order of addition of the reagents has been found to be important; the highest yields were obtained when the alkyne, copper(II) chloride and the TEA were combined prior to the addition [^{125}I]NaI and the azide.[184] This protocol was followed using the azide-functionalised rhodamine B **76** and the alkyne functionalised maleimide **71** (Scheme 2.27).

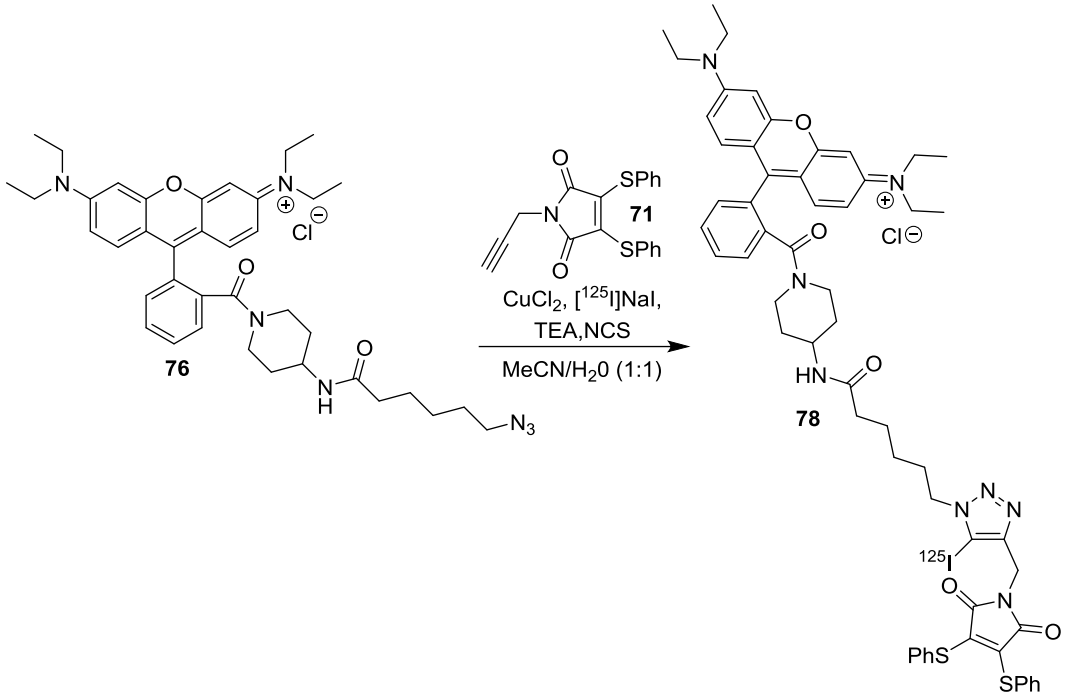

Scheme 2.27: Synthesis of the radiolabelled maleimide **78**.

2.3.4.2 Characterisation of Radioactive [^{125}I] Multimodal Maleimide

In order to characterise and quantify the radiolabelled maleimide **78**, radio-HPLC was employed.[184] To determine the exact retention time expected for the desired product, the nonradioactive compound **77** was run as a reference. The LC-chromatogram obtained is shown below in Figure 2.66.

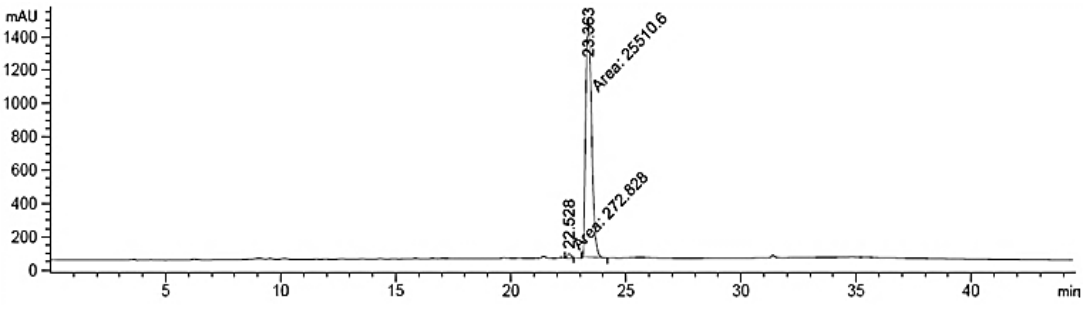

Figure 2.66: The LC chromatogram of maleimide **77** (retention time: 23.4 min).

A sharp peak was observed for compound **77** and a retention time of 23.36 minutes was recorded. Subsequently, the reaction in Scheme 2.27 was carried out, and the reaction mixture analysed by radio-HPLC using exactly the same conditions as previously employed. The LC-chromatogram (**A**) and the radio-chromatogram (**B**) are shown in Figure 2.67.

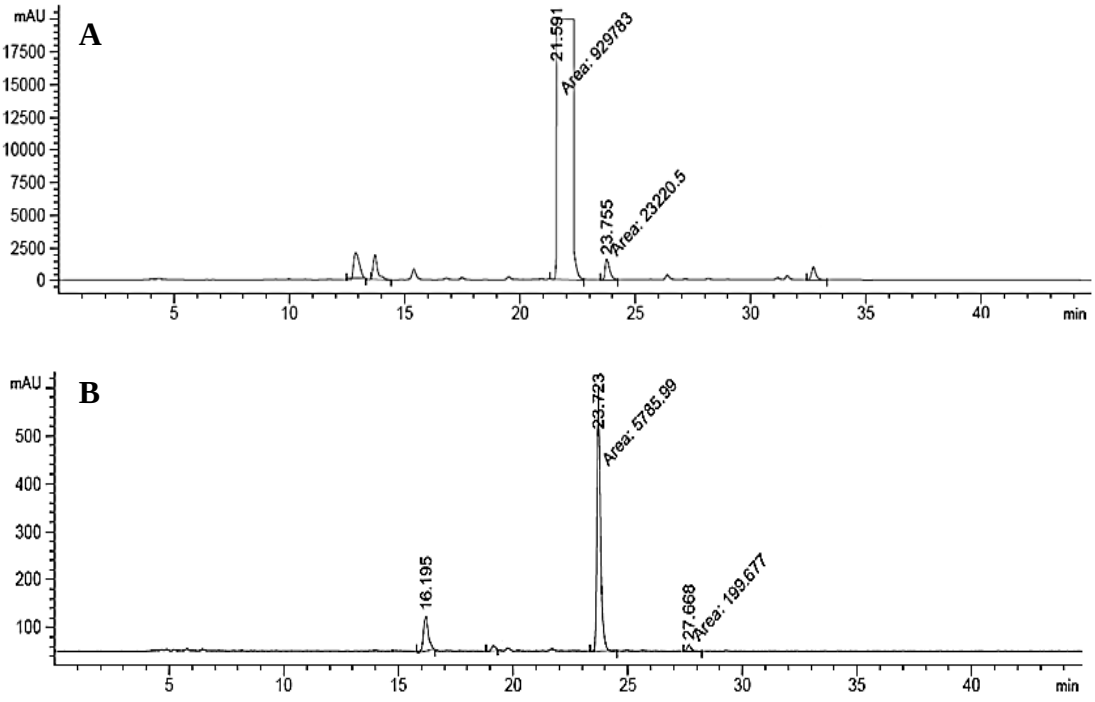

Figure 2.67: **A**) The LC chromatogram of the 'click' cycloaddition reaction mixture (retention time of non-iodinated product: 21.6 min, retention time of iodinated product: 23.8 min), **B**) The radio-chromatogram of the 'click' cycloaddition reaction mixture (retention time of iodinated product: 23.7 min).

From the comparison of the LC-chromatogram **A** with that of the reference compound in Figure 2.66, we can assign the peak of retention time 23.76 minutes as the radiolabelled maleimide **78**. The large peak at 21.59 minutes is most likely the non-iodinated triazole which is the competing reaction in such a protocol. Comparing LC-chromatogram **A** with the radio-chromatogram **B** provides complimentary evidence. The peaks in chromatogram **B** show products that have incorporated ^{125}I; the major peak in this case being that with a retention time of 23.72 minutes, which correlates well with the retention time of the assigned product **78** in chromatogram **A**. In addition, there is no peak in the radio-chromatogram at or around 21.59 minutes, again suggesting that this is the non-iodinated derivative.

To fully confirm that the product at 23.76 minutes is the desired radiolabelled maleimide **78**, this peak was collected and co-injected with the non-radiolabelled reference compound **77**. If the compounds are atomically identical, besides the isotopic nature of the iodine, then co-elution should be observed. The LC- and radio-chromatograms are shown in Figure 2.68.

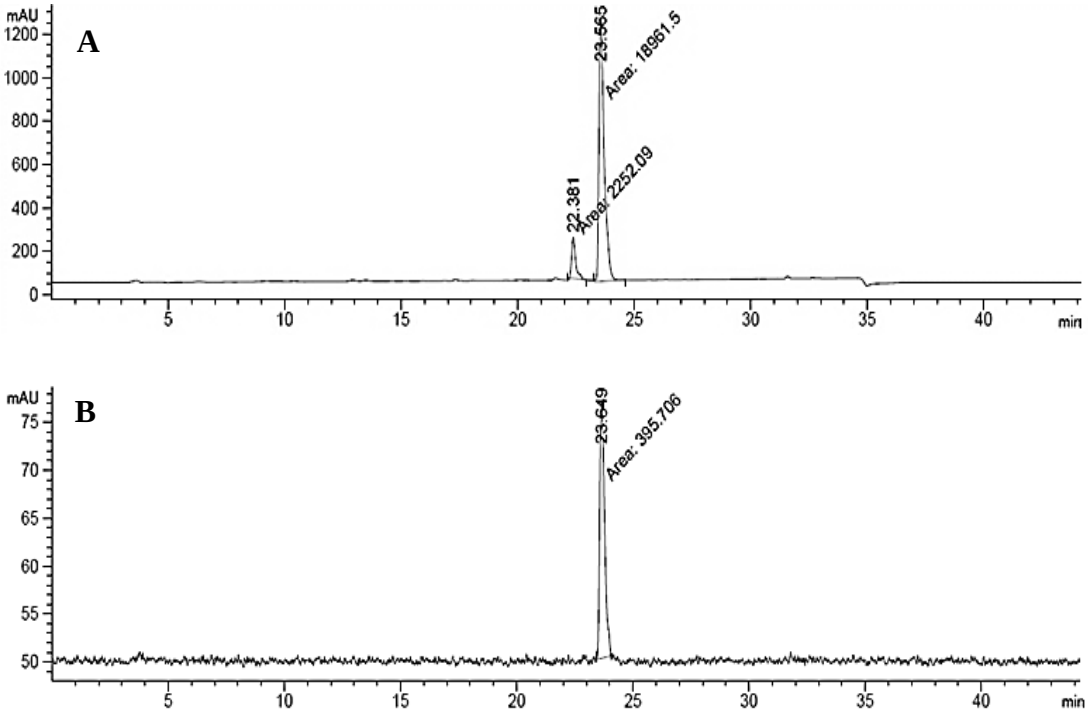

Figure 2.68: **A**) The LC chromatogram of maleimide **77** and maleimide **78** co-injection (retention time: 23.6 min), **B**) The radio-chromatogram of maleimide **77** and maleimide **78** co-injection (retention time: 23.7 min).

Besides a small impurity at 22.38 minutes, we observed very good co-elution of both the non-radiolabelled maleimide **77** and the labelled derivative **78** at 23.57 minutes confirming formation of the desired product.

Confident that formation of the desired product was successful, it was then quantified. The analytical radiochemical yield (RCY), which is determined from the area under the peak in the radio-chromatogram **B** (Figure 2.67), was determined to be 58%. The isolated RCY is determined by the amount of product-associated radioactivity isolated from a known amount of radioactivity added into the reaction.[184] In this case, 1.263 MBq of radioactivity was added into the reaction in the form of [^{125}I]NaI and 0.58 MBq of product-associated radioactivity was isolated following the reaction. This equated to an isolated RCY of 49%. Considering the bulky nature of the azide participating in the

reaction and the competing formation of the non-iodinated triazole, a yield of around 50% of the desired product is pleasing.

2.3.4.3 Maleimide Modification of Octreotide

In order to examine the bridging efficacy of the doubly functionalised maleimide, the nonradioactive derivative was used to reduce unnecessary exposure to radioactivity; this and the radioactive compound should act identically. As with all other octreotide bridging experiments, octreotide **34** was first reduced using 1.2 equivalents of TCEP before addition of 1.2 equivalents of maleimide **77** in a step wise protocol (Scheme 2.28).

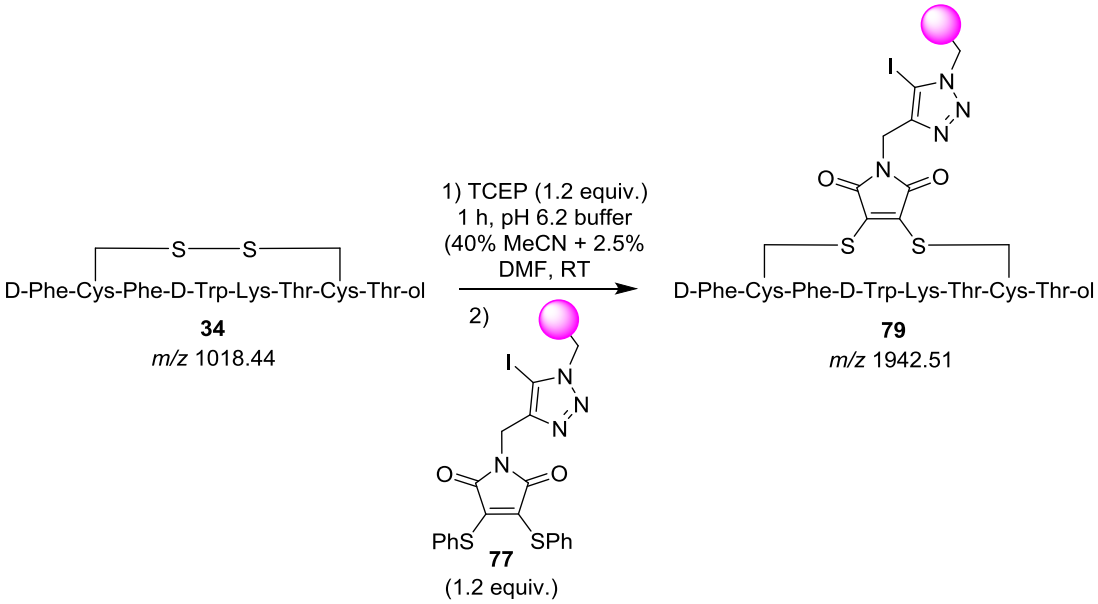

Scheme 2.28: Step wise bridging of octreotide **34** by reduction with TCEP (1.2 equiv.) followed by addision of maleimide **77** (1.2 equiv.).

Full conversion to the bridged peptide **79** was observed within 15 minutes. This suggests that, despite the bulky substituents attached to the maleimide, insertion into the disulfide bond is still efficient. The mass spectra of the reaction are shown below in Figure 2.69.

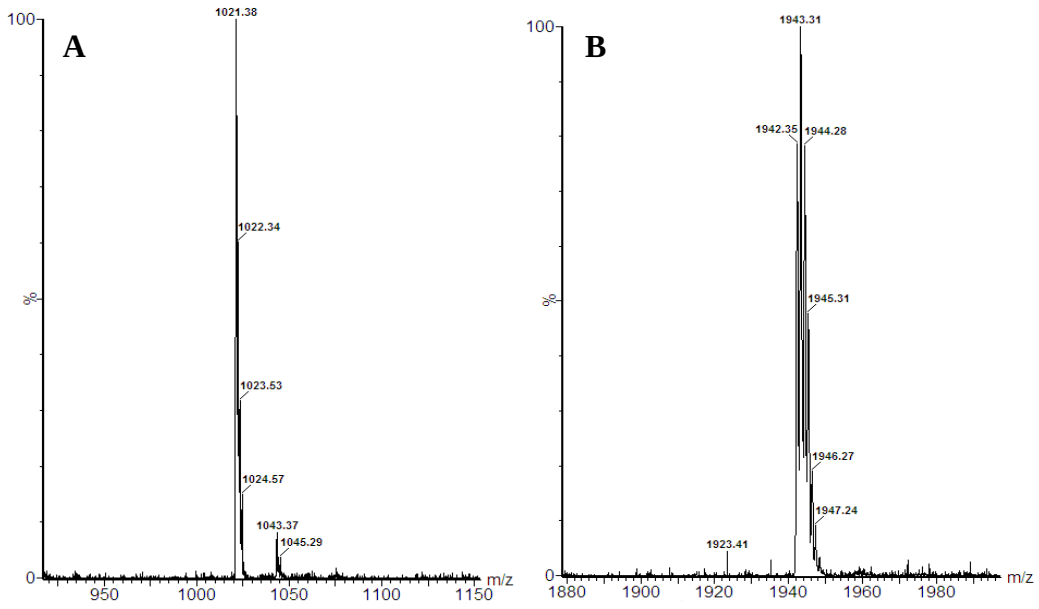

Figure 2.69: ESI mass spectrum of **A**) peak at *m/z* 1021.7 corresponding to reduced octreotide (expected mass = *m/z* 1021. 3) and **B**) peak at *m/z* 1943.31 corresponding to modified octreotide **79** (expected mass = *m/z* 1942.51).

In order to remove the organic solvents, buffer salts and any excess reducing agent and maleimide, the modified octreotide was purified by dialysis. The product was then dried by centrifugation *in vacuo* before being redissolved in deionised water. This product was then analysed for its purity by LC-MS analysis (Figure 2.70).

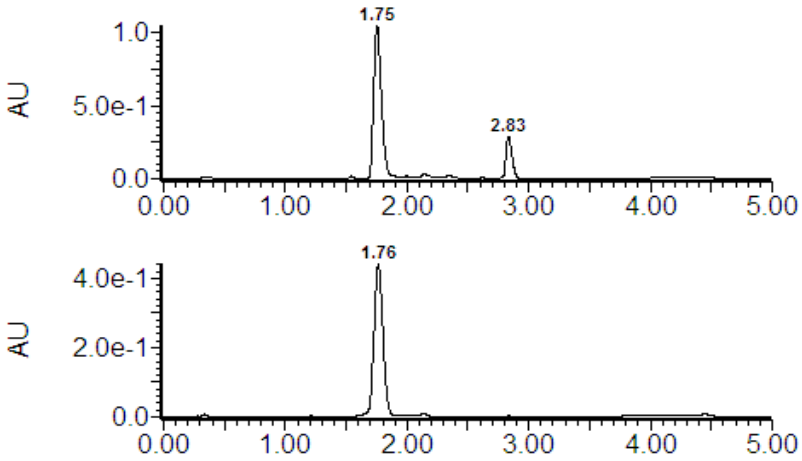

Figure 2.70: LC chromatogram of **A**) crude reaction before dialysis **B**) after dialysis. (Modified peptide **79** retention time: 1.75-1.76 min, maleimide **77** retention time: 2.83 min).

A very clean UV-vis spectrum of the desired product was obtained after dialysis. Purity was confirmed from the mass spectrum (not shown) confirming no contaminating small molecules remained. This product was used for further experimentation.

2.3.4.4 Imaging Studies Using Octreotide-MOMIA

With the functionalised octreotide derivative **79** in hand, analysis of its utility as a MOMIA began. It is imperative that, despite conjugation, octreotide retained its specificity for the somatostatin receptor and that the rhodamine and radioisotopic iodine retained their activity to enable visualisation.

In order to determine whether the functionalised peptide still bound to the receptor and whether the fluorescence of the attached rhodamine moiety could be visualised effectively, confocal microscopy experiments were carried out. Three cell models were employed in these experiments:

- Cell line with endogenous expression of the somatostatin receptor: human pancreatic BON-1 cells derived from a neuroendocrine tumour, which are reported to display somatostatin receptor subtype 2 expression.[186,187]
- Cell line with heterologous expression of the somatostatin receptor: HEK293 cells transiently transfected with somatostatin receptor subtype 2, which should display high levels of receptor expression. These were co-transfected with eGFP to determine precisely which cells express the receptor.
- Negative control cell line: HEK293 cells with no somatostatin receptor expression.

These cell lines were cultured onto glass bottomed petri dishes and the 'engineered' cell line transfected with the somatostatin receptor subtype 2. Each cell line was incubated with 1 μM of the octreotide-MOMIA **79** for 20 minutes at room temperature before removal and washing with buffer to remove excess unbound octreotide-MOMIA. The cells were then visualised by confocal microscopy at two excitation wavelengths; 488 nm was used to visualise fluorescence from eGFP as a marker of successful cell transfection and 543 nm was used to visualise rhodamine fluorescence. Some images from these experiments are shown below in Figures 2.71 and 2.72.

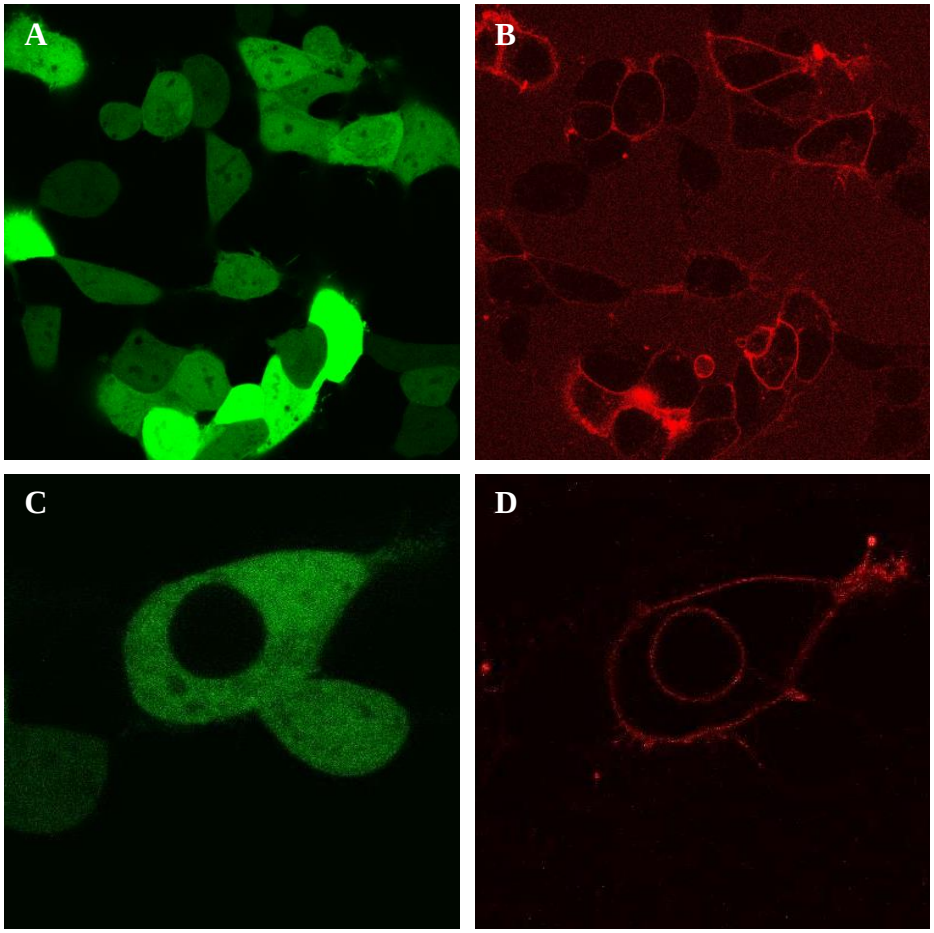

Figure 2.71: Confocal images of HEK293 cells transfected with the somatostatin receptor subtype 2 and eGFP after incubation with 1 µM octreotide-MOMIA **79** for 20 min. **A**) & **C**) Visualisation at 488 nm shows positively expressing cells fluorescing green. **B**) & **D**) Visualisation at 543 nm shows rhodamine fluorescing red. **A**) and **B**) Visualisation before removal of octreotide-MOMIA and buffer wash. **C**) and **D**) Visualisation after removal of octreotide-MOMIA and buffer wash.

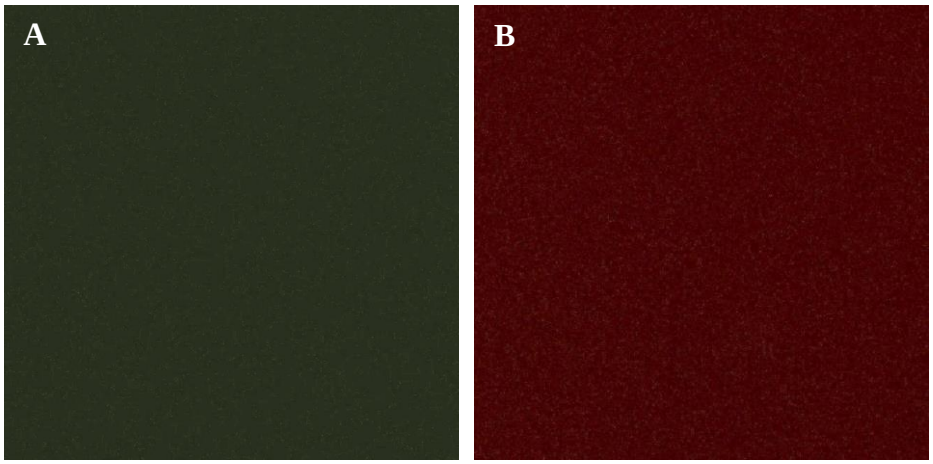

Figure 2.72: Confocal images of non-transfected HEK293 cells after incubation with 1 µM octreotide-MOMIA **79** for 20 min. **A**) Visualisation at 488 nm. **B**) Visualisation at 543 nm.

Fluorescence imaging at a wavelength of 488 nm allowed effective visualisation of cells expressing eGFP and therefore expressing the somatostatin receptor subtype 2. Subsequent visualisation of the same field of cells at 543 nm allowed for visualisation of the red fluorescence of the rhodamine bearing octreotide-MOMIA **79**. From Figure 2.71, localisation of fluorescence in images **A** and **B** suggests octreotide-MOMIA **79** can effectively target somatostatin receptor positive cells. To determine whether this cell binding is specific and due to interaction with the somatostatin receptor, identical experiments were carried out on the same cell line but without transfection with the receptor. No fluorescence was observed at 543 nm (Figure 2.72 **B**), suggesting no binding of the octreotide-MOMIA **79** to the cells.

Identical experiments were also carried out the BON-1 cells which were originally derived from a young male presenting a lymph node metastatic pancreatic tumour (Figure 2.73). This neuroendocrine cell line is commonly used as the cells display the morphology and cell-surface markers characteristic of such tumours.[186] As discussed in the introduction, up-regulation of somatostatin receptor expression is well known in neuroendocrine tumours and so we chose them as a suitable model for our experiments. Using a cell line such as BON-1 that naturally expresses the receptor allows a more physiologically relevant analysis of the utility of octreotide-MOMIA **79** as levels of expression are more representative of what they would be in tumour tissue *in vivo*.

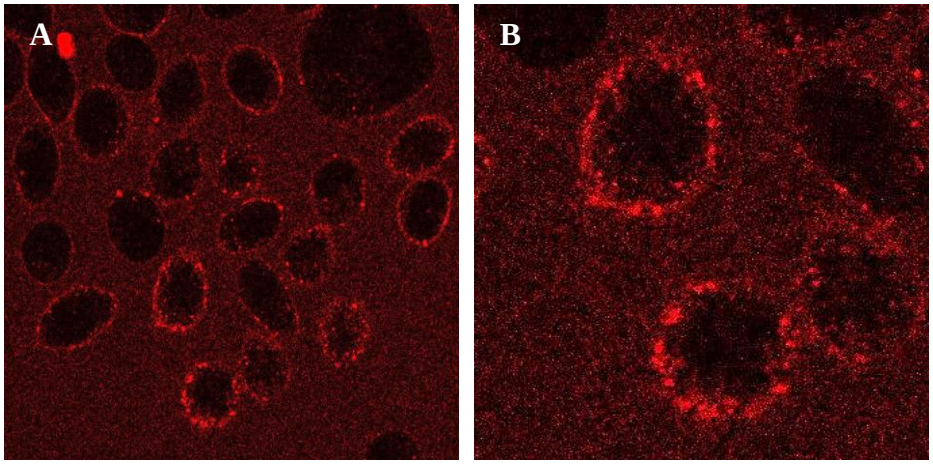

Figure 2.73: **A**) Confocal image of BON-1 cells at 543 nm after incubation with octreotide-MOMIA **79** for 20 min **B**) a zoomed image of a group of cells from Figure 2.73 **A**.

From Figure 2.73, cell membrane localisation of the octreotide-MOMIA **79** can be seen. These experiments give more promising evidence to suggest that the peptide has

retained the ability to bind to its target. Unlike the previous images of the transfected HEK293 cells where fluorescence seemed to be quite uniform around the cell membrane, localisation in this case appears to be more punctuated around the membrane. This could be as a result of receptor internalisation upon binding of octreotide-MOMIA **79**, as known, and previously discussed, for the somatostatin receptor upon binding of its agonists. The punctuation on the periphery of the cells could be the formation of vesicles; a common route by which receptor internalisation and trafficking occurs.[188] Such endocytosis could be further investigated by experiments with longer incubation times.

Altogether, these confocal imaging studies suggest that the MOMIA **79** still has the ability to selectively bind to its receptor target, meaning the tumour-cell targeting aspect of the bioconjugate is still functional. In addition, good fluorescence was observed during visualisation, showing that the rhodamine had maintained its fluorescent nature during synthesis of MOMIA **79**. Although the compound tested in this case was the non-radiolabelled derivative, comparable results would be expected from the radiolabelled maleimide **78** when incorporated into octreotide. This bioconjugate could then also be employed in SPECT imaging.

2.3.5 Summary of Octreotide Modification

Octreotide presented itself as in ideal candidate for maleimide modification at its disulfide bond. Considerable coverage in the literature of creating functionalised bioconjugates from this peptide highlighted the utility of octreotide in this field. Presence of a single disulfide made the modification procedure considerably more straightforward than with tertiapin Q as issues with disulfide scrambling were circumvented.

To accurately determine the effect of the insertion of a maleimide bridge into the disulfide bond of such a small peptide, a non-functionalised maleimide was first utilised. The modification was rapid and efficient and the desired product was purified and characterised before being tested for any alteration to biological activity. The ability of the modified peptide **61** to activate the somatostatin receptor was monitored using whole-cell patch clamp experiments. The modified peptide was still able to activate the receptor, with an EC_{50} of 118 nM. Compared to native octreotide **35** with an EC_{50} of 0.66 nM, the agonistic activity of our modified derivative had been attenuated. A

decrease in agonist efficacy was also observed, suggesting partial agonist characteristics. This was reasoned to be as a result of the proximity of the cysteine residues to the pharmacophore of the peptide which is a region where perturbations to structure and conformation are not well tolerated.

As agonistic activity was still in the nanomolar range, work progressed on to synthesising functionalised octreotide bioconjugates. Our first target was an alkyne-linked derivative, with the aim of using this as a precursor onto which a variety of azide-functionalised biomolecules could be attached. The alkyne-functionalised octreotide **64** was again synthesised with relative ease. When examined for its agonistic activity, the expected attenuation was again observed; an EC_{50} of 105 nM was obtained. The agonistic efficacy of this modified derivative was not compromised in this case however, and maximal current increase was observed at higher concentrations. Work progressed onto optimising the conditions for an efficient 'click' cycloaddition reaction between alkyne-functionalised octreotide and an azide. Preliminary experiments with a small azide were promising, but this did not translate well when a larger, functional azide was employed. Doxorubicin-azide did not react well under any conditions attempted.

After concluding that this may not be the most efficient route to a functionalised octreotide bioconjugate, our focus altered towards creating the desired functionalised maleimide prior to incorporation into the disulfide bond. Concurrent with this was the discovery of the field of targeted, multimodal imaging agents within the literature. We postulated that, using the *N*-alkyne maleimide, we could create such a molecule. In collaboration with the Arstad group at UCL, and utilising their one-pot, three-component approach to forming iodinated triazoles via a 'click' cycloaddition, we pursued this. A maleimide functionalised with both the fluorophore rhodamine and the radiolabel ^{125}I was synthesised using this strategy, and subsequently incorporated into the disulfide bond of octreotide. In this way we hoped to have created a new candidate for the next generation of MOMIA – octreotide as the targeting moiety for localising somatostatin receptor positive tumours, rhodamine to enable subsequent fluorescent imaging and ^{125}I to facilitate SPECT imaging.

Confocal microscopy imaging was employed to visualise the possible binding of the octreotide-MOMIA **79** to the somatostatin receptor. Efficient fluorescence intensity from the rhodamine moiety allowed visualisation of the bioconjugate binding to cells. Pleasingly, the octreotide-MOMIA showed specific binding to cells endogenously expressing the somatostatin receptor (BON-1 cell line) and those transfected with the receptor. Fluorescence appeared to accumulate in to what we predict to be vesicles, suggesting internalisation of the octreotide-MOMIA could be occurring upon receptor binding. Further experiments are required to confirm this hypothesis.

In conclusion, maleimide modification of the disulfide bond of octreotide is relatively straightforward. However, incorporation of a two-carbon bridge between the cysteine residues is not completely tolerated and, as a result, agonistic activity towards its receptor target is attenuated. Despite this, biological activity remained within the nanomolar range. An octreotide bioconjugate linked to a fluorophore and a radiolabel has been synthesised and promising imaging studies suggest this could be a new novel candidate for a MOMIA to aid the diagnosis and localisation of somatostatin receptor positive tumours. Such diagnostic agents serve to minimise the number of compounds administered to patients during diagnosis and, as a result, helps reduce pharmacokinetic variance and associated side-effects. Current methods to incorporate multiple visualisation agents into one molecule efficiently are currently limited; our methodology provides a novel and straightforward strategy to address this issue.

Chapter 3

Concluding Remarks & Future Directions

Cysteine residues present themselves as a convenient target for site-selective modification, owing largely to their low natural abundance and significant nucleophilicity. The concept of targeting disulfide bonds as a site of modification is relatively new, and has been recently advanced by the advent of the 'modification by re-bridging' strategy. Exploiting naturally occurring disulfide bonds with this methodology allows the incorporation of a desired functional moiety whilst maintaining the structural integrity conferred by the original bond. It also means that no prior manipulation of the peptide or protein, such as incorporation of a non-natural amino acid residue, needs to be carried out prior to the modification. This methodology continues to be developed and fine-tuned, which the work in this project aimed to further.

The 3,4-disubstituted maleimides pioneered and developed by our group have proved efficient in the modification of disulfide bonds. They act fast, with incorporation into a reduced disulfide occurring in minutes. Recent work has allowed their utility in an *in situ* methodology, serving to re-bridge the two cysteine residues as soon as they are exposed by reduction. Work in this project has helped further the development of both the reagents and the protocols employed. The way in which the maleimides can be tailored towards the desired application with significant ease was demonstrated; the reactivity of the reagent can be varied by altering the chemistry of the leaving groups, depending on whether a faster or slower acting reagent is sought. The properties of the compounds can also be adjusted by design, for example improving water-solubility to remove the need for organic solvents in the protocols means that aqueous conditions can be employed – highly desirable when working with biological systems. Finally, by careful design and employing the right chemistry, the nitrogen of the maleimide ring provides a convenient site for attachment to a functional moiety of choice. The library of functionalised maleimides available continues to expand; a novel bi-modal example synthesised within this project has enabled the scope of this to be furthered. Pleasingly, development of such bi-modal reagents is set to continue.

Despite the efficiency and scope of these reagents, they are not without limitations which became apparent over the course of this project. Disulfide bonds are fundamental, most predominantly in cases where the geometry of the local environment is integral to the biological activity and target specificity of the peptide or protein. In small peptides limited structural constraint is conferred by the non-covalent interactions between amino acid side chains, for which disulfide bonds must compensate. It is this which makes the modification of these bonds very challenging.

Although the maleimides studied are indisputably fast reacting and selective for cysteine thiolates over other nucleophilic sites within the peptide, their incorporation into the disulfide bond is not without detriment. From the work on octreotide it is clear that the incorporation of an unnatural two-carbon bridge is not completely tolerated in small peptides; there is an associated attenuation of biological activity. It appears that the, albeit relatively small, increase in distance between the cysteines is enough of a geometric alteration to hinder binding to the target. This is compounded by the proximity of the disulfide to the pharmacophore of the peptide, a limitation which will be common amongst many small peptides.

In addition, small peptides with multiple disulfide bonds in proximity also bring challenges. Limited tertiary structure means that such peptides effectively lack a significant hydrophobic core - the site at which larger proteins bury residues and bonds that are integral to their structure and function. As a result, the disulfides of small peptides are often all solvent accessible and have similar reactivity towards both reducing agents and modification reagents. In this way, selectively targeting one disulfide bond as a site of modification is very difficult, as observed in the work on tertiapin Q.

These issues present themselves as the limitations to the maleimide modification strategy. In such cases alternative routes to bioconjugates may be superior; *N*- or *C*-terminal attachment of a functional moiety for example. In this way, the pharmacophore of the peptide can hopefully remain unperturbed.

Despite the discussed challenges and limitations encountered, the value and efficacy of the analytical techniques employed throughout this project should be highlighted.

Although a relatively complex technique, the patch clamp analysis proved to be an informative and accurate method for monitoring the biological activity of the studied peptides upon binding to their targets. Such high-resolution current recordings allowed for precise determination of IC_{50} or EC_{50} values and the utility of such a technique for the detailed study of physiological systems was quickly realised. In addition, the tandem MS analysis presented itself as another invaluable technique; it facilitated the unequivocal location of the maleimide modification within a peptide chain. Detailed and informative data was obtained in minutes using very small amounts of product and, in some cases, without the need for prior purification. The scope of such an analytical method is undoubtedly huge.

With regards to the future directions for this study, the aforementioned limitations to maleimide modification are predicted to be overcome with careful consideration of the target. Larger peptides or proteins with significantly greater structural integrity are more likely to tolerate the incorporation of a maleimide bridge without detriment to their biological activity. In this way, the multimodal maleimide incorporating a radiolabel and fluorophore would perhaps be of increased value if employed on a larger protein. The protein would of course need high affinity for a desirable receptor, one that is overexpressed on tumour cells, but we postulate that this affinity is less likely to be attenuated after incorporation of our multimodal maleimide. As a result, a superior MOMIA could effectively be created. Such a hypothesis is supported by recent publications from our group where antibody fragments have been efficiently modified using the maleimide bridging strategy, with full maintenance of their target binding affinity.[59,189] In these cases incorporation of the maleimide proves not to have detrimental effect on the structure of the protein.

Further to this, the multimodality of this reagent is not limited to diagnostics. One can envisage incorporation of a drug, instead of a fluorophore, alongside the radiolabel to create a reagent that confers both diagnostic and therapeutic functionality. Such constructs are often termed ‘theranostics’.[190] In order to do this, the drug of choice will require activation as an azide to be able to participate in the ‘click’ cycloaddition reaction.

When considering tertiapin Q, and other small peptides with multiple disulfides in close proximity, the outlook is not so clear. There are other strategies that could be considered to attempt to circumvent the issue of disulfide scrambling; the employment of additives which could help stabilise the tertiary structure of the peptide is one example. If the issue cannot be overcome in this fashion, it would seem that the most facile way to selectively target one disulfide would be during solid-phase synthesis of the peptide. In this way cysteines can be selectively protected as desired, facilitating with confidence the modification of only the desired residues.

Overall, it is clear that every peptide or protein target should be considered individually when attempting modification to produce bioconjugates. The chemistry and structure of peptides and proteins is extensively variable and, as a result, no one strategy for modification will be universal. Extensive consideration and careful design of reagents and protocols is required with each case. Combined, however, the continually increasing variety of modification technologies is proving hugely successful in the pursuit and development of novel bioconjugates for diagnostic and therapeutic applications.

Chapter 4

Experimental Procedures

4.1 General Information

Synthetic reactions were all carried out at room temperature and under an inert atmosphere unless otherwise stated. All commercially available reagents were used as received without further purification.

^{1}H and ^{13}C NMR spectra were recorded on either a Brüker Avance-500 machine or a Brüker Avance-600 machine (as stated), ran at a frequency of 500 MHz and 600 MHz respectively for ^{1}H spectra and 125 MHz and 150 MHz respectively for ^{13}C spectra. Deuterated solvents used were obtained from Sigma Aldrich. Peaks are assigned as singlet (s), doublet (d), triplet (t) or multiplet (m) and are sharp peaks unless denoted as broad (br). Chemical shifts are recorded in parts per million (ppm) denoted by δ. Proton coupling constants (*J* values) are reported in Hertz (Hz). Where necessary, assignments were confirmed with the aid of DEPT spectra.

Mass spectra were recorded on a VG70-SE mass spectrometer running in EI or CI mode.

Matrix-assisted laser desorption/ionisation (MALDI) mass spectra were recorded on an Axima-CFR (Shimadzu) instrument.

Infra-red (IR) spectra were recorded on a PerkinElmer Spectrum 100 FT-IR spectrometer operating in ATR mode.

Melting points were measured using a Gallenkamp apparatus and are uncorrected.

LC-MS measurements were taken on an Acquity Ultra Performance LC instrument. LC data was recorded at a wavelength of 280 nm and MS data obtained in ES^{+} and ES^{-} mode with a detection range between *m/z* 90 – 2000. LC solvent solutions: A - H_2O (0.1% TFA); B – MeCN (0.1% TFA); running conditions: Gradient 5-95% B in 5 min; injection volume: 10 µl. Masses are assigned as a mass to charge ratio (*m/z*). For tertiapin Q analysis, LC-MS spectra are de-convoluted. This was done using the maximum entropy algorithm MaxEnt-1. The output mass ranges were set to 2000-4000 *m/z*, with a resolution of 2 Da/channel. The damage model used uniform Gaussian, with a peak width at half height of 0.75 Da. The minimum intensity ratios were set at 33% for either side of the peak.

For peptide purification by RP-HPLC, a Shimadzu LC-10AT instrument fitted with a C_{18} column, 150 x 4.60 mm (Phenomenex) was used. Solvent solutions: A - H_2O (0.1% TFA); B – MeCN (0.1% TFA). Flow rate: 1 mL/min.

Somatostatin (83% peptide content), equine heart cytochrome c (95% peptide content) and equine heart myoglobin (90% peptide content) used were all obtained from Sigma Aldrich. Octreotide was obtained from LKT Laboratories. Tertiapin Q (73% peptide content) was obtained from Abcam. Lyophilised somatostatin (1 mg) was resolubilised in buffer (2 mL, 50 mM $NaHPO_4^-$, pH 6.2, 40% MeCN, 2.5 % DMF) and stored at 4 °C until use. Lyophilised tertiapin Q (1mg) was resolubilised in buffer (2 mL, 50 mM, $NaHPO_4^-$, pH 6.2), flash frozen with liquid nitrogen and stored as 150 µL aliquots at -20°C until use.

Peptide concentrations were determined using a nanodrop ND-1000 spectrophotometer.

'Peptide buffer' employed in experiments consisted of pH 6.2 phosphate buffer (50 mM) with 40 % MeCN and 2.5 % DMF.

4.2 Syntheses

4.2.1 Synthesis of dithiophenolmaleimide[24]

3,4-Bis-phenylsulfanyl-pyrrolidine-2,5-dione (**22**)

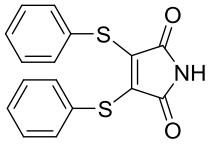

To a solution of 3,4-dibromomaleimide (80.9 mg, 0.318 mmol) and sodium hydrogen carbonate (129 mg, 1.54 mmol) in methanol (6 mL) was added thiophenol (66.6 µL, 0.648 mmol) in methanol (1 mL) drop-wise and the reaction mixture stirred for 15 min. The solvent was removed *in vacuo* to afford a yellow solid which was purified by flash chromatography on silica gel (petroleum ether : ethyl acetate, gradient elution from 9 : 1 to 7:3) to afford the product (**22**) as a yellow solid (84.7 mg, 84 % yield).

m.p. 101-103 °C (literature value: 123-126 °C); IR υ_{max}(solid): 3231 (m), 3060 (w), 1774 (m), 1701 (s) cm^{-1}; ^1H NMR (600 MHz, MeOD): δ = 7.29-7.24 (m, 6H, Ar-*H*), 7.16-7.14 (m, 4H, Ar-*H*); ^{13}C NMR (150 MHz, MeOD): δ = 165.5 (*C*=O), 135.5 (*C*), 132.4 (*C*H), 130.6 (*C*), 130.1 (*C*H), 129.2 (*C*H); MS (EI+) *m/z*: 313 (36%, M^+), 133 (100%); Mass calculated for [$C_{16}H_{11}O_2NS_2$]: 313.0226; Found: 313.0230.

4.2.2 Synthesis of di-*ortho*-thiocresolmaleimide

3,4-Bis-*o*-tolylsulfanyl-pyrrole-2,5-dione (**41**)

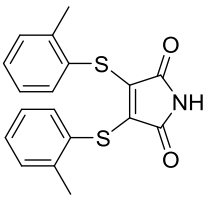

To a solution of 3,4-dibromomaleimide (99.3 mg, 0.390 mmol) and sodium hydrogen carbonate (130 mg, 1.55 mmol) in methanol (10 mL) was added a solution of thiocresol (92.4 µL, 0.784 mmol) in methanol (2 mL) drop-wise and the reaction mixture stirred for 2 h. The solvent was removed *in vacuo* to afford a yellow solid which was purified by flash chromatography on silica gel (petroleum ether : ethyl acetate, gradient elution from 9 : 1 to 7 : 3) affording the product (**41**) as a yellow solid (99.9 mg, 75 % yield).

m.p. 137-138 °C; IR υ_{max}(solid): 3172 (m), 3059 (m), 1771 (m), 1694 (s) cm^{-1}; ^{1}H NMR (600 MHz, MeOD): δ = 7.21 (td, 2H, *J* = 7.2, 1.4 Hz, Ar-*H*), 7.16 (t, 4H, *J* = 7.3 Hz, Ar-*H*), 7.12-7.08 (m, 2H, Ar-*H*), 2.19 (s, 6H, CH_3); ^{13}C NMR (150 MHz, MeOD): δ = 169.3 (*C*=O), 141.1 (*C*), 137.5 (*C*H), 133.7 (*C*), 131.6 (*C*H), 130.3 (*C*H), 129.8 (*C*), 127.6 (*C*H), 20.8 (*C*H_3); MS (EI+) *m/z*: 341 (100%, M^+), 91 (58%); Mass calculated for [$C_{18}H_{15}O_2NS_2$]: 341.0539; Found: 341.0529.

4.2.3 Synthesis of di-*ortho*-chlorothiophenolmaleimide

3,4-Bis-(2-chloro-phenylsulfanyl)-pyrrole-2,5-dione (**42**)

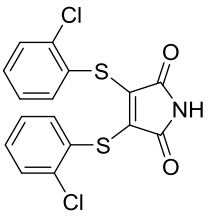

To a solution of 3,4-dibromomaleimide (498 mg, 1.96 mmol) and sodium hydrogen carbonate (655 mg, 7.84 mmol) in methanol (25 mL) was added *ortho*-chlorothiophenol (445 µL, 3.92 mmol) in methanol (5 mL) drop-wise and reaction mixture stirred for 20 min. The solvent was removed *in vacuo* to afford an orange solid which was purified by flash chromatography on silica gel (petroleum ether : ethyl acetate, gradient elution from 9 : 1 to 7 : 3) affording the product (**42**) an orange solid (685 mg, 91 % yield).

m.p. 135-137 °C; IR υ_{max}(solid): 3189 (w), 3063 (w), 2451 (w), 2340 (w), 2324 (w), 1776 (m), 1703 (s) cm^{-1}; ^{1}H NMR (500 MHz, MeOD): δ = 7.36 (d, 2H, *J* = 8.1 Hz, Ar-*H*), 7.30-7.28 (m, 4H, Ar-*H*), 7.21 (td, 2H, *J* = 7.6, 1.4 Hz, Ar-*H*); ^{13}C NMR (125 MHz, MeOD): δ = 168.6 (*C*=O), 137.5 (*C*), 136.8 (*C*), 134.5 (*C*H), 131.0 (2x*C*H), 129.9 (*C*), 128.6 (*C*H); MS (EI+) *m/z*: 381 (63%, M^+), 383 (42%), 385 (7%), 350 (5%), 348 (55%), 346 (100%), 144 (45%); Mass calculated for [$C_{16}H_9O_2NS_2{}^{35}Cl_2$]: 380.9446; Found: 380.9437.

4.2.4 Synthesis of di-*ortho*-methylthiosalicylatemaleimide

3,4-Bis-(2-methyl ester-phenylsulfanyl)-pyrrole-2,5-dione (**43**)

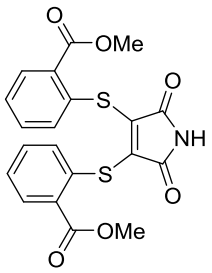

To a solution of 3,4-dibromomaleimide (210 mg, 0.823 mmol) and sodium hydrogen carbonate (264 mg, 3.14 mmol) in methanol (40 mL) was added *ortho*-methylthiosalicylate (216 µL, 1.57 mmol) in methanol (2 mL) drop-wise and reaction mixture stirred for 30 min. The solvent was removed *in vacuo* to afford an orange solid which was purified by flash chromatography on silica gel (petroleum ether : ethyl acetate, gradient elution from 9 : 1 to 7 : 3) to afford the product (**43**) as a deep orange solid (168.3 mg, 48 % yield).

m.p. 146-149 °C; IR υ_{max}(solid): 3190 (w), 2947 (w), 2344 (w), 1769 (m), 1686 (s) cm^{-1}; ^{1}H NMR (500 MHz, DMSO): δ = 11.40 (s, 1H, N-*H*), 7.69 (dd, *J* = 7.9, 1.4 Hz, 2H, Ar-*H*), 7.40 (td, *J* = 7.7, 1.6 Hz, 2H, Ar-*H*), 7.26 (td, *J* = 7.6, 1.5 Hz, 2H, Ar-*H*), 7.21 (dd, *J* = 8.0, 1.5 Hz, 2H, Ar-*H*), 3.78 (s, 6H, O*CH*$_3$); ^{13}C NMR (125 MHz, DMSO): δ = 170.1 (*C*=O), 167.3 (*C*=O), 137.2 (*C*), 133.1 (*C*), 133.0 (*C*), 132.4 (CH), 132.3 (*C*H), 130.1 (*C*H), 128.1 (*C*H), 52.7 (*C*H$_3$); MS (EI+) *m/z*: 428 (100%, M^+); Mass calculated for [$C_{20}H_{14}NO_6S_2$]: 428.0263; Found: 428.0246.

4.2.5 Synthesis of di-*N*-Boc-L-cysteine methyl ester maleimide

2-*tert*-Butoxycarbonylamino-3-[4-(2-*tert*-butoxycarbonylamino-2-methoxy carbonyl -ethylsulfanyl)-2,5-dioxo-2,5-dihydro-1H-pyrrol-3-ylsulfanyl]-propionic acid methyl ester (**44**)

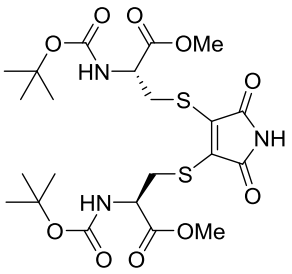

To a solution of maleimide **22** (31.4 mg, 0.100 mmol) in DMF (1.25 mL), was added buffer (21.3 mL, 50 mM $NaHPO_4^-$, pH 6.2, 1.25 mL DMF) slowly, with stirring. *N*-Boc-Cys-OMe (50.9 mg, 0.216 mmol) in DMF (1.25 mL) was added drop-wise to the maleimide solution (final concentration of DMF, 15%) and the mixture stirred for 30 min. A yellow precipitate formed which was dissolved in ethyl acetate (25 mL) and the organic phase washed with distilled water (2 x 25 mL), saturated aqueous LiCl (3 x 25 mL) and brine (2 x 25 mL). The solvent was removed *in vacuo* and the crude product purified by flash chromatography on silica gel (petroleum ether : ethyl acetate, gradient elution from 9 : 1 to 6 : 4) to afford the product (**44**) as a yellow solid (47.8 mg, 85 % yield).

IR υ_{max}(in MeOH): 3367 (w), 2972 (w), 1730 (s), 1513 (m) cm^{-1}; ^1H NMR (600 MHz, $CDCl_3$): δ = 7.82 (s, 1H, CON*H*), 5.84 (d, 2H, *J* = 7.5 Hz, N*H*$CO_2{}^t$Bu), 4.70-4.67 (m, 2H, NHC*H*CH_2), 3.82-3.79 (m, 2H, SC*H*H), 3.77 (s, 6H, CO_2CH_3), 3.70 (m, 2H, SCH*H*), 1.42 (s, 18H, $CO_2C(CH_3)_3$) ; ^{13}C NMR (150 MHz, $CDCl_3$): δ = 170.8 (*C*=O), 165.7 (*C*=O), 155.1 (*C*=O), 137.2 (*C*), 80.4 (*C*), 53.9 (*C*H), 53.0 (CH_3) 33.8 (CH_2), 28.4 (3xCH_3); MS (EI+) *m/z*: 564 (27%, M^+), 408 (100%), 364 (12%); Mass calculated for [$C_{22}H_{34}O_{10}N_3S_2$]: 564.1686; Found: 564.1664.

4.2.6 Synthesis of di-*ortho*-thiosalicylicacidmaleimide

(3,4-Bis-(2-mercapto-benzoic acid)-pyrrole-2,5-dione) (**45**)

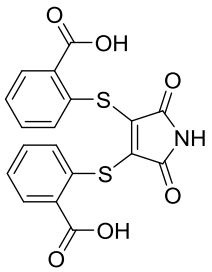

To a solution of 3,4-dibromomaleimide (201 mg, 0.787 mmol) and sodium hydrogen carbonate (532 mg, 6.34 mmol) in methanol (20 mL) was added *ortho*-thiosalycylic acid (247 mg, 1.60 mmol) in methanol (4 mL) drop-wise and the reaction mixture stirred for 45 min. The solvent was removed *in vacuo* to afford a yellow solid crude product. The crude product was re-dissolved in water (40 mL), acidified with aqueous HCl (2M, 80 mL) and extracted with ethyl acetate (4 x 100 mL). The organic layers were combined, dried ($MgSO_4$) and the solvent removed *in vacuo* to afford maleimide (**45**) as a yellow solid (301 mg, 95 %).

m.p. 257-258 °C; IR υ_{max}(solid): 3042 (w), 1772 (s), 1681 (m) cm^{-1}; ^{1}H NMR (500 MHz, MeOD): δ = 7.80 (d, *J* = 8.0 Hz, 2H, Ar-*H*), 7.36 (t, *J* = 7.0 Hz, 2H, Ar-*H*), 7.22 (t, *J* = 7.5 Hz, 2H, Ar-*H*) 7.09 (d, *J* = 8.0 Hz, 2H, Ar-*H*); ^{13}C NMR (125 MHz, MeOD): δ = 170.1 (*C*=O), 168.8 (*C*=O), 137.8 (*C)*, 133.0 (*C)*, 132.9 (*C)*, 132.7 (*C*H), 132.5 (*C*H), 130.7 (*C*H), 128.1 (*C*H); MS (EI+) *m/z*: 401 (55%, M^+), 136 (100%); Mass calculated for [$C_{18}H_{11}NO_6S_2$]: 401.0022; Found: 401.0025.

4.2.7 Synthesis of *N*-methyl diphenoxymaleimide

3,4-diphenoxy-1*H*-pyrrole-2,5-dione (**53**)

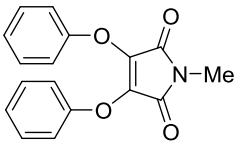

A solution of phenol (100 mg, 1.07 mmol) in dry dioxane (2 mL) was added drop-wise to a solution of potassium *tert*-butoxide (143 mg, 1.27 mmol) and 18-crown-6 (333 mg, 1.26 mmol) in dry dioxane (3.5 mL). The mixture was stirred for 20 min before being added drop-wise to a solution of *N*-methyl-3,4-dibromomaleimide (137 mg, 0.510

mmol) in dry dioxane (2 mL) over 20 min. The reaction mixture was stirred at room temperature for 48 h. The solvent was removed *in vacuo* and the crude product re-dissolved in ethyl acetate (20 mL), washed with aqueous NaOH (1M, 3 x 3 mL) and brine (3 x 5 mL) before being dried ($MgSO_4$) and the solvent removed *in vacuo.* The product was purified by flash chromatography on silica gel (petroleum ether : ethyl acetate, gradient elution from 9 : 1 to 8 : 2) to afford the product (**53**) as a white solid (50.2 mg, 33 % yield).

m.p. 110-111 °C; IR υ_{max}(solid): 3058 (w), 2923 (w), 1712 (m), 1681 (m), 1588 (m) cm^{-1}; ^1H NMR (500 MHz, $CDCl_3$): δ = 7.19-7.16 (m, 4H, Ar-*H*), 7.04 (t, *J* = 6.7 Hz, 2H, Ar-*H*), 6.85-6.83 (m, 4H, Ar-*H*) 3.08 (s, 3H, NC*H*$_3$); ^{13}C NMR (125 MHz, $CDCl_3$): δ = 165.5 (*C*=O), 154.9 (*C*), 133.3 (*C)*, 129.5 (*C*H), 124.6 (*C*H), 117.3 (*C*H), 23.7 (*C*H_3) ; MS (EI+) *m/z*: 295 (100%, M^+); Mass calculated for [$C_{17}H_{13}NO_4$]: 296.09228 ; Found: 296.091210.

4.2.8 Synthesis of *N*-methoxycarbonyl-3,4-dibromomaleimide[170]

Methyl 3,4-dibromo-2,5-dioxo-2,5-dihydro-1*H*-pyrrole-1-carboxylate (**62**)

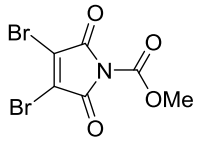

To a solution of 3,4-dibromomaleimide (511 mg, 2.00 mmol) and *N*-methylmorpholine (220 µL, 2.00 mmol) in THF (20 mL) was added methylchloroformate (160 µL, 2.00 mmol) and the mixture was stirred for 20 min. DCM (30 mL) was added and the organic phase was washed with water (3 x 20 mL) and dried ($MgSO_4$) before the solvent was removed *in vacuo* to afford the product (**62**) as a purple solid (557 mg, 90 % yield).

m.p. 111-112 °C; IR υ_{max}(solid): 3240 (w), 3005 (w), 1807 (m), 1723 (s), 1599 (m) cm^{-1}; ^1H NMR (500 MHz, $CDCl_3$): δ = 4.00 (s, 3H, COOC*H*$_3$); ^{13}C NMR (125 MHz, $CDCl_3$): δ = 159.3 (*C*=O), 147.0 (*C*=O), 131.5 (*C*), 54.9 (*C*H_3); MS (EI+) *m/z*: 311 (100%, M^+), 310 (40%); Mass calculated for [$C_6H_3NO_4Br_2$]: 310.8429; Found: 310.8425.

4.2.9 Synthesis of *N*-propargyl dibromomaleimide[170]

3,4-dibromo-1-(prop-2-yn-1-yl)-1*H*-pyrrole-2,5-dione (**63**)

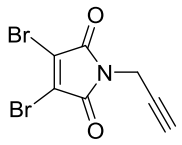

Propargylamine (26.0 µL, 0.400 mmol) was added to a stirred solution of *N*-methoxycarbonyl-3,4-dibromomaleimide (**62**) (101 mg, 0.321 mmol) in DCM (4 mL) and the mixture stirred for 30 min. EtOAc (4 mL) was added and the organic phase washed with saturated ammonium chloride solution (3 x 10 mL) and water (3 x 10 mL) before being dried ($MgSO_4$) and the solvent removed *in vacuo*. The crude product was purified by flash chromatography on silica gel (DCM) to afford the product (**63**) as a pale yellow solid (77 mg, 82 %).

m.p. 115-118 °C; IR υ_{max}(solid): 3264 (w), 2905 (w), 1718 (s), 1589 (m) cm^{-1}; ^1H NMR (500 MHz, $CDCl_3$): δ = 4.38 (d, *J* = 2.5 Hz, 2H, NC*H*$_2$,), 2.26 (t, *J* = 2.5 Hz, 1H, CC*H*); ^{13}C NMR (125 MHz, $CDCl_3$): δ = 162.7 (*C*=O), 129.9 (*C*), 76.1 (*C*), 72.6 (*C*H), 28.6 (*C*H_2); MS (EI+) *m/z*: 295 (50%), 293 (100%, M^+), 291 (60%), 246 (13%); Mass calculated for [$C_7H_4NO_2Br_2$]: 291.8603; Found: 291.8605.

4.2.10 Synthesis of *N*-methoxycarbonyl-3,4-dithiophenolmaleimide[170]

Methyl 2,5-dioxo-3,4-bis(phenylthio0-2,5-dihydro-1H-pyrrole-1-carboxylate (**80**)

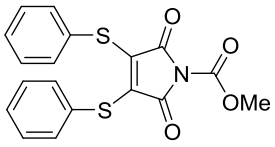

To a solution of 3,4-dithiophenolmaleimide (**22**) (49.8 mg, 0.160 mmol) and *N*-methylmorpholine (18.0 µL, 0.160 mmol) in EtOAc (6 mL) was added methylchloroformate (14.0 µL, 0.170 mmol) and the mixture stirred for 30 min. The organic phase was washed with water (3 x 10 mL), dried ($MgSO_4$) and the solvent removed *in vacuo* to afford the product (**80**) as an orange solid (57.7 mg, 97 % yield).

m.p. 105-107 °C; IR υ_{max}(solid): 3103 (w), 2913 (w), 1803 (m), 1761 (m), 1713 (m), 1438 (m) cm^{-1}; ^1H NMR (500 MHz, $CDCl_3$): δ = 7.34-7.26 (m, 10H, Ar-*H*), 3.91 (s, 3H,

$COOCH_3$); ^{13}C NMR (125 MHz, $CDCl_3$): δ = 161.8 (*C*=O), 137.3 (*C*=O), 132.7 (2x*C*), 129.3 (*C*H), 129.1 (*C*H) 128.2 (*C*H), 54.4 (CH_3); MS (EI+) *m/z*: 372 (100%, M^+), 369 (35%), 367 (30%); Mass calculated for [$C_{18}H_{13}NO_4S_2$]: 372.0481; Found: 372.0478.

4.2.11 Synthesis of *N*-alkyne dithiophenol maleimide[170]

3,4-bis(phenylthio)-1-(prop-2-yn-1-yl)-1*H*-pyrrole-2,5-dione (**71**)

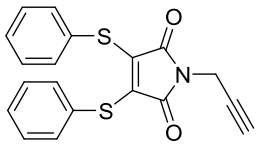

Propargylamine (6.20 µL, 0.0960 mmol) was added to a stirred solution of maleimide (**80**) (33.9 mg, 0.0960 mmol) in DCM (6 mL) for 2 h before silica was added and the reaction mixture left to stir overnight. The silica was removed by filtering under vacuum andthe filtrate concentrated *in vacuo*. The resulting product was purified by flash chromatography on silica gel (petroleum ether : ethyl acetate, gradient elution from 9 : 1 to 8 : 2) to afford the product (**71**) as a yellow solid (25.7 mg, 76 % yield).

m.p. 123-124 °C; IR υ_{max}(solid): 3269 (m), 3000 (w), 1771 (m), 1704 (s) cm^{-1}; ^1H NMR (500 MHz, $CDCl_3$): δ = 7.32-7.21 (m, 10H, Ar-*H*), 4.26 (d, 2H, *J* = 2.4 Hz, NCH_2), 2.20 (t, 1H, *J* = 2.2 Hz, CC*H*); ^{13}C NMR (125 MHz, $CDCl_3$): δ = 165.5 (*C*=O), 136.0 (*C*), 132.2 (*C*H), 129.1 (*C*H), 128.8 (*C*), 128.6 (*C*H), 76.8 (*C*), 71.8 (*C*H), 27.8 (CH_2); MS (EI+) *m/z*: 351 (100%, M^+); Mass calculated for [$C_{19}H_{13}NO_2S_2$]: 351.03877; Found: 351.03830.

4.2.12 Synthesis of Boc-protected aminopiperidine-rhodamine B[46]

N-(9-(2-(4-((*tert*-butoxycarbonyl)amino)piperidine-1-carbonyl)phenyl)-6-(diethylamino)-3*H*-xanthen-3-ylidene)-*N*-ethylethanaminium chloride (**73**)

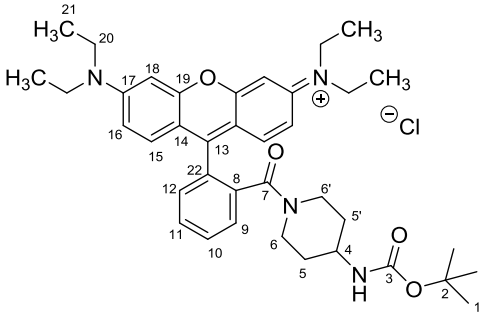

Rhodamine B (427 mg, 0.891 mmol) was dissolved in DCM (30 mL), oxalyl chloride (2.5 mL) was added and the reaction mixture stirred for 2 h. The solvent and excess oxalyl chloride was removed *in vacuo*. The purple residue was re-dissolved in DCM (15 mL) before being slowly added to a solution of Cs_2CO_3 (1.50 g. 4.56 mmol) and 4-(*N*-Boc-amino)-piperidine (913 mg, 4.56 mmol) in DCM (15 mL). The mixture was stirred for 18 h before the solvent was removed *in vacuo* to yield the crude product as a purple solid. This was purified by flash chromatography on silica gel (DCM : MeOH, gradient elution from 98 : 2 to 90 : 10) to afford the product (**73**) as a dark purple solid (331 mg, 59%).

m.p. 205-207 °C; IR υ_{max}(oil): 2977 (w), 2910 (w), 1702 (m), 1584 (m) cm^{-1}; ^1H NMR (500 MHz, MeOD): δ = 7.76-7.73 (m, 2H, C*H-10 & 11*), 7.65 (dd, 1H, *J* = 6.0, 3.0 Hz, C*H-9*), 7.49 (dd, 1H, *J* = 6.0, 2.5 Hz, C*H-12*), 7.27 (d, 2H, *J* = 9.5 Hz, 2xC*H-15*), 7.09-7.04 (m, 2H, 2xC*H-16*), 6.97 (d, 2H, *J* = 2.5 Hz, 2xC*H-18*), 4.05 (m, 1H, C*H-6 eq.*), 3.71 (m, 1H, C*H-4*), 3.69 (q, 8H, *J* = 7.5 Hz, 4xCH_2*-20*), 3.45-3.42 (m, 1H, C*H-6' eq.*), 3.03 (bs, 1H, C*H-6' ax.*), 2.68 (m, 1H, C*H-6 ax.*) 1.77-1.72 (m, 2H, C*H-5 eq. & 5' eq.*), 1.40 (s, 9H, 3xCH_3*-1*), 1.31 (t, 12H, *J* = 7.5 Hz, 4xC*H3-21*), 1.16 (m, 2H, C*H-5 ax. & 5' ax.*); ^{13}C NMR (125 MHz, MeOD): δ = 169.3 (*C*=O), 159.3 (*C*), 157.6 (*C*=O), 157.2 (*C*), 157.0 (*C*), 137.1 (*C*), 133.3 (*C*H), 132.0 (*C*), 131.7 (*C*H), 131.3 (*C*H), 131.0 (*C*H), 128.6 (*C*H), 115.4 (*C*H), 114.8 (*C*), 97.3 (*C*H), 80.1 (*C*), 49.9 (*C*H), 47.7 (CH_2), 46.9 (CH_2), 41.8 (*C*H_2), 33.5 (*C*H_2), 32.3 (*C*H_2), 28.7 (*C*H_3), 12.9 (*C*H_3); MS (EI+) *m/z*: 625 (100%, M^+), 372 (30%); Mass calculated for [$C_{38}H_{49}N_4O_4$]: 625.3754; Found: 625.3761.

4.2.13 Synthesis of aminopiperidine-rhodamine B[46]

1-(2-(6-(diethylamino)-3-(diethyliminio)-3*H*-xanthen-9-yl)benzoyl)piperidin-4-aminium 2,2,2-trifluoroacetate chloride (**74**)

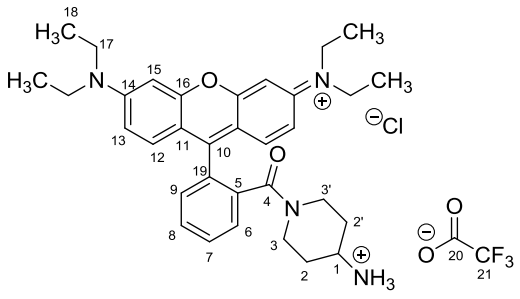

TFA (15 mL) was added to a stirred solution of Boc-protected rhodamine (**73**) (257 mg, 0.410 mmol) in DCM (15 mL) and the solution stirred for 4 h. The solvent was then removed azeotropically using toluene (3 x 15 mL) followed by chloroform (4 x 10 mL) to yield the product (**74**) as a purple solid (402 mg, quantitative yield).

m.p. 231-234 °C; ^{1}H NMR (500 MHz, MeOD): δ = 7.78-7.76 (m, 2H, C*H-7 & 8*), 7.66-7.64 (m, 1H, C*H-6*), 7.50-7.48 (m, 1H, C*H-9*), 7.26 (d, 2H, *J* = 9.5 Hz, 2xC*H-12*), 7.07-7.05 (m, 2H, 2xC*H-13*), 6.97-6.95 (m, 2H, 2xC*H-15*), 4.31 (m, 1H, C*H-3 eq.*), 3.84 (m, 1H, C*H-3' eq.*), 3.71-3.70 (m, 1H, C*H-1*), 3.69-3.67 (m, 8H, 4xCH_2*-17*), 2.97-2.92 (m, 1H, C*H-3 ax.*), 2.57-2.55 (m, 1H, C*H-3' ax.*), 1.95 (m, 2H, *J* = 11.5 Hz, C*H-2 eq. & 2' eq.*), 1.42-1.39 (m, 2H, C*H-2 ax. & 2' ax.*), 1.31 (t, 12H, *J* = 7.5, 4xCH_3*-18*); ^{13}C NMR (125 MHz, MeOD): δ = 169.6 (*C*=O), 159.3 (*C*), 157.3 (*C*=O), 157.2 (*C*), 156.8 (*C*), 136.7 (*C*), 133.4 (*C*H), 132.0 (*C*), 131.9 (*C*H), 131.4 (*C*H), 131.3 (*C*H), 128.4 (*C*H), 117.0 (*C*), 115.4 (*C*H), 115.3 (*C*H), 115.1 (*C*), 97.4 (*C*H), 46.9 (*C*H_2), 31.4 (*C*H_2), 30.5 (*C*H_2), 12.8 (*C*H_3); MS (EI+) *m/z*: 525 (100%, M^+), 338 (10%); Mass calculated for [$C_{38}H_{41}N_4O_2$]: 525.3230; Found: 525.3238.

4.2.14 Synthesis of azidohexanoic acid[185]

6-Azidohexanoic acid (**75**)

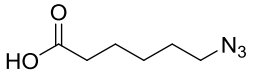

A mixture of 6-bromohexanoic acid (402 mg, 2.06 mmol) and sodium azide (668 mg, 10.3 mmol) in DMF (1.5 mL) was stirred at 50°C for 3 h. The mixture was cooled to room temperature and DCM (30 mL) added. The organic phase was washed with water (2 x 30 mL), saturated aqueous LiCl (5 x 30 mL) and brine (2 x 30 mL), dried ($MgSO_4$) and the solvent removed *in vacuo*. The crude product was purified by flash chromatography on silica gel (petroleum ether : ethyl acetate, gradient elution from 8 : 2 to 6 : 4) to afford the product (**75**) as a colourless liquid (124 mg, 39 %).

IR υ_{max}(oil): 3200 (m), 2925 (m), 2095 (m), 1702 (s)cm^{-1}; ^{1}H NMR (500 MHz, $CDCl_3$): δ = 3.28 (t, 2H, *J* = 7.0 Hz, HOOCCH_2), 2.37 (t, 2H, *J* = 7.5 Hz, CH_2), 1.70-1.59 (m, 4H, 2xCH_2), 1.46-1.40 (m, 2H, CH_2); ^{13}C NMR (125 MHz, $CDCl_3$): δ = 180.0 (*C*=O), 51.3 (*C*H_2), 33.9 (*C*H_2), 28.6 (*C*H_2), 26.2 (*C*H_2), 24.4 (*C*H_2); MS (EI+) as sodium

adduct *m/z*: 180 (100%, $M+Na^+$); Mass calculated for [$C_6H_{11}N_3O_2Na$]: 180.0749; Found: 180.0733.

4.2.15 Synthesis of rhodamine B-azide

N-(9-(2-(4-(6-azidohexanamido)piperidine-1-carbonyl)phenyl)-6-(diethylamino)-3*H*-xanthen-3-ylidene)-*N*-ethylethanaminium chloride (**76**)

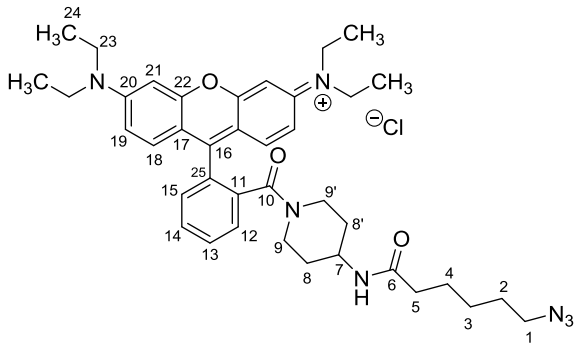

To a solution of 6-azidohexanoic acid (**75**) (29.5 mg, 0.189 mmol), HBTU (71.7 mg, 0.189 mmol), and HOBt (25.5 mg, 0.189 mmol) in DMF (2 mL) was added DIPEA (99.0 µL, 0.576 mmol) in DMF (2 mL). The reaction mixture was stirred for 20 min before a solution of rhodamine B-amine (**74**) (99.3 mg, 0.189 mmol) in DMF (2 mL) was added drop-wise and the mixture stirred for 3 h. The solvent was then removed *in vacuo* and the crude product re-dissolved in DCM (10 mL) before being washed with saturated aqueous LiCl (3 x 10 mL), 15 % aqueous K_2CO_3 (2 x 10 mL), 15 % aqueous citric acid (2 x 10 mL) and water (2 x 10 mL). The resulting product was dried ($MgSO_4$) and the remaining solvent removed *in vacuo* before being purified by flash chromatography on silica gel (DCM : MeOH, gradient elution from 100 : 0 to 96 : 4) to yield the product (**76**) as a purple solid (96.9 mg, 77 % yield).

m.p. 199-202 °C; IR υ_{max}(solid): 2963 (w), 2928 (w), 2875 (w), 2090 (s) 1582 (m) cm^{-1}; ^{1}H NMR (500 MHz, MeOD): δ = 7.75 (m, 2H, *J* = 7.0, 2.5 Hz, C*H-13&14*), 7.65-7.63 (m, 1H, C*H-12*), 7.50-7.48 (m, 1H, C*H-15*), 7.26 (d, 2H, *J* = 9.5 Hz, 2xC*H-18*), 7.07-7.03 (m, 2H, 2xC*H-19*), 6.95 (d, 2H, *J* = 2.5 Hz, 2xC*H-21*), 4.10 (m, 1H, *J* = 15.7 Hz, C*H-9 eq.*), 3.77-3.75 (m, 2H, C*H-7 & 9' eq.*), 3.68 (q, 8H, *J* = 7.5 Hz, 4xCH_2*-23*), 3.27 (t, 2H, J = 7.0 Hz, CH_2*-1*), 3.06-3.03 (m, 1H, C*H-9' ax.*), 2.69-2.65 (m, 1H, C*H-9 ax.*), 2.15-2.14 (m, 2H, CH_2*-5*), 1.80-1.70 (m, 2H, C*H-8 eq. & 8' eq.*), 1.67-1.55 (m, 4H, CH_2*-2 & 4*), 1.41-1.39 (m, 2H, CH_2*-3*), 1.38-1.36 (m, 1H, C*H-8 ax.*), 1.31 (t, 12H, *J* =

6.5 Hz, 4xC*H*$_3$-*24*), 1.29-1.20 (m, 1H, C*H-8' ax.*); ^{13}C NMR (125 MHz, MeOD): δ = 175.3 (*C*=O), 169.4 (*C*=O), 159.3 (*C*), 157.2 (*C*), 157.0 (*C*), 137.0 (*C*), 133.3 (*C*H), 132.0 (*C*), 131.7 (*C*H), 131.3 (*C*H), 131.1 (*C*H), 128.5 (*C*H), 115.4 (*C*H), 114.8 (*C*), 97.3 (*C*H), 52.3 (*C*H$_2$), 47.7 (*C*H), 46.9 (*C*H$_2$), 41.8 (*C*H$_2$), 36.8 (*C*H$_2$), 33.0 (*C*H$_2$), 31.9 (*C*H$_2$), 29.6 (*C*H$_2$), 27.3 (*C*H$_2$), 26.5 (*C*H$_2$), 25.6 (*C*H$_2$), 12.9 (*C*H$_3$); MS (EI+) *m/z*: 664 (100%, M$^+$); Mass calculated for [$C_{39}H_{50}N_7O_3$]: 664.3975; Found: 664.3950.

4.2.16 Synthesis of rhodamine B-[^{127}I]-dithiophenol maleimide

N-(6-(diethylamino)-9-(2-(4-(6-(4-((2,5-dioxo-3,4-bis(phenylthio)-2,5-dihydro-1*H*-pyrrol -1-yl)methyl)-5-iodo-1*H*-1,2,3-triazol-1-yl)hexanamido)piperidine-1-carbonyl) phenyl)-3*H*-xanthen-3-ylidene)-*N*-ethylethanaminium (**77**)

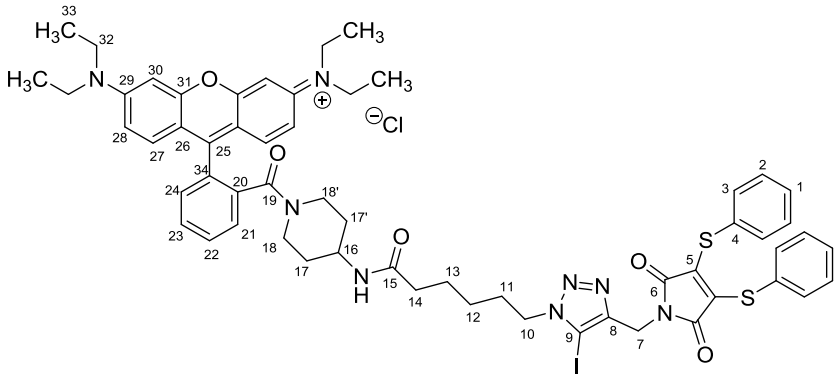

To a solution of copper (I) iodide (8.00 mg, 0.0420 mmol) in dry acetonitrile (5 mL) was added *N*-alkyne dithiophenolmaleimide (**71**) (13.4 mg, 0.0380 mmol), rhodamine-azide (**76**) (27.9 mg, 0.0420 mmol), triethylamine (5.3 µL, 0.0380 mmol) and *N*-chlorosuccinimide (6.10 mg, 0.0460 mmol) and the reaction mixture stirred overnight. The copper was removed by gravity filtration and the filtrate concentrated *in vacuo*. The crude product was purified by flash chromatography on silica gel (DCM : MeOH, gradient elution from 100 : 0 to 95 : 5) to afford the product (**77**) as a purple solid (15.9 mg, 37 % yield).

m.p. 223-224 °C; IR υ_{max}(solid): 2969 (m), 2904 (m), 1709 (m), 1583 (m) cm^{-1}; ^{1}H NMR (600 MHz, MeOD): δ = 7.75 (td, 1H, *J* = 7.6 Hz, 1.6, C*H-22*), 7.74 (td, 1H, *J* = 7.6, 1.6 Hz, C*H-23*), 7.66-7.64 (m, 1H, C*H-21*), 7.50-7.48 (m, 1H, C*H-24*), 7.28 (d, 2H, *J* = 9.6 Hz, 2xC*H-27*), 7.28-7.26 (m, 2H, 2xC*H-1*), 7.23-7.21 (m, 4H, 4xC*H-2*), 7.15-7.13 (m, 4H, 4xC*H-3*), 7.06 (m, 2H, 2xC*H-28*), 6.94 (d, 1H, *J* = 2.0 Hz, C*H-30*), 6.93

(d, 1H, *J* = 2.0 Hz, C*H-30*), 4.73 (d, 1H, *J* = 15.7 Hz, C*H-7*), 4.69 (d, 1H, *J* = 15.7 Hz, C*H-7*), 4.40 (t, 2H, *J* = 6.8 Hz, CH_2*-10*), 4.10 (m, 1H, *J* = 13.2 Hz, C*H-18 eq.*), 3.75-3.73 (m, 1H, C*H-16*), 3.72-3.70 (m, 1H, C*H-18' eq.*), 3.65 (bq, 8H, *J* = 7.0 Hz, 4xCH_2*-32*), 3.08-3.02 (m, 1H, C*H-18' ax.*), 2.68-2.64 (m, 1H, C*H-18 ax.*), 2.11 (td, 2H, *J* = 7.1, 2.0 Hz, CH_2*-14*), 1.89-1.85 (m, 2H, CH_2*-11*), 1.75 (d, 1H, *J* = 12.5 Hz, C*H-17' eq.*), 1.73 (d, 1H, *J* = 12.5 Hz, C*H-17 eq.*), 1.62-1.58 (m, 2H, CH_2*-13*), 1.30 (t, 12H, *J* = 7.0 Hz, 4xCH_3*-33*), 1.28-1.26 (m, 1H, C*H-17' ax.*), 1.26-1.24 (m, 2H, CH_2*-12*), 1.25-1.20 (m, 1H, C*H-17 ax.*); ^{13}C NMR (125 MHz, MeOD): δ = 175.3 (*C*), 169.5 (*C*), 167.7 (*C*), 159.3 (*C*), 157.2 (*C*), 157.0 (*C*), 147.2 (*C*), 137.1 (*C*), 137.0 (*C*), 133.3 (*C*H), 132.4 (*C*H), 131.9 (*C*), 131.8 (*C*H), 131.4 (*C*H), 131.1 (*C*H), 130.4 (*C*), 130.2 (*C*H), 129.3 (*C*H), 128.6 (*C*H), 115.4 (*C*H), 114.8 (*C*), 97.3 (*C*H), 81.1 (*C*), 51.6 (*C*H_2), 47.8 (*C*H_2), 47.6 (*C*H), 46.9 (*C*H_2), 41.9 (*C*H_2), 36.6 (*C*H_2), 35.5 (*C*H_2), 33.1 (*C*H_2), 31.8 (*C*H_2), 30.4 (*C*H_2), 26.6 (*C*H_2), 26.2 (*C*H_2), 12.9 (*C*H_3); MS (EI+) *m/z*: 1141 (100%, M^+), 285 (20%); Mass calculated for [$C_{58}H_{62}IN_8O_5S_2$]: 1141.33; Found: 1141.3103.

4.2.17 Synthesis of rhodamine B-[^{125}I]-dithiophenol maleimide (78)[184]

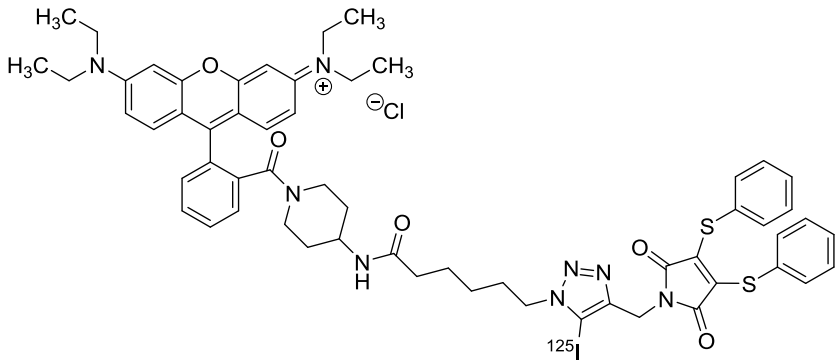

Radio-HPLC analysis was performed with an Agilent 1200 HPLC system equipped with a GABI Star NaI(Tl) scintillation detector and a Knauer Smartline fixed wavelength 254 nm UV-detector. A ZORBAX column (300SB-C18, 9.4 x 250 mm) was used. Reductant free [125I]NaI was purchased from Perkin Elmer with a concentration of 370 mCi/mL (13.69 GBq/mL) and specific activity of 629 GBq/mg in 10-5 M NaOH (pH 8-11) aqueous solution.

To copper(II) chloride (13.4 mg, 0.100 mmol) was added anhydrous acetonitrile (4 mL) followed by anhydrous triethylamine (20.9 µL, 0.150 mmol), and the mixture was mixed by vortex.

To the alkyne **71** (0.35 mg, 1.0 µmol) was added the above solution of the $CuCl_2$/triethylamine complex in acetonitrile (40 µL) and the mixture vortexed. After 5 min, $Na^{125}I$ in water (6.00 µL, 1.438 MBq) was added to the mixture. Azide **76** (6.64 mg, 10.0 µmol) was dissolved in MeCN (200 µL) before 20 µL (1.00 µmol) was added to the reaction mixture. The tube was capped and the reaction was heated at 60 °C for 90 min. The reaction was quenched with acetonitrile and water (1:1, 400 µL) and the resulting solution was purified by HPLC (Buffer A: water + 0.1 % TFA, Buffer B: methanol + 0.1 % TFA, gradient elution from 60-90 % Buffer B over 30 min, flow rate 3 mL/min). The labelled compound **78** was identified by co-injection and co-elution with the non-radioactive reference compound **77**. The isolated RCY of **78** was 47%.

4.3 TCEP Cross Reactivity Studies

To a solution of **22** (35.0 mg, 0.112 mmol) in DMF (6.25 mL) was added TCEP (31.8 mg, 0.111 mmol) fully dissolved in peptide buffer (43.75 mL) (final concentration of DMF, 15 %). The reaction was stirred for 15 min before being extracted with ethyl acetate (50 mL). The organic phase was washed with saturated aqueous LiCl (3 x 50 mL), saturated aqueous NaCl (3 x 50 mL) and water (2 x 50 mL). The organic phase was then dried ($MgSO_4$) and the solvent removed *in vacuo* to regain maleimide **22** (31.9 mg, 94 %).

A control reaction was run, with TCEP absent, to determine the amount of product lost by experimental procedures. For this, peptide buffer (43.75 mL) was added to **1** (35.8 mg, 0.114 mmol) in DMF (6.25 mL). The solution was left stirring for 15 min before extracted, washed and dried as before to regain maleimide **22** (34.9 mg, 97.4%).

This procedure was repeated using maleimides **41**, **42** and **43** and using the same molar equivalents ratio.

4.4 Maleimide Bridging of Somatostatin

N.B. These general bridging procedures were repeated with some changes in the number of equivalents used, as described in the Results and Discussion.

4.4.1 General Step Wise Protocol with TCEP

Somatostatin (344 µL, 199.7 µM) was diluted to a concentration of 152.6 µM with peptide buffer (106 µL). TCEP (3.91 mg) was prepared at a concentration of 15.26 mM using peptide buffer (894 µL). 1.7 equivalents of the TCEP solution (7.5 µL, 0.114 mmol) was then added to the diluted somatostatin (450 µL, 0.0687 mmol) and left to reduce for 1 h. Stock solutions of 3,4-dibromomaleimide and maleimides **22** and **41**-**43** were prepared at a concentration of 15.26 mM using DMF (50%) and peptide buffer (50%). An aliquot of reduced somatostatin (30 µL, 0.00458 mmol) was taken and 5 equivalents of 3,4-dibromomaleimide (1.5 µL, 0.0229 mmol) was added and left to react for 10 min. This mixture was removed and analysed by LC-MS to test for full reduction of somatostatin. Full conversion to maleimide-bridged somatostatin was observed (LC retention time: 1.30 min, *m/z* 866.9 (*m/2*)), confirming complete reduction of all disulfides.

From the remaining reduced somatostatin stock, 4 aliquots (90 µL, 0.0137 mmol) were taken and to each 1.1 equivalents of a different maleimide (**22** and **41**-**43**) (0.99 µL, 0.0151 mmol) was added and left to react for 10 min. From these, aliquots (30 µL) were removed at 1, 10 and 60 min and analysed by LC-MS. The percentage of bridged (LC retention time: 1.30 min, *m/z* 866.90 (*m/2*)) and reduced, non-bridged (LC retention time: 1.23 min, *m/z* 820.34 (*m/2*)) somatostatin was recorded in each case.

4.4.2 General *In-situ* Protocol

4.4.2.1 Using TCEP

Somatostatin (474 µL, 199.7 µM) was diluted to a concentration of 152.6 µM with peptide buffer (146 µL). TCEP (3.68 mg) was prepared at a concentration of 15.26 mM using peptide buffer (841 µL). Stock solutions of maleimides **22** and **41**-**43** were prepared at a concentration of 15.26 mM using DMF (50%) and peptide buffer (50%). The diluted somatostatin (620 µL, 0.0946 mmol) was split into 4 aliquots (150 µL, 0.0229 mmol) and to each 5 equivalents of one of the maleimides **22** and **41**-**43** stock solution (7.5 µL, 0.114 mmol) was added and left to react for 10 min. 3 equivalents of

the TCEP solution (4.5 µL, 0.0687 mmol) was then added to each and aliquots (30 µL) removed at 1, 5, 10, 20 and 30 min and analysed by LC-MS. The percentage of bridged (LC retention time: 1.30 min, *m/z* 866.90 (*m/2*)) and reduced, non-bridged (LC retention time: 1.23 min, *m/z* 820.34 (*m/2*)) somatostatin was recorded.

4.4.2.2 Using Benzeneselenol

Somatostatin (322 µL, 293.6 µM) was diluted to a concentration of 152.6 µM using peptide buffer (298 µL) and 4 aliquots (150 µL, 0.0229 mmol) were taken. Stock solutions of maleimides **22** and **41**-**43** were prepared at a concentration of 15.26 mM using DMF (50%) and peptide buffer (50%). To each somatostatin aliquot, 10 equivalents of the maleimide **22** and **41**-**44** stock solution (15 µL, 0.229 mmol) were added. Benzeneselenol (1.62 µL) was prepared at a concentration of 15.26 mM using DMF (50 µL) and peptide buffer (950 µL). 5 equivalents (7.5 µL, 0.114 mmol) of this were added to the somatostatin solution[iv]. Aliquots (30 µL) of the reaction mixture were removed at 1, 5, 10, 20 and 30 min and analysed by LC-MS. The percentage of bridged (LC retention time: 1.30 min, *m/z* 866.90 (*m/2*)) and reduced, non-bridged (LC retention time: 1.23 min, *m/z* 820.34 (*m/2*)) somatostatin was recorded.

4. 5 Double Maleimide Bridging of Tertiapin Q

N.B. These general bridging procedures were repeated with some changes in the maleimide reagent employed and the number of equivalents of both this and reducing agent used, as described in the Results and Discussion.

4.5.1 General Step Wise Protocol with TCEP

Tertiapin Q (299 µL, 127 µM) was diluted to a concentration of 100 µM using pH 6.2 phosphate buffer (81 µL). TCEP (2.50 mg) was prepared at a concentration of 10 mM using peptide buffer (872 µL) before 3 equivalents (11.4 µL, 0.114 mmol) of this was added to the tertiapin Q solution (380 µL, 0.038 mmol). The peptide was left to reduce for 1 h and reduction was confirmed as previously described using a 30 µL aliquot. A solution of maleimide **45** (2.06 mg) was prepared at a concentration of 10 mM using DMF (77.0 µL) and peptide buffer (436 µL). 3 equivalents (10.5 µL, 0.105 mmol) of the maleimide solution were added to the remaining reduced tertiapin Q (350 µL, 0.035 mmol) and, after 10 min, an aliquot (30 µL) of this reaction mixture was removed and

[iv] Note: Due to the formation of the unwanted diselenide product upon exposure to air, fresh solutions of the benzeneselenol stock were made for each reaction.

analysed by LC-MS to ensure full conversion from reduced, non-bridged peptide (LC retention time: 0.89 min, *m/z* 2457.0) to the bridged product (LC retention time: 0.99 min, *m/z* 2642.0).

4.5.2 General *In Situ* Protocol

4.5.2.1 Using TCEP:

Tertiapin Q (307 µL, 130.4 µM) was diluted to a concentration of 100 µM by addition of pH 6.2 phosphate buffer (93.0 µL). Maleimide **45** (2.60 mg) was prepared at a concentration of 10 mM using DMF (65.0 µL) and peptide buffer (583 µL). An aliquot (150 µL, 0.0150 mmol) of the diluted tertiapin Q was removed and 2.1 equivalents (3.20 µL, 0.0320 mmol) of the maleimide were added to the peptide. TCEP (2.53 mg) was prepared at a concentration of 10 mM using pH 6.2 phosphate buffer (882 µL) before 2.1 equivalents (3.20 µL, 0.0320 mmol) were added to the reaction mixture. Aliquots (30 µL) were taken at 1, 5, 10, 30 and 60 min analysed by LC-MS. The percentage of bridged (LC retention time: 0.99 min, *m/z* 2642.0) and reduced, non-bridged (LC retention time: 0.89 min, *m/z* 2457.0) peptide was recorded.

4.5.2.2 Using Benzeneselenol:

Tertiapin Q (184 µL, 130.4 µM) was diluted to a concentration of 100 µM by addition of DMF (5.0 µL) and MeCN (61.0 µL). Maleimide **22** (2.24 mg) was prepared at a concentration of 10 mM using DMF (143 µL) and peptide buffer (572 µL). An aliquot (120 µL, 0.0120 mmol) of the diluted tertiapin Q was taken and 20 equivalents (24.0 µL, 0.240 mmol) of the maleimide were added to the peptide. Benzeneselenol (1.1 µL) was prepared at a concentration of 10 mM using DMF (99 µL) before 5 equivalents (6.0 µL, 0.0600 mmol) were added to the reaction mixture. Aliquots (30 µL) were taken at 1, 15, 30 and 60 min and analysed by LC-MS. The percentage of bridged (LC retention time: 0.99 min, *m/z* 2642.0) and reduced, non-bridged (LC retention time: 0.89 min, *m/z* 2457.0) peptide was recorded.

4. 6 Single Maleimide Bridging of Tertiapin Q

N.B. These general bridging procedures were repeated with some changes in the number of equivalents used, as described in the Results and Discussion.

4.6.1 General Step Wise Protocol Using TCEP

Tertiapin Q (193 µL, 144.9 µM) was diluted to a concentration of 100 µM by addition of pH 6.2 phosphate buffer (87.0 µL). Maleimide **53** (1.00 mg) was prepared at a concentration of 10 mM using DMF (339 µL) and 1.5 equivalents (4.20 µL, 0.0420 mmol) were added to the peptide. TCEP (2.27 mg) was prepared at a concentration of 10 mM using pH 6.2 phosphate buffer (792 µL) before 1.5 equivalents (4.20 µL, 0.0420 mmol) were added to the reaction mixture. An aliquot (30 µL) was removed at 60 min and analysed by LC-MS. A further 0.5 equivalent (1.3 µL, 0.0130 mmol) of TCEP was added to the peptide and after 60 min an aliquot (30 µL) was taken and analysed by LC-MS. A final 0.5 equivalent (1.1 µL, 0.0110 mmol) of TCEP was added to the peptide and after 60 min, an aliquot (30 µL) was taken and analysed by LC-MS. The percentage of bridged (LC retention time: 1.20 min, *m/z* 2567.0) and reduced, non-bridged (LC retention time: 0.89 min, *m/z* 2457.0) peptide was recorded.

4.6.2 With Capping of Free Thiols

Tertiapin Q (98.0 µL, 154.8 µM) was diluted to a concentration of 100 µM by addition of pH 6.2 phosphate buffer (52.0 µL). Maleimide **45** (0.63 mg) was prepared at a concentration of 10 mM using DMF (213 µL) and 1.5 equivalents (2.25 µL, 0.0225 mmol) were added to the peptide. TCEP (2.35 mg) was prepared at a concentration of 10 mM using pH 6.2 phosphate buffer (820 µL) before 1.5 equivalents (2.25 µL, 0.0225 mmol) were added to the reaction mixture. This was left to react for 1 h. Meanwhile, maleimide (0.79 mg) was prepared at a concentration of 10 mM using pH 6.2 phosphate buffer (814 µL). An aliquot (30 µL) of the tertiapin Q reaction mixture was taken, and to this 10 equivalents (3 µL, 0.0300 mmol) of maleimide was added and mixed. This was left to react for 10 min before analysis by LC-MS. The percentage of bridged (LC retention time: 1.20 min, *m/z* 2567.0), reduced, non-bridged (LC retention time: 0.89 min, *m/z* 2457.0) and thiol-capped (LC retention time: 1.24 min, *m/z* 2757.0) peptide was recorded.

4.7 Maleimide Bridging of Octreotide

N.B. ‘Peptide buffer’ employed in these experiments consisted of pH 6.2 phosphate buffer (50 mM) with 40 % MeCN and 2.5 % DMF.

This general bridging procedure was repeated variation in the maleimide reagent employed.

4.7.1 General Step Wise Protocol using TCEP

Octreotide (140 µL, 643 µM) was diluted to a concentration of 300 µM using peptide buffer (160 µL). TCEP (5.93 mg) was prepared at a concentration of 30 mM using peptide buffer (690 µL) before 1.5 equivalents (4.50 µL, 0.135 mmol) of this was added to the octreotide solution and mixed. The peptide was left to reduce for 1 h before an aliquot (30 µL) was removed and analysed by LC-MS to ensure complete disulfide reduction. A solution of maleimide **63** (2.71 mg) was prepared at a concentration of 30 mM using DMF (144 µL). 1.5 equivalents (4.05 µL, 0.122 mmol) of the maleimide solution were added to the reduced octreotide and mixed. After 10 min, an aliquot (30 µL) of this reaction mixture was removed and analysed by LC-MS to ensure full conversion to the bridged product (LC retention time: 1.10 min, *m/z* 1152.8).

4.8 Step Wise Click Modification of Octreotide

General Information

The 11, azido-3,6,9-trioxaundecan-1-amine, sodium ascorbate, $CuSO_4$, amino guanidine and tris-(hydroxypropyltriazolylmethyl)-amine (THPTA) used were all obtained from Sigma Aldrich. The doxorubicin-azide was kindly provided by Dr. João Nunes (UCL)[180].

4.8.1 Using a Small PEG-azide

Step 1: The above procedure (**4.7.1**) was repeated.

Step 2: $CuSO_4$ (2.5 µL, 0.2 mM) was added to THPTA (5 µL, 1 mM) and mixed until a blue coloration appeared. Meanwhile, 11, azido-3,6,9-trioxaundecan-1-amine (6 µL) was prepared at a concentration of 30 mM in DMF (1 mL) before 5 equivalents (5 µL) were added to the alkyne-maleimide bridged octreotide from Step 1 (100 µL) and mixed. To this was added 1 µL of the $CuSO_4$:THPTA solution before mixing. Next, amino guanidine (10 µL, 5 mM) and sodium ascorbate (10 µL, 5 mM) were added before the solution was mixed thoroughly and left to react for 1 h at room temperature. The reaction was analysed by LC-MS to ensure full conversion to the bridged product (LC retention time: 1.00 min, *m/z* 685.7 (*m/2*)).

This protocol was repeated using 10, 20 and 50 equivalents of 11, azido-3,6,9-trioxaundecan-1-amine. It was also repeated with reaction time of 24 h.

4.8.2 Using Doxorubicin-azide

Step 1: Octreotide (47 µL, 643 µM) was diluted to a concentration of 200 µM using peptide buffer (103 µL). TCEP (2.0 mg) was prepared at a concentration of 20 mM using peptide buffer (349 µL) before 1.5 equivalents (1.50 µL, 0.0300 mmol) of this was added to the octreotide solution and mixed. The peptide was left to reduce for 1 h. A solution of maleimide **63** (1.65 mg) was prepared at a concentration of 20 mM using DMF (282 µL). 1.5 equivalents (1.5 µL, 0.0300 mmol) of the maleimide solution were added to the reduced octreotide and mixed. After 10 min, an aliquot (30 µL) of this reaction mixture was removed and analysed by LC-MS to ensure full conversion to the bridged product. (LC retention time: 1.10 min, *m/z* 1152.8).

Step 2: $CuSO_4$ (2.5 µL, 0.2 mM) was added to THPTA (5 µL, 1 mM) and mixed until a blue coloration appeared. Meanwhile, 20 equivalents (33 µL, 12 mM) of doxorubicin-azide in DMF were added to the alkyne-maleimide bridged octreotide from Step 1 (100 µL) and mixed. To this was added 1 µL of the $CuSO_4$:THPTA solution before mixing. Next, amino guanidine (10 µL, 5 mM) and sodium ascorbate (10 µL, 5 mM) were added before the solution was mixed thoroughly and left to react for 90 mins at room temperature. The reaction was analysed by LC-MS to ensure full conversion to the bridged product (LC retention time: 1.35 min, *m/z* 1957.01).

4.9 Purification of Peptide Products

i) Dialysis

The remaining reaction mixture was added to a Slide-A-Lyzer Mini Dialysis Unit (2000 MWCO, ThermoScientific) and dialysed into distilled water for 24 h at 4 ˚C with stirring.

ii) RP-HPLC

A Shimadzu LC-10AT instrument fitted with a C_{18} column, 150 x 4.60 mm (Phenomenex) was used for all purification procedures. The mobile phases were water, 0.1% TFA (solvent A) and acetonitrile, 0.1 % TFA (solvent B). Flow rate of 1 mL/min. Species eluting from the column was monitored by measuring the absorbance at 280 nm. A fraction collector was used to collect the desired peaks (1 mL fractions) and identical fractions were pooled before being lyophilised using a Scanvac vacuumed

centrifuge (Labmode). The residual peptide was reconstituted in distilled water (RP-HPLC-grade, Fisher Chemicals).

Tertiapin Q product purification method:

Time (min)	*Solvent B (%)*
1.0	0
15.0	30
19.0	90
22.0	90
24.50	0
30.0	0

Octreotide product purification method:

Time (min)	*Solvent B (%)*
1.0	0
15.0	60
19.0	60
22.0	90
24.50	0
30.0	0

4.10 Cell Culture

4.10.1 Cell Line and Cell Culture Reagents

The cells used in this study were:

- Human Embryonic Kidney (HEK293) cell line stably expressing GIRK channel subtype 1/4 and the gene encoding zeocin resistance (referred to as GIRK1/4 cells).
- HEK293 cell line stably expressing GIRK channel subtype 1/2a and the gene encoding G418 resistance (referred to as GIRK1/2a cells).
- Human pancreatic neuroendocrine tumour cell line BON-1.

The HEK293 cell line is an immortalised human cell line derived from primary embryonic kidney cells and was already stored in the frozen cell line stock library at the William Harvey Research Institute, Queen Mary University of London. The BON-1 cell

line is an immortalised human cell line derived from a metastatic carcinoid tumour of the pancreas and was kindly donated by Professor Meyer (UCL).

For the GIRK1/4 cell line: The medium used was Minimum Essential Medium (MEM) containing Earle's salts obtained from PAA Laboratories. This was supplemented with 10% Foetal Bovine Serum (FBS) and the antibiotic zeocin (364 µg/mL) (Invitrogen).
For the GIRK1/2a cell line: The medium used was MEM containing Earle's salts supplemented with 10% FBS and the antibiotic G-418 (800 µg/mL) (Melford).
For the BON-1 cell line: The medium used was 1:1 MEM:Ham's F-12 K Nutrient Mixture (F-12K) supplemented with 10% FBS and 1% penicillin/streptomycin (Life Technologies).
The Phosphate Buffered Saline (PBS) and 0.25% trypsin solutions used were obtained from Gibco Life Technologies. The culture medium, PBS and trypsin were all warmed to 37 ˚C prior to use.

4.10.2 Cell Culture Procedure

The cell culture procedure was identical for all cell lines used.

4.10.2.1 Revival of Frozen Stocks, Subculture and General Maintenance

A 1 mL aliquot of cells stored in dimethyl sulfoxide (DMSO) at -80 ˚C was taken and defrosted in a water bath at 37 ˚C. The cells were pipetted into a 10 mL Falcon tube and ~6 mL of supplemented MEM media added. This was centrifuged for 2 min at 1000 rpm. The media was removed and 2 mL of fresh media added to resuspend the cell pellet. This was pipetted into a T75 flask (Nunclon) containing 8 mL of fresh media. The flask was incubated at 37 ˚C in a humidified atmosphere with 95% air and 5% CO_2.

Once the cells were 90% confluent they were passaged. The medium was removed and the remaining cells washed with PBS. Cells were detached from the flask base by adding 3 mL of trypsin and incubating at room temperature for 2-3 min. 7 mL of fresh medium was added to inhibit the trypsin and the mixture centrifuged at 1000 rpm for 3 min. The medium was removed and the cell pellet resuspended in 2 mL of fresh medium. A dilution of the resuspended pellet was made (typically to a ratio of 1:20) with fresh media in a new T75 flask. This was incubated at 37 ˚C. Passaging was carried out weekly.

4.10.2.2 Culture of Cells for Patch Clamp Experiments

When cells were required for patch clamp experiments they were passaged directly onto glass coverslips (10 mm diameter, borosilicate glass, VWR International). Once the cell pellet was resuspended in 2 mL of fresh medium (see above), ~0.2 mL of the resuspension was added to 12 mL of fresh media. This was then added in 1 mL aliquots to the wells of a 12 well plate (Nunclon) containing a single glass coverslip. The plate was incubated at 37 ˚C for 2 days before use.

4.10.3 Bacterial Transformation

4.10.3.1 General Information

The competent cells used for the transformation were TOP10 *E. coli* cells (Life Technologies). The DNA used was encoding the somatostatin receptor subtype 2 and eGFP. The DNA fragment encoding the somatostatin receptor was cloned into the plasmid vector pcDNA3.1+ (Life Technologies), also encoding ampicillin resistance. The eGFP was encoded in the pEGFP-N1 plasmid (Life Technologies), also encoding kanamycin resistance.

The antibiotics kanamycin and carbenicillin were purchased from Sigma Aldrich. The carbenicillin stock solution was made at 100 mg/mL in molecular grade water (Sigma Aldrich). The kanamycin stock solution was made at 25 mg/mL in molecular grade water.

4.10.3.2 Preparation of Liquid Broth (LB) Medium

20 LB medium tablets (Sigma Aldrich) were dissolved in 1 L of distilled water. This was autoclaved for sterilisation and allowed to cool to room temperature before use.

LB for somatostatin receptor transformation:

To 54 mL of liquid broth medium was added 54 µL of carbenicillin stock solution (stock solution at 100 mg/mL in distilled water) to make a final carbenicillin concentration of 100 µg/mL.

LB for eGFP transformation:

To 54 mL of liquid broth medium was added 54 µL of kanamycin stock solution (stock solution at 25 mg/mL in distilled water) to give a final kanamycin concentration of 25 µg/mL.

4.10.3.3 Preparation of LB-Agar Plates

To 100 mL of liquid broth medium was added 1.5 g of agar (Life Technologies). This was heated in the microwave on full power for 90 seconds. The agar was allowed to cool to 50 °C before the relevant antibiotics were added (100 µg/mL carbenicillin or 25 µg/mL kanamycin). Once the antibiotics were added, the LB-agar was mixed by inversion before being poured into sterile 100 x 20 mm tissue culture dishes (Sarstedt) and left to set at room temperature. The plates were stored at 4 °C until future use.

4.10.3.4 Transformation of Plasmid DNA

On ice, 30 µL of TOP10 *E. coli* cells were mixed with 1 µL of plasmid DNA. This was then incubated for 30 mins on ice. The bacteria were heat shocked for 90 seconds at 42 °C in a water bath before being returned to the ice. 1 mL of liquid broth medium (antibiotic free) was added and the bacteria then left for 30 mins at 37 °C. Lastly, 150 µL of bacteria was plated onto agar plates with the correct selective antibiotic. The plates were left overnight in an incubator at 37 °C.

4.10.3.5 Purification of Plasmid DNA

An individual colony from a plate was picked using a sterile pipette tip. This tip was added to 4 mL of liquid broth medium containing the correct selective antibiotic and shaken overnight at 37 °C.

The desired plasmids were then extracted and purified using the QIAGEN Plasmid Purification kit which contained all reagents required and mentioned below. The reagents were prepared as described in the enclosed handbook. The procedure for a midi-preparation from a bacterial suspension was described and followed from the enclosed handbook.

In brief:

The bacterial cells were harvested by centrifugation at 6000 *x g* for 15 min at 4 °C and the bacterial pellet was re-suspended in 4 mL of re-suspension buffer P1. 4 mL of lysis buffer P2 was added and mixed thoroughly by inversion several times before being incubated at room temperature for 5 mins to allow the bacteria to lyse and release the plasmid DNA. Next, 4 mL of chilled (4 °C) neutralisation buffer P3 was added and mixed immediately by inversion several times. This was then incubated on ice for 15

mins before being centrifuged at 20, 000 *x g* for 30 mins at 4 °C. The supernatant containing the plasmid DNA was removed promptly.

A QIAGEN-tip 100 column was equilibrated with 4 mL of equilibration buffer QBT. The collected supernatant was applied to the column and allowed to enter the resin by gravity flow. The column was washed with 2 x 10 mL of wash buffer QC and the plasmid DNA was then finally eluted with 5 mL of elution buffer QF. The plasmid DNA was precipitated by the addition of 3.5 mL of room temperature isopropanol; this was mixed and centrifuged immediately at 15, 000 *x g* for 30 mins at 4 °C. The supernatant was decanted and the DNA pellet washed with 2 mL of room temperature ethanol (70%) before being centrifuged at 15, 000 *x g* for 10 mins. The supernatant was again decanted and the pellet left to air-dry for 10 minutes. The pellet was re-suspended in 100 µL of molecular grade water and stored at -20 °C until further use.

The concentration of plasmid DNA stock solutions were determined by absorbance at 260 nm using a nanophotometer (Geneflow). The concentration of somatostatin receptor subtype 2 DNA stock solution was determined to be 766 ng/µL. The concentration of eGFP DNA stock solution was determined to be 974 ng/ µL.

4.10.4 Transfection of Cells

In a 1.5 mL Eppendorf was mixed 50 ng eGFP plasmid DNA (from stock solution), 800 ng SSTR2 plasmid DNA (from stock solution) and 97 µL of MEM media (containing no antibiotics or serum) per transfection well. This was mixed thoroughly by vortex. To this was added 5 µL of Fugene HD (Promega) per transfection well and mixed by gentle inversion. The mixture was incubated for 15 mins at room temperature.

Meanwhile, cells cultured onto 12 or 6 well plates for patch clamp experiments (as previously described in Section 4.5.2.2) were prepared for transfection. The antibiotic-conatining media was carefully removed, the coverslips washed with 2 mL of antibiotic-free media and replaced with 2 mL of antibiotic-free media per transfection well. 100 µL of the transfection mixture prepared above was added to each transfection well. Following incubation at 37 °C for 4 h, the media was removed, the cells were washed with 2 mL of antibiotic-free media and lastly the media replaced with 2 mL of G418 media. The cells were incubated at 37 °C until experiments commenced.

4.11 Electrophysiology

4.11.1 Patch Clamp Equipment Setup

A Faraday cage was used to reduce the effects of electrostatic noise and this was mounted on an air table to minimise vibrations. Prior to use, a glass-bottomed recording chamber, which is mounted above a microscope, is perfused with extracellular solution using a gravity-driven perfusion system. A vacuum pump system was used to remove the extracellular solution and to allow a continuous perfusion flow; a solution depth of around 5 mm was maintained throughout experiments. The microscope was fitted with a UV light source to allow visualisation of transfected cells. A glass coverslip with cells adhered was placed in the recording chamber. The recording chamber was grounded by an Ag/AgCl reference electrode (Axon instruments).

Patch pipettes were pulled from borosilicate glass (1.17 mm internal diameter, Harvard Apparatus) and a pipette puller (PP-830, Narishige). Pipettes were pulled to have a resistance of close to 2 MΩ when filled with intracellular solution. The pipette was filled with intracellular solution and attached onto the headstage. A slight positive pressure is applied to prevent the pipette tip being blocked with debris. The course controls on the manipulator (Sutter Instruments) is used to roughly position the pipette above the cell and the fine control is then used to touch the cell membrane. In order to achieve the gigaohm seal on the membrane, gentle suction is often required; to achieve this, the pipette holder is attached to tubing allowing suction and positive pressure to be applied by the experimenter. After a gigaohm seal is formed (cell-attached configuration, see Figure 1.19), increased suction leads to membrane rupture (whole-cell configuration, see Figure 1.20). At this point, after the membrane capacitance has been corrected, the whole-cell voltage clamp protocol can begin. From a holding potential of -50 mV, 20 mV steps were applied from -120 mV to +40 mV. The micropipette electrode was connected to a unitary voltage gain headstage amplifier (HS-2, Axon Instruments) containing a 10 MΩ resistor. Signals were further amplified by an Axopatch 200B amplifier (Axon Instruments), converted from analogue to digital signals by a Digidata 1440 converter, and captured and analysed using pClamp software (version 10.0, Axon Instruments). Voltage commands were generated using pClamp10 software.

4.11.2 Solutions Used for Whole Cell Patch Clamp Experiments

Extracellular (Bath) Solution:

KCl (20 mM), NaCl (120 mM), $CaCl_2$ (2 mM), $MgCl_2$ and HEPES (10 mM) were dissolved in high quality 18 Ω distilled water in a 1 L volumetric flask. The pH of the solution was adjusted to pH7.4 using NaOH (5 M) as required. The solution was stored at 4 ˚C and warmed to room temperature before use.

Intracellular (Pipette) Solution:

KCl (130 mM), NaCl (10 mM), $MgCl_2$ (1 mM), MgATP (2 mM), EGTA (2 mM), GTP (0.3 mM) and HEPES (10 mM) were dissolved in high quality 18 Ω distilled water in a 100 mL volumetric flask. The pH of the solution was adjusted to pH7.4 using KOH (5 M) as required. The solution was pipetted into 1 mL aliquots and stored at -20 ˚*C*. An aliquot was defrosted and sterile filtered before use ad incubated on ice throughout the experiments to reduce breakdown of ATP.

Tertiapin Q Solutions:

The concentration of the native and bridged tertiapin Q products was determined by UV absorption at 280 nm and the extinction coefficient of the peptide (5,750 $L\ mol^{-1}\ cm^{-1}$). With this a serial dilution to 100 nM, 50 nM, 30 nM, 10 nM, 5 nM and 1 nM was made in the extracellular solution prepared previously. 10 mL batches of each concentration were made on the day of the experiment.

Octreotide Solutions:

The concentration of native and bridged tertiapin Q products was determined by UV absorption at 280 nm and the extinction coefficient of the peptide (5, 630 $L\ mol^{-1}\ cm^{-1}$). With this a serial dilution to 10 µM, 1 µM, 100 nM, 10 nM, 1 nM, 0.1 nM and 0.01 nM was made in the extracellular solution prepared previously. 10 mL batches of each concentration were made on the day of the experiment.

4.11.3 Dose-Response Analysis of Tertiapin Q

Whole-cell patch clamp was carried out on HEK293 cells stably expressing the GIRK1/4 channel prepared as described in Section 2.8.2. Once a satisfactory seal to the cell membrane was formed (>1 GΩ), and a whole-cell had been achieved, transient spikes caused by cell capacitance were negated using the amplifier-circuitry. The cells

were voltage-clamped at -50 mV and the current measuring protocol (voltage steps from -120 to 50 mV in 10 mV increments) was run every minute until maximum inwards K^+ current was observed. At this point, the perfusion solution was switched to that of 1nM tertiapin Q. Again, the protocol was run every minute until K^+ current reduction by GIRK inhibition stabilised. At this point, the perfusion solution was switched to that of 5 nM tertiapin Q and again the protocol was run until the current reduction stabilised. This was repeated with tertiapin Q concentrations of 10, 30, 50 and 100 nM.

This procedure was repeated with bridged tertiapin Q concentrations of 10, 30, 50 and 100 nM.

4.11.4 Wash-Out Study of Tertiapin Q

After the above procedure was completed, the perfusion was switched back to extracellular solution and the voltage-clamp protocol run every 5 min to test for reversal of the drug effect.

4.11.5 Dose-Response Analysis of Octreotide

Whole-cell patch clamp was carried out on HEK293 cells stably expressing the GIRK1/2a channel and transiently transfected with both the somatostatin receptor subtype 2 and eGFP to enable identification of transfected cells (as described in Section 4.5.4). Once a fluorescent cell on the coverslip had been located, current recordings were conducted, as described in Section 2.9.4. In this case, agonist activity of octreotide was monitored by activation of the somatostatin receptor leading to increased K^+ current through GIRK channels. This was monitored by sequential perfusion with 0.01, 0.1, 1, 10 and 100 nM octreotide.

This procedure was repeated with bridged octreotide concentrations of 1, 10, 100, 10^3 and 10^4 nM.

4.11.6 Wash-Out Study of Octreotide

After the above procedure was completed, the perfusion was switched back to extracellular solution and the voltage-clamp protocol run every 2 min to test for regeneration of resting K^+ currents.

4.12 Confocal Microscopy Imaging

4.12.1 General Information

For these experiments, HEK293 cells stably expressing the GIRK1/2a channel and BON-1 cells were used.

Tyrode's solution:

NaCl (135 mM), KCl (5.4 mM), $CaCl_2$ (2 mM), $MgCl_2$ (1 mM), HEPES (5 mM) and glucose (10 mM) were dissolved in distilled water in a 500 mL volumetric flask. The pH of the solution was adjusted to pH 7.4 using NaOH (5 M) as required. The solution was stored at 4 ˚C and warmed to room temperature before use.

4.12.2 Cell Preparation

When ~80% confluent, cells were passaged, as described previously in Section 4.10.2.2, onto glass bottomed petri dishes (40 mm). One dish of HEK293 cells was transfected, as described in Section 4.10.4, with SSTR 2 and eGFP and these cells were imaged 48 h after transfection. Prior to imaging, the cells were washed with Tyrode's solution (2 x 1 mL) and 2 mL of Tyrode's solution added.

To each petri dish, maleimide **77** in distilled water (1 µM, 33 µL) was added and left either at room temperature or 37 °C for 20 minutes before confocal imaging. After preliminary imaging, the solution containing maleimide **77** was removed and the cells washed with Tyrode's solution (3 x 1 mL) before 2 mL of Tyrode's solution was added and the cells imaged again.

4.12.3 Microscopy Imaging

Live cells were imaged using a Zeiss LSM510 (Mark 4) confocal microscope and a Plan-Apochromat 63× oil lens objective (1.4 numerical aperture). eGFP was visualized using a multi-line Argon laser (wavelength 488 nm) and filtered using a BP505-530 (band pass) emission filter. Rhodamine B was visualised using a helium/neon laser (wavelength 543 nm) and filtered using a BP560-615 emission filter. To avoid 'cross-talk' between eGFP and rhodamine B signals, images were acquired sequentially. Images were taken at 1024×1024 frame size, a bit depth of 16 bit, and were averaged twice.

4.13 Mass Spectrometry Analysis

These IM-MS/MS experiments were performed in a hybrid quadrupole-ion mobility-orthogonal acceleration time-of-flight (oa-TOF) mass spectrometer (Synapt HDMS, Waters, Manchester, UK).

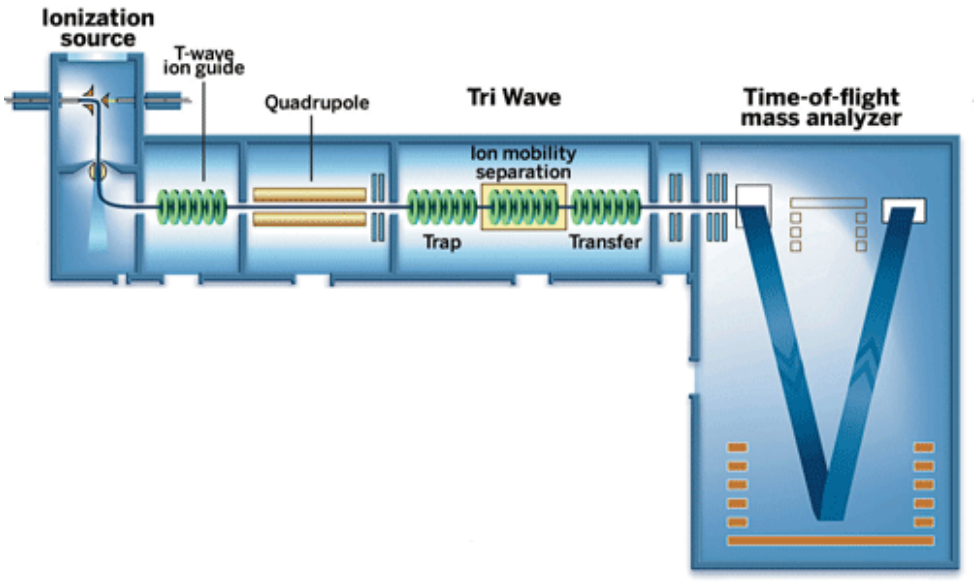

Figure 2.2: A schematic of the IM-MS/MS instrument.[v]

4.13.1 Ion-Mobility-Mass Spectrometry/Mass Spectrometry (IM-MS/MS)

The instrument was fitted with a nanoflow electrospray ion source and operated at a source temperature of 40 °C. The cone was optimized between 30 V and 70 V for electrospray ionisation mass spectrometry/mass spectrometry (ESI-MS/MS) experiments and the collision energy was increased from 20 eV to 80 eV during the each acquisition. Samples were introduced into the instrument by direct infusion ESI and ions were subsequently mass selected, prior to MS/MS experiments, by use of an installed quadrupole. All MS/MS experiments were performed after ion mobility separation in the Tri-wave transfer cell. The pressure in the Tri-wave IM cell was 0.58 mbar with nitrogen employed as the mobility gas. The T-wave height and velocity were set at 7 V and 300 m/s respectively. The time-of-flight (TOF) mass analyzer recorded 200 pushes, each one representing a single mass spectrum. Mass spectra were acquired at an acquisition rate of two spectra per second with a scan time of 1 s. Data acquisition and subsequent processing were carried out using Mass Lynx (v4.1) software (Waters Corp., Milford, MA).

[v] Arnaud, C. H. *Chemical & Engineering News Archive* **2008**, *86*, 11.

4.13.2 Calibration for Ion-Mobility Analysis

Equine myoglobin and cytochrome c data were used to create a calibration curve for ion mobility experiments. Absolute cross sections for myoglobin and cytochrome c were previously obtained from drift-time ion mobility mass spectrometry (DTIMS) experiments. Normalised cross sections (corrected for charge state) were plotted against corrected drift times (corrected to exclude time spent outside the ion mobility cell) to produce a calibration curve. This curve could then be used to determine unknown cross sections from known drift times.

To compare the experimental cross sections of native and modified tertiapin with theoretical values, cross sections were calculated using the open source software programme MOBCAL, a program to calculate mobilities from published X-ray structure files held at the RCSB Protein Data Bank. In these experiments, cross sections were calculated using both the projection approximation (PA) and exact hard-sphere scattering (EHSS) model methods on the RCSB Protein Data Bank file 1TER.

4.13.3 Capillary Liquid Chromatography/Mass Spectrometry (capLC/MS, -MS^2)

Chromatographic separation was performed using an Accela capillary LC system (Thermo Scientific, UK). The LC system is consisted of an Accela solvent rack, Accela 600 pressure dual gradient pumping system with an on-line solvent degasser and an Accela autosampler.

The LC system was fitted with a Hypersil Gold, C_{18} column, 100 x 2.1 mm, 1.9 µL (Thermo Scientific, UK) and coupled to a Finnigan LTQ mass spectrometer (Thermo Scientific, UK). The mobile phases were water, 0.1% formic acid (solvent A) and methanol, 0.1 % formic acid (solvent B). A linear gradient was utilised for the LC-MS, -MS^2 analyses as shown in Table 4.1, with a total run time of 10 minutes. An injection loop of 25 µL was used, and between sample injections the needle and injection loop were washed with methanol - water (1:1) to eliminate sample carry-over.

Table 4.1: LC method conditions

Time (min)	*Solvent A (%)*	*Solvent B (%)*	*Flow rate (µL/min)*
0	*99*	*1*	*200*
8.0	*5*	*95*	*200*
9.0	*5*	*95*	*200*
9.1	*99*	*1*	*200*
10	*99*	*1*	*200*

10 µL of the sample was diluted with 90 µL water, 0.1% formic acid. The sample was centrifuged at 13,000 *x g* for 3 minutes. 20 µL was injected onto the reversed phase column via the injection loop. Eluent from the C_{18} column was continuously directed to the capillary electrospray source of the Finnigan LTQ mass spectrometer via a fused silica emitter. The LTQ mass spectrometer was operated in the positive ion ES mode with four scan events over the 10 min gradient LC run. The scan events were MS and MS^2. MS^2 was programmed on $[M+H]^+$, $[M+2H]^{2+}/2$, $[M+3H]^{3+}/3$ and $[M+4H]^{4+}/4$. For acquisition of the MS^2 spectra, the collision energy was 35%. The mass spectrometer was operated under the following settings:-spray voltage 4.5 kV, capillary temperature 280 °C, sheath gas flow rate 40, auxiliary gas flow rate 10. MS, MS^2 scans consisted of three averaged "microscans" each with a maximum injection time of 200 ms.

Appendix

Table 1: Data for the dose-response curve of native tertiapin Q (0-100 nM).

Concentration (nM)	*Log Concentration*	*Average Current Inhibition*	*No. of experiments*	*Standard Error of the Mean*	*Normalised Average Current Inhibition (%)*
0	-6.00	0	-	-	0
1	-3.00	18.032	4	4.051	22.69
5	-2.30	43.494	7	4.726	54.72
10	-2.00	54.820	6	5.249	68.97
30	-1.52	72.162	5	5.064	90.79
50	-1.30	77.562	4	4.314	97.58
100	-1.00	79.485	5	5.483	100.00

Table 2: Expected fragment ions produced from MS/MS of reduced tertiapin Q.

Fragment	*Exact mass*	*Fragment*	*Exact mass*
b1	72.04	y1	145.12
b2	185.13	y2	273.22
b3	288.14	y3	330.24
b4	402.18	y4	433.25
b5	505.19	y5	561.34
b6	619.23	y6	689.44
b7	777.35	y7	875.52
b8	890.43	y8	978.53
b9	1003.52	y9	1106.59
b10	1116.6	y10	1243.65
b11	1213.65	y11	1340.7
b12	1350.71	y12	1453.78
b13	1478.77	y13	1566.87
b14	1581.78	y14	1679.97
b15	1767.86	y15	1838.07
b16	1895.96	y16	1952.11
b17	2024.05	y17	2055.12
b18	2127.06	y18	2169.16
b19	2184.08	y19	2272.17
b20	2312.18	y20	2385.26
b21	2456.29	y21	2456.29

Table 3-5: Expected fragment ions produced from MS/MS of doubly modified tertiapin Q.

Table 3: C3-C14/C5-C18 disulfide connectivity

Fragment	*Exact mass*		*Fragment*	*Exact mass*	
b1	72.04	no mal	y1	145.12	no mal
b2	185.13	no mal	y2	273.22	no mal
b3	n/a	mal	y3	330.24	no mal
b4	n/a	mal	y4	n/a	mal
b5	n/a	mal	y5	n/a	mal
b6	n/a	mal	y6	n/a	mal
b7	n/a	mal	y7	n/a	mal
b8	n/a	mal	y8	n/a	mal
b9	n/a	mal	y9	n/a	mal
b10	n/a	mal	y10	n/a	mal
b11	n/a	mal	y11	n/a	mal
b12	n/a	mal	y12	n/a	mal
b13	n/a	mal	y13	n/a	mal
b14	n/a	mal	y14	n/a	mal
b15	n/a	mal	y15	n/a	mal
b16	n/a	mal	y16	n/a	mal
b17	n/a	mal	y17	n/a	mal
b18	2311.01	mal	y18	n/a	mal
b19	2368.04	mal	y19	2458.14	mal
b20	2496.13	mal	y20	2571.23	mal
b21	2642.26	mal	y21	2642.26	mal

Table 4: C3-C5/C14-C18 disulfide connectivity

Fragment	*Exact mass*		*Fragment*	*Exact mass*	
b1	72.04	no mal	y1	145.12	no mal
b2	185.13	no mal	y2	273.22	no mal
b3	n/a	mal	y3	330.24	no mal
b4	n/a	mal	y4	n/a	mal
b5	598.17	mal	y5	n/a	mal
b6	712.23	mal	y6	n/a	mal
b7	868.34	mal	y7	n/a	mal
b8	981.42	mal	y8	1071.51	mal
b9	1094.50	mal	y9	1199.57	mal
b10	1207.60	mal	y10	1337.34	mal
b11	1304.67	mal	y11	1434.71	mal
b12	1441.71	mal	y12	1547.78	mal
b13	1569.77	mal	y13	1660.86	mal
b14	n/a	mal	y14	1773.95	mal
b15	n/a	mal	y15	1930.05	mal
b16	n/a	mal	y16	2044.09	mal
b17	n/a	mal	y17	n/a	mal
b18	2311.01	mal	y18	n/a	mal
b19	2368.04	mal	y19	2458.14	mal
b20	2496.13	mal	y20	2571.23	mal
b21	2642.26	mal	y21	2642.26	mal

Table 5: C3-C18/C5-C14 disulfide connectivity

Fragment	*Exact mass*		*Fragment*	*Exact mass*	
b1	72.04	no mal	y1	145.12	no mal
b2	185.13	no mal	y2	273.22	no mal
b3	n/a	mal	y3	330.24	no mal
b4	n/a	mal	y4	n/a	mal
b5	n/a	mal	y5	n/a	mal
b6	n/a	mal	y6	n/a	mal
b7	n/a	mal	y7	n/a	mal
b8	n/a	mal	y8	n/a	mal
b9	n/a	mal	y9	n/a	mal
b10	n/a	mal	y10	n/a	mal
b11	n/a	mal	y11	n/a	mal
b12	n/a	mal	y12	n/a	mal
b13	n/a	mal	y13	n/a	mal
b14	n/a	mal	y14	n/a	mal
b15	n/a	mal	y15	n/a	mal
b16	n/a	mal	n/a	n/a	mal
b17	n/a	mal	y17	n/a	mal
b18	2311.01	mal	y18	n/a	mal
b19	2368.04	mal	y19	2458.14	mal
b20	2496.13	mal	y20	2571.23	mal
b21	2642.26	mal	y21	2642.26	mal

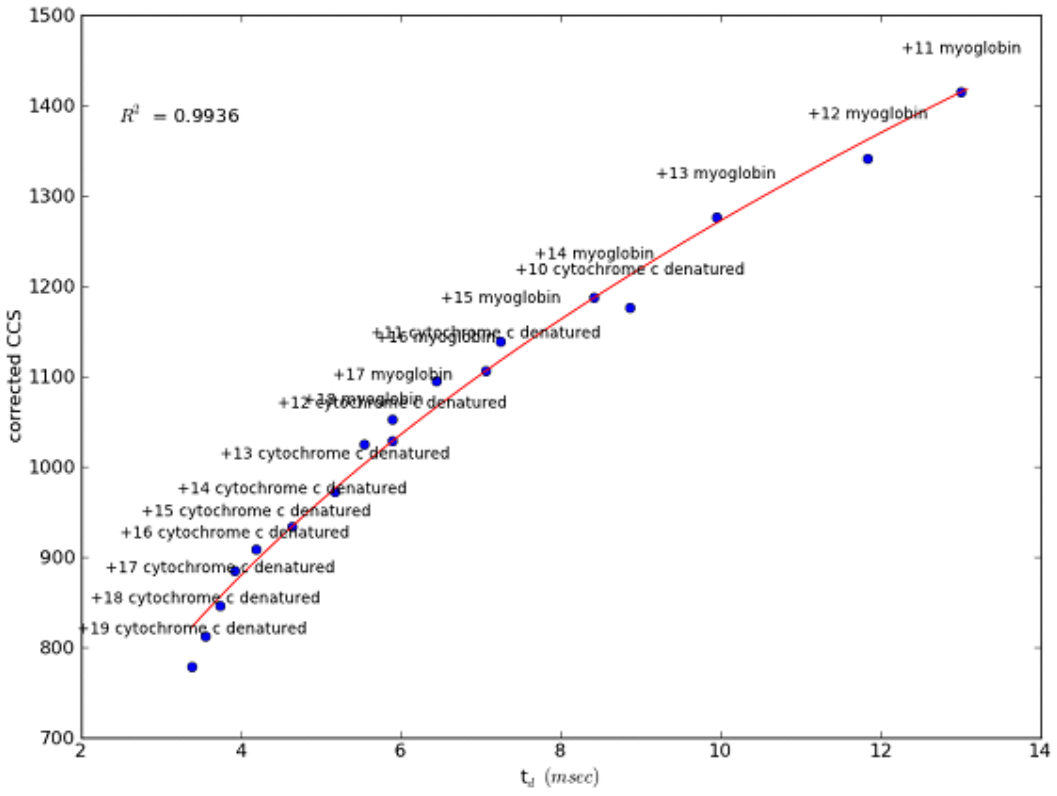

Figure 1: Calibration curve of corrected collision cross section against drift time created using myoglobin and cytochrome c.

Table 6-11: Expected fragment ions produced from MS/MS of singly modified tertiapin Q.

Table 6: C3-C5 disulfide connectivity

Fragment	*Exact mass*		*Fragment*	*Exact mass*	
b1	72.04	no mal	y1	144.11	no mal
b2	185.13	no mal	y2	272.21	no mal
b3	n/a	mal	y3	329.23	no mal
b4	n/a	mal	y4	432.24	no mal
b5	612.19	mal	y5	560.33	no mal
b6	726.23	mal	y6	688.43	no mal
b7	884.35	mal	y7	874.51	no mal
b8	997.43	mal	y8	977.52	no mal
b9	1110.52	mal	y9	1105.58	no mal
b10	1223.6	mal	y10	1242.64	no mal
b11	1320.66	mal	y11	1339.69	no mal
b12	1457.71	mal	y12	1452.77	no mal
b13	1585.77	mal	y13	1565.86	no mal
b14	1688.78	mal	y14	1678.96	no mal
b15	1874.86	mal	y15	1837.06	no mal
b16	2002.96	mal	y16	1951.1	no mal
b17	2131.05	mal	y17	n/a	mal
b18	2234.06	mal	y18	n/a	mal
b19	2291.08	mal	y19	2378.16	mal
b20	2419.18	mal	y20	2491.25	mal
b21	2563.29	mal	y21	2563.29	mal

Table 7: C14-C18 disulfide connectivity

Fragment	*Exact mass*		*Fragment*	*Exact mass*	
b1	72.04	no mal	y1	144.11	no mal
b2	185.13	no mal	y2	272.21	no mal
b3	288.14	no mal	y3	329.23	no mal
b4	402.18	no mal	y4	n/a	mal
b5	505.19	no mal	y5	n/a	mal
b6	619.23	no mal	y6	n/a	mal
b7	777.35	no mal	y7	n/a	mal
b8	890.43	no mal	y8	1084.52	mal
b9	1003.52	no mal	y9	1212.58	mal
b10	1116.6	no mal	y10	1349.64	mal
b11	1213.65	no mal	y11	1446.69	mal
b12	1350.71	no mal	y12	1559.77	mal
b13	1478.77	no mal	y13	1672.86	mal
b14	n/a	mal	y14	1785.94	mal
b15	n/a	mal	y15	1944.06	mal
b16	n/a	mal	y16	2058.1	mal
b17	n/a	mal	y17	2161.11	mal
b18	2234.06	mal	y18	2275.15	mal
b19	2291.08	mal	y19	2378.16	mal
b20	2419.18	mal	y20	2491.25	mal
b21	2563.29	mal	y21	2563.29	mal

Table 8: C3-C14 disulfide connectivity

Fragment	*Exact mass*		*Fragment*	*Exact mass*	
b1	72.04	no mal	y1	144.11	no mal
b2	185.13	no mal	y2	272.21	no mal
b3	n/a	mal	y3	329.23	no mal
b4	n/a	mal	y4	432.24	no mal
b5	n/a	mal	y5	560.33	no mal
b6	n/a	mal	y6	688.43	no mal
b7	n/a	mal	y7	874.51	no mal
b8	n/a	mal	y8	n/a	mal
b9	n/a	mal	y9	n/a	mal
b10	n/a	mal	y10	n/a	mal
b11	n/a	mal	y11	n/a	mal
b12	n/a	mal	y12	n/a	mal
b13	n/a	mal	y13	n/a	mal
b14	1688.78	mal	y14	n/a	mal
b15	1874.86	mal	y15	n/a	mal
b16	2002.96	mal	y16	n/a	mal
b17	2131.05	mal	y17	n/a	mal
b18	2234.06	mal	y18	n/a	mal
b19	2291.08	mal	y19	2378.16	mal
b20	2419.18	mal	y20	2491.25	mal
b21	2563.29	mal	y21	2563.29	mal

Table 9: C5-C18 disulfide connectivity

Fragment	*Exact Mass*		*Fragment*	*Exact Mass*	
b1	72.04	no mal	y1	144.11	no mal
b2	185.13	no mal	y2	272.21	no mal
b3	288.14	no mal	y3	329.23	no mal
b4	402.18	no mal	y4	n/a	mal
b5	n/a	mal	y5	n/a	mal
b6	n/a	mal	y6	n/a	mal
b7	n/a	mal	y7	n/a	mal
b8	n/a	mal	y8	n/a	mal
b9	n/a	mal	y9	n/a	mal
b10	n/a	mal	y10	n/a	mal
b11	n/a	mal	y11	n/a	mal
b12	n/a	mal	y12	n/a	mal
b13	n/a	mal	y13	n/a	mal
b14	n/a	mal	y14	n/a	mal
b15	n/a	mal	y15	n/a	mal
b16	n/a	mal	y16	n/a	mal
b17	n/a	mal	y17	2161.11	mal
b18	2234.06	mal	y18	2275.15	mal
b19	2291.08	mal	y19	2378.16	mal
b20	2419.18	mal	y20	2491.25	mal
b21	2563.29	mal	y21	2563.29	mal

Table 10: C3-C18 disulfide connectivity

Fragment	*Exact mass*		*Fragment*	*Exact mass*	
b1	72.04	no mal	y1	144.11	no mal
b2	185.13	no mal	y2	272.21	no mal
b3	n/a	mal	y3	329.23	no mal
b4	n/a	mal	y4	n/a	mal
b5	n/a	mal	y5	n/a	mal
b6	n/a	mal	y6	n/a	mal
b7	n/a	mal	y7	n/a	mal
b8	n/a	mal	y8	n/a	mal
b9	n/a	mal	y9	n/a	mal
b10	n/a	mal	y10	n/a	mal
b11	n/a	mal	y11	n/a	mal
b12	n/a	mal	y12	n/a	mal
b13	n/a	mal	y13	n/a	mal
b14	n/a	mal	y14	n/a	mal
b15	n/a	mal	y15	n/a	mal
b16	n/a	mal	y16	n/a	mal
b17	n/a	mal	y17	n/a	mal
b18	2234.06	mal	y18	n/a	mal
b19	2291.08	mal	y19	2378.16	mal
b20	2419.18	mal	y20	2491.25	mal
b21	2563.29	mal	y21	2563.29	mal

Table 11: C5-C14 disulfide connectivity

Fragment	*Exact mass*		*Fragment*	*Exact mass*	
b1	72.04	no mal	y1	144.11	no mal
b2	185.13	no mal	y2	272.21	no mal
b3	288.14	no mal	y3	329.23	no mal
b4	402.18	no mal	y4	432.24	no mal
b5	n/a	mal	y5	560.33	no mal
b6	n/a	mal	y6	688.43	no mal
b7	n/a	mal	y7	874.51	no mal
b8	n/a	mal	y8	n/a	mal
b9	n/a	mal	y9	n/a	mal
b10	n/a	mal	y10	n/a	mal
b11	n/a	mal	y11	n/a	mal
b12	n/a	mal	y12	n/a	mal
b13	n/a	mal	y13	n/a	mal
b14	1688.78	mal	y14	n/a	mal
b15	1874.86	mal	y15	n/a	mal
b16	2002.96	mal	y16	n/a	mal
b17	2131.05	mal	y17	2161.11	mal
b18	2234.06	mal	y18	2275.15	mal
b19	2291.08	mal	y19	2378.16	mal
b20	2419.18	mal	y20	2419.18	mal
b21	2563.29	mal	y21	2563.29	mal

Table 12: Data for the dose-response curve of native octreotide (0-100 nM).

Concentration (nM)	*Log Concentration*	*Absolute Current Activation (pA/pF)*	*No. of experiments*	*Standard Error of the Mean (pA/pF)*
0	-6.00	-12.237	7	1.372
0.01	-5.00	-15.730	4	1.129
0.10	-4.00	-24.606	7	1.203
1.00	-3.00	-41.777	5	4.063
10.0	-2.00	-59.441	4	5.164
100	-1.00	-62.824	4	4.429

Table 13: Data for the dose-response curve of modified octreotide (0-10 μM).

Concentration (nM)	*Log Concentration*	*Absolute Current Activation (pA/pF)*	*No. of experiments*	*Standard Error of the Mean (pA/pF)*
0	-6.00	-11.292	7	1.174
1.00	-3.00	-11.642	7	1.123
10.00	-2.00	-18.417	6	1.151
100.00	-1.00	-26.093	4	2.971
1×10^3	0	-36.800	4	4.245
1×10^4	1.00	-43.680	4	6.494

Table 14: Data for the dose-response curve of alkyne modified octreotide (0-10 μM).

Concentration (nM)	*Log Concentration*	*Absolute Current Activation (pA/pF)*	*No. of experiments*	*Standard Error of the Mean (pA/pF)*
0	-6.00	-17.303	7	3.030
1.00	-3.00	-18.079	5	4.436
10.00	-2.00	-24.193	6	3.506
100.00	-1.00	-40.784	8	3.582
1×10^3	0	-62.323	6	5.454
1×10^4	1.00	-65.167	5	5.934

References

(1) Whitford, D. *Proteins: Structure and Function*; Wiley, 2005.

(2) Walsh, C. T. *Posttranslational Modification of Proteins: Expanding Nature's Inventory*; Roberts & Co, 2005.

(3) Seet, B. T.; Dikic, I.; Zhou, M. M.; Pawson, T. *Nat. Rev. Mol. Cell Biol.* **2006**, *7*, 473.

(4) Ehrlich, J. R. *J. Cardiovasc. Pharmacol.* **2008**, *52*, 129.

(5) McGregor, D. P. *Curr. Opin. Pharmacol.* **2008**, *8*, 616.

(6) Clardy, S. M.; Allis, D. G.; Fairchild, T. J.; Doyle, R. P. *Expert Opin. Drug Deliv.* **2011**, *8*, 127.

(7) Lu, Z. R.; Shiah, J. G.; Sakuma, S.; Kopeckova, P.; Kopecek, J. *J. Control. Release* **2002**, *78*, 165.

(8) Werle, M.; Bernkop-Schnürch, A. *Amino Acids* **2006**, *30*, 351.

(9) Heller, A.; Feldman, B. *Chem. Rev.* **2008**, *108*, 2482.

(10) Olsen, J. O.; Pozderac, R. V.; Hinkle, G.; Hill, T.; Odorisio, T. M.; Schirmer, W. J.; Ellison, E. C.; Odorisio, M. S. *Seminars in Nuclear Medicine* **1995**, *25*, 251.

(11) Parker, D. *Chem. Soc. Rev.* **1990**, *19*, 271.

(12) Shreve, P.; Aisen, A. M. *Magn.Reson.Med.* **1986**, *3*, 336.

(13) Ruan, G.; Agrawal, A.; Marcus, A. I.; Nie, S. *J. Am. Chem. Soc.* **2007**, *129*, 14759.

(14) Achilefy, S.; Dorshow, R. B.; Bugaj, J. E.; Rajagopalan, R. *Investigative Radiology* **2000**, *35*, 479.

(15) Hershfield, M. S.; Chaffee, S.; Korojohnson, L.; Mary, A.; Smith, A. A.; Short, S. A. *Proc. Natl. Acad. Sci. U. S. A.* **1991**, *88*, 7185.

(16) Chari, R. V. J. *Accounts of Chemical Research* **2008**, *41*, 98.

(17) Baslé, E.; Joubert, N.; Pucheault, M. *Chemistry & Biology* **2010**, *17*, 213.

(18) Chalker, J. M.; Bernardes, G. J. L.; Lin, Y. A.; Davis, B. G. *Chemistry-an Asian Journal* **2009**, *4*, 630.

(19) Smith, M. E. B.; Schumacher, F. F.; Ryan, C. P.; Tedaldi, L. M.; Papaioannou, D.; Waksman, G.; Caddick, S.; Baker, J. R. *J. Am. Chem. Soc.* **2010**, *132*, 1960.

(20) Miseta, A.; Csutora, P. *Mol. Biol. Evol.* **2000**, *17*, 1232.

(21) Rosendahl, M. S.; Doherty, D. H.; Smith, D. J.; Carlson, S. J.; Chlipala, E. A.; Cox, G. N. *Bioconjugate Chem.* **2005**, *16*, 200.

(22) Davis, B. G.; Lloyd, R. C.; Jones, J. B. *Journal of Organic Chemistry* **1998**, *63*, 9614.

(23) Balan, S.; Choi, J. W.; Godwin, A.; Teo, I.; Laborde, C. M.; Heidelberger, S.; Zloh, M.; Shaunak, S.; Brocchini, S. *Bioconjugate Chem.* **2007**, *18*, 61.

(24) Schumacher, F. F.; Nobles, M.; Ryan, C. P.; Smith, M. E. B.; Tinker, A.; Caddick, S.; Baker, J. R. *Bioconjugate Chem.* **2011**, *22*, 132.

(25) Sun, M. M. C.; Beam, K. S.; Cerveny, C. G.; Hamblett, K. J.; Blackmore, R. S.; Torgov, M. Y.; Handley, F. G. M.; Ihle, N. C.; Senter, P. D.; Alley, S. C. *Bioconjugate Chem.* **2005**, *16*, 1282.

(26) Singh, R.; Maloney, E. K. *Anal. Biochem.* **2002**, *304*, 147.

(27) Hermanson *Bioconjugate Techniques*; Academic Press, 2008.

(28) Riener, C. K.; Kada, G.; Gruber, H. J. *Anal. Bioanal. Chem.* **2002**, *373*, 266.

(29) Hallaway, B. E.; Hedlund, B. E.; Benson, E. S. *Arch. Biochem. Biophys.* **1980**, *203*, 332.
(30) Bernardes, G. J. L.; Chalker, J. M.; Errey, J. C.; Davis, B. G. *J. Am. Chem. Soc.* **2008**, *130*, 5052.
(31) Chalker, J. M.; Gunnoo, S. B.; Boutureira, O.; Gerstberger, S. C.; Fernandez-Gonzalez, M.; Bernardes, G. J. L.; Griffin, L.; Hailu, H.; Schofield, C. J.; Davis, B. G. *Chemical Science* **2011**, *2*, 1666.
(32) Lemieux, G. A.; Bertozzi, C. R. *Trends in Biotechnology* **1998**, *16*, 506.
(33) Pignataro, B. *Ideas in Chemistry and Molecular Sciences: Where Chemistry Meets Life*; Wiley VCH, 2010.
(34) Seifried, S. E.; Yan, W.; Vonhippel, P. H. *J. Biol. Chem.* **1988**, *263*, 13511.
(35) Davis, N. J.; Flitsch, S. L. *Tetrahedron Lett.* **1991**, *32*, 6793.
(36) Schelte, P.; Boeckler, C.; Frisch, B.; Schuber, F. *Bioconjugate Chem.* **2000**, *11*, 118.
(37) Ghosh, S. S.; Kao, P. M.; McCue, A. W.; Chappelle, H. L. *Bioconjugate Chem.* **1990**, *1*, 71.
(38) Ratner, D. M.; Adams, E. W.; Disney, M. D.; Seeberger, P. H. *Chembiochem* **2004**, *5*, 1375.
(39) Tuesca, A. D.; Reiff, C.; Joseph, J. I.; Lowman, A. M. *Pharm. Res.* **2009**, *26*, 727.
(40) Veronese, F. M. *PEGylated Protein Drugs: Basic Science and Clinical Applications*; Birkhauser, 2009.
(41) Baldwin, A. D.; Kiick, K. L. *Bioconjugate Chem.* **2011**, *22*, 1946.
(42) Smyth, D. G.; Konigsberg, W.; Blumenfeld, O. O. *Biochem. J.* **1964**, *91*, 589.
(43) Tedaldi, L. M.; Smith, M. E. B.; Nathani, R. I.; Baker, J. R. *Chem. Commun.* **2009**, 6583.
(44) Schafer, F. Q.; Buettner, G. R. *Free Radic. Biol. Med.* **2001**, *30*, 1191.
(45) Mannhold, R.; Kubinyi, H.; Folkers, G. *Prodrugs and Targeted Delivery: Towards Better ADME Properties*; Wiley VCH, 2010.
(46) Moody, P.; Smith, M. E. B.; Ryan, C. P.; Chudasama, V.; Baker, J. R.; Molloy, J.; Caddick, S. *Chembiochem* **2012**, *13*, 39.
(47) Schmiedl, A.; Breitling, F.; Winter, C. H.; Queitsch, I.; Dubel, S. *Journal of Immunological Methods* **2000**, *242*, 101.
(48) Walsh, C. T. *Post-translational Modification of Protein Biopharmaceuticals*; Wiley VCH, 2009.
(49) Loferer, H.; Hennecke, H. *Trends Biochem.Sci.* **1994**, *19*, 169.
(50) Noiva, R. *Protein Expr. Purif.* **1994**, *5*, 1.
(51) Britto, P. J.; Knipling, L.; Wolff, J. *J. Biol. Chem.* **2002**, *277*, 29018.
(52) Wang, Z. Z., Y. Zhang, H. Harrington, P. Chen, H. *American Society for Mass Spectrometry* **2012**, *23*, 520.
(53) Wedemeyer, W. J.; Welker, E.; Narayan, M.; Scheraga, H. A. *Biochemistry* **2000**, *39*, 4207.
(54) Jornvall, H.; Philipson, L. *Eur. J. Biochem.* **1980**, *104*, 237.
(55) Thornton, J. M. *J. Mol. Biol.* **1981**, *151*, 261.
(56) Brocchini, S.; Godwin, A.; Balan, S.; Choi, J. W.; Zloh, M.; Shaunak, S. *Adv. Drug Deliv. Rev.* **2008**, *60*, 3.
(57) Freda, P. U. *J. Clin. Endocrinol. Metab.* **2002**, *87*, 3013.
(58) Rajesh Singh, R.; Chang, J. Y. *Biochimica et biophysica acta* **2003**, *1651*, 85.

(59) Schumacher, F. F.; Sanchania, V. A.; Tolner, B.; Wright, Z. V. F.; Ryan, C. P.; Smith, M. E. B.; Ward, J. M.; Caddick, S.; Kay, C. W. M.; Aeppli, G.; Chester, K. A.; Baker, J. R. *Scientific Reports* **2013**, *3*.

(60) Ruddy, K.; Mayer, E.; Partridge, A. *CA: A Cancer Journal for Clinicians* **2009**, *59*, 56.

(61) Castaneda, L.; Maruani, A.; Schumacher, F. F.; Miranda, E.; Chudasama, V.; Chester, K. A.; Baker, J. R.; Smith, M. E. B.; Caddick, S. *Chem. Commun.* **2013**, *49*, 8187.

(62) Palanki, M. S. S.; Bhat, A.; Bolanos, B.; Brunel, F.; Del Rosario, J.; Dettling, D.; Horn, M.; Lappe, R.; Preston, R.; Sievers, A.; Stankovic, N.; Woodnut, G.; Chen, G. *Bioorganic & Medicinal Chemistry Letters* **2013**, *23*, 402.

(63) Marculescu, C.; Kossen, H.; Morgan, R. E.; Mayer, P.; Fletcher, S. A.; Tolner, B.; Chester, K. A.; Jones, L. H.; Baker, J. R. *Chem. Commun.* **2014**, *50*, 7139.

(64) Ryan, C. P.; Smith, M. E. B.; Schumacher, F. F.; Grohmann, D.; Papaioannou, D.; Waksman, G.; Werner, F.; Baker, J. R.; Caddick, S. *Chem. Commun.* **2011**, *47*, 5452.

(65) Martin, E. A. *A Dictionary of Science*; OUP Oxford, 2010.

(66) Lewis, R. J.; Garcia, M. L. *Nat. Rev. Drug Discov.* **2003**, *2*, 790.

(67) Bisset, N. G. *J. Ethnopharmacol.* **1991**, *32*, 71.

(68) Nasiripourdori, A.; Taly, V.; Grutter, T.; Taly, A. *Toxins* **2011**, *3*, 260.

(69) Soroceanu, L.; Manning, T. J.; Sontheimer, H. *J. Neurosci.* **1999**, *19*, 5942.

(70) Livett, B. G.; Gayler, K. R.; Khalil, Z. *Curr. Med. Chem.* **2004**, *11*, 1715.

(71) Barton, M. E.; White, H. S.; Wilcox, K. S. *Epilepsy Res.* **2004**, *59*, 13.

(72) Steinmetzer, T.; Sturzebecher, J. *Curr. Med. Chem.* **2004**, *11*, 2297.

(73) Tsetlin, V. I.; Hucho, F. *FEBS Lett.* **2004**, *557*, 9.

(74) Livett, B. G.; Sandall, D. W.; Keays, D.; Down, J.; Gayler, K. R.; Satkunanathan, N.; Khalil, Z. *Toxicon* **2006**, *48*, 810.

(75) Jin, W. L.; Lu, Z. *Biochemistry* **1998**, *37*, 13291.

(76) Xu, X. B.; Nelson, J. W. *Proteins* **1993**, *17*, 124.

(77) Jin, W. L.; Klem, A. M.; Lewis, J. H.; Lu, Z. *Biochemistry* **1999**, *38*, 14294.

(78) Protein Data Bank, www.rcsb.org/pdb/explore.do?structureId=1TER, (last accessed 14.09.2014)

(79) Jin, W. L.; Lu, Z. *Biochemistry* **1999**, *38*, 14286.

(80) Lewohl, J. M.; Wilson, W. R.; Mayfield, R. D.; Brozowski, S. J.; Morrisett, R. A.; Harris, R. A. *Nat. Neurosci.* **1999**, *2*, 1084.

(81) Hille, B. *Neuron* **1992**, *9*, 187.

(82) Karschin, C.; Dissmann, E.; Stuhmer, W.; Karschin, A. *J. Neurosci.* **1996**, *16*, 3559.

(83) Lopatin, A. N.; Makhina, E. N.; Nichols, C. G. *Nature* **1994**, *372*, 366.

(84) Matsuda, H.; Saigusa, A.; Irisawa, H. *Nature* **1987**, *325*, 156.

(85) Iwanir, S.; Reuveny, E. *Pflugers Arch.* **2008**, *456*, 1097.

(86) Signorini, S.; Liao, Y. J.; Duncan, S. A.; Jan, L. Y.; Stoffel, M. *Proc. Natl. Acad. Sci. U. S. A.* **1997**, *94*, 923.

(87) Surmeier, D. J.; Mermelstein, P. G.; Goldowitz, D. *Proc. Natl. Acad. Sci. U. S. A.* **1996**, *93*, 11191.

(88) Drici, M. D.; Diochot, S.; Terrenoire, C.; Romey, G.; Lazdunski, M. *Br. J. Pharmacol.* **2000**, *131*, 569.

(89) Mark, M. D.; Herlitze, S. *Eur. J. Biochem.* **2000**, *267*, 5830.

(90) Tinker, A.; Jan, Y. N.; Jan, L. Y. *Cell* **1996**, *87*, 857.

(91) Doyle, D. A.; Cabral, J. M.; Pfuetzner, R. A.; Kuo, A. L.; Gulbis, J. M.; Cohen, S. L.; Chait, B. T.; MacKinnon, R. *Science* **1998**, *280*, 69.

(92) Sadja, R.; Alagem, N.; Reuveny, E. *Neuron* **2003**, *39*, 9.

(93) Nishida, M.; MacKinnon, R. *Cell* **2002**, *111*, 957.

(94) Lujan, R.; Maylie, J.; Adelman, J. P. *Nat. Rev. Neurosci.* **2009**, *10*, 475.

(95) Kitamura, H.; Yokoyama, M.; Akita, H.; Matsushita, K.; Kurachi, Y.; Yamada, M. *J. Pharmacol. Exp. Ther.* **2000**, *293*, 196.

(96) Kanjhan, R.; Coulson, E. J.; Adams, D. J.; Bellingham, M. C. *J. Pharmacol. Exp. Ther.* **2005**, *314*, 1353.

(97) Felix, J. P.; Liu, J.; Schmalhofer, W. A.; Bailey, T.; Bednarek, M. A.; Kinkel, S.; Weinglass, A. B.; Kohler, M.; Kaczorowski, G. J.; Priest, B. T.; Garcia, M. L. *Biochemistry* **2006**, *45*, 10129.

(98) Dobrev, D.; Friedrich, A.; Voigt, N.; Jost, N.; Wettwer, E.; Christ, T.; Knaut, M.; Ravens, U. *Circulation* **2005**, *112*, 3697.

(99) Ehrlich, J. R.; Biliczki, P.; Hohnloser, S. H.; Nattel, S. *J. Am. Coll. Cardiol.* **2008**, *51*, 787.

(100) Hashimoto, N.; Yamashita, T.; Tsuruzoe, N. *Pharmacol. Res.* **2006**, *54*, 136.

(101) Harris, A. G. *Gut* **1994**, *35*, S1.

(102) Breeman, W. A. P.; de Jong, M.; Kwekkeboom, D. J.; Valkema, R.; Bakker, W. H.; Kooij, P. P. M.; Visser, T. J.; Krenning, E. P. *European Journal of Nuclear Medicine* **2001**, *28*, 1421.

(103) Patel, Y. C. *Frontiers in Neuroendocrinology* **1999**, *20*, 157.

(104) Wolin, E. M. *Gastrointestinal cancer research : GCR* **2012**, *5*, 161.

(105) Martin-Gago, P.; Aragon, E.; Gomez-Caminals, M.; Fernandez-Carneado, J.; Ramon, R.; Martin-Malpartida, P.; Verdaguer, X.; Lopez-Ruiz, P.; Colas, B.; Alicia Cortes, M.; Ponsati, B.; Macias, M. J.; Riera, A. *Molecules* **2013**, *18*, 14564.

(106) Veber, D. F.; Holly, F. W.; Paleveda, W. J.; Nutt, R. F.; Bergstrand, S. J.; Torchiana, M.; Glitzer, M. S.; Saperstein, R.; Hirschmann, R. *Proc. Natl. Acad. Sci. U. S. A.* **1978**, *75*, 2636.

(107) Bauer, W.; Briner, U.; Doepfner, W.; Haller, R.; Huguenin, R.; Marbach, P.; Petcher, T. J.; Pless, J. *Life Sciences* **1982**, *31*, 1133.

(108) Davies, P. H.; Stewart, S. E.; Lancranjan, I.; Sheppard, M. C.; Stewart, P. M. *Clinical Endocrinology* **1998**, *48*, 673.

(109) Krenning, E. P.; Breeman, W. A. P.; Kooij, P. P. M.; Lameris, J. S.; Bakker, W. H.; Koper, J. W.; Ausema, L.; Reubi, J. C.; Lamberts, S. W. J. *Lancet* **1989**, *1*, 242.

(110) Ur, E.; Bomanji, J.; Mather, S. J.; Britton, K. E.; Wass, J. A. H.; Grossman, A. B.; Besser, G. M. *Clinical Endocrinology* **1993**, *38*, 501.

(111) Bakker, W. H.; Albert, R.; Bruns, C.; Breeman, W. A. P.; Hofland, L. J.; Marbach, P.; Pless, J.; Pralet, D.; Stolz, B.; Koper, J. W.; Lamberts, S. W. J.; Visser, T. J.; Krenning, E. P. *Life Sciences* **1991**, *49*, 1583.

(112) Weinel, R. J.; Neuhaus, C.; Stapp, J.; Klotter, H. J.; Trautmann, M. E.; Joseph, K.; Arnold, R.; Rothmund, M. *Annals of Surgery* **1993**, *218*, 640.

(113) Otte, A.; Jermann, E.; Behe, M.; Goetze, M.; Bucher, H. C.; Roser, H. W.; Heppeler, A.; MuellerBrand, J.; Maecke, H. R. *European Journal of Nuclear Medicine* **1997**, *24*, 792.

(114) Forrer, F.; Valkema, R.; Kwekkeboom, D. J.; de Jong, M.; Krenning, E. P. *Best Practice & Research Clinical Endocrinology & Metabolism* **2007**, *21*, 111.

(115) Otte, A.; Herrmann, R.; Heppeler, A.; Behe, M.; Jermann, E.; Powell, P.; Maecke, H. R.; Muller, J. *European Journal of Nuclear Medicine* **1999**, *26*, 1439.

(116) Albert, R.; Smith-Jones, P.; Stolz, B.; Simeon, C.; Knecht, H.; Bruns, C.; Pless, J. *Bioorganic & Medicinal Chemistry Letters* **1998**, *8*, 1207.

(117) Becker, A.; Hessenius, C.; Licha, K.; Ebert, B.; Sukowski, U.; Semmler, W.; Wiedenmann, B.; Grotzinger, C. *Nature Biotechnology* **2001**, *19*, 327.

(118) Folli, S.; Westermann, P.; Braichotte, D.; Pelegrin, A.; Wagnieres, G.; Vandenbergh, H.; Mach, J. P. *Cancer Research* **1994**, *54*, 2643.

(119) Licha, K.; Hessenius, C.; Becker, A.; Henklein, P.; Bauer, M.; Wisniewski, S.; Wiedenmann, B.; Semmler, W. *Bioconjugate Chem.* **2001**, *12*, 44.

(120) Ferrari, M.; Mottola, L.; Quaresima, V. *Canadian Journal of Applied Physiology-Revue Canadienne De Physiologie Appliquee* **2004**, *29*, 463.

(121) Fottner, C.; Mettler, E.; Goetz, M.; Schirrmacher, E.; Anlauf, M.; Strand, D.; Schirrmacher, R.; Kloeppel, G.; Delaney, P.; Schreckenberger, M.; Galle, P. R.; Neurath, M. F.; Kiesslich, R.; Weber, M. M. *Endocrinology* **2010**, *151*, 2179.

(122) Trubetskoy, V. S. *Adv. Drug Deliv. Rev.* **1999**, *37*, 81.

(123) Josephson, L.; Kircher, M. F.; Mahmood, U.; Tang, Y.; Weissleder, R. *Bioconjugate Chem.* **2002**, *13*, 554.

(124) Zhang, Z. R.; Liang, K. X.; Bloch, S.; Berezin, M.; Achilefu, S. *Bioconjugate Chem.* **2005**, *16*, 1232.

(125) Edwards, W. B.; Xu, B.; Akers, W.; Cheney, P. P.; Liang, K.; Rogers, B. E.; Anderson, C. J.; Achilefu, S. *Bioconjugate Chem.* **2008**, *19*, 192.

(126) Alberts, B.; Bray, D.; Hopkin, K.; Johnson, A.; Lewis, J.; Raff, M.; Roberts, K.; Walter, P. *Essential Cell Biology, Fourth Edition*; Taylor & Francis Group, 2013.

(127) Neher, E.; Sakmann, B. *Pflugers Arch.* **1976**, *362*, R31.

(128) Neher, E.; Sakmann, B.; Steinbach, J. H. *Pflugers Arch.* **1978**, *375*, 219.

(129) Penner, R. In *Single-Channel Recording*; Sakmann, B., Neher, E., Eds.; Springer US: 1995, p 3.

(130) Sigworth, F. J.; Neher, E. *Nature* **1980**, *287*, 447.

(131) Ashcroft, F. M.; Rorsman, P. *Nature Reviews Endocrinology* **2013**, *9*, 660.

(132) Molleman, A. *Patch Clamping: An Introductory Guide to Patch Clamp Electrophysiology*; Wiley, 2003.

(133) Leica Microsystems, www.leica-microsystems.com/science-lab/the-patch-clamp-technique/, (last accessed 01.09.2014)

(134) Hille, B. *Ionic Channels of Excitable Membranes*; Mass., 1992.

(135) Edwards, F. A.; Konnerth, A.; Sakmann, B.; Takahashi, T. *Pflugers Arch.* **1989**, *414*, 600.

(136) Hestrin, S. *Neuron* **1992**, *9*, 991.

(137) Silver, R. A.; Traynelis, S. F.; Cullcandy, S. G. *Nature* **1992**, *355*, 163.

(138) Gibb, A. J.; Colquhoun, D. *Proceedings of the Royal Society B-Biological Sciences* **1991**, *243*, 39.

(139) Edwards, F. A.; Konnerth, A.; Sakmann, B.; Busch, C. *Journal of Physiology-London* **1990**, *430*, 213.

(140) Bhattacharjya, S.; Balaram, P. *Proteins: Structure, Function, and Bioinformatics* **1997**, *29*, 492.

(141) Ogino, H.; Ishikawa, H. *Journal of Bioscience and Bioengineering* **2001**, *91*, 109.

(142) Singh, R.; Kats, L. *Anal. Biochem.* **1995**, *232*, 86.

(143) Lundblad, R. L. *Chemical Reagents for Protein Modification, Fourth Edition*; Taylor & Francis, 2014.

(144) Mattos, C.; Ringe, D. *Current Opinion in Structural Biology* **2001**, *11*, 761.

(145) Hacker, M.; Messer, W. S.; Bachmann, K. A. *Pharmacology: Principles and Practice*; Elsevier Science, 2009.

(146) Luján, R.; Marron Fernandez de Velasco, E.; Aguado, C.; Wickman, K. *Trends in Neurosciences* **2014**, *37*, 20.

(147) Hibino, H.; Inanobe, A.; Furutani, K.; Murakami, S.; Findlay, I.; Kurachi, Y. *Inwardly Rectifying Potassium Channels: Their Structure, Function, and Physiological Roles*, 2010; Vol. 90.

(148) Zhu, G.; Zhang, Y.; Xu, H.; Jiang, C. *Journal of Neuroscience Methods* **1998**, *81*, 73.

(149) Gilbert, H. F. *Biothiols, Pt A* **1995**, *251*, 8.

(150) Bednar, R. A. *Biochemistry* **1990**, *29*, 3684.

(151) Hansen, R. E.; Winther, J. R. *Anal. Biochem.* **2009**, *394*, 147.

(152) Aguilar, M. I. *HPLC of Peptides and Proteins: Methods and Protocols*; Humana Press, 2004.

(153) Hilton, G. R.; Jackson, A. T.; Thalassinos, K.; Scrivens, J. H. *Analytical Chemistry* **2008**, *80*, 9720.

(154) Hunt, D. F.; Yates, J. R.; Shabanowitz, J.; Winston, S.; Hauer, C. R. *Proceedings of the National Academy of Sciences* **1986**, *83*, 6233.

(155) Kjeldsen, F.; Haselmann, K. F.; Budnik, B. A.; Sørensen, E. S.; Zubarev, R. A. *Analytical Chemistry* **2003**, *75*, 2355.

(156) Larsen, M. R.; Trelle, M. B.; Thingholm, T. E.; Jensen, O. N. *Biotechniques* **2006**, *40*, 790.

(157) Roepstorff, P.; Fohlman, J. *Biomedical Mass Spectrometry* **1984**, *11*, 601.

(158) Johnson, R. S.; Martin, S. A.; Biemann, K.; Stults, J. T.; Watson, J. T. *Analytical Chemistry* **1987**, *59*, 2621.

(159) Sela, M.; Lifson, S. *Biochimica et biophysica acta* **1959**, *36*, 471.

(160) Yen, T. Y.; Yan, H.; Macher, B. A. *Journal of Mass Spectrometry* **2002**, *37*, 15.

(161) Bohrer, B. C.; Mererbloom, S. I.; Koeniger, S. L.; Hilderbrand, A. E.; Clemmer, D. E. In *Annual Review of Analytical Chemistry* 2008; Vol. 1, p 293.

(162) Matthews, C. R. *Annual Review of Biochemistry* **1993**, *62*, 653.

(163) Mamathambika, B. S.; Bardwell, J. C. *Annual Review of Cell and Developmental Biology* **2008**, *24*, 211.

(164) Kreienkamp, H. J.; Honck, H. H.; Richter, D. *FEBS Lett.* **1997**, *419*, 92.

(165) Ferrante, E.; Pellegrini, C.; Bondioni, S.; Peverelli, E.; Locatelli, M.; Gelmini, P.; Luciani, P.; Peri, A.; Mantovani, G.; Bosari, S.; Beck-Peccoz, P.; Spada, A.; Lania, A. *Endocrine-Related Cancer* **2006**, *13*, 955.

(166) Beaumont, V.; Hepworth, M. B.; Luty, J. S.; Kelly, E.; Henderson, G. *J. Biol. Chem.* **1998**, *273*, 33174.

(167) Liu, Q. S.; Schonbrunn, A. *J. Biol. Chem.* **2001**, *276*, 3709.

(168) Thornton, J. M. *J. Mol. Biol.* **1981**, *151*, 261.

(169) Bodige, S. G.; Mendez-Rojas, M. A.; Watson, W. H. *J. Chem. Crystallogr.* **1999**, *29*, 57.

(170) Castaneda, L.; Wright, Z. V. F.; Marculescu, C.; Tran, T. M.; Chudasama, V.; Maruani, A.; Hull, E. A.; Nunes, J. P. M.; Fitzmaurice, R. J.; Smith, M. E. B.; Jones, L. H.; Caddick, S.; Baker, J. R. *Tetrahedron Lett.* **2013**, *54*, 3493.

(171) Moses, J. E.; Moorhouse, A. D. *Chem. Soc. Rev.* **2007**, *36*, 1249.

(172) Kolb, H. C.; Sharpless, K. B. *Drug Discov. Today* **2003**, *8*, 1128.

(173) Hein, C.; Liu, X.-M.; Wang, D. *Pharm. Res.* **2008**, *25*, 2216.

(174) Seo, T. S.; Li, Z.; Ruparel, H.; Ju, J. *The Journal of Organic Chemistry* **2002**, *68*, 609.

(175) Hong, V.; Presolski, S. I.; Ma, C.; Finn, M. G. *Angewandte Chemie-International Edition* **2009**, *48*, 9879.

(176) O'Brien, M. E. R.; Wigler, N.; Inbar, M.; Rosso, R.; Grischke, E.; Santoro, A.; Catane, R.; Kieback, D. G.; Tomczak, P.; Ackland, S. P.; Orlandi, F.; Mellars, L.; Alland, L.; Tendler, C.; Grp, C. B. C. S. *Annals of Oncology* **2004**, *15*, 440.

(177) Chun, C.; Lee, S. M.; Kim, C. W.; Hong, K.-Y.; Kim, S. Y.; Yang, H. K.; Song, S.-C. *Biomaterials* **2009**, *30*, 4752.

(178) Arencibia, J. M.; Schally, A. V.; Krupa, M.; Bajo, A. M.; Nagy, A.; Szepeshazi, K.; Plonowski, A. *International Journal of Oncology* **2001**, *19*, 571.

(179) Lau, A.; Berube, G.; Ford, C. H. J. *Bioorganic & Medicinal Chemistry* **1995**, *3*, 1299.

(180) Schumacher, F. F.; Nunes, J. P. M.; Maruani, A.; Chudasama, V.; Smith, M. E. B.; Chester, K. A.; Baker, J. R.; Caddick, S. *Organic & Biomolecular Chemistry* **2014**, *12*, 7261.

(181) Weissleder, R.; Pittet, M. J. *Nature* **2008**, *452*, 580.

(182) Kubin, R. F.; Fletcher, A. N. *Journal of Luminescence* **1982**, *27*, 455.

(183) Nicolas, J.; Miguel, V. S.; Mantovani, G.; Haddleton, D. M. *Chem. Commun.* **2006**, 4697.

(184) Yan, R.; Sander, K.; Galante, E.; Rajkumar, V.; Badar, A.; Robson, M.; El-Emir, E.; Lythgoe, M. F.; Pedley, R. B.; Årstad, E. *J. Am. Chem. Soc.* **2012**, *135*, 703.

(185) Yamakoshi, H.; Dodo, K.; Palonpon, A.; Ando, J.; Fujita, K.; Kawata, S.; Sodeoka, M. *J. Am. Chem. Soc.* **2012**, *134*, 20681.

(186) Ludvigsen, E.; Stridsberg, M.; Taylor, J.; Culler, M.; Öberg, K.; Janson, E. *Med Oncol* **2004**, *21*, 285.

(187) Lamberts, S. W. J.; Bakker, W. H.; Reubi, J. C.; Krenning, E. P. *New England Journal of Medicine* **1990**, *323*, 1246.

(188) Cescato, R.; Schulz, S.; Waser, B.; Eltschinger, V.; Rivier, J. E.; Wester, H.-J.; Culler, M.; Ginj, M.; Liu, Q.; Schonbrunn, A.; Reubi, J. C. *Journal of Nuclear Medicine* **2006**, *47*, 502.

(189) Hull, E. A.; Livanos, M.; Miranda, E.; Smith, M. E. B.; Chester, K. A.; Baker, J. R. *Bioconjugate Chem.* **2014**, *25*, 1395.

(190) Kelkar, S. S.; Reineke, T. M. *Bioconjugate Chem.* **2011**, *22*, 1879.